

Development of a durable and efficacious pre-erythrocytic malaria vaccine

THESIS SUBMITTED FOR THE DEGREE OF
DOCTOR OF PHILOSOPHY

MICHAELMAS TERM 2022

INDRA RUDIANSYAH
BRASENOSE COLLEGE

WORD COUNT ~ 40.000
(EXCLUDING BIBLIOGRAPHY, APPENDICES TABLES AND DIAGRAMS)

DPhil Supervisors

Dr Alexandra J. Spencer

Prof Adrian V. S. Hill KBE, FRCP, FRS

College Advisor

Professor Russell Foster

This work was supported by funding from the European Union's Horizon 2020 research and innovation programme under grant agreement No 733273.
I. Rudiansyah D.Phil scholarship is funded by LPDP

Table of Contents

Abstract *4*

Acknowledgements *5*

Author's and Authorship Statement *6*

Table of Figures *7*

Table of Tables *9*

Abbreviations *10*

Introduction *13*

1.1 Malaria diseases and global burden **13**

1.1.1 Malaria control and prevention 14

1.1.2 Life cycle of Plasmodium falciparum 17

1.1.3 Clinical feature and pathogenesis of severe malaria. 20

1.2 Immunity against malaria **22**

1.2.1 Summary of key component of human immune system 22

1.2.2 Immune response to malaria infection and vaccination 24

1.3 Malaria vaccine development **30**

1.3.1 Transgenic parasites as innovative tools to evaluate human malaria vaccines in murine model. 31

1.3.2 Current update on malaria vaccine landscape 32

1.3.3 Whole Sporozoite Vaccines 35

1.3.4 Subunit pre-erythrocytic vaccines 39

1.4 Thesis aim **43**

Materials and method *45*

2.1 Key Resources Table **45**

2.2 Resources availability **48**

2.2.1 Viral vector vaccine 48

2.3 Experimental models and subject details **50**

2.3.1 Ethics statement 50

2.3.2 Mice 50

2.3.3 Parasites 50

2.4 Method Details **50**

2.4.1 Antigen construction and plasmid preparation 50

2.4.2 ChAdOx1-BAC preparation 52

2.4.3 MVA-Shuttle plasmid preparation 53

2.4.4 Generation of ChAdOx1 vectored vaccines 54

2.4.5 Generation of MVA vectored vaccines 54

2.4.6 Generation of DNA vaccines 55

2.4.7 Vaccine preparations 55

2.4.8 Mice immunisation 56

2.4.9 Sporozoite challenge 56

2.4.10 Serum collection 57

2.4.11 Lymphocytes isolation 57

2.4.12 Endpoint titre ELISA 58

2.4.13 Single dilution, standardised ELISA 58

2.4.14 Avidity ELISA 59

2.4.15 Inhibition of sporozoite invasion assay. 60
2.4.16 *Ex-vivo* IFN-γ ELISpot assay 60
2.4.17 Intracellular cytokines staining 61
2.4.18 Identification of liver-tissue resident memory 62
2.4.19 Identification of Antigen-specific B-cells. 63
2.4.20 Indirect Immunofluorescent (IFA) Assay 63
2.4.21 Identification of antigen expression on the cell surface 64
2.4.22 SDS and Western Blot Assay 65
2.4.23 Statistical analysis 65

Optimisation of viral vectors encoding P. falciparum TRAP antigen: Impact of human-codon optimisation and strain selection on the immunogenicity and efficacy against liver-stage malaria 67

3.1 Introduction 67

3.2 Implementing human-codon optimised technique on TRAP sequences. 69
3.2.1 Human codon-optimised TRAP induced higher T-cells responses than the TRAP native sequence vaccine. 71

3.3 Head-to-head comparison of Adenoviral and MVA vaccines encoding *Pf.* TRAP T9/96 or 3D7 strain. 74
3.3.1 Immunogenicity following single-dose ChAdOx1 vaccinations. 76
3.3.2 Immunogenicity following single-dose MVA vaccinations. 84
3.3.3 Immunogenicity following heterologous ChAdOx1-MVA vaccinations. 88
3.3.3 Viral vectors encoding TRAP 3D7 elicit higher levels of protection in mice. 96

3.4 Adjuvanting Adenoviral vector vaccines encoding Pf. TRAP 3D7. 102
3.4.1 Addition of SHIC enhanced T-cell responses in the suboptimal antigen but not in the optimised TRAP 3D7. 103

3.5 Inducing $CD8^+$ Tissue Resident (TRM) Memory in the liver using TRAP 3D7 encoded viral vectors. 108
3.5.1 Prime-target vaccination using *Pf*. TRAP 3D7 encoded viral vectors induced $CD8^+$ liver-TRM in C57BL/6 mice. 109

3.6 Discussion 115
3.6.1 Chapter summary 122

Design of a nanoparticle CSP antigen encoded in chimpanzee adenoviral vectors..... 123

4.1 Introduction 123

4.2. Construction of chimpanzee adenoviral, ChAdOx1, vector encoding CSN nanoparticle. 126

4.3. Increased immunogenicity of ChAdOx1 encoding nanoparticle CSP in BALB/c mice. 129

4.4. Confirmation of antigens expression encoded in ChAdOx1. 134

4.5. Two doses of ChAdOx1 did not protect mice from malaria following sporozoite challenge 138

4.6. Towards multi-antigen pre-erythrocytic malaria vaccines. 141

4.7. Discussion. 145
4.7.1 Chapter summary 149

Broadening antibody responses towards different CSP domains by heterologous vaccination..... 150

5.1 Introduction 150

5.2. Comparison of immune response induced by viral vector and protein VLP vaccines in outbred mice. 154

5.3. Heterologous vaccinations induced broad antibody responses to different regions of CSP in inbred mice. 158

5.4 Heterologous vaccinations induced broad antibody responses to different regions of CSP in outbred mice. 164

5.5. Cellular immunity following homologous and heterologous vaccination in CD-1 mice. 169

5.6. All vaccination regimens induced high-level protection against the first malaria challenge. 170

5.7. Broad antibody responses to different regions of CSP were maintained in heterologous C,G1,G1 vaccination regimen prior the second challenge. 172

5.8. Homologous G1,G1,G1 and Heterologous C,G1,G1 vaccination regimens conferred high-level protection against the second malaria challenge. 173

5.9. Correlation analysis between antibody responses and protection. 175

5.10. Serum from homologous and heterologous vaccination inhibit sporozoite invasion *in-vitro*. 177

5.11. Discussion 180

5.11.1 Chapter summary: 185

Concluding remarks* *187

6.1 Summary findings 187

6.2 Future directions 190

6.2.1 Head-to-Head comparison of viral vectors vaccine encoding ME-TRAP and tPA-TROP in clinical trial 190

6.2.2 Optimisation of nanoparticle CSP encoded in chimpanzee adenoviral vectors. 190

6.2.3 Multi-antigen and multi-stage malaria vaccine. 191

6.2.4 Investigating mRNA vaccine technology to deliver large and complex malaria antigen. 191

6.3 Final remarks 192

References* *193

Appendix* *217

8.1 Supplemental Figures 217

8.2 Supplemental Tables 221

Development of a durable and efficacious pre-erythrocytic malaria vaccine

Indra Rudiansyah, Brasenose College, University of Oxford

Thesis submitted for the degree of Doctor of Philosophy, Michaelmas term 2022

Abstract

Despite the licensing of RTS,S/AS01 as the first malaria vaccine by WHO, development of a durable and efficacious malaria vaccine is still needed to achieve 75% efficacy as targeted in Malaria Vaccine Technology Roadmap. While the identification of more immunogenic pre-erythrocytic malaria antigens is still ongoing, CSP and TRAP are two of the most promising antigens for the subunit pre-erythrocytic malaria vaccines. This thesis aims to improve the subunit pre-erythrocytic malaria vaccines targeting CSP and TRAP that have been evaluated in clinical trials. First, Adenovirus and MVA vaccines encoding TRAP antigen were improved by substituting the antigen sequence with the African strain sequence that is more relevant to the vaccine deployment region. The vaccines induced high T-cell response and protected more mice against malaria infection following challenge with transgenic *P. berghei* sporozoite expressing homologous *P. falciparum* TRAP compared to Adenovirus-MVA vector vaccine encoding ME-TRAP, which contain heterologous strain antigen sequence. Secondly, the concept of combining virus-like particle vaccine modalities with an Adenovirus vector was investigated, using CSP antigen as a model, to produce a vaccine that induced high antibody and CD8 T-cell responses, which are required for protection against malaria infection. Subsequently, the strategy was expanded to include multiple antigens, CSP and TRAP, that may improve the protection by inducing broad immune responses against different pre-erythrocytic antigens. Lastly, the strategy to broaden the antibody response against subdominant epitope within CSP antigen, which is known to contain protective epitope, was evaluated using heterologous vaccinations. This strategy induces a high antibody response against subdominant epitope that correlates with protection against sporozoite infection in vivo and in vitro. Together, these preclinical studies have provided valuable information for the clinical development of pre-erythrocytic malaria vaccines targeting CSP and TRAP antigens.

Acknowledgements

First and foremost, thanks to my supervisors, Dr. Alexandra J. Spencer and Prof Adrian V. S. Hill KBE, FRCP, FRS, for their excellent supervision, constant support, guidance and mentorship throughout the D.Phil. You have inspired, challenged, and broaden my knowledge in vaccinology and became my role model as a professional scientist and leader. To Adrian, thank you for the massive opportunity to conduct this project and your contagious enthusiasm for malaria vaccine development. For Alex, working directly under your supervision was one of the luckiest experiences of my entire DPhil. Thank you for the technical aspect, stories, and encouragement to participate in any opportunity to build my professional career actively. To both of you, hopefully, we will have another cross path and more collaborations in the future. Secondly, thanks to my scholarship, LPDP. Without this financial support, it is impossible for me to pursue my D.Phil.

Special thanks to Prof. Sarah Gilbert DBE, Prof. Teresa Lambe OBE, Associate Prof. Alexander Douglas, and Prof. Ellie Barnes for your constructive advice on my project. I would also like to thank all members of the Vector Core Facility, Heather Gray, Viv Clark and all staff at the FGF for their help during my D.Phil. Also, thanks to Adam Truby and Marta Ulaszewska for always being available to help with my experiments. Thank you to Susan Morris and Reshma Kailath for sharing your extensive knowledge of viral vector vaccines. Thanks to Ekta Mukhopadhyay, Ahmed Salman, Rames Segireddy, Duncan Bellamy and Edmund Wee for sharing the resources I used for this study.

Many thanks to Amy Flaxman, Mustapha Bittaye, Jordan Barret, Sandra Belij-Rammerstorfer and Marco Polo Peralta Alvarez for the massive collaboration during COVID-19 clinical trial. Many thanks to all, past and present, members and students at the Jenner Institute, especially Andrew Worth, Mariya Mykhaylyk, Julie Furze, Andres Noe, Daniel Wright, Alexander Sampson, Carina Joe, Sarah Batawi and Cameron Bisset for your help and support.

Thanks to my support system in Oxford, my partner and friends, Dominic Armsby, Javier Gilbert, Catriona Rooney, and Ujang Purnama, for countless laughs, joy, and support. Finally, I thank my parents for always keeping my name in their praying.

Author's and Authorship Statement

The COVID-19 pandemic has brought a significant collateral impact on the progress of experiments and data collection. For example, the lab facility was closed for non- COVID-19 projects to comply with government regulations on national lockdown for at least six months during the first year of the pandemic, followed by limited access for experimenting for at least the next six months after the laboratories open. Despite these circumstances, most of the data have been collected and presented in this thesis.

Additionally, during the pandemic, I was involved in the clinical trial of Oxford-AstraZeneca's COVID-19 vaccine to evaluate the antibody responses for eight months during phase I/II and phase II/III across the UK and Brazil. Additionally, I interned for six months at COVAX Facility/GAVI to support the technical and policy team for the Office of COVAX Facility in Geneva. These experiences, indeed, have enriched my professional career throughout my D.Phil.

This thesis has been composed by myself and is entirely based on my own work unless stated otherwise. In summary, the following contributions are acknowledged:

1. Another scientist of the Jenner institute has cloned some DNA plasmids, and the DNA plasmids I generated during this study were stated in Chapter 2.
2. The viral vector core facility produced the viral vector vaccines used in this study using the plasmids that were generated by myself or already available at Jenner.
3. Dr. Ahmed Salman and Ekta Mukhopadhyay produced the R21 and R21/G1 used in this study, and these contributions are acknowledged explicitly in Chapter 2.
4. Adam Truby has prepared the culture of sporozoites at the Jenner Insectary Facility, and intravenous administration of this sporozoite was performed with the help of Marta Ulaszewska and Dr. Alex Spencer.

Table of Figures

FIGURE 1.1 LIFE CYCLE OF P. FALCIPARUM 18
FIGURE 2.1 INTRACELLULAR CYTOKINES STAINING GATING STRATEGY. 62
FIGURE 3.1 IMMUNOGENICITY OF DNA VACCINES MEASURED BY EX-VIVO IFN-γELISPOT ASSAY. 73
FIGURE 3.2 ANTIGEN INSERT IN CHADOX1 AND MVA VACCINES..... 76
FIGURE 3.3 T-CELL RESPONSES INDUCED BY SINGLE DOSE CHADOX1 VACCINATION. 79
FIGURE 3.4 FUNCTIONALITY OF $CD4^+$ AND $CD8^+$ T-CELL RESPONSES FOLLOWING VACCINATION WITH A SINGLE DOSE OF CHADOX1. 82
FIGURE 3.5 ANTIBODY RESPONSES FOLLOWING A SINGLE DOSE CHADOX1 VACCINATION. 83
FIGURE 3.6 T-CELL RESPONSES INDUCED BY SINGLE DOSE MVA VACCINATION. 86
FIGURE 3.7 FUNCTIONALITY OF $CD4^+$ AND $CD8^+$ T-CELL RESPONSES FOLLOWING VACCINATION WITH A SINGLE DOSE OF MVA..... 87
FIGURE 3.8 ANTIBODY RESPONSES FOLLOWING SINGLE DOSE MVA VACCINATION. 88
FIGURE 3.9 T-CELL RESPONSES INDUCED FOLLOWING HETEROLOGOUS CHADOX1-MVA VACCINATIONS. 90
FIGURE 3.10 FUNCTIONALITY OF TRAP-SPECIFIC $CD4^+$T-CELL RESPONSES FOLLOWING VACCINATION WITH CHADOX1-MVA. 93
FIGURE 3.11 FUNCTIONALITY OF TRAP-SPECIFIC $CD8^+$T-CELL RESPONSES FOLLOWING VACCINATION WITH CHADOX1-MVA. 94
FIGURE 3.12 ANTIBODY RESPONSES FOLLOWING CHADOX1-MVA VACCINATIONS. 96
FIGURE 3.13 EFFICACY OF CHADOX1-MVA VACCINATION IN CD-1 AND C57BL/6 MICE..... 98
FIGURE 3.14 TRAP-SPECIFIC $CD8^+$ T-CELL RESPONSES FROM PROTECTED VS UNPROTECT CD-1 MICE. 99
FIGURE 3.15 CORRELATION BETWEEN $CD8^+$ T-CELL RESPONSES WITH TIME TO 1% PARASITAEMIA. 100
FIGURE 3.16 IMPACT OF THE ADDITION OF SHIC ADJUVANT TO THE IMMUNOGENICITY TROP ENCODED CHADOX-1 VECTOR. 105
FIGURE 3.17 IMPACT OF THE ADDITION OF SHIC ADJUVANT TO THE IMMUNOGENICITY TROP ENCODED CHADOX-1 VECTOR. 106
FIGURE 3.18 T-CELL RESPONSES INDUCED BY PRIME-BOOST OR PRIME-TARGET VACCINATION. 111
FIGURE 3.19 PRIME-TARGET VACCINATION WITH VIRAL VECTORS. 114
FIGURE 4.1 ILLUSTRATION OF DIFFERENT TYPES OF VLPS. 127
FIGURE 4.2 CONSTRUCTION OF CHADOX1 ENCODING NANOPARTICLE CSP. 129
FIGURE 4.3 IMMUNOGENICITY OF SINGLE DOSE CHADOX1 VACCINES. 130
FIGURE 4.4 HUMORAL AND CELLULAR RESPONSE INDUCED BY PRIME-BOOST VACCINATION OF CHADOX1.. 132
FIGURE 4.5 EXPRESSION OF CSN ANTIGENS. 136
FIGURE 4.6 EFFICACY OF TWO-DOSES CHADOX1 AND FUNCTIONALITY OF ANTIBODY RESPONSE FOLLOWING PRIME-BOOST VACCINATION OF CHADOX1. 140
FIGURE 4.7 IMMUNOGENICITY OF DNA VACCINES ENCODING MULTI-PRE-ERYTHROCYTIC ANTIGENS..... 144
FIGURE 5.1 SCHEMATIC DIAGRAM OF PF. CSP 3D7. 151
FIGURE 5.2 HUMORAL AND CELLULAR RESPONSES INDUCED BY VLP OR VIRAL VECTOR VACCINATIONS..... 157

FIGURE 5.3 ANTIBODY RESPONSES FOLLOWING HOMOLOGOUS AND HETEROLOGOUS VACCINATIONS IN BALB/C MICE. 162
FIGURE 5.4 T-CELLS RESPONSES FOLLOWING HOMOLOGOUS AND HETEROLOGOUS VACCINATIONS IN BALB/C MICE. 163
FIGURE 5.5 EFFICACY FOLLOWING HOMOLOGOUS AND HETEROLOGOUS VACCINATIONS. ..**ERROR! BOOKMARK NOT DEFINED.**
FIGURE 5.6 ANTIBODY RESPONSES FOLLOWING HOMOLOGOUS AND HETEROLOGOUS VACCINATION IN CD-1 MICE. .....**ERROR! BOOKMARK NOT DEFINED.**
FIGURE 5.7 ANTIBODY RESPONSES FOLLOWING HOMOLOGOUS AND HETEROLOGOUS VACCINATION IN CD-1 MICE AT THE SECOND CHALLENGE TIME POINT.....**ERROR! BOOKMARK NOT DEFINED.**
FIGURE 5.8 CELLULAR RESPONSES FOLLOWING HOMOLOGOUS AND HETEROLOGOUS VACCINATION IN CD-1 MICE. .....**ERROR! BOOKMARK NOT DEFINED.**
FIGURE 5.9 SERUM FROM MICE VACCINATED WITH HOMOLOGOUS AND HETEROLOGOUS VACCINATION INHIBIT SPOROZOITE INVASION IN-VITRO. 178

Table of Tables

TABLE 1.1 WHO PPC FOR MALARIA VACCINE TO PREVENT INFECTION (PRE-ERYTHROCYTIC MALARIA)[16] 16

TABLE 1.2 CURRENT MALARIA VACCINE LANDSCAPE (DEC 2022) 33

TABLE 2.1 KEY RESOURCES TABLE 45

Table 1.2 Viral vector vaccines produced in the study 49

Table 2.3 TRAP antigen constructs produced or used in this study 52

TABLE 2.4 CSN ANTIGEN CONSTRUCTS PRODUCED OR USED IN THIS STUDY. 52

TABLE 5.1 SUMMARY OF ANTIBODY RESPONSES INDUCED BY FOUR DIFFERENT VACCINATION REGIMENT IN CD-1 MICE. 179

Abbreviations

Ag	Antigen
AMA1	Aapical Membrane Antigen 1
AP	Alkaline Phosphatase
APC	Antigen Presenting Cells
AS	Adjuvant System
BAC	Bacterial Artificial Chromosome
BCRs	B-cell Receptors
CD	Cluster of Differentiation
CEF	Chick Embryo Fibroblast
ChAd	Chimpanzee Adenovirus
CHMI	Controlled Human Malaria Infection
CPS	Administration of Infectious Sporozoite with Chemoprophylaxis
CSA	Chondroitin Sulphate A
CSP	Circumsporozoite Proteins
CT	Cytoplasmic Tail
DNA	Deoxyribonucleic Acid
EBA	Erythrocyte-Binding Antigens
EBA	Erythrocytes Binding Antigen
EEF	Exo-Erythrocytic
ELISA	Enzyme-Linked Immunoassay
ELISpot	Enzyme-Linked Immunosorbent Spot
EMP1	Erythrocyte Membrane Protein 1
EPI	Expanded Immunisation Programme
EVs	Extracellular Vesicles
Fab	Variable Regions
Fc	Constant Region
FCS	Fetal Calf Serum
GAP	Genetically Attenuated Parasite
GFP	Green Fluorescence Protein
GLURP	Glutamine-Rich Protein
GMP	Good Manufacturing Practice
GPI	Glycosylphosphatidylinositol
HA	Haemagglutinin A
HAc	Hyaluronic Acid
HBsAg	Hepatitis B Surface Antigen
HIV	Human Immunodeficiency Virus
HRP2	Histidine-Rich Protein 2
ICAM-1	Intracellular Adhesion Molecule 1
IFA	Indirect Immunofluorescence Assay
IFN	Interferon
Ig	Immunoglobulin

IL	Interleukin
IPTp	Intermittent Preventive Treatment of Malaria in Pregnancy
IPTsc	Intermittent Preventive Treatment of Malaria in School-Aged Children
IRSs	Indoor Residual Spray
ISI	Inhibition Of Sporozoite Invasion
ITNs	Insecticide-Treated Nets
LSA1	Liver-Stage Antigen 1
mAb	Monoclonal Antibody
MBL	Mannose Binding Lectin
MDA	Mass Drug Administration
ME	Multiple Epitope String
MHC	Major Histocompatibility Complex
MPLA	Monophosphoryl-Lipid A
MSP	Merozoite Surface Protein
MVA	Modified Vaccinia Ankara
NAI	Natural Acquired Immunity
NHP	Non-Human Primate
P2A	Porcine Teschovirus-1 2A Sequence
PAMPs	Pathogen-Associated Molecular Patterns
PBS	Phosphate Buffer Saline
PDMC	Post-Discharge Malaria Chemoprevention
PEV	Pre-Erythrocytic Malaria Vaccine
PMC	Perennial Malaria Chemoprevention
PRRs	Pattern Recognition Receptors
PVM	Parasitophorous Vacuole Membrane
RAS	Radiate Attenuated Sporozoite
RBCs	Red Blood Cells
RDTs	Rapid Diagnostic Tests
RFP	Red Fluorescent Protein
RH	Reticulocyte Binding Homologs
RIFIN	Repetitive Interspersed Family Proteins
RNA	Ribonucleic Acid
RSV	Respiratory Syncytial Virus
SHIC	Transmembrane Domain of Shark Invariant Chain
SHIC65	Transmembrane Domain and Cytoplasmic Tail of Shark Invariant Chain
SMC	Seasonal Malaria Chemoprevention
spz	Sporozoites
STARP	Sporozoite Threonine-Asparagine-Rich Protein
STEVOR	Sub-Telomeric Variable Open Reading Frame Proteins
SURFIN	Surface-Associated Interspersed Gene Family Proteins
t-SNE	T-Distributed Stochastic Neighbor Embedding
T2A	Thosea Asigna Virus 2A Sequence

TCRs	T-Cell Receptors
Tfh	T Follicular Helper
TLR	Toll-Like Receptor
TM	Transmembrane Domain
TNF	Tumor Necrosis Factor
tPA	Tissue Plasminogen Activator Signal Peptide
TRAP	Thromobospondin-Related Adhesion Protein
Treg	Regulatory T-Cells
TRM	Tissue Resident Memory Cells
VCAM1	Vascular Cell Adhesion Molecule 1
VLP	Virus Like-Particle
VSAs	Variants Surface Antigens
VVCF	Viral Vector Core Facility
WHO	World Health Organisation
WSV	Whole Sporozoite Vaccination
wt	Wild-Type

1

Introduction

1.1 Malaria diseases and global burden

Malaria is a vector-borne disease that remains a significant global health problem. The disease is caused by infection of Plasmodium parasites that are spread by female Anopheles *sp.* mosquitoes during feeding. Fever, headache, and chill are the most common symptoms that appear 10-15 days after the parasite inoculation by mosquitoes. If the infection is left untreated, it can progress to severe acute febrile illness and death. Five species of *Plasmodium* are known to be the causative agent for malaria disease in humans: *P. falciparum*, *P. vivax*, *P. ovale*, *P. knowlesi* and *P. malariae*. Two *Plasmodium* species, *P. falciparum* and *P. vivax* pose a significant threat to public health as infection by these parasites can lead to severe malaria and death. *P. falciparum* is also responsible for highest proportion of malaria cases and death worldwide, with 95% of cases in sub-Saharan Africa.

According to World Malaria Report 2022, there were an estimated 247 million malaria cases and 619 000 malaria death in 2021 [1]. In the last two decades malaria prevention has relied on vector control and chemo-preventive programmes which have significantly reduced malaria incidence from around 82.3 in 2000 (cases per 1000 population at risk) to 60.1 in 2015; however, this progress has been stalled since 2015 [1, 2]. Furthermore, the COVID-19 pandemic has disrupted the supply chain and distribution of malaria control tools, increasing malaria cases globally. It is estimated that COVID-19 disruption has led to 13.4 million additional malaria cases between 2019 and 2021 [1]. These data highlight the need

for additional tools, such as vaccines, to complement existing control strategies and bring down malaria incidents globally.

1.1.1 Malaria control and prevention

Vector control is one of strategy that effectively reduces malaria transmission and infection. Insecticide-Treated Nets (ITNs) and Indoor Residual Spray (IRSs) are two major interventions in controlling malaria vectors that have both significantly contributed to a reduction of the malaria burden between 2000-2015 in moderate to high transmission settings. However, the efficacy of ITNs and IRSs have been threatened by the emergence of vector resistance to the insecticides [3, 4]. Moreover, it has been reported that vectors with behavioural changes, for example, feeding earlier and resting outdoors, have become more dominant and can significantly impact the effectivity of ITNs and IRS [5].

Another strategy that has significantly brought down malaria cases is administering antimalarial treatments in malaria-endemic countries to high-risk populations. This strategy covers Perennial Malaria Chemoprevention (PMC), Seasonal Malaria Chemoprevention (SMC), Intermittent Preventive Treatment of malaria in pregnancy (IPTp) and school-aged children (IPTsc), post-discharge malaria chemoprevention (PDMC) and mass drug administration (MDA). However, the emergence of antimalarial drug resistance, such as artemisinin-partial resistance in the Greater Mekong Subregion and Africa region, can jeopardise the effectiveness of this strategy to control malaria globally [6-8]. Additionally, active malaria parasite surveillance has strengthened the effort to control malaria infection and diseases, especially to detect and map out the spread of antimalarial drug resistance. Indeed, continuous improvement is required to increase sensitivity and specify, notably in

the appearance of parasites with histidine-rich protein 2 (HRP2) gene deletion that becomes a target for Rapid Diagnostic Tests (RDTs) [9, 10].

Despite the success of these tools in controlling and preventing malaria diseases, since 2015 progress has stalled. Any disruption to the distribution and implementation of these preventive tools, such as occurred during the COVID-19 pandemic, could diminish the achievement of malaria control in the last two decades [11]. The WHO recently approved the use of the first malaria vaccine, RTS,S/AS01, as a new tool to control malaria diseases and transmission [12, 13]. The vaccine is recommended for children living in moderate to high malaria transmission regions. Data from phase 3 clinical trial involving 15000 children across 7 countries in sub-Saharan Africa showed that the vaccine has an efficacy of around 30-50% [14, 15]. Table 1.1 summarised the Preferred Product Characteristic (PPC) for pre-erythrocytic malaria vaccine that published by WHO in 2022. According to this WHO PPC, a pre-erythrocytic malaria vaccine is expected to have efficacy more than 90% and long lasting (more than 1 year) [16]. This suggesting that there is still room for improvement in pre-erythrocytic malaria vaccine development.

Table 1.1 WHO PPC for malaria vaccine to prevent infection (pre-erythrocytic malaria)[16]

Parameter	Preferred Product Characteristics
Indication for use	Prevention of blood-stage infection due to *P. falciparum* and/or *P. vivax* malaria at the individual level The vaccine may be indicated for malaria control, elimination and/or prevention of reintroduction post-elimination, and may have application in low-, moderate- and high-transmission settings.
Target population	To maximize the public health impact of an infection-prevention vaccine, the immediate need will be to target populations or age groups who experience high incidence of infection. However, community-wide effects on transmission could be achieved by vaccinating a substantial proportion of the population that infects mosquitoes. Potential changes in malaria epidemiology should be considered, anticipating shifts in ages with the highest infection incidence at the time vaccines become available.
Safety	The safety and reactogenicity of the vaccine should be comparable to or better than WHO-recommended vaccines in use in LMICs. Safety should also be demonstrated in high-risk or immunocompromised groups, such as HIV-infected children or adults. Developers should be aware of possible deferred increases in morbidity due to the dynamics of waning vaccine-induced immunity and reductions in naturally acquired immunity. Plans for assessment of such effects may be required either in Phase 3 or Phase 4 evaluation.
Efficacy and duration	The vaccine should dramatically reduce incidence of blood-stage infection (e.g. 90% over 12 months of follow-up post-immunization) at the individual level. A rational target level of efficacy should be justified in conjunction with targets for the duration of protection, variation of efficacy over time and other key drivers of public health impact in the primary target group. Thus, the initial efficacy and long-term dynamics of protection will be considered together.
Dose regimen and schedule	Single dose for primary immunization is preferred, but additional doses (including annual doses) are likely to be needed for strong and/or long-lasting immunity (e.g. efficacy > 90% and/or duration > 1 year).
Co-administration	Immunogenicity data are required if the malaria vaccine may be co-administered with vaccines against other pathogens. Data should provide confidence that immunogenicity and safety of both the malaria and non-malaria vaccines are maintained and there is no clinically relevant interference.

Parameter	Preferred Product Characteristics
Formulation/ Presentation	Vaccines seeking WHO prequalification should meet WHO-defined criteria for programmatic suitability regarding formulation, presentation, packaging, thermostability and disposal.
Route of administration	Vaccines seeking WHO prequalification should not require an intravenous route of administration, a mandatory requirement by the PSPQ Working Group whereby compliance is compulsory at time of application to WHO prequalification.
Product stability and storage	Vaccines stable under refrigerated conditions (2–8°C) for 24 months are preferred. Vaccines or any component presented for WHO prequalification should not require storage at less than -20°C, a mandatory requirement by the PSPQ Working Group whereby compliance is compulsory at time of application to WHO prequalification.
Programmatic suitability	Vaccines presented for WHO prequalification will be assessed for programmatic suitability according to mandatory, critical, unique or innovative, and preferred characteristics. The vaccine should be prequalified in order to support purchasing by United Nations (UN) agencies, according to the process outlined in *Procedure for assessing the acceptability, in principle, or vaccines for purchase by the United Nations agencies* (WHO/BS/10.2155).
Access and affordability	Dosage, regimen and cost of goods should enable affordable supply. Favourable cost-effectiveness should be established and price should not be a barrier to access, including in LMICs.

1.1.2 Life cycle of Plasmodium falciparum

The life cycle of *Plasmodium* parasites is complex, involving female *Anopheles* sp. mosquitoes and vertebrata hosts. In a single malaria life cycle, at each stage a specific parasite forms will infect different cell types. While the process is unique to every *Plasmodium* sp., the detail of the life cycle of *P. falciparum* is described as this thesis focuses on vaccine development targeting *P. falciparum* (Figure 1.1).

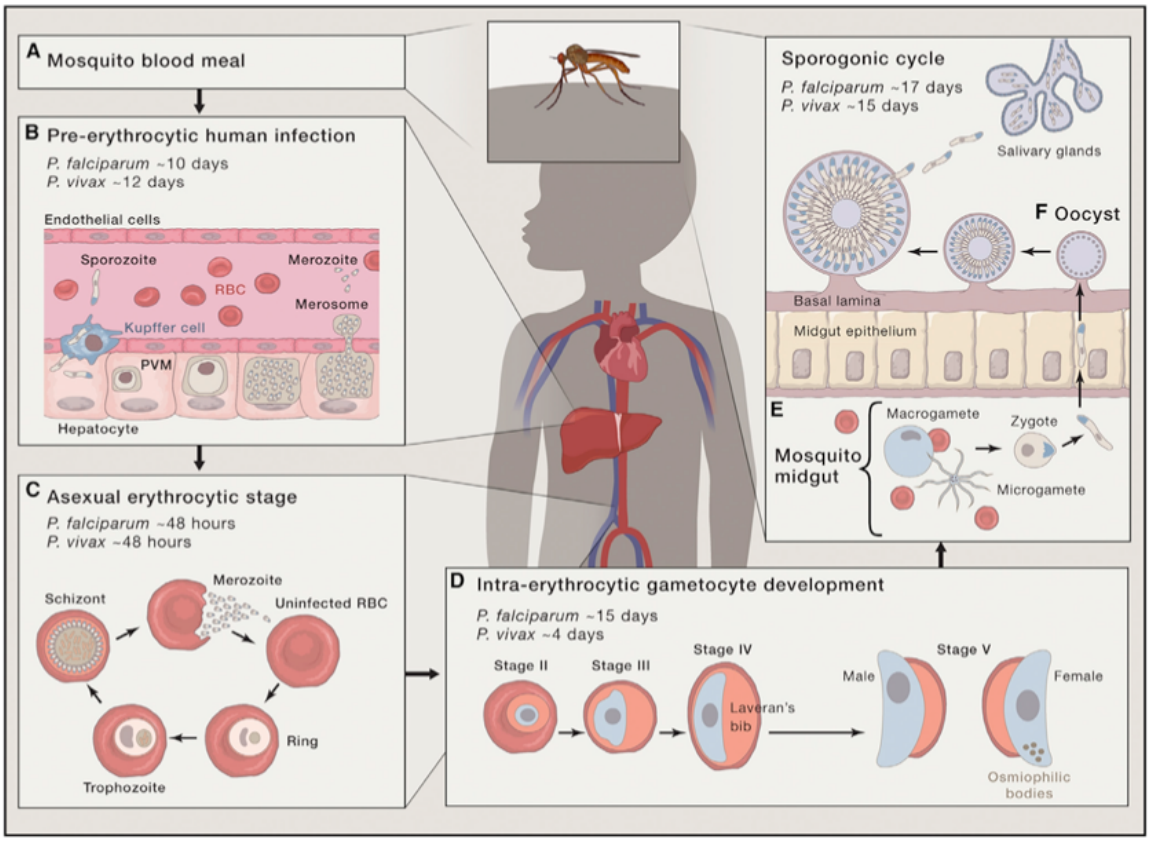


Figure 1.1 Life cycle of *P. falciparum.* Image taken from [17].

A. Sporozoites from the salivary gland of female Anopheles sp. are deposited in the dermis during a blood meal. **B.** After parasite migration to the liver, the sporozoites invade hepatocytes, develop and release merozoites into the bloodstream. **C.** The parasites start their erythrocytic development in the blood, exponentially releasing more parasites. **D.** Some parasites commit to undergoing sexual development, releasing male and female gametes. **E.** The gametes are taken by female Anopheles sp. during a blood meal, fused into zygotes and developed in the midgut, resulting in new sporozoites and ready to start a new cycle.

Pre-erythrocytic stage

Malaria parasites are transferred from female *Anopheles* sp. to humans in the form of sporozoites during mosquito feeding. Infection in humans begins with inoculation of tens to hundreds sporozoites into the dermis, followed by parasite gliding to reach blood vessels and get into the bloodstream [18, 19]. Some sporozoites remain in the skin and are eventually destroyed or reach the lymph node through lymphatic drainage process [20, 21]. Parasites in the bloodstream migrate to the liver and enters the liver lobule via the portal vein or portal field. Next, sporozoites start to glide along the liver sinusoids and traverse the fenestrated

endothelial and Kupfer cells (a liver resident macrophage) before reaching the space of Disse. Sporozoites then traverses several hepatocytes before settling in one hepatocyte to establish an infection. Once Circumsporozoite proteins (CSP) on the sporozoite surface are activated by the proteo-cleavage mechanism, the invasion of hepatocytes begins [22]. It is estimated that the migration of sporozoite from the site of inoculation to the liver takes around 1-3 hours, resulting in a short window for the immune system to eliminate the sporozoite [23]. Parasites establish a Parasitophorous Vacuole Membrane (PVM) in the infected hepatocytes and it is within this PVM that the sporozoites undergo exo-erythrocytic (EEF) or liver-stage development for between 2 to 10 days (species dependant) culminating in the release of merosomes, each containing 10000 – 40000 merozoites, into the bloodstream [23, 24].

Erythrocytic stage

In the bloodstream, the merosomes rupture and release merozoites allowing parasites to come into contact with erythrocytes, this is mediated by the MSP complex which initiates pre-invasion [25, 26]. After the MSP contact event, merozoites reorientate until the apical end of the merozoite is directly facing towards the erythrocyte, this enables ligand-receptor interaction, mediated by Erythrocytes Binding Antigen (EBA) and Reticulocyte Binding Homologs (RH), resulting in host cell deformation and activation of downstream invasion events [27, 28]. The invasion process begins with a binding event between the host-cell receptor and Rh5 ligand in a complex form with RIPR and CYRPA proteins, followed by the formation of a PVM that encloses the merozoite [27, 29-31]. Inside the infected erythrocyte, the parasite undergoes development marked by initial formation of ring-stage trophozoite, followed by mature trophozoite and, finally, erythrocytic schizont. When the schizont-containing erythrocytic rupture, new merozoites are released into the bloodstream and the invasion and replication cycle is repeated.

Sexual stage

During rounds of merozoite replication, a proportion of parasites commit to undergoing sexual development into male and female gametocytes. Whilst the factor that influence parasites to commit to sexual development remain unclear, the timing point of this transition is predicted to occur between the trophozoites and formation of schizont [32, 33]. The length of the maturation process varies between Plasmodium species. In *P. falciparum*, the maturation of gametocytes lasts for 11 days, and the early phase gametocytes are sequestered in the bone marrow [34]. Meanwhile, only mature, infectious gametocytes circulate in the peripheral until taken up into the mosquito midgut during feeding. Once inside the mosquito midgut, male and female gametes are activated, fused, and produce zygotes which subsequently develop into ookinetes and invade the mid-gut wall and form Oocysts. Once Oocysts ruptures, sporozoites are released and migrate to the mosquito salivary gland, ready to start another malaria cycle.

1.1.3 Clinical feature and pathogenesis of severe malaria.

The infection of hepatocytes during the pre-erythrocytic development stage is asymptomatic. In contrast, the infection of erythrocytes by merozoite induces clinical symptoms and is associated with malaria pathology, with outcomes ranging from mild symptoms to severe disease and even death. However, the clinical symptoms induced by blood-stage infection are not malaria specific and commonly include fever, chills, sweats, headaches, body aches, malaise, nausea and vomiting. Complete treatment in the early stage of malaria infection can clear the parasite in the bloodstream and stop the clinical symptom of malaria developing. However, incomplete treatment or new infections will lead to the development of clinical symptoms. If the infection is left untreated, the disease can progress

into severe malaria with various outcomes such as cerebral malaria (coma), severe anaemia, acute respiratory distress syndrome, metabolic acidosis, multiple organ failure or death.

Many malaria pathologies are the result of host cell interactions with the malaria parasites. Infection of erythrocytes by malaria parasite change the cells' structure and contributes to the virulence of *P. falciparum* [35]. The infected red-blood cells expressed *P. falciparum* EMP1, a knob-like adhesive protein, on its surface that can bind to a broad range of receptors, including thrombospondin, CD36, vascular cell adhesion molecule 1 (VCAM1), intracellular adhesion molecule 1 (ICAM-1), E-selectin, chondroitin sulphate A (CSA), CD31 and hyaluronic acid (HA) [36-41]. Interaction of malaria-infected red blood cells with receptor ICAM-1 is associated with cerebral malaria [40]. Meanwhile, binding to the CSA and HA receptors is essential to establishing placenta malaria in a pregnant individual [39, 42]. Notably, infected erythrocytes can adhere to capillary and postcapillary venular endothelium (cytoadherence) or uninfected erythrocytes and form red cell rosettes (this process is called rosetting) [43]. Both cytoadherence and rosetting can lead to the sequestration of infected erythrocytes in various organs, resulting in tissue damage [44, 45]. Additionally, uncontrolled reactions from the host immune system in response to malaria infection can also result in pathological diseases (immunopathology) [46-48]. Excessive expression of early pro-inflammatory cytokines can result in progressive immune pathology and increased disease severity.

1.2 Immunity against malaria

1.2.1 Summary of key component of human immune system

Innate Immunity

In the grand scheme, components of the immune system are sub-divided into either the innate or adaptive immune system. Epithelial surfaces serve as an initial physical barrier against pathogens. In addition, they secrete various chemical and antimicrobial substances, including lysozyme, secretory phospholipase A2 and antimicrobial peptides (defensins, cathelicidins, histatins) that directly attack pathogens. Once physical and initial chemical deference barriers are breached, the innate immune system encounters the pathogens. The innate immune system consists of secreted (complement) and cellular components. Complement is soluble proteins present in the blood and other body fluids that interact with immune components enabling pathogen clearance. Complement components circulate in an inactive form (zymogen) in the absence of infection and recognition of foreign substances triggers activation of the complement pathway by either via classical, alternative or Mannose Binding Lectin (MBL) pathways. All these pathways lead to the generation of a C3 convertase which activates C3 through proteolysis, resulting in effector functions to promote either inflammation, attract phagocytic cells or formation of a membrane-attack complex on the surface of the pathogens [49, 50].

The innate immune system also contains cellular components such as dendritic cells, macrophages, mast cells, neutrophils, eosinophils, and basophils derived from common myeloid progenitors. While neutrophils, eosinophils and basophils are primarily found in the circulation, macrophages, dendritic cells, and mast cells primarily reside in tissues. Macrophages, neutrophils and dendritic cells have essential roles in the innate system as

they detect an infection and directly activate their effector function to release pro-inflammatory cytokines. Notably, these classes of innate cellular immunity can act as Antigen Presenting Cells (APC) and activate the adaptative immune system [51, 52]. Although the innate immune response is non-specific, the innate immune system components can differentiate pathogens from other host components via Pattern Recognition Receptors (PRRs) that recognise Pathogen-Associated Molecular Patterns (PAMPs) that are conserved in many microorganisms [53, 54]. Notably, many vaccines adjuvant have been developed based on PRRs agonist to enhance the immune response.

Adaptive Immunity

The adaptive immune response is activated at the later phase of infection with the help of innate immunity. However, unlike innate immunity, the adaptive immune system can generate immunological memory to each specific pathogens [55]. This feature has become the interest of vaccination to provide long-term protection against infections. Similar to innate immunity, the adaptive immune system also consists of humoral and cellular components.

The cellular component of the adaptive immune system, B-cells and T-cells, are derived from a common lymphoid progenitor. B-cell contains membrane immunoglobulin called B-cell receptors (BCRs) that recognise linear or conformational epitopes contained in the antigen. When the BCRs bind to the antigen, it will lead to the activation of B-cells either via thymus-dependent antigen or thymus-independent antigen, resulting in B-cells proliferation and differentiation into plasmablast or plasma cells. Similar to the B-cells, T-cells express T-cell receptors (TCRs) that recognise linear epitopes presented by the Major

Histocompatibility Complex (MHC) on the surface of APC [56, 57]. T-cells can be subdivided by the expression of surface markers CD4 and CD8, which have different effector functions [58]. The CD8 T cells (also known as cytotoxic T-cell lymphocytes) recognise the complex of epitope peptide from intracellular pathogen presented by MHC class I on infected cells. Peptide-MHC recognition activates CD8 T-cell effector function to enable direct killing of the infected cell [59]. Meanwhile, CD4 T cells (also known as T-helper lymphocytes) recognise epitope peptides, mainly from the extracellular pathogen, in complex with MHC class II presented by the APCs. This recognition activates T-cell to produce cytokines and "help" other components of immune cells, such as the activation of B-cells by T follicular helper (Tfh), a subset of CD4 T-cells. Based on the phenotype characteristic, CD4 T-cells can be divided into Th1, Th2, Th17, regulatory T-cells (Treg) and T follicular helper cells (Tfh) [60].

Antibodies are the humoral component of the adaptive immune system and are secreted forms of B-cell receptor (BCR) which are produced by activated B-cells that have differentiated into plasmablast or plasma cells. An antibody consists of two identical heavy chains bound to two identical light chains. Together, the heavy and light chains form a variable regions (Fab) containing two-antigen binding sites that recognise the antigen's epitope. The C-terminus of the antibody contains a constant region (Fc) that mediates the effector functions of the different antibody subclasses through binding with Fc receptors [61].

1.2.2 Immune response to malaria infection and vaccination

Despite many studies characterising the immune response to malaria infections, it is still only partially understood. It is evident that Natural Acquired Immunity (NAI) against

malaria can develop in individuals living in endemic regions as a result of prolonged and continuous exposure to malaria infections [62-64]. However, such immunity wanes rapidly after malaria exposure ceases. Significantly the rate of immunity acquisition depends on exposure intensity and appears to be species-specific [65]. Although the underlying mechanism of protection provided by NAI remained elusive, NAI has been characterised by the capability to control diseases and reduce parasite density. In *P. falciparum*, a high level of parasitaemia is associated with inflammation, which, if left untreated, will lead to immunopathology [35]. NAI can directly decrease parasitaemia in the blood by neutralising the parasite (antiparasitic immunity) or diminish proinflammatory cytokines to reduce the severity of the disease (anti-disease immunity). It has been reported that immunity against severe malaria and death is rapidly developed [66]. In contrast, 'antiparasitic immunity' is slowly acquired [62, 63, 67]. Additionally, evidence suggests that such immunity is not sterilising, which is corroborated by many adults who developed asymptomatic infections after prolonged exposure during childhood [63, 68, 69]. However, pregnant women remain susceptible to severe malaria despite pre-existing immunity [70], adding more complexity to the immune response against malaria infection.

Immunity to pre-erythrocytic stage

Innate immunity is the first line of defence against malaria infection. During infectious Anopheles mosquito feeding, the sporozoites are deposited in the skin and enter the blood capillary via gliding motility [71]. Studies in mice using murine malaria, *P. berghei,* demonstrated that dendritic cells captured and degraded some sporozoite that remained in the skin [71, 72]. Additionally, *P.berghei* sporozoite, which reached the lymph node during intradermal vaccination, also induced immune responses, shown by the increase of lymph node size in response to parasites [21]. Sporozoites that reach the blood capillary rapidly migrate to the liver and infect hepatocytes. During liver infection, the host elicits a weak

cellular immune response shown by formation inflammatory foci that populate by neutrophils, eosinophils, and macrophages [73, 74] around the hepatocytes after injection with infectious, but not heat-killed, sporozoites in murine models [75-77].

Sterilising immunity against malaria infection can be achieved by stopping the parasites' egress from hepatocytes to initiate a blood-stage infection. However, studies in naturally exposed individuals suggest malaria infections do not produce sterile immunity against liver-stage development [63, 68]. It remains poorly understood why natural infection fails to induce such protection against liver-stage malaria. The low number of sporozoites being deposited (10-100 sporozoite) during mosquitoes feeding, thus low overall antigen load, could be one of the explanations, as repeat vaccination with a high dose of live-attenuated sporozoite (around 1000-3000 bites or 4-5 intravenous injections with 135.000 sporozoite/injection) is able to induce sterile protection [18, 19, 78].

In addition, the capability of sporozoites to evade the innate immune system during pre-erythrocytic development may have a role in the absence of sterile immunity at this stage. Firstly, sporozoite rapidly migrate from injection site to the blood vessels and reach hepatocyte by traversing Kupffer cells [79]. Secondly, it has been reported that the sporozoites can suppress respiratory bursts during the traversal of Kupfer cells, by hijacking the production of reactive oxygen [21, 80, 81]. Thirdly, the sporozoite able to supress expression of pro-inflammatory gene, mainly mediated through sporozoite CSP [82]. Next, the sporozoite infected hepatocytes are found to increase the expression of Hemeoxygenase-1, which regulates inflammatory responses, allowing the parasite to develop inside hepatocytes [75]. Lastly, the parasite able to inhibit apoptosis of the host cell by releasing host-cell membrane vesicle containing developed parasite (merozoite) [83, 84].

Regarding antibody responses, natural infections induce anti-sporozoites antibodies among individuals in endemic countries [85]. Most of these antibodies bind to CSP, the major antigen expressed on the sporozoite surface [86, 87]. It has been demonstrated that anti-sporozoite antibodies can inhibit sporozoite infection through different mechanisms at any phase of pre-erythrocytic stage development [88]. During blood feeding, anti-sporozoite antibodies in mice previously vaccinated with Radiate Attenuated Sporozoite (RAS) form an antibody complex with soluble CSPs released by sporozoite into mosquito saliva, resulting in lower sporozoites deposited in the dermis compared to naïve mice [19]. Notably, passive serum transfer from RAS-vaccinated mice or monoclonal antibodies against CSP can inhibit mouse hepatocyte infection following a lethal dose challenge [87, 89]. Additionally, serum from mice vaccinated with *P. falciparum* RAS is shown to inhibit sporozoite motility and cell invasion *in vitro* [90]. Serum from a naturally exposed individuals has also been shown to recognise other sporozoite antigens such as Thromobospondin-related adhesion protein (TRAP), Liver-stage antigen 1 (LSA1) sporozoite threonine-asparagine-rich protein (STARP) and apical membrane antigen 1 (AMA1) [91, 92]. However, antibodies induced by subunit vaccines targeting these antigens are not protective.

In the context of the adaptive cellular response, sporozoite antigen-specific T-cell have been detected among individuals naturally exposed to malaria, although low in magnitude. This response is primarily directed against TRAP, LSA1 and CSP antigen [93-95]. The role of CD8 T-cells in providing immunity against malaria infection was demonstrated in the 1980s following RAS vaccinations [78, 96-99]. At least 1% of CSP-specific CD8 T-cells in peripheral blood are required to protect mice against malaria infection following challenge with *P. berghei*, suggesting a high number of Ag-specific T-cells are required to induce

sterile protection against liver-stage malaria [100], a number that is not achieved by natural infection. Indeed, investigation of RAS vaccination in humans resulted in high protection, mediated mainly by CD8 T-cells [78]. This protection was achieved after administering four to five doses of a high number of sporozoites. Alternatively, high-numbers of CD8 T-cells can be achieved by targeting individual antigens using viral vectors [101]. Several studies have demonstrated a role for CD4 T-cells in helping CD8 T-cell expansion and survival and promoting the production of antibodies by B-cell [93, 102, 103]. However, further exploration is needed to dissect this T-cell subset's contribution to protection against liver-stage malaria.

Immunity to erythrocytic stage

During the erythrocytic stage, parasites grow exponentially. Therefore, it is not surprising that most naturally acquired immunity is directed towards blood-stage development, albeit it is not sterilising [66, 104, 105]. Blood-stage infection induces a high level of inflammation either induced directly by the molecule produced from the parasite or generated towards components from infected red blood cells [106]. For instance, some merozoite antigens contain glycosylphosphatidylinositol (GPI) -an anchor that activates TLR2/TLR6 and TLR-2/TLR1 heterodimer or TLR-4 homodimer that leads to inflammation [107-109]. Repeating cycles of blood-stage development leads to excessive and persistent inflammation that influences disease progression.

There is limited evidence on the role T-cell mediated immunity against erythrocytic stage development. A longitudinal study in children from malaria endemic regions, ie naturally exposed to malaria, showed that Ag-specific $CD4^+$ T-cells were detected in almost all children [93, 110-112] and was associated with recent malaria exposure but not protection. However, in murine models, $CD4^+$ T-cells have been shown to play a significant role in

immunity against blood-stage malaria by helping B-cells to produce antibodies. Additionally, the production of IFN-γ by malaria antigen-specific $CD4^+$ T-cells has been shown to control the peak of parasitaemia in acute infection against *P. chaubadi* [113-116]. Indeed, our understanding of how T-cell response mediated protection against blood-stage infection still needs to be developed.

In contrast, the role of antibodies in mediating protection against blood-stage development is well described. In a seminal study, passive transfer of IgG from immune adults reduced parasitaemia by around 3-4 logs when it was given to Gambian children with clinical malaria [117]. However, defining which antigen are the targets of protective antibodies remains challenging. Generally, blood-stage antigens targeted by protective antibodies can be classified into two groups. The first group is variants surface antigens (VSAs) which are expressed and transferred to the surface of the infected erythrocytes [118]. Several VSAs have been identified as a targets of protective antibodies: *P. falciparum* erythrocyte membrane protein 1 (PfEMP1; ~50 members/parasite), repetitive interspersed family proteins (RIFIN; ~150 members/parasite), sub-telomeric variable open reading frame proteins (STEVOR: ~30 members/parasite), and surface-associated interspersed gene family proteins (SURFIN; 10 members/parasite). It is likely that antibodies targeting VSAs work by interfering with the adhesion or sequestration process of infected erythrocytes. The other antigens targets are proteins on the parasite's surface that act as a ligand for erythrocyte invasion [119-121]. In individuals with NAI, antibodies against apical membrane antigen 1 (AMA1), glutamine-rich protein (GLURP), merozoite surface protein (MSP)-3, $MSP\text{-}1_{19}$ (a fragment of MSP-1 that remained on the surface of Merozoite), and erythrocyte-binding antigens (EBA) have been associated with protection. However, using these antigens in subunit vaccines has been challenging as these antigens are highly polymorphic. In recent

work, PfRh5 antigen has gained more attention as this antigen is highly conserved and importantly, less immunogenic in natural infection suggesting this antigen not under immune pressure. Therefore, PfRh5 is an attractive target for blood-stage malaria vaccine and currently under investigation [122].

1.3 Malaria vaccine development

According to the WHO PPC for pre-erythrocytic malaria vaccine 2022, a malaria vaccine candidate preferably need to have 90% protective efficacy against malaria infection for at least 12 months [16]. Malaria parasites infect hepatocytes and erythrocytes in two different forms with use different machinery to establish invasion. Therefore, malaria vaccines have been designed to target different stages of the parasite life-cycle: pre-erythrocytic, blood-stage and sexual-stage (transmission blocking). A malaria vaccine targeting the pre-erythrocytic stage is an attractive candidate as infection at this stage results is asymptomatic. Therefore, a successful vaccine candidate that can effectively reduce the sporozoite burden, killing the infected hepatocytes and preventing the merozoite egress to the bloodstream would prevent clinical diseases and transmission. However, developing such vaccines has been challenging, as one successful parasite development in an infected hepatocyte can lead to release of hundreds of merozoites and development of blood-stage malaria [123]. On the other hand, vaccines targeting blood-stage malaria are likely to reduce the severity of clinical disease, as shown in naturally exposed adults with asymptomatic infection resulting from prolonged and consistent exposure [104, 105, 124]. Additionally, a transmission-blocking vaccine aims to inhibit parasite development in the *Anopheles* sp. vector by targeting *de-novo* antigen expressed during parasite development in the mosquitoes, resulting in incomplete parasite development and preventing transmission during *Anopheles* sp. feeding [125].

Most conventional vaccines are developed to induce immunity, mimicking NAI without disease progression. However, in the case of malaria, the NAI induced by infection is not sterilising and develops slowly [63, 67, 68]. Notably, only a low-level immune response against antigens/stage development that are thought to be the bottleneck for parasite development have been observed, eg a low-level T-cells response against liver-stage antigens and antibody response against PfRh5 (Blood stage antigen) [122, 126]. In the last two decades, many attempts to develop malaria vaccines that can induce high-level cellular immunity have been made. Novel platforms such as viral vector vaccines have been shown to effectively induce a high number of circulating antigen-specific CD8+ T-cells, which are associated with protection against pre-erythrocytic stage malaria [127-129]. Importantly, innovation in vaccination regimens such as prime-target has allowed us to harness a localised-protective immune response in the liver that is not naturally induced by natural infections [130]. Furthermore, focusing immune responses to antigens with a low degree of polymorphism, such as the PfRh5 antigen, has shown reduced parasite growth *in vitro* and *in vivo* in humanised mice [122, 131]. Taken together, these data support the notion that an "unnatural" form of malaria immunity that can be induced by vaccination may prevent infection, prevent diseases, and stop transmission.

1.3.1 Transgenic parasites as innovative tools to evaluate human malaria vaccines in murine model.

Controlled human infection models are powerful tools to accelerate vaccine development and for malaria, Controlled Human Malaria Infection (CHMI) has been widely used to evaluate malaria vaccines in early clinical trials before conducting studies in endemic regions [132]. In order to achieve a collective goal of obtaining a high-efficacious malaria

vaccine by 2030, CHMI has been used in many clinical trial research centres and led to harmonisation of the methodology enabling comparison between studies [133]. Although CHMI can be performed using a well-characterised laboratory strain clone, the *P. falciparum* strain NF54 and its laboratory clone 3D7 or 7G8 are most frequently used in the CHMI studies [132]. Importantly these strains were found to be sensitive to chloroquine.

Applying the challenge infection model in preclinical studies requires some adaptation as *P. falciparum* does not infect small animal models; hence cannot be used in mice. Several malarial parasites, such as *P. berghei*, *P. yoelii*, and *P. chabaudi* have been isolated and infect mice and have been frequently used in murine malaria studies [134, 135]. The advancement of biotechnology has allowed scientists to generate transgenic murine sporozoites such as *P. berghei* or *P. yoelii* to express *P. falciparum* antigens; whether as a substitution or complement of endogenous antigen [136-139]. Although the major caveat of this model is an inability to identically recapitulate the infection of *P. falciparum* in humans, it has significantly contributed to antigen screening before progressing vaccines to preclinical study in higher order animal model, such as a non-human primate (NHP) that can be infected by *P. falciparum* [134]. Alternatively, chimeric mice with the humanised liver can be used to evaluate pre-erythrocytic malaria vaccines [140].

1.3.2 Current update on malaria vaccine landscape

The following database were used to summarise the current malaria vaccine candidates that currently being evaluated in clinical trials: 1. WHO Global Observatory on Health Research and Development database (https://www.who.int/observatories/global-observatory-on-health-research-and-development/monitoring/who-review-of-malaria-vaccine-clinical-development, accessed on 20 December 2022) with selection criteria/keywords: “active”

and "*P. falciparum",* and *"pre-erythrocytic"* and *"blood stage"* and *"sexual stage";* 2. US National Library of medicine (https://clinicaltrials.gov, accesed on 3 April 2023) with selection criteria/keywords: "malaria,falciparum" and "vaccine" and "not yet recruiting" and "recruiting" and "active, not recruiting". Table 1.2 summarised 26 candidates that fit with criteria/keywords. The candidate vaccines targeting the pre-erythrocytic stage will be discussed further, as this thesis will focus on developing a pre-erythrocytic malaria vaccine (PEV).

Table 1.2 Current malaria vaccine landscape (Dec 2022)

Vaccines	Vaccine platform/Antigen construct	Target antigen	Current phase	References
Pre-erythrocytic vaccines				
FMP013/ALFQ	Protein recombinant, near full-length CSP epressed in E. coli formultaed in ALFQ (liposom containing synthetic MPLA+QS21)	PfCSP	Phase I	[141]
FMP014/ALFQ	Self Assembly Nanoparticle, CSP epitope based expressed in E. coli with SAPN scaffold formulated in ALFQ (liposom containing synthetic MPLA+QS21)	PfCSP	Phase I	[142]
PfGAP3-KO	Whole sporoizte vaccine (WSV), Genetically attenuated sporozoite Pf. NF45	Multiple	Phase I	[143]
PfSPZ	Whole sporoizte vaccine (WSV), Raddiated attenuated sporozoite Pf. NF45	Multiple	Phase II	[144]
PfSPZ-Cvac	Whole sporoizte vaccine (WSV), Infectious sporozoite Pf. NF45 adminstered with chemoprophylaxis	Multiple	Phase II	[145]
PfSPZ-GA1	Whole sporoizte vaccine (WSV), Genetically attenuated sporozoite Pf. NF45	Multiple	Phase I	[146]
PfSPZ-GA2 with Adjuvants (CoGA)	Whole sporoizte vaccine (WSV), Genetically attenuated sporozoite Pf. NF45	Multiple	Phase I	[147]
PfSPZ-CVac	Whole sporoizte vaccine (WSV), wild-type Pf. NF45 followed by administration of Pyronaridine/ Tetraphosphate/ Artesunate Drug Combination	Multiple	Phase I	
R21/AS01B	Recombinant protein (VLP), truncated CSP (18 NANP repeat + C-terminal domain fused to HBsAg) formulated in AS01 adjuvant	PfCSP	Phase I	

Vaccines	Vaccine platform/Antigen construct	Target antigen	Current phase	References
R21/Matrix M1	Recombinant protein(VLP), truncated CSP (18 NANP repeat + C-terminal domain fused to HBsAg) formulated in Matrix M	PfCSP	Phase III	[148, 149]
R21/Matrix M1; Chad63-MVA ME-TRAP	Recombinant protein(VLP), truncated CSP (18 NANP repeat + C-terminal domain fused to HBsAg) formulated in Matrix M. Viral vector vaccines, Pf TRAP T9/96 naïve sequence fused to multiepitope string (ME-TRAP)	PfCSP, PfTRAP	Phase IIb	
rCSP/AP10-602	Recombinant protein, Full-length CSP expressed in Pseudomonas fluorescent formulated in Glucopyranosyl Lipid A-liposome QS21 (GLA-LSQ) adjuvant)	PfCSP	Phase I	[150]
RTS,S/AS01E	Recombinant protein (VLP), truncated CSP (18 NANP repeat + C-terminal domain fused to HBsAg) formulated in AS01 Adjuvant	PfCSP	Phase IV	
VLPM01	CHIK-VLP displaying NANP repeat epitope formulated in Alum	PfCSP	Phase I	[151]
Erythrocytic vaccines				
BK-SE36/CpG	Recombinant protein, N-terminal domain of Pf SERA5 produced in E. coli formulated in Alum and CpD	PfSERA5	Phase I	[152]
ChAd63-MVA Rh5	Viral vector vaccine, Pf RH5 3D7	PfRh5	Phase Ia/Ib	[153]
Chemically attenuated Pf7G8	Whole merozoite vaccine, Pf 7G8 merozoite chemically attenuated with tafuramycin-A	Multiple	Phase I	[154]
Rh5.1/Matrix M1	Recombinant protein, Full-length ectodomain PfRH5 3D7 antigen formulated in matrix M	PfRh5	Phase Ib	
Rh5/AS01B	Recombinant protein, Full-length ectodomain PfRH5 3D7 antigen formulated in AS01	PfRh5	Phase IIa	[155]
MSP3-CRM-Vac4All/ Alhydrogel® Vaccine	Recombinant protein, MSP3 antigen fused to CRM protein carrier formulated with Alhydrogel	MSP3	Phase Ia/IIb	[156]
Matrix M with R78C and/or RH5.1	Recombinant protein, Full-length ectodomain PfRH5 3D7 antigen, and/or truncated RIPR and CyRPA antigen formulated in matrix M.	PfRh5, PfRIPR, PfCyRPA	Phase I	[157]
Matrix-M with RH5.2 VLP and/or R21	Recombinant protein, Full-length ectodomain PfRH5 3D7 antigen expressed as a VLP mix with Recombinant protein (VLP), truncated	PfRh5, CSP (Multi-stage)	Phase I	

Vaccines	Vaccine platform/Antigen construct	Target antigen	Current phase	References
	CSP (18 NANP repeat + C-terminal domain fused to HBsAg)			
Transmission Blocking Vaccine & other				
Pfs25-IMX313/Matrix M1	Self-Assembly Nanoparticle, recombinant Pfs25 antigen fused to C4 bp oligomerisation domain (IMX313) expressed in P. pastoris and formulated in Matrix M	Pfs25	Phase II	[158]
Pfs25/AS01B; Pfs230D1M-EPA	Recombinant protein, recombinant Pfs25 antigen expressed in P. pastoris and formulated in AS01 Recombinant protein, recombinant Pfs230 antigen conjugated to detoxified Exo- Protein A from Pseudomonas aeruginosa. expressed in P. pastoris and formulated in Alum	Pfs25, Pf230	Phase II	
PRIMVAC/Alum PRIMVAC/GLA-SE	Recombinant protein, DBL1x-2x region of Pf VAR2CSA 3D7 formulated in Alum or GLA-SE	Pf VAR2CSA / Placenta malaria	Phase I	[159]
Pfs48/45 in Matrix-M	Recombinant protein, full-length of gamete surface protein Pfs48/45 with Matix M	Pfd48/45	Phase I	[160]

1.3.3 Whole Sporozoite Vaccines

The use of the whole sporozoite for a malaria vaccine was first demonstrated in 1967 using irradiated *P. berghei* sporozoites to immunise mice which protected them from subsequent challenge with *P. berghei* sporozoites [96]. Since then, the concept of whole sporozoite vaccination (WSV) has been investigated in humans [78, 98, 99, 161, 162]. Studies in humans using radiated attenuated sporozoites induced a high-level protection against malaria infection. For this reason, WSV has become a gold standard in pre-erythrocytic vaccine development [78]. Several challenges have been acknowledged to bring the whole sporozoite vaccine from lab/pilot scale production to commercial scale: 1. Sporozoite requires mosquitoes to grow; hence the mass production of WSV requires a massive amount of mosquito culture that becomes the bottleneck for scaling up. 2. The WSV vaccine is required to be stored in liquid nitrogen. 3. Current cold-chain infrastructure for vaccine

distribution is limited to -80°C (most vaccines distribute using -20°C or 2-8°C) as applicable in the distribution of mRNA vaccine during the COVID-19 pandemic, hence currently cannot yet accommodate the distribution of WSV that requires liquid nitrogen.. Nonetheless, some progress has been made in producing these vaccines to Good Manufacturing Practice (GMP) conditions [163]. In addition, various strategies to attenuate or deliver the vaccine have been developed: Radiate Attenuated Sporozoite (RAS), Genetically Attenuated Parasite (GAP) or administration of infectious sporozoite with chemoprophylaxis (CPS). All to prevent parasite replication while preserving metabolic activity to induce a diverse immune response.

Radiation Attenuated Sporozoite

The use of γ-irradiation to produce the RAS vaccine was based on the experiments conducted in the late 1960s where mice vaccinated by mosquitoes bites containing *P. berghei* attenuated sporozoite made through the y-irradiation of the *Anopheles* sp. vector were protected from infection upon challenge [96]. This study has become a foundation for developing RAS vaccines against *P. falciparum* [164]. Early human studies involving 9 clinical visits for immunisation, with over 1000 mosquito bites per volunteer, protected 24 out of 26 volunteers after challenge with *P. falciparum* infected mosquitoes [99]. The method to deliver the RAS vaccine has been developed further. Recently, complete protection was achieved by administering five doses of the RAS vaccine (1.35×10^5 sporozoite/dose) administered intravenously [78]. The protection induced by the RAS vaccine in humans appears to be dose-dependent, as decreasing the number of dose to four reduces the efficacy down to 66%. Notably, the anti-sporozoite antibody and Ag-specific $CD8^+$ T-cell responses in protected volunteers was higher than in the unprotected group [78].

Indeed, the protection induced by RAS vaccination appears to be pre-erythrocyte specific as no antibodies were detected against erythrocytes-stage antigens.

γ-irradiation maintains sporozoite's viability and ability to invade hepatocytes but prevents complete asexual replication inside hepatocytes. Thin-section electron microscopy analysis reveals that γ-irradiation does not change the integrity of the cells. However, irradiated sporozoites appear to be more vacuous with a partially disrupted plasma membrane and inner membrane complex. Gene-microarray analysis shows that at least 180 liver-stage parasite genes are transcriptionally altered, and 7 of those genes involve cell cycle arrest of the parasite inside hepatocytes [165]. The process development (led by Sanaria) to produce the RAS vaccine that complies with GMP regulation has reached significant progress. The robust and reproducible γ-irradiation process has been achieved with no breakthrough infection [163, 166]. However, the challenge of scaling up for mass production, storage and distribution remain to be addressed.

Genetically Attenuated Parasite

An alternative method to attenuate the sporozoite is the genetic knock-out of genes essential for parasite development inside hepatocytes. The concept of Genetically Attenuated Parasite (GAP) was first introduced in 2005 using murine malaria models [167, 168]. Mice immunised with GAP parasites were sterilely protected to a level comparable with RAS vaccination [169]. Similar to RAS, the idea of GAP is to produce a whole sporozoite vaccine where sporozoites can invade hepatocytes but development is restricted. However, unlike RAS, which has limited parasite development inside hepatocytes, GAP can be adjusted to produce parasites that arrests at mid to late stages during liver-stage development, enabling a broader range of antigens to be expressed. An early human study using the *P. falciparum*

sporozoite NF54 strain with deletion at P52 and P36 gene (Pf52-/Pf36-) showed that the vaccine is well tolerated, and the volunteers remained blood-stage negative after receiving low and medium doses via mosquitoes bite [170-172]. However, high dose administration of GAP (>200 mosquito bite) lead to breakthrough blood-stage infection [173], suggesting incomplete attenuation using only these gene knock-outs. Further genetic deletions to achieve high-level attenuation at mid-late liver-stage development is still being investigated. Currently, parasites with a deletion on the slarp/sap1 gene, in addition to the deletion of one or more 6-Cys family genes (p52/p36/b9), are the most advanced GAP candidate for human use. Early pre-clinical assesement in mice with human liver tissue engrafted demonstrates that the *P. falciparum* GAP sporozoite with p52-/p36-/sap1- (named GAP3KO) or b9-/slarp-deletion completely abort intrahepatic development [174, 175], suggesting this combination of mutations may be safe to use in human, and currently progressing to clinical trial in human.

Sporozoite vaccination under chemoprophylaxis

Another innovative strategy for whole sporozoite vaccination is inoculation using fully infectious sporozoite followed by the administration of anti-malaria drugs that kill the parasite in the early stage of erythrocytic development, such as chloroquine [176-179]. Chloroquine inhibits the metabolism of haemoglobin by the parasites, resulting in the accumulation of the toxic product in the vacuole that kills the parasites [180, 181]. Hence, this drug is specific for blood-stage treatment and does not impact liver parasite development. CHMI study have been used to assess the efficacy of chloroquine and mefloquine based vaccine strategy. Other anti-malaria drugs, including artesunate, azithromycin, clindamycin, piperaquine, primaquine, and pyrimethamine, are currently being investigated as an alternative to chloroquine and have shown promising results in pre-

clinical trials [182-186]. In addition, the protection induced by CPS vaccination appears to be stage-specific, targeting pre-erythrocytic development, as CHMI study using mosquito bites among CPS-vaccinated individuals protects the volunteer but does not protect when volunteers were challenged with the blood-stage parasite [182].

1.3.4 Subunit pre-erythrocytic vaccines

Despite the success of WSV being able to induce a high level of protection and manufacturing process improvements, the use of WSV, with currently available infrastructure (e.g. storage condition and cold-chain), in the endemic areas still needs to be optimised to be able to successfully deploy WSV. Subunit vaccine, such as Hepatitis B vaccines, have been widely used globally as part of the Expanded Immunisation Programme (EPI) with storage and cold-chain infrastructure available widely, including rural-malaria endemic areas. Additionally, novel technology platforms such as viral vector vaccines have been licensed in COVID-19, providing a blueprint for manufacturing and authorisation process for global use [187]. Therefore, the subunit vaccine approach can overcome the logistical challenges of WSV. Early studies in identifying immune responses induced by RAS vaccination have pointed to Circumsporozoite protein (CSP) as a dominant antigen and potential protective target [86, 87, 188, 189]. Subsequently, immune responses against other pre-erythrocytic antigens, including TRAP, LSA1 and EXP1, have also been detected [92, 93]. Here the current status of CSP and TRAP-based antigens is discussed as these antigens are the main focus of this thesis.

<u>PEV: PfCSP based vaccines</u>

Circumsporozoite protein (CSP) is the major protein on the surface of malaria sporozoites. The structure of CSP contains an N-terminal domain, central repeat region and C-terminal

domain. It is evident that the immune response against CSP has been dominated by the NANP-repeat contained within the central repeat region [86, 89]. Moreover, the dominance of the NANP epitope is not only within the CSP antigen but also the whole sporozoites antigen, as immune responses induced by RAS vaccination are primarily directed towards this epitope.

Many pre-erythrocytic subunit malaria vaccines have been developed based on this CSP, yet early studies showed major challenges in expressing CSP as a full-length antigen. RTS,S/AS01, the first licensed malaria vaccine, is designed based on a truncated CSP, fused to Hepatitis B surface antigen protein (HBsAg) and co-expressed with additional free HBsAg protein to create a virus-like particle (VLP) structure in *S. cerevisiae* [190]. The ratio between malaria antigen and HBsAg in RTS,S vaccine is estimated to be 1:4. Although it has been granted licensing approval, the vaccine only provides partial protection, with only 25-50% of children and infants protected against malaria in endemic settings [191, 192]. Another promising CSP-based vaccine, R21, has a similar antigen construct to RTS,S. However, this vaccine is not co-expressed with free HBsAg protein and is expressed in a different host system, resulting in a higher density of malaria antigen [193, 194]. The vaccine is currently in clinical development, with interim data showing promising results [148, 149]. Other strategies to develop CSP-based vaccines, including full-length recombinant CSP, genetic vaccines (DNA, mRNA and viral vector) and epitope-based vaccines, have been extensively evaluated in preclinical and clinical settings with various outcomes [150, 195-197].

In RAS vaccination, the protection in mice is primarily mediated by CSP-specific CD8 T-cell response is able to destroy malaria infected hepatocytes [78, 97]. In contrast, protection

afforded by the RTS,S vaccine is mainly mediated via antibodies, which likely targets the extracellular phase of sporozoite during parasite migration from the site injection to the liver [191, 192]. Data suggests that antibody and T-cell response against CSP can mediate protection against malaria infection. In recent years, immunological exploration from humans vaccinated with RAS revealed CSP contains an additional protective epitope in a region not included in RTS,S or R21 [198, 199]. This protective epitope, called the junctional epitope, appears superior to the NANP as passive transfer of mAb against this epitope protects more mice than an mAb against the NANP epitope. Indeed, many next generation CSP-based vaccines are exploring inclusion of this epitope.

PEV: PfTRAP based vaccines

Another antigen that has been extensively evaluated as a target for subunit pre-erythrocytic vaccines is a microneme protein called Thrombospondin Related Adhesion Protein (TRAP) [200]. This protein plays a significant role during sporozoite traversal and hepatocyte invasion [201, 202]. TRAP from *P. falciparum* T9/96 fused to the multiepitope string (ME-TRAP) encoded in Adenovirus (ChAd63) and MVA vector is the most advanced sub-unit vaccine encoding TRAP to date [129, 203]. The vaccine proved partial protection in malaria naïve adults but not infants and children in malaria-endemic regions and vaccination induced high-levels of Ag-specific CD8 T-cells that was associated with protection. Unlike CSP, immunity induced by TRAP likely targets the intracellular phase of sporozoite during liver-stage development, as antibodies induced by TRAP do not inhibit sporozoite invasion [128, 204, 205]. Heterologous prime-boost of ChAd63A -MVA encoding ME-TRAP have been extensively used in clinical trials in sub-Saharan Africa; however, the antigen sequence used in the construct derived from the *P. falciparum* strain that primarily circulated in South-East Asia [200, 206, 207]. Data from whole sporozoite vaccination shows that vaccine

efficacy is significantly reduced when the parasite used for the challenge differs from the strain used in the vaccine [208]. The vaccine efficacy reduction may be due to antigenic variability, raising the question of whether antigen sequence based on strain circulated in sub-Saharan Africa will provide higher protection than current ME-TRAP constructs [207].

1.4 Thesis aim

As introduced above, significant progress has been achieved in malaria vaccine development with the licensing of RTS,S/AS01. However, more research is still needed to produce a pre-erythrocytic vaccine with higher protection. Whilst the whole sporozoite vaccination has been shown to induce a high level of protection, the application of such vaccines for global use requires further optimisation in terms of manufacturing and distribution. Meanwhile, using a subunit vaccine platform for the pre-erythrocytic malaria vaccine could ease deployment, especially in malaria-endemic regions.

The pre-clinical and clinical data shows that both humoral and cellular immune responses are able to mediate protection against pre-erythrocytic malaria [97, 191, 204]. Subunit CSP vaccines are found to induce humoral responses that target the extracellular phase of sporozoite during parasite migration; meanwhile, viral vector encoding TRAP induced protective CD8 T-cell responses that act upon the intracellular phase of sporozoite liver-stage development. Together, TRAP and CSP are two pre-erythrocyte antigens that consistently show their potential as protective antigens in many pre-clinical and clinical studies. Nevertheless, these vaccines are still require further optimisation to improve protection. Hence, work described in this thesis aimed to further investigate strategies to improve the current TRAP and CSP-based viral vector vaccines. This platform has been shown to generate robust antibodies and high-level antigen-specific cellular responses. ME-TRAP encoded in ChAd63 and MVA is the leading vaccine targeting parasite liver-stage development. While heterologous prime-boost ChAd63-MVA is found to exceptionally induce high T-cell responses, further improvement can be made through optimising the antigen insert, including codon optimisation and selecting the most relevant antigen strain.

CSP antigen is the target of protective antibody and T-cell response. The current malaria vaccine, RTS,S is designed using VLPs technology, a platform that is known able to induce high antibody responses. On the other hand, viral vector vaccines such as adenovirus appear to be potent in inducing T-cell responses. Therefore, it is interesting to investigate whether combining these two modalities into a single platform can result in a higher immune response that can lead to higher levels of protection. Suggestions to incorporate different regions of CSP, including the junctional epitope, have been raised in many studies as a

mechanism to broaden the immune response against CSP and increase the target of protective antibodies. In this thesis, strategies to achieve such a goal will be investigated.

Lastly, it has been thought that to achieve high protection, multiple antigens might be required in subunit pre-erythrocytic vaccine to broaden immune response against sporozoite antigen, as has been shown in vaccination using WSV. Therefore, this thesis will provide an early investigation into whether a multi-antigen approach targeting the pre-erythrocytic stage is feasible. In detail, the major aims of this thesis are:

- To investigate the strategies to improve the immunogenicity and efficacy of viral vectors encoding liver-stage antigen Pf. TRAP.
- To develop an adenovirus vector vaccine encoding CSP antigen expressed as nanoparticle VLPs.
- To develop a multi-antigen vaccine targeting pre-erythrocytic vaccine using Pf. TRAP and Pf. CSP antigen
- To investigate the strategies to broaden immune response against CSP antigen.

2

Materials and method

2.1 Key Resources Table

Table 2.1 Key Resources Table

Reagent or Resource	Source	Identifier
Antibodies		
Anti-mouse B220/CD45 R (Clone: RA3-6B2) PECy7	Biolegend	Cat. No. 115553
Anti-mouse CD11a (Clone: M17/4) PE-Cy7	Biolegend	Cat. No. 101121
Anti-mouse CD138 (Clone: 281-2) BV421	Biolegend	Cat. No. 142508
Anti-mouse CD183 (CXCR3)(Clone: CXCR3-173) APC	Biolegend	Cat. No. 126511
Anti-mouse CD186 (CXCR6)(Clone: SA051D1) BV711	Biolegend	Cat. No. 151111
Anti-mouse CD19 (Clone: 6D5) PEDazzle	Biolegend	Cat. No. 115553
Anti-mouse CD279 (PD1)(Clone: 29F.1A12) BV605	Biolegend	Cat. No. 135219
Anti-mouse CD3 (Clone: 145-2C11) BUV496	BD Horizon	Cat. No. 612955
Anti-mouse CD38 (Clone: 90) PECY5	eBioscience	Cat. No. 15-0381-82
Anti-mouse CD4 (Clone: GK1.5) BV650	Biolegend	Cat. No. 100469
Anti-mouse CD4 (Clone: RM4-5) e450	eBioscience	Cat. No. 48-0042-82
Anti-mouse CD44 (Clone: IM7) A700	BD Horizon	Cat. No. 560567
Anti-mouse CD69 (Clone: H1.2F3) Pe-CY5	Biolegend	Cat. No. 104509
Anti-mouse CD8 (Clone: 53-6.7) PerCPcy5.5	Biolegend	Cat. No. 100733
Anti-mouse CD95 (Clone: SA367H8) BV605	Biolegend	Cat. No. 152612
Anti-mouse GL7 (Clone: GL7) PerCP Cy5.5	Biolegend	Cat. No. 144609
Anti-mouse IFN-y (Clone: XMG1.2) APC	Biolegend	Cat. No. 505809
Anti-mouse IFN-y (Clone: XMG1.2) BV421	Biolegend	Cat. No. 505829
Anti-mouse IgD[a] (Balb/c) (Clone: 11-26c) A700	eBioscience	Cat. No. 17114033
Anti-mouse IgM (Clone: RMM-1) APCCy7	Biolegend	Cat. No. 406515
Anti-mouse IL-2 (Clone: JES6-5H4) PE	Biolegend	Cat. No. 503807
Anti-mouse TNF-a (Clone: MP6-XT22) AF488	Biolegend	Cat. No. 506315
Donkey Anti-mouse IgG AF488	Thermo Fischer Scientific	Cat. No. A21202
mAb: 2A10	Genescript	N/A

Reagent or Resource	Source	Identifier
TruStain FcX™ anti-mouse CD16/32 (Clone: 93)	Biolegend	Cat. No. 101319
Chemical, peptide, recombinant proteins, viral vector vaccines		
Ammonium chloride NH_4Cl	Sigma Aldrich	Cat. No. A-4514
AP Conjugate substrate kit	Bio-Rad	Cat. No. 1706432
BD Perm/Wash™ buffer	BD	Cat. No. 554723
Blocker™ Casein in PBS	Thermo Fischer Scientific	Cat. No. 37528
Bovine serum albumine	PAA Laboratories	Cat. No. K41-001
ChAdOx1-ME-TRAP	Jenner Institute	N/A
ChAdOx1-tPA-TRIP	Jenner Institute	N/A
ChAdOx1-TRAP(wt)	Jenner Institute	N/A
Color Prestained Protein Standard, Board Range (10-250 kDa)	New England Biolabs	Cat. No. P7719S
DAPI	Sigma Aldrich	Cat. No. 101101353
Dulbecco's modified eagle medium (DMEM)	Sigma Aldrich	Cat. No. 6546
Endotoxin free water	Sigma Aldrich	Cat. No. W3500
Fetal Calf Serum (FCS)	Sigma Aldrich	Cat. No. F-2442
Formalin, neutral buffered 10%	Sigma Aldrich	Cat. No. HT5011-1CS
Gateway® LR Clonase® II enzyme mix	Invitrogen	Cat. No. 11791-020
GeneRuler 1kb, DNA Ladder ready-to-use	Thermo Fischer Scientific	Cat. No. SM0310
Gibco PBS 10x, pH 7.4	Thermo Fisher Scientific	Cat. No. 70011044
Giemsa	Sigma Aldrich	Cat. No. GS1L
Golgi-Plug	BD	Cat. No. 555028
In Fusion® Snap Assembly Master mix with competent cells	Takara Bio	Cat. No. 638952
Kanamycin	Sigma Aldrich	Cat. No. K0254
Lipofectamine	Invitrogen	Cat. No. 11668-019
LIVE/DEAD™ Fixable Aqua Dead Cell Stain Kit	Thermo Fisher Scientific	Cat. No. L34957
MVA-ME-TRAP	Jenner Institute	N/A
MVA-tPA-TRIP	Jenner Institute	N/A
MVA-TRAP(wt)	Jenner Institute	N/A
M-PER™ Mammalian Protein Extraction	Thermo Fischer Scientific	Cat. No. 78501
Minimum Essential Medium (MEM) Eagle a-modification	Sigma Aldrich	Cat. No. M4526
Mowiol® 20-98	Sigma Aldrich	Cat. No. 11773
NuPAGE® 4-12% Bis-Tris Midi Gel	Thermo Fischer Scientific	Cat. No. WG1403BX10
NuPAGE® LDS Sample Buffer (4x)	Invitrogen	Cat. No. NP0007

Reagent or Resource	Source	Identifier
NuPAGE® MES Running buffer 20x	Thermo Fischer Scientific	Cat. No. NP0002
NuPAGE® Sample Reducing Agent (10x)	Invitrogen	Cat. No. NP0009
P. falciparum CSP 3D7 pool peptides	Mimitopes	Custom order (appendix)
P. falciparum N-interface peptide	ProImmune	Custom order
P. falciparum PF16 peptide	Mimitopes	Custom order
P. falciparum repeat $NANP_6C$-peptide	Mimitopes	Custom order
P. falciparum repeat $NANP_9C$ biotinylated peptide	Mimitopes	Custom order
P. falciparum TRAP 3D7 pool peptides	Mimitopes	Custom order (appendix)
P. falciparum TRAP T9/96 pool peptides	Mimitopes	Custom order (appendix)
Phusion® 2x Master mix with HF Buffer	New England Biolabs	Cat. No. F-351
Phusion® High-Fidelity DNA Polymerase	New England Biolabs	Cat. No. M0530L
PNPP Substrate Tablets	Thermo Fisher Scientific	Cat. No. 34047
Proteinase K	Sigma Aldrich	Cat. No. P2308
R21	Jenner Institute	N/A
R21-G1	Jenner Institute	N/A
Recombinant CSP (rCSP)	Jenner Institute	N/A
Recombinant TRAP 3D7	Jenner Institute	N/A
RPMI-1640 medoum	Sigma Aldrich	R0883
SIGMA*FAST*™ p-Nitrophenyl phosphate tablets	Sigma Aldrich	Cat No. N2770
Sodium thiocyanate solution, 8M	Sigma Aldrich	Cat. No 80518
Streptavidin AF488	Invitrogen	Cat. No. S11223
Streptavidin AF647	Invitrogen	Cat. No. S21374
Streptavidin PE	Biolegend	Cat. No. 405204
SYBR Safe in DMSO	Invitrogen	Cat. No. S33102
Trans-Blot® Turbo™ Transfer Pack	Bio-Rad Laboratories	Cat. No. 170-4158
Triton™ X-100	Sigma Aldrich	Cat. No. X100
Trpan Blue	Sigma Aldrich	Cat. No. T8154
TrypLE™ Express Enzyme (1x)	Thermo Fischer Scientific	Cat. No. 12605-010
Critical commercial assays		
Mouse IFN-γ ELISpot Kit (ALP)	Mabtech	Cat. No. 3321-2A
Qiagen EndoFree Plasmid Giga Kit	Qiagen	Cat. No. 12362
Qiagen plasmid midi kit	Qiagen	Cat. No. 12142
DNA plasmid		

Reagent or Resource	Source	Identifier
pBAC/ChAdOx1-Dest	Jenner Institute	P2563
pBAC/ChAdOx1-ME-TRAP	Jenner Institute	
pBAC/ChAdOX1-tPA.TRIP	Jenner Institute	
pENTR4/LPTOS-CSN	Jenner Institute	P2360
pENTR4/LPTOS-ME-TRAP	Jenner Institute	P2084
pENTR4/LPTOS-tPA.TRIP	Jenner Institute	P2158
pENTR4/LPTOS-tPA.TROP	Jenner Institute	P2157
pENTR4/LPTOS-TRAP	Jenner Institute	P2161
pENTR4/Mono-(tr)shark/Ii-LSA1	Jenner Institute	P4292
pENTR4/Mono-HA5-VN04	Jenner Institute	P3159
pENTR4/Mono-sharkTM/Ii-LSA1	Jenner Institute	P4295
Experimental models: Organism/Strain		
A549 cells	Jenner Institute	N/A
HeLa S3 cells	Jenner Institute	N/A
Huh-7 cells	Jenner Institute	N/A
Mouse: BALB/c JOlaHsd	Envigo	Model code 162
Mouse: C57BL/6JOlaHsd	Envigo	Model code 057
Mouse: Hsd:ICR(CD-1)	Envigo	Model code 030
Parasite: ***P. berghei*** (Pf TRAP$_{\mathbf{Pbuis4}}$ GFP::Luc$_{\mathbf{Pbeef1a}}$) sporozoites	Jenner Insectary Facility	Stock no 2281
Parasite: ***P. berghei*** (PfCS(r)PbCS +[GFP::Luc$_{\mathbf{Pbeef1a}}$]) sporozoites	Jenner Insectary Facility	Stock no 2257
Oligonucleotides (See Appendix)		
Software and algorithms		
DNASTAR Lasergene 12 Core Suite	DNASTAR	
FlowJo	FlowJo	
Gen5 Microplate reader	BioTEK	
GraphPad Prism 9	GraphPad Software	
SPICE 6	NIAID	

2.2 Resources availability

2.2.1 Viral vector vaccine

This study generated new viral vector vaccines (listed below), and the master seeds were stored in the Viral Vector Core Facility (VVCF) at the Jenner Institute.

Table 2.2 Viral vector vaccines produced in the study

Vaccines	Antigen construct
ChAdOx1 tPA-TRAP(opt)	Full-length of Pf. TRAP T9/96 strain human-codon optimised
ChAdOx1 tPA-TROP	Full-length of Pf. TRAP 3D7 strain human-codon optimised
ChAdOx1 SHIC-TRAP(wt)	Full-length of Pf. TRAP T9/96 wild-type sequence fused to transmembrane domain of shark invariant chain
ChAdOx1 SHIC-TROP	Full-length of Pf. TRAP 3D7 human-codon optimised fused to transmembrane domain of shark invariant chain
ChAdOx1 SHIC-TRIP	Truncated Pf. TRAP 3D7 human-codon optimised fused to transmembrane domain of shark invariant chain
MVA tPA-TRAP(opt)	Full-length of Pf. TRAP T9/96 strain human-codon optimised
MVA tPA-TROP	Full-length of Pf. TRAP 3D7 strain human-codon optimised
ChAdOx1 CSN	Full-length of CSP antigen with 15 NANP repeat without GPI anchor
ChAdOx1 gag::CSN	Full-length of CSP antigen with 15 NANP repeat without GPI anchor and SIVmac239 gag separated by GSG linker and P2A sequence
ChAdOx1 gag::CSN(SHIC65)	Full-length of CSP antigen with 15 NANP repeat without GPI anchor fused to transmembrane and cytoplasmic domain of shark invariant chain, and SIVmac239 gag separated by GSG linker and P2A sequence

2.2.2 Virus like particle protein

The R21 vaccine was constructed by Katherine A. Collins as described in Collins et al. [193] and was used in some experiments in this study. Additionally, The VLPs displaying junction epitope of CSP, R21-G1, were constructed, produced, and kindly provided by Ekta Mukhopadhyay and Ahmed Salman (manuscript in preparation) used in some experiments in this study.

2.3 Experimental models and subject details

2.3.1 Ethics statement

All animal procedures were conducted in compliance with the UK Animals (Scientific Procedures) Act 1986 and approved by the University of Oxford Animal Care and Ethical Review Committee under Project License P9804B4F1 (from October 2018-January 2022) and PP3331087 (From January 2022 – July 2022).

2.3.2 Mice

All C57BL/6, BABL/c and CD-1 mice were purchased from Envigo (UK). All experiments conducted in this study used female mice aged at least six weeks. The mice were kept in individually ventilated cages and maintained at the Wellcome Trust Centre for Human Genetics Functional Genetics Facility in a specific, pathogen-free environment. The mice were feed ad-libitum, and a 12:12h or 13:11h light-dark cycle conditions.

2.3.3 Parasites

Transgenic *P. berghei* parasites containing a single additional copy of *P. falciparum* TRAP 3D7 (Pf $TRAP_{Pbuis4}$ $GFP::Luc_{Pbeef1a}$) and transgenic *P. berghei* parasites containing a single replacement copy of *P. falciparum* CSP 3D7 ($PfCS(r)_{PbCS}$ +[$GFP::Luc_{Pbeef1a}$]) were provided by Jenner Insectary Facility. The parasites and *Anopheles stephensi* mosquitoes were maintained kindly by Adam Truby.

2.4 Method Details

2.4.1 Antigen construction and plasmid preparation

The tPA-TRAP(opt) and SIVmac293 pr55 gag were synthesised in the pUC19 plasmid using GeneArt Gene synthesis service. Once the plasmids were received, the antigen sequences

were inserted into the pENTR™4 plasmid downstream of long version of human CMV immediate early (CMV) promoter. In addition, the bovine growth hormone (BGH) poly(A) tail was added downstream of the antigen sequence. The ME-TRAP, TRAP(wt), tPA-TROP, tPA-TRIP, CSN antigen constructs, as well as a transmembrane and cytoplasmic (TM-CT) domain of Haemagglutinin 5 (HA5), TM-CT of Shark Invariant chain (SHIC) and thosea asigna virus 2A (T2A) sequence were available from within the Jenner plasmid repository in pENTR™4 plasmid backbone and used in this study to generated other constructs

The TRAP(opt), SHIC-TRAP(wt), SHIC-TROP, SHIC-TRIP, gag::CSN, gag::CSN(HA5), gag::CSN(SHIC65), tPA-TROP::gag::CSN(SHIC65) and gag::CSN(SHIC65)::tPA-TROP antigen constructs were generated using polymerase chain reaction (PCR) cloning using Phusion High-Fidelity PCR Master Mix with HF Buffer. Subsequently, the amplicons were ligated using NEB T4 DNA Ligase or assembled using the In-Fusion® HD Cloning Kit or NEBuilder HIFI DNA Assembly Kit into pENTR™ 4 plasmid backbone before transformed into *E. coli* Stellar™ Competent Cells followed by clone selection using Kanamycin. Following clone selection, bacterial cultures were set up using Luria-Bertani (LB) Broth media containing Kanamycin and incubated overnight at 37°C, 230 rpm. Following overnight incubation, the cultures were harvested by centrifugation at 6000 g, 4°C for 15 minutes. Subsequently, the plasmid DNA were isolated and purified using the QIAGEN Plasmid Plus Midi Kit according to the manufacturer's standard instructions. The concentration of plasmids was measured by NanoDrop Spectrophotometer, and the inserts were confirmed by restriction digest analysis. Additionally, the validity of antigen sequences pENTR™ 4 plasmids was confirmed by sanger sequencing, and the data was analysed using SeqMan pro™ from DNASTAR Lasergene 12 Core Suite. The antigen constructed or used in this study are listed below:

Table 2.3 TRAP antigen constructs produced or used in this study.

Vaccine	Detail construct				Sources
	Leading sequence	Endogenous signal	Core antigen sequence	TMD	
ME-TRAP	Multi-epitope string	Yes	T9/96 native codon	Yes	Jenner repository
TRAP(wt)	-	Yes	T9/96 native codon	Yes	Jenner repository
TRAP(opt)	-	Yes	T9/96 human codon opt.	Yes	This study
tPA-TRAP(opt)	tPA	Yes	T9/96 human codon opt.	Yes	This study
tPA-TROP	tPA	Yes	3D7 human codon opt	Yes	This study
tPA-TRIP	tPA	Yes	3D7 human codon opt	No	Jenner repository
SHIC-TRAP(wt)	Shark invariant chain (TMD)	No	T9/96 native codon	Yes	This study
SHIC-TROP	Shark invariant chain (TMD)	No	3D7 human codon opt	Yes	This study
SHIC-TRIP	Shark invariant chain (TMD)	No	3D7 human codon opt	No	This study

Table 2.2 CSN antigen constructs produced or used in this study.

Vaccine	VLP structural protein	Linker	Core antigen	TMD
CSN	-	-	Near full length CSP 3D7 (CSN)	-
gag::CSN	SIVmac239 gag	P2A	CSN	-
gag::CSN(HA5)	SIVmac239 gag	P2A	CSN	TM-CT from Haemaglutinin 5
gag::CSN(SHIC65)	SIVmac239 gag	P2A	CSN	TM-CT from Shark Ii-chain

2.4.2 ChAdOx1-BAC preparation

Bacterial artificial chromosome (BAC) containing ΔE1 and ΔE3 ChAdOx1 genome (p2563) was used as a destination vector to generate ChAdOx1 vector vaccines. The antigen constructs, including CMV promotor and BGH-poly A-tail, were cloned from the pENTR™4 entry vector by attL-attR site recombination using the Gateway®LR Clonase® II Enzyme following manufacturer protocol. After the recombination process, the BACs

were transformed into *E. coli* Stellar™ competent cells, followed by clone selection using chloramphenicol and kanamycin.

Following clone selection, the cultures were set up using LB broth containing chloramphenicol. After overnight incubation, the cells were harvested by centrifugation at 6000 g, 4 °C for 15 minutes. Subsequently, BACs were extracted using the QIAGEN Plasmid Plus Midi Kit following the manufacturer's standard instructions with some modifications. Briefly, the cells were resuspended in 10 mL of buffer P1, followed by adding 10 mL of buffer P2 and incubated for 5 minutes. After incubation, 10 mL of neutralising buffer P3 was added and preparation incubated on ice for 15 minutes. Following incubation, debris cells were separated by centrifugation at 10 000 g, 4°C for 15 minutes; subsequently, the supernatants were removed and transferred to a clean tube. Next, the DNA volume was brought down by precipitating the DNA using isopropanol, followed by centrifugation at 15 000 g, 4°C for 30 minutes. Pellets were resuspended in 5 mL of TE Buffer pH8 and buffer QBT, followed by purification by passing the BAC solution through the Qiagen-20 column using gravitational flow. After DNA was captured, the columns were washed as standard protocol, followed by DNA elution using elution buffer. The validity of antigen sequences in ChAdOx1-BAC was confirmed by sanger sequencing, and the data was analysed using SeqMan pro™ from DNASTAR Lasergene 12 Core Suite.

2.4.3 MVA-Shuttle plasmid preparation

To produce recombinant MVA vaccines, the antigens were constructed in MVA-shuttle plasmid under the p7.5 promotor. Briefly, the antigen sequences from existing plasmid, e.g. pENTR™4 entry vector, were digested using restriction enzymes Acc65I and NotI, followed by ligation into MVA-shuttle plasmid using NEB T4 DNA Ligase. Subsequently, the

plasmids were transformed into *E. coli* Stellar™ competent cells and purified using the QIAGEN Plasmid Plus Midi Kit according to the manufacturer's standard instructions.

2.4.4 Generation of ChAdOx1 vectored vaccines

The ChAdOx1-BACs containing antigen constructs were sent to the Viral Vector Core Facility (VVCF) at the Jenner Institute for vaccines production. Briefly, after linearising ChAdOx1-BAC, the BACs were transfected to T-REX™ 293 cells, followed by incubation at 37^{o}C with 5% CO_2. When the optimum cytopathic effect was observed, the Adenovirus was harvested and purified using caesium chloride gradient centrifugation. The infectious virus titre was determined by plaque immunostaining, and the PCR method was used to measure the viral particle (VP) titre.

2.4.5 Generation of MVA vectored vaccines

The MVA vector vaccines were produced by VVCF using Chick Embryo Fibroblast (CEF). Briefly, the Green Fluorescent Protein (GFP)-containing MVA shuttle plasmid was transfected into the MVA expressing Red Fluorescent Protein (RFP) infected-CEF cells. This step allows the transfer of antigen construct from the MVA shuttle plasmid to the MVA genome via homologous recombination, resulting in unstable intermediate cells expressing GFP and RFP. Subsequently, the cells were sorted using MoFlo Legacy MLS High-Speed Cell Sorter, followed by cell lysis. Next, new CEF cells were infected with the cell lysate, followed by plaque selection. Subsequently, the virus was bulked up and purified using the selected MVA plaque. The PCR method and plaque-forming titration assays were used to determine virus identity and titre, respectively.

2.4.6 Generation of DNA vaccines

The pENTR™4 entry plasmids containing relevant antigen constructs were used for DNA vaccination in several experiments in this study. The DNA vaccines were prepared using Qiagen Endo Free plasmid purification Giga Kits per the standard manufacturer's protocol. Briefly, after setting up the bacterial cultures, the cells were harvested by centrifugation at 6000g for 15 minutes at 4°C. Next, the pellet was resuspended using buffer P1, followed by cell lysis with the addition of buffer P2 and subsequently incubated at room temperature for 5 minutes. After the incubation, the mixtures were neutralised by adding buffer P3 and mixed thoroughly. The lysate was separated from the debris cell by passing the mixture into QIAfilter Giga Cartridge, followed by adding buffer ER to remove endotoxin. Subsequently, the plasmids were purified by passing the supernatant through the Qiagen tip, followed by column washing. Finally, the plasmids were eluted from the column, concentrated using isopropanol precipitation, and resuspended in endotoxin-free buffer TE.

2.4.7 Vaccine preparations

For viral vector vaccinations, the Adenovirus and MVA vector vaccines were prepared fresh from master aliquots by dilution using PBS, with working concentrations of $2x10^8$ (low dose) or $2x10^9$ (high dose) IU/mL for Adenoviral vaccine, and $2x10^9$ PFU/mL for MVA. When the viral vector vaccines were used for intravenous administration, the Adenovirus vaccines were prepared at a working concentration of $1x10^9$ IU/mL; meanwhile, the MVA vaccines were prepared at a working concentration of $1x10^8$ PFU/mL.

In addition, DNA vaccines were prepared by diluting the master aliquots using endotoxin-free PBS and endotoxin nuclease-free water to the working concentration of 1mg/mL. Meanwhile, for protein (VLPs) vaccination, the proteins were diluted from master aliquots

to a concentration of 20μg/mL; subsequently, the vaccines were formulated with Adjuvant Addavax at the ratio between the vaccine and adjuvant 1:1, resulting in a working concentration of 10μg /mL.

2.4.8 Mice immunisation

Before immunisation, mice were anaesthetised with 3.5% isoflurane carried in medical oxygen at 2L/min. The mice were immunised intramuscularly at *M. tibialis* with 50 μL of prepared vaccine, resulting in mice receiving 10^7 or 10^8 IU of Adenovirus, 10^7 PFU of MVA, 50μg of DNA or 0.5 μg of VLP vaccines. For prime-target vaccinations, after intramuscular administration, mice were immunised intravenously with 10^8 IU of Adenovirus or 10^7 PFU of MVA vaccines. Alexandra J. Spencer kindly administered the intravenous vaccination.

2.4.9 Sporozoite challenge

On the day of the sporozoite challenge, the infected mosquitoes kindly prepared previously by Adam Truby at Insectary Facility were sedated by placing a petri-dish containing mosquitoes in the fridge for 5 minutes. Subsequently, the sedated mosquitoes were put on the slide with dissection media (RPMI) and dissected, followed by the harvesting of salivary glands. After dissecting a sufficient number of mosquitoes, the salivary glands were homogenised to release the sporozoites. The number of sporozoites was counted using a haemocytometer and adjusted to the working concentration (10000 sporozoites per ml, enabling injection of 1000 sporozoites per mouse) using RPMI media. Vaccinated or naive-control mice were intravenously injected with the sporozoites and monitored for blood parasitaemia for 11-14 days. Alexandra J. Spencer and Marta Ulaszewska kindly performed the intravenous injections.

2.4.10 Serum collection

Blood was collected from mice via the lateral tail vein or cardiac puncture (terminal time point). The blood was left overnight to clot and separated from the serum by centrifugation at 13500 rpm for 4 minutes. The serum fraction was collected and transferred to the clean tube for later analysis.

2.4.11 Lymphocytes isolation

Spleen samples were collected at the end of the experiment. After cervical dislocation, the spleen was removed and processed. Single spleen cell suspensions were prepared by crushing spleens with the back of a 5ml syringe and passing the cell suspension through a 70 μm cell strainer and centrifugation at 400g for 5 minutes. The supernatant was removed and the red blood cells (RBC) were lysed by addition of ACK lysis buffer and incubation at room temperature for less than 5 minutes. PBS was added to the cell suspension to stop the lysis reaction, followed by centrifugation. Lymphocytes were resuspended in 5 mL complete α-MEM and counted using CasyCounter before being used for further analysis.

To isolate liver lymphocytes, the mouse liver was perfused immediately after cervical dislocation by injecting the PBS into the portal vein, prior to collection of the liver once separated from the gallbladder. To prepare a single cell suspension, the liver was crushed with the back of a 2ml syringe prior to passage through a 70 μm cell strainer and transfer to to a clean tube and centrifugation at 700g for 7 minutes. After removing the supernatant, the pellet was resuspended in 10 mL of 33% isotonic percoll, followed by centrifugation at 693g for 12 minutes without applying the break. The hepatocytes' debris (cell layer at top of the percoll solution) and percoll were removed, followed by resuspending the pellet in ACK

lysis buffer. The reaction was stopped by adding PBS and centrifugation at 700g for 5 minutes. Finally, lymphocytes were resuspended in complete α-MEM and counted using CasyCounter.

2.4.12 Endpoint titre ELISA

Maxisorp Nunc-Nucleon 96 flat bottom plates were coated with 2 μg/mL NANP(6) peptide and incubated overnight at 4°C. The following day, plates were washed six times with PBS/0.05% Tween and blocked with 2% BSA and incubated for 1-2 hours at room temperature. During this period, samples were prepared by diluting serum samples in 1% BSA/PBS solution. Following removal of blocking buffer; samples were loaded into relevant wells, followed by serial 1 in 3 dilutions of samples down the plate prior to incubation for 2 hours at room temperature. Subsequently, the plates were washed, and the alkaline phosphatase conjugated-anti-mouse IgG (diluted 1:3000 in 1%BSA/PBS) was added and plates incubated at room temperature for 1 hour prior to washing and addition of the development solution (pNPP substrate buffer) with well absorbance detected on an ELISA reader.

2.4.13 Single dilution, standardised ELISA

Maxisorp Nunc-Nucleon 96 flat bottom plates were coated overnight at 4ºC with either TRAP 3D7 protein (1μg/mL), CSP protein (1 μg/mL), NANP(6)C peptide (2 μg/mL), N-interface peptide (KLKQPADGNPDPNANPNVDP; at 2 μg/mL) or PF16 peptide (EPSDKHIKEYLNKIQNSLSTEWSPCSVTCGNGIQVRIKPGSANKPKDELDYANDIEK KICKMEKCS; at 2 ug/mL). A Pool of positive serum from mice vaccinated with ChAd63-MVA encoding TRAP or ChAd63-MVA encoding CSN were used on each plate to generate a standard curve in which anti-TRAP IgG or anti-CSP IgG could be quantified.

Alternatively, the monoclonal antibody mAb 2A10 or positive serum from mice vaccinated with R21 or R21-G1 were used as a standard to measure anti-NANP, anti-N-interface or anti-PF18 IgG, respectively. Following overnight incubation with coating protein, plates were washed six times with PBS/0.05% Tween and blocked by addition of casein solution and incubation for 1-2 hours at room temperature. During this incubation period, serum sample and standard were prepared by diluting in casein. Blocking solution was subsequently removed and samples (triplicate) and standard (duplicate) were added to the relevant well. In addition, several wells were loaded with casein as a background control. Plates were incubated at room temperature for two hours, prior to washing (six times with PBS-Tween) and addition of detection antibody alkaline phosphatase conjugated-anti-mouse IgG (diluted 1:3000 in casein), followed by incubation at room temperature for 1 hour. Plates were washed prior to addition of development solution, pNPP substrate buffer, and absorbance measured on an ELISA reader.

2.4.14 Avidity ELISA

A modified endpoint titre ELISA method was used to measure the avidity of antibodies induced by vaccinations. Briefly, after Maxisorp Nunc-Nucleon 96 flat bottom plates were coated with the relevant antigen, plates were blocked for 1-2 hours with Casein solution. In parallel, using the titre obtained from a standardised ELISA, serum samples were normalised and diluted to achieve 1 Elisa Unit/well then added to wells and incubated at room temperature for 2 hours. During this period, different concentrations of NaSCN from (0.5-8 M) were prepared. Following serum incubation, varying concentration of NaSCN solution were added to wells and incubated for 15 minutes at room temperature, prior to washing and addition of alkaline phosphatase conjugated-anti-mouse IgG (diluted 1:3000 in Casein) detection antibody. Following incubation at room temperature for 1 hour, plates were

washed and addition of development solution, pNPP substrate buffer, with absorbance read on an ELISA reader.

2.4.15 Inhibition of sporozoite invasion assay.

To evaluate the functionality of antibodies induced by vaccination, the Inhibition of sporozoite invasion (ISI) assay was used [209]. Briefly, 30 000 (100µl of 3 x10^5 cells/mL) Huh7 cells were seeded overnight in sterile Nunc™ Edge™ 96-Well, Flat-Bottom Microplate. The following day, infected mosquitoes were dissected to isolated transgenic Pb(PfCSP) sporozoites (spz) from the salivary glands, prior to dilution of sporozoites in RMPI media to achieve 600 000 spz/mL. In parallel, serum samples were diluted in RPMI complete media to a the final concentration of 1-2%. Following gentle removal of supernatant from Huh7 cells, 50 µL of serum was added to wells in duplicate, followed by addition of 50 µL of sporozoites solution. Control wells contained with media only, naïve serum or 1µg/mL mAb 2A10. The plates were centrifuged at 500g for 5 minutes prior to overnight incubation at 37°C. The following day, media was removed from the plates and cells were dissociated by addition of 50 µL of trypsin, followed by incubation at 37°C for 5 minutes. Cells were transferred to the cluster tube and washed using 10% FCS/PBS, followed by resuspension in 2%FCS/PBS. Immediately prior to sample acquisition on a flow cytometer, 5µL of DAPI was added to the cells .

2.4.16 *Ex-vivo* IFN-γ ELISpot assay

ELISpot plates were coated with 50 µL (5 µg/mL) of anti-IFN-γ monoclonal antibody (mAb) AN18 followed by overnight incubation at 4°C before use. The following day, the plates were blocked by addition of complete α-MEM for at least 1 hour. Following lymphocyte isolation, 50 µL of lymphocytes at concentration 1 x 10^7 cells/mL were seeded

and titrated two-fold and cells stimulated by addition of relevant peptide at a final concentration 1 μg/mL (or media as negative control) and incubated at 37°C for 16-18 hours. Following overnight incubation, cells were removed by washing plates with PBS prior to addition of IFN-γ detection antibody, rat anti-mouse IFN-γ (1 μg/mL). Following incubation for 2 hours at RT, plates were washed 6 times with PBS, followed by adding Streptavidin Alkaline Phosphatase Polymer (1μg/ml) and incubation at room temperature for 1 hour. Plates were washed prior to addition of development solution, alkaline phosphatase (AP) conjugate development buffer for 5-10 until spots were visible. The plates were washed and dried overnight before being counted using the ELISpot plate counter.

2.4.17 Intracellular cytokines staining

Following lymphocyte isolation, 150 μL of cells were seeded to the U bottom 96 well plate and stimulated for 6 hours with relevant peptides at a final concentration of 1 μg/mL (or media as an unstimulation control) together with addition of 1 μg/mL BD GolgiPlug™. Cells were stained for surface molecules by addition of an antibody cocktails containing anti-CD4-e450 (1:200), anti-CD8-PerCP-Cy5.5 (1:100), and LIVE/DEAD® (1:200) Fixable Aqua Dead Cell Stain Kit and incubated at 4°C for 30 minutes. Following centrifugation (for 3 minutes at 800g) and supernatant removal, cells were fixed by addition of 100 μL Neutral buffered formalin for 5 minutes at 4°C, followed by adding 100 μL of BD Perm/Wash™ buffer (Becton Dickinson). Subsequently, intracellular cytokines were stained by antibody cocktails containing anti-IFNγ-Alexa647 (1:100), anti-TNFα-Alexa488 (1:100) and anti-IL2-PE (1:100) and incubation for 30 minutes at 4°C. Cells were washed two times using BD Perm/Wash™ buffer and then resuspended in 1%BSA/PBS for sample acquisition on a BD Fortessa. The data were analysed using FlowJo software, and the gating strategies used in the experiment are shown below (Figure 2.1).

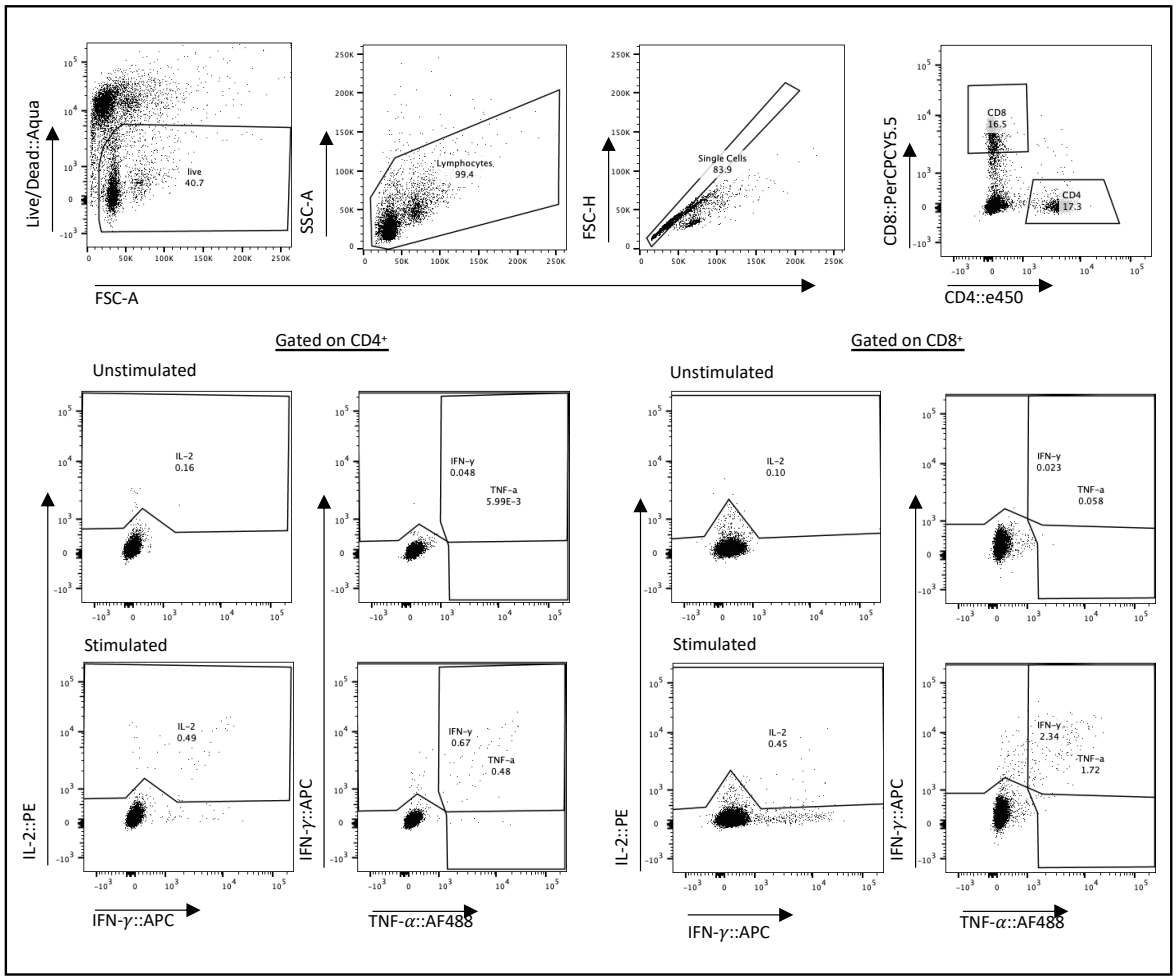


Figure 2.1 Intracellular cytokines staining gating strategy.

After gating on live cells, lymphocytes and single cells, cells were stratified based on CD4 and CD8 T-cell marker expression. Subsequently, within $CD4^+$ and $CD8^+$ T-cell populations, cells were gating based on the expression of IFN-γ, TNF-α and IL-2 cytokines. In addition, the representative of stimulated and unstimulated samples are presented.

2.4.18 Identification of liver-tissue resident memory

Similar to the ICS assays, lymphocytes isolated from the liver and spleen (for comparison) were seeded into the U bottom 96 well plates and stimulated for 5 hours with relevant peptide at a final concentration of 1 µg/mL in the presence of 1 µg/mL BD GolgiPlug. Following stimulation, surface molecules were stained by addition of an antibody cocktail containing Live-Dead Aqua (1:200), CD3-UV496 (1:200), CD4-BV650 (1:100), CD8-PerCPCy5.5 (1:100), CD69-PECy5 (1:100), CD11a-PECy7 (1:100), CD44-A700 (1:100), CXCR6-

BV711 (1:100), CXCR3-APC (1:100), and PD1-BV605 (1:100) prior to fixation with 100 μL Neutral buffered formalin for 5 minutes at 4°C. Cells were stained for cytokine expression using an antibody cocktail containing IFN-γ- BV421 (1:100), TNF-α-AF488 (1:100) and IL-2-PE (1:100). Cells were washed and transferred to clean cluster tubes before acquisition on the flow cytometer.

2.4.19 Identification of Antigen-specific B-cells.

To detect the presence of NANP-specific B-cells in the spleen, double NANP(9)C tetramer were used. The tetramers were prepared in house by mixing biotinylated NANP(9)C peptide with streptavidin conjugated-AF488 or AF647 in a 4:1 molar ratio and incubation on ice for at least 30 minutes before use. 200 μL of isolated lymphocytes were seeded to the U bottom 96 well plate and washed with 200 μL of PBS/BSA. Next, the cells were stained with Live-Dead Aqua (1:200) and Fc block (anti-CD16/32 mAb, 1:50) for 30 minutes. Cells were washed (addition of PBS-BSA, centrifugation and removal of supernatant) and stained with an antibody cocktail containing tetramer NANP(9)C-AF488 (0.4mM), tetramer NANP(9)C-F467 (0.4mM), tetramer, GL7-PerCPCy5.5 (1:100), CD138-BV421 (1:100), IgM-APCCy7 (1:100), CD19-PEDazzle (1:200), IgD-A700 (1:100), CD38-PECy5 (1:200), CD45R-PECy7 (1:200), CD3 BUV496 (1:200), and CD95-BV605 (1:100) and incubation for 30 minutes at 4°C. Unbound antibody was removed by washing (as above) prior to samples being transferred to the clean cluster tube prior for sample acquisition on a flow cytometer.

2.4.20 Indirect Immunofluorescent (IFA) Assay

The human adenocarcinoma epithelial cell line (A549) was used to measure antigen expression analysis using an Indirect Immunofluorescence Assay (IFA). Sterile coverslips were placed in the sterile 24-well Nunc™ Cell-Culture Multidishes, and subsequently, 1 mL

of cells with density $1x10^5$ cells/mL were seeded into the wells, followed by incubation overnight at 37°C with 5%CO_2. The following day, plasmids encoding antigen construct were diluted in OPTI-MEM media. Following overnight incubation of cells to enable adherence to coverslips, media was removed from the well and cells washed by addition of sterile PBS twice prior to transfection of cells with 800ng of plasmid DNA diluted in lipofectamine 2000 with the ratio between plasmid and lipofectamine 1:2. The cells were incubated for 48-72 hours at 37°C with 5%CO_2. Following the incubation, the cells were fixed with 4% paraformaldehyde and incubated for 30 minutes, followed by adding 50 mM NH_4CL diluted in PBS for 5 minutes. Subsequently, the cells were permeabilised by adding 0.2% Triton for 5 minutes. Next, the cells were blocked with 15% of goat serum before being labelled with primary antibodies using serum-vaccinated mice or monoclonal antibodies. The binding was detected by adding Alexa Fluor 488 (AF488) conjugated donkey-anti-mouse IgG for 30 minutes. Finally, the cells were washed and air dried. Immediately before microscope analysis, the coverslips were mounted on the microscope slides using Mowiol media containing 1μg/ml DAPI.

2.4.21 Identification of antigen expression on the cell surface

Hela S3 cells ($4x10^5$ cells/well) were seeded into 6-well Nunc™ Cell-Culture Multidishes and incubated overnight at 37°C with 5% CO_2. Cells were infected by addition of ChAdOx1 vector vaccines, encoding different constructs of CSP, at a MOI of 10 and incubated for 48-72 hours. After incubation, cells were dissociated by addition of 500 μL of trypsin for 5 minutes prior to washing with 10% FCS/PBS twice, pelleted by centrifugation at 500g for 5 minutes and resuspended in PBS/BSA 0.5%. Cells were split into three groups of alternative staining, the mAb 2A10 (1 μg/mL), sera from mice vaccinated with ChAd63-MVA encoding CSN (1:50) or R21 (1:100) and incubated at room temperature for 2 hours.

Following incubation, cells were washed three times with 0.5% of BSA/PBS prior to detection by addition of AF488 conjugated Goat-anti-mouse IgG for 1 hour at room temperature. Cells were washed three times and resuspended in 0.5% of BSA/PBS before the level of antibody binding was measured by flow cytometry. As a control, cells infected with a ChAdOx1 encoding an irrelevant antigen, tPA-TROP, or left uninfected were used for comparison.

2.4.22 SDS and Western Blot Assay

Protein samples were mixed with 4x LDS loading buffer with/without reducing agent. For reduced conditions, the mixtures were boiled at 95°C for 10 minutes. The samples were loaded into NUPAGE™ 12% Bis-Tris Protein Gels and run in a 1x MES buffer for 50 minutes at 200 Volt. The gel was stained using Coomassie staining until the bands were developed. For Western Blot analysis, the gel was transferred onto the Trans-Blot® Turbo™ Nitrocellulose membrane using Trans-Blot® Turbo™ Transfer System for 7 minutes. The membrane, subsequently, was blocked with 3% BSA/PBS or Casein for 1 hour at RT, then stained with primary antibody either from mice-vaccinated serum or mAbs. Subsequently, the binding was detected by adding alkaline phosphatase conjugated-antibody anti-mouse and developed by the addition of SIGMAFAST™ p-Nitrophenyl phosphate.

2.4.23 Statistical analysis

Statistical analyses were performed in GraphPad Prism. To compare the data between two groups, a non-parametric Mann-Whitney rank test was used. Meanwhile, a non-parametric One-way ANOVA (Kruskall-Wallis) test followed by Dunn's multiple comparison post-hoc test or two-way ANOVA with Tukey multiple comparison post-hoc test was used to compare the difference between more than two groups. Spearman correlation analysis was

used to analyse the correlation between variables. In addition, efficacy data were presented in the Kaplan-Meier survival graphs. The survival curves were compared by Log-rank (Manter-Cox) with Bonferroni correction.

3

Optimisation of viral vectors encoding *P. falciparum* TRAP antigen: Impact of human-codon optimisation and strain selection on the immunogenicity and efficacy against liver-stage malaria

3.1 Introduction

The thrombospondin-related adhesion protein, TRAP, was first identified in 1988 from *P. falciparum* T9/96 haplotype [200], a laboratory clone derived from a clinical isolate in Thailand [210]. Initially, TRAP was thought to be expressed only in the erythrocytic stage [211]. However, the protein was later found predominantly expressed in microneme inside sporozoites [212, 213]. TRAP is necessary for gliding motility, active during cell traversal and hepatocyte invasion [212, 214]. Since identification, the protein has been targeted as a liver-stage malaria antigen and extensively evaluated using various platforms and vaccination regimens in pre-clinical and clinical settings [101, 128, 129, 203, 204, 206, 215-226].

To date, *Pf.* TRAP vaccines administered in heterologous prime-boost regimen, using chimpanzee Adenovirus 63 (ChAd63) and Modified Vaccinia Ankara (MVA) viral vector with an eight week interval, is the most clinically advanced liver-stage malaria vaccine candidate. The vaccine construct contains a core antigen of full-length *Pf.* TRAP T9/96 fused to the multiple-epitope (ME) string. The ME string consists of 14 *P. falciparum* $CD8^+$ T-cell restricted epitopes covering human HLA B35, B53, B7, B8, A2.1, A2.2, B17 and

B58 derived from a number of pre-erythrocytic malaria proteins; Liver-stage antigen 1 (LSA-1), TRAP, Circumsporozoite protein (CSP), and Sporozoite Threonine and Asparagine Rich Protein (STARP). Additionally, three CD4 universal epitopes from *Pf.* CSP, BCG and tetanus toxoid; a Heparin-binding motif of *Pf.* TRAP T9/96 and a mouse H-2^d restricted immunodominant P9 epitope from *P. berghei* CSP [206, 217, 227] were also included into antigen cassettes. These targeted HLAs are found in most Caucasian and African individuals. Additionally, most of these epitopes are conserved across *P. falciparum* strains. These epitopes were included to support induction of effective immune responses against most *P. falciparum* strains. ChAd63-MVA regimen induces exceptionally high T-cell responses in murine models, human malaria naïve, semi-immune adults [101, 128, 204], and Gambian and Burkinabe children, albeit the response in Burkinabe is lower than detected in Gambian children [226].

In terms of efficacy, the vaccine conferred partial protection against infection in malaria naïve adults in Controlled-Human Malaria Infection (CHMI) studies when the *P. falciparum* sporozoites 3D7 haplotype was used as the challenge parasite. Protection positively correlated with a high frequency of TRAP-specific IFN-γ^+ $CD8^+$ T-cells [204]. From the field study, the vaccine was also shown to partially protect semi-immune Kenyan adults during a malaria transmission season [228]. However, sterile protection was not observed in Senegalese adults and Burkinabe children [203, 225], which was likely associated with lower TRAP-specific T-cells responses observed in these populations. While many factors could contribute to reductions in vaccine induced immunogenicity, e.g. previous exposure to malaria, nutrition status and endemic status [229-232], intrinsic elements of vaccine construct, e.g. sequence optimisation and source of antigen haplotype, are worth considering when trying to optimise vaccine immunogenicity and efficacy. The choice of TRAP protein

as a liver-stage antigen remains a debate. Indeed, many endeavours have been made to identify other liver-stage antigens [233-235]. Nevertheless, to our knowledge, no other identified liver-stage antigen has shown comparable or higher levels of immunogenicity and efficacy. Moreover, efficacy data that showed partial protection in exposed Kenyan adults indicated the potential of ME-TRAP to prevent against liver-stage malaria infections in endemic countries.

In parallel with assessment of other liver-stage antigens in our group, this study has focused on improving the immunogenicity and efficacy of TRAP-encoded viral vector vaccines. Using two murine models, C57BL/6 and CD-1 mice, four strategies were investigated: 1. Implementing human-codon optimised technique on the TRAP sequence; 2. Investigate *Pf.* TRAP 3D7 haplotype as the core antigen and compared with *Pf.* TRAP T9/96 strain; 3. Addition of molecular adjuvant; 4. Induction of TRAP-specific $CD8^+$ tissue-resident memory using optimised TRAP-encoded viral vector vaccines. Unlike previous preclinical studies, vaccines were not tested in BALB/c mice, as the $H\text{-}2^d$ restricted immunodominant Pb9 epitope contained in the ME sequence could hinder the evaluation of the core antigen in the ME-TRAP construct [216].

3.2 Implementing human-codon optimised technique on TRAP sequences.

Since the first construction of the ME-TRAP antigen, delivered either in DNA or viral vector vaccines [206, 217, 232], the sequence of the core antigen, TRAP, but not the ME, has been encoded using the native codons of *P. falciparum* T9/96. The advancement of biotechnology in the early 2000s has enabled us to maximise protein expression in a heterologous host by implementing codon-optimisation of the coding sequence. Codon optimisation is a genetic engineering approach to synonymously change the codon assignment from rare to the most

frequently used codons in a target host species. This technique increases the translation rate and led to a higher yield of protein [236]. In recent years, this approach has been widely used for either *in-vitro* expression for recombinant protein production or *in vivo*, such as in gene therapy and vaccinations [237-245]. Unfortunately, this technique was not widely used at the time of original ME-TRAP construction.

In regard to vaccination, human/mammalian codon optimisation in DNA, RNA or viral vector vaccines has been shown to improve immunogenicity against antigens from Malaria, *Mycobacterium tuberculosis*, Influenza, Respiratory Syncytial Virus (RSV), and Human Immunodeficiency Virus (HIV)[239, 242, 243, 245]. However, the codon optimisation strategy is only sometimes beneficial. For instance, in HPV therapeutic vaccines, the human codon-optimised E7 oncogene revealed the cryptic epitope that reduced the recognition of immune response to the native protein, reducing the efficacy of the treatment [241]. Another study has shown that optimising the coding sequence of CelTOS, another pre-erythrocytic antigen, led to amino acid misincorporation and abruptly changed the secondary structure when the protein was expressed in *Escherichia coli*, resulting in poor antibody responses when the proteins were used for vaccinations [246]. This indicates that codon-optimisation benefits could be antigen and purpose specific.

In the context of malaria vaccines, it is widely known that the genome composition of *P. falciparum* contains exceptionally high Adenosin and Thymine (AT) content and is different in the frequency of codon usage compared with humans [238]. Consequently, it is possible that the expression of malaria antigens, such as TRAP, encoded with native codons in DNA or viral vector vaccines could be sub-optimal. The work described in this section aimed to determine the impact of codon optimisation on the immunogenicity of *Pf.* TRAP T9/96.

Results:

3.2.1 Human codon-optimised TRAP induced higher T-cells responses than the TRAP native sequence vaccine.

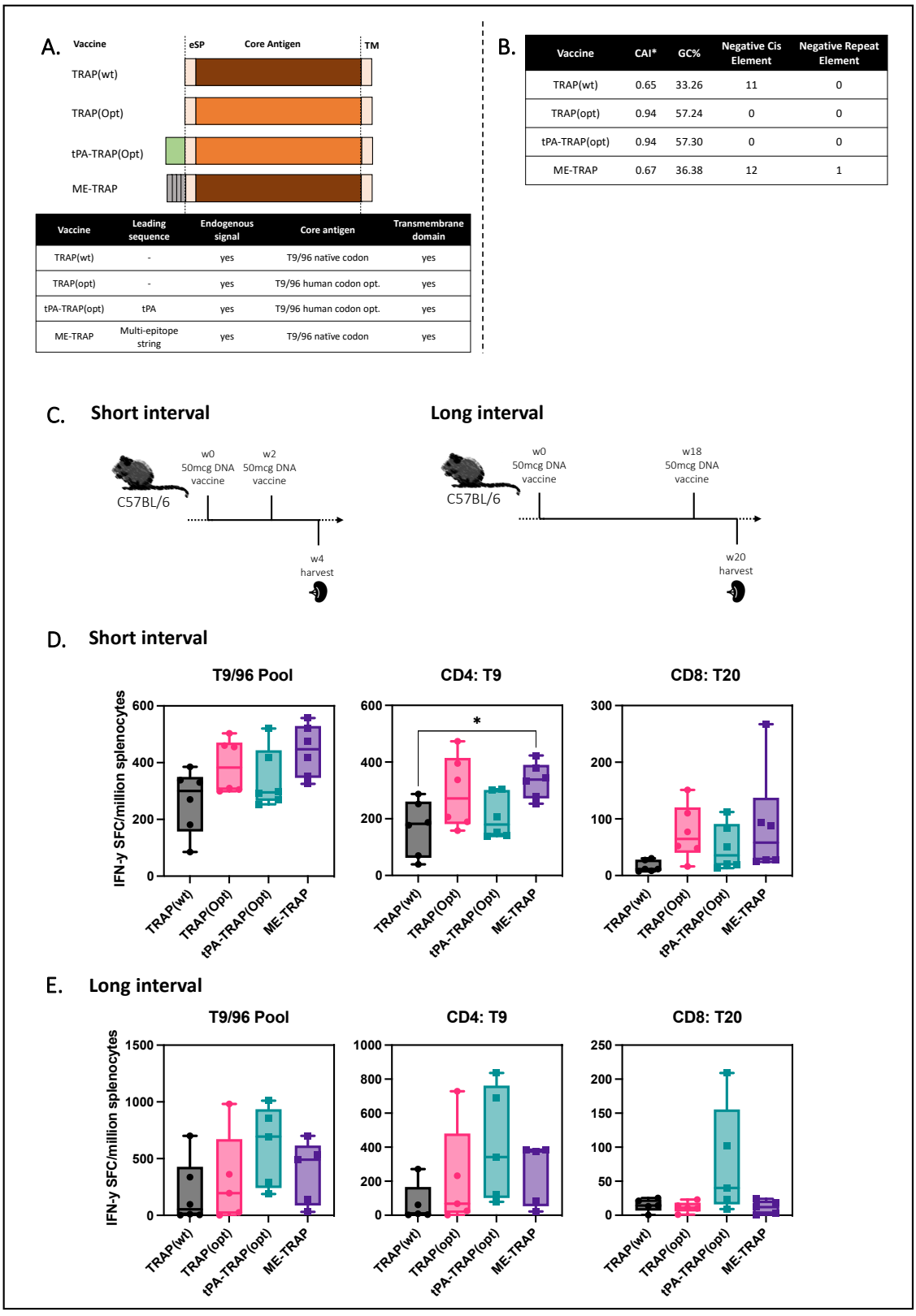
Four DNA vaccines were produced using a pENTR4^{TM} plasmid backbone with antigen insert based on *Pf.* TRAP T9/96, as illustrated in Figure 3.1A. The first construct encoded *Pf.* TRAP T9/96 in native sequence and denoted as TRAP(wt). The second construct, TRAP(opt), is a human-codon optimised version of TRAP T9/96. The third one was similar to the second but was fused to the signal peptide of human tissue plasminogen activator (tPA); which has been shown to improve the expression and immunogenicity in DNA and viral vectored vaccines [247-249]. The last vaccine, ME-TRAP, was used as a benchmark. All constructs had Kozak's sequence for expression in mammalian cells, expression was controlled by a CMV long-sequence promotor (LPTOS) and all constructs were tailed with BGH Poly-A.

Rare codon analysis revealed that without human-codon optimisation, lower codon adaptation index (CAI) and GC% content were found in TRAP(wt) and ME-TRAP compared to TRAP(opt) or tPA-TRAP(opt). Also higher negative cis element content was present in native TRAP sequences (Figure 3.1 B). To determine whether codon optimisation could improve the immunogenicity of TRAP, six-week-old C57BL/6 mice, six per group, were primed with 50 μg of each DNA vaccine and boosted two weeks later with the corresponding vaccine; alternatively, mice were boosted with a longer 18 week interval. Mice were sacrificed two weeks after the last vaccination, and spleens harvested and processed for *ex-vivo* IFN-γ T-cells ELISpot assays. Splenocytes were stimulated with three different conditions: a pool of 20 mer peptides representing a full length of TRAP T996

sequence (T9/96 pool), a single peptide T9 or T20 containing either a $CD4^+$ or $CD8^+$ T cell restricted epitope in H-2^b mice (Figure 3.1 C)[127].

Following short-interval vaccination, a nonsignificant lower total T-cell responses against T9/96 pool in mice vaccinated with TRAP(wt) were observed compared to TRAP(opt) or ME-TRAP vaccination groups. Interestingly, vaccination with TRAP(wt) or tPA-TRAP(opt) induced a comparable T-cell response against T9/96 pool. When a T9 peptide was used for stimulation, significant ($p<0.05$) lower $CD4^+$ T-cell responses were observed in TRAP(wt) compared with ME-TRAP. Meanwhile, comparable $CD4^+$ T-cell responses were observed in mice vaccinated with TRAP(opt) and ME-TRAP. Additionally, comparable $CD8^+$ T-cell responses were induced after stimulation with T20 peptide in TRAP(opt), tPA-TRAP(opt) and ME-TRAP vaccination groups. While vaccination with TRAP(wt) induced lower $CD8^+$ T-cell responses compared to other vaccination groups, albeit this was not statistically significant (Figure 3.1D)

When the interval between vaccinations was increased to 18 weeks, tPA-TRAP(opt) induced higher total T-cell responses against T9/96 pool compared to all other vaccination groups, albeit this was not statistically significant. Meanwhile, mice vaccinated with the TRAP(wt) vaccine elicited the lowest total T-cell response against T9/96 pool. Non-significant higher $CD4^+$ and $CD8^+$ T-cell responses were also observed in mice vaccinated with tPA-TRAP (opt) after stimulation with T9 or T20 peptides compared to TRAP(wt), TROP(opt) or ME-TRAP group (Figure 3.1 E).



Vaccine	Leading sequence	Endogenous signal	Core antigen	Transmembrane domain
TRAP(wt)	-	yes	T9/96 native codon	yes
TRAP(opt)	-	yes	T9/96 human codon opt.	yes
tPA-TRAP(opt)	tPA	yes	T9/96 human codon opt.	yes
ME-TRAP	Multi-epitope string	yes	T9/96 native codon	yes

Vaccine	CAI*	GC%	Negative Cis Element	Negative Repeat Element
TRAP(wt)	0.65	33.26	11	0
TRAP(opt)	0.94	57.24	0	0
tPA-TRAP(opt)	0.94	57.30	0	0
ME-TRAP	0.67	36.38	12	1

Figure 3.1 Immunogenicity of DNA vaccines measured by ex-vivo IFN-γ ELISpot assay.

A. Four different DNA vaccines were constructed based on Pf. TRAP T9/96 antigen, namely TRAP(wt), TRAP(opt), tPA-TRAP opt and ME-TRAP. **B.** Experimental design to evaluate the impact of codon optimisation on TRAP antigen immunogenicity. **C.** Box and whisker plot of T-cell responses from mice vaccinated in short or **D.** long intervals. Splenocytes were stimulated with a T9/96 pool, a pool of peptides spanning the entire length of the antigen (left), and a single peptide, T9 or T20, containing a CD4 or CD8 T-

cell restricted epitope in C57BL/6 mice. Single points indicates the response from individual mice. Data in each graph was analysed with Kruskal-Wallis's test followed by Dunn's multiple comparison tests to compare the difference between vaccination groups. The data presented were representative of a single study. Asterisks indicate significant differences (* indicates $p<0.05$).

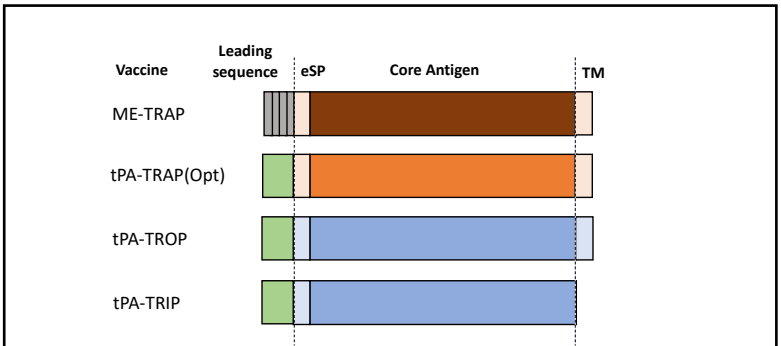
3.3 Head-to-head comparison of Adenoviral and MVA vaccines encoding *Pf.* TRAP T9/96 or 3D7 strain.

P. falciparum 3D7 strain is a laboratory clone derived from *P. falciparum* NF54, a clinical isolate from a malaria case in the Netherlands [250]. This malaria case was considered an imported case, as the patient never left the country. Although the origin of the isolate remains unknown, genomic characterisation data demonstrated that *P. falciparum* 3D7 is of African origin [251]. In addition, the strain is sensitive to chloroquine. Therefore, sporozoites from the 3D7 haplotype are used as a challenge parasite in the CHMI studies [132]. As more than 95% of malaria's global burden of disease is concentrated in sub-Saharan Africa, whole sporozoite vaccines have been developed based on the *P. falciparum* NF54 strain. Additionally, many subunits of malaria vaccines in clinical development, for instance, RTS,S, R21, AMA1, Rh5, and Pfs25, have been designed using antigen sequences from the *P. falciparum* 3D7 haplotype [122, 193, 252].

Data from whole sporozoite vaccination regimens have demonstrated that these approaches can provide 100% short-term and long-term protection after homologous challenge with *P. falciparum* 3D7 sporozoites [78]. However, efficacy was reduced significantly when volunteers were challenged with a heterologous strain [208, 253, 254]. This indicated that matching the strain in the vaccine construct with the strain circulating in the targeted region would likely improve vaccine mediated protection. In regard to the ME-TRAP vaccine, the core antigen was constructed based on the *P. falciparum* T9/96, a parasite strain that differs in geographic prevalence from the 3D7 strain. It has been shown that TRAP is a polymorphic

protein, albeit to less extent than another pre-erythrocytic antigen such as CSP. The difference in amino acid sequence between *Pf.* TRAP T9/96 and 3D7 is around 6.1%. In addition, polymorphism and phylogenetic network analysis showed that the 3D7 strain and other African-origin *P. falciparum* were positioned in a different cluster with TRAP T9/96 strain [207]. Therefore, the protection afforded by this vaccine against challenges with the 3D7 strain was considered heterologous protection.

During clinical development, the immunogenicity of ME-TAP has been measured toward both TRAP T9/96 and 3D7. The data showed that ME-TRAP induced cross-reactive responses to TRAP 3D7 [206], albeit lower in frequency compared to the homologous peptide. Nevertheless, the immunogenicity of viral vector encoded *Pf.* TRAP 3D7 strain has never been compared to ME-TRAP, nor has protection against a homologous challenge been investigated. Therefore, a head-to-head comparison of viral vectors encoded *Pf.* TRAP antigen from T9/96 and 3D7 haplotype was performed in this study. Adenoviral (ChAdOx1) [255] and MVA vectors expressing different antigens inserts based on *Pf.* TRAP from T9/96 and 3D7 haplotypes were generated (Figure 3.2). The original T9/96 ME-TRAP was used as a benchmark, given it has progressed through to Phase II clinical testing. The second construct, tPA-TRAP (opt), was generated based on the previous experiment. The third insert, tPA-TROP, was constructed based on the full-length TRAP 3D7, fused to the tPA leading sequence and human-codon optimised as this strategy has been shown, previously, to induce higher T-cell responses compared to TRAP in the native sequence. The fourth construct is similar to the third but with the truncation on the transmembrane and cytoplasmic (CT-TM) domain; as it was hypothesised that removing the CT-TM of the TRAP protein may increase the secretion of the antigen, allowing improved antigen uptake by antigen-presenting cells.



Vaccine	Leading sequence	Endogenous signal	Core antigen	Transmembrane domain
ME-TRAP	Multie-pitope string	yes	T9/96 native codon	yes
tPA-TRAP(opt)	tPA	yes	T9/96 human codon opt.	yes
tPA-TROP	tPA	yes	3D7 human codon opt.	yes
tPA-TRIP	tPA	yes	3D7 human codon opt.	no

Figure 3.2 Antigen insert in ChAdOx1 and MVA vectors.

Four different versions of the transgene were designed based on the TRAP sequence from *P. falciparum* T9/96 and 3D7 strain. The ME-TRAP contains wild-type TRAP T9/96 fused sequence to the human-codon optimised multi-epitope (ME) string. The second construct, tPA-TRAP (opt), is a human-codon optimised TRAP T9/96 with a tPA-leading sequence. The third one, tPA-TROP, is similar to tPA-TRAP(opt) but encodes TRAP 3D7 haplotype. The fourth transgene is 3D7 TRAP but truncated to remove the transmembrane and cytoplasmic domain.

Results:

3.3.1 Immunogenicity following single-dose ChAdOx1 vaccinations.

To compare the immunogenicity of each transgene after a single dose of ChAdOx1, six 6-week-old C57BL/6 or CD-1 mice per group were vaccinated with 10^7 or 10^8 infectious units (IU) of ChAdOx1 expressing each antigen. The mice were sacrificed 14 days later, representing the peak point after vaccination with adenoviral vectors (Figure 3.3A) [127]. Spleens were harvested, processed, and stimulated with TRAP T9/96, TRAP 3D7 or a common pool consisting of peptides with identical sequences in both TRAP T9/96 and 3D and responses were measured by *ex-vivo* IFN- γ ELISpot assay. Splenocytes from C57BL/6 mice were also stimulated with single peptides T9/TD9 and T20 that contain the $CD4^+$ and

$CD8^+$ T cell restricted epitope in H-2^b mice. Unlike peptide T20, which is identical between the two strains, the peptides that contain $CD4^+$ T cell epitope differ between T9/96 and 3D7 strain and are denoted as T9 and TD9.

Following single dose ChAdOx1 vaccination of CD-1 mice, total T-cell responses induced by tPA-TRAP(opt) and tPA-TROP were comparable across peptides pool and significantly ($p<0.05$) higher than mice vaccinated with ME-TRAP when cells were stimulated with common peptides. A significantly higher ($p<0.01$) T-cell response was also observed in tPA-TRAP(opt) compared to tPA-TRIP following T9/96 peptide pool stimulation. Conversely, ME-TRAP induced significantly lower ($p<0.01$) IFN-γ responses against the 3D7 pool compared with tPA-TROP. Interestingly a nonsignificant lower total T-cell responses against T9/96 pool were observed in ME-TRAP compared to tPA-TRAP(opt).

Meanwhile, in C57BL/6 mice, the total T-cell responses against T9/96 pool in ME-TRAP and tPA-TRAP (opt) were significantly higher ($p<0.05$) compared to tPA-TRIP. However, T-cell responses against T9/96 pool, induced by ME-TRAP or tPA-TRAP(opt) vaccines, were comparable to mice vaccinated with tPA-TROP. Conversely, significantly higher ($p<0.01$) total T-cell responses against 3D7 pool were observed in mice immunised with tPA-TROP or tPA-TRIP immunisation compared to mice receiving ME-TRAP. In addition, lower but nonsignificant total T-cell responses against the 3D7 pool were induced after vaccination with tPA-TRAP(opt) compared to tPA-TROP or tPA-TRIP vaccines. Interestingly, when the common pool was used for stimulation, the responses were higher in tPA-TROP, with a significant difference ($p<0.05$) observed compared to ME-TRAP.

Stimulation with individual T9 or TD9 peptides clearly distinguished the responses between vaccine strains in C57BL/6 mice after a single dose of ChAdOx1. We observed that the ME-

TRAP elicited significantly higher $CD4^+$ T-cell responses ($p<0.01$) compared to tPA-TROP and tPA-TRIP when T9 peptide was used for stimulation. Meanwhile, comparable $CD4^+$ T-cell responses after T9 peptide stimulation were observed in mice receiving ME-TRAP or tPA-TRAP (opt). In contrast, when the splenocytes were stimulated with TD9 peptide, the tPA-TRAP(opt) vaccine induced significantly ($p<0.01$) lower $CD4^+$ T-cell responses compared to tPA-TROP or tPA-TRIP. Meanwhile, lower (non-significant) $CD4^+$ T-cell responses were observed in mice vaccinated with ME-TRAP compared to tPA-TROP and tPA-TRIP after stimulation with TD9 peptide. Interestingly, tPA-TROP elicited significantly higher ($p<0.05$) $CD8^+$ T-cells responses after stimulation with T-20 peptide compared to ME-TRAP or tPA-TRAP(opt). Higher $CD8^+$ T-cell responses were also observed in mice immunised with tPA-TRIP compared to ME-TRAP or tPA-TRAP(opt), albeit this was not statistically significant. Meanwhile, comparable $CD8^+$ T-cell responses were produced by tPA-TROP and tPA-TRIP vaccines. (Figure 3.3 C).

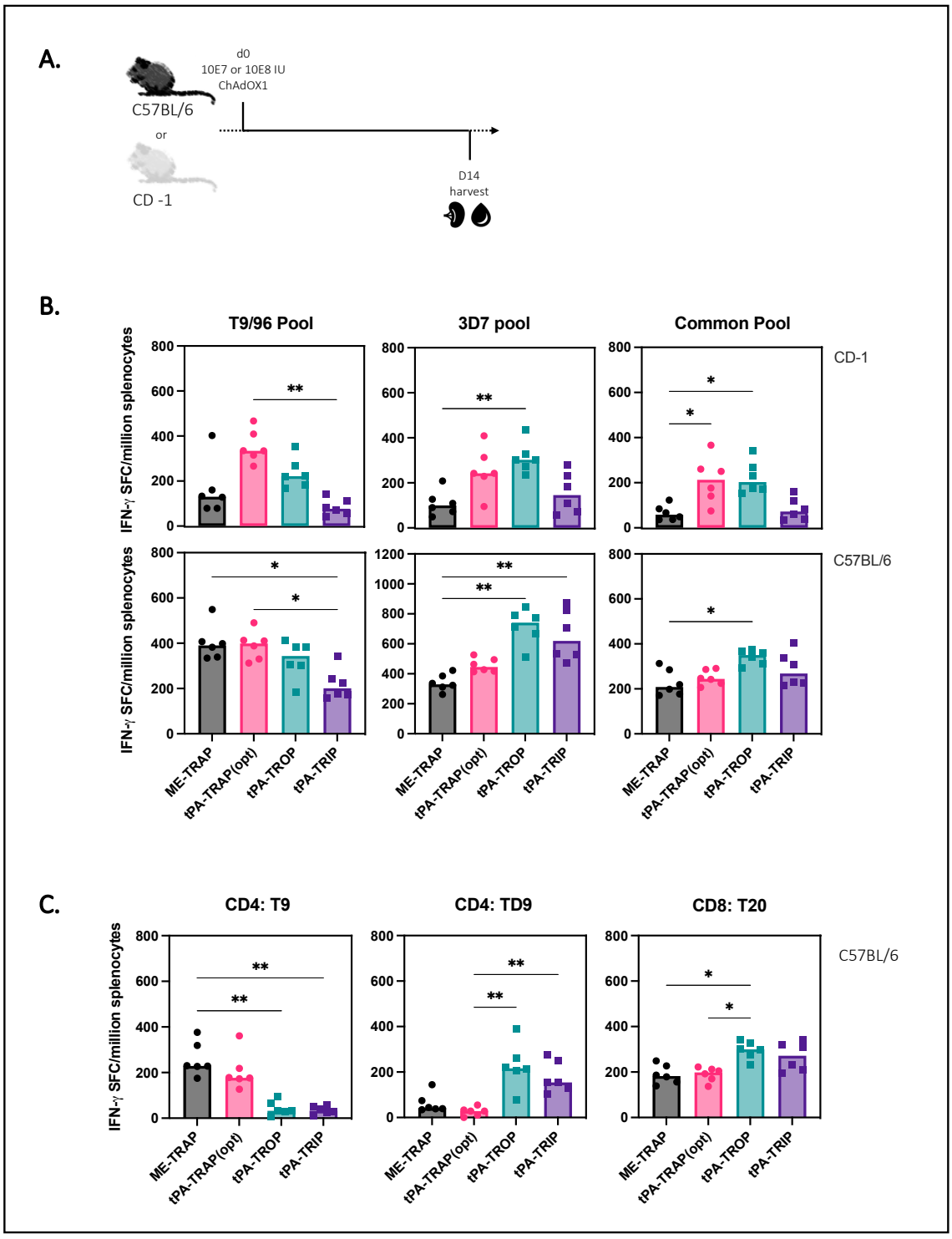


Figure 3.3 T-cell responses induced by a single dose ChAdOx1 vaccine.

A. Inbred and outbred mice were vaccinated with 10^7 (C57BL/6) or 10^8 IU (CD1) of ChAdOx1, encoding different versions of TRAP antigen. Two weeks later, mice were sacrificed, and spleens and blood harvested. T-cell responses were measured by *ex-vivo* IFN-γ ELISpot assay following stimulation with **B.** T9/96, 3D7 and a common peptide pool to measure total T cell responses. **C**. Splenocytes from C57BL/6 mice were also stimulated with individual peptides, T9, TD9 and T20, that contain $CD4^+$ and $CD8^+$ T cell restricted epitope in H-2^b mice. The bar represents each group's median (SFC/million splenocytes), and each mouse represented

by a single point. Data in each graph was analysed with Kruskal-Wallis's test followed by Dunn's multiple comparison test to compare the difference between vaccination groups. The data presented were representative of a single study. Asterisks indicate significant differences (*=$p<0.05$, **=$p<0.01$).

To evaluate the functional capacity of $CD4^+$ and $CD8^+$ T-cells after a single dose of ChAdOx1 vaccine, splenocytes were stimulated with either T9/96 or 3D7 pool and the production of cytokines measured by intracellular cytokine staining (ICS). In CD-1 mice, the levels of $CD4^+$ T-Cell producing IFN-γ, TNF-α or IL-2 were higher in mice vaccinated with tPA-TRAP (opt) or tPA-TROP compared to ME-TRAP or tPA-TRIP after stimulation with the T9/96 or 3D7 pool. Although the previous study showed that responses against the transmembrane domain of TRAP were minimal, we observed a significantly lower ($p<0.01$) frequency of $CD4^+$ T-cells expressing TNF-α or IL-2 in mice vaccinated with tPA-TRIP compared to tPA-TROP after stimulation with 3D7 peptide pool. Additionally, tPA-TROP induced significantly higher frequencies of TNF-α^+ or IL-2^+ $CD4^+$ T-cell responses compared to ME-TRAP following stimulation with 3D7 peptides. In C57BL/6 mice, the frequency of $CD4^+$ T-cells producing IFN-γ, TNF-α or IL-2 was significantly higher when splenocytes were stimulated with a pool of peptides that matched the vaccine strain. Consistent with ELISpot data against single peptide T9 or TD9, $CD4^+$ T-cells responses were shown to be more strain-specific in C57BL/6 mice (Figure 3.4 A).

Single-dose ChAdOx1 vaccination induced a comparable frequency of $CD8^+$ T-cells producing IFN-γ, TNF-α or IL-2 in CD-1 mice across vaccination groups regardless of the strain of peptide used to stimulate cells. Meanwhile, in C57BL/6 mice, tPA-TROP and tPA-TRIP induced higher frequencies of $CD8^+$ T-cells producing IFN-γ or TNF-α, but not IL-2 cytokine compared to ME-TRAP ($p<0.01$) or tPA-TRAP(opt) ($p<0.01$) against the 3D7 peptide pool. Meanwhile, the frequency of IFN-γ^+ or TNF-α^+ $CD8^+$ T-cells induced by tPA-TRAP(opt) immunisation in response to the T9/96 pool was significantly higher ($p<0.05$)

than ME-TRAP. Remarkably, a significantly higher frequency of IFN-γ^+ or TNF-α^+ $CD8^+$ T-cells were also observed in tPA-TROP ($p<0.01$) compared to ME-TRAP following stimulation with T9/96 peptide pool. Additionally, a higher frequency of IFN-γ^+ $CD8^+$ T-cells were also observed in mice receiving the tPA-TRIP vaccine, compared with mice immunised with ME-TRAP following stimulation with T9/96 pool. Suggesting a high level of $CD8^+$ T-cell cross reactivity was induced by the TRAP 3D7 vaccine strain against T9/96 peptide pool in C57BL/6 mice. Meanwhile, significantly higher IFN-γ^+ or TNF-α^+ $CD8^+$ T-cell frequencies were observed in tPA-TROP or tPA-TRIP compared to ME-TRAP or tPA-TRAP(opt) following stimulation with the 3D7 pool peptide (Figure 3.4 B).

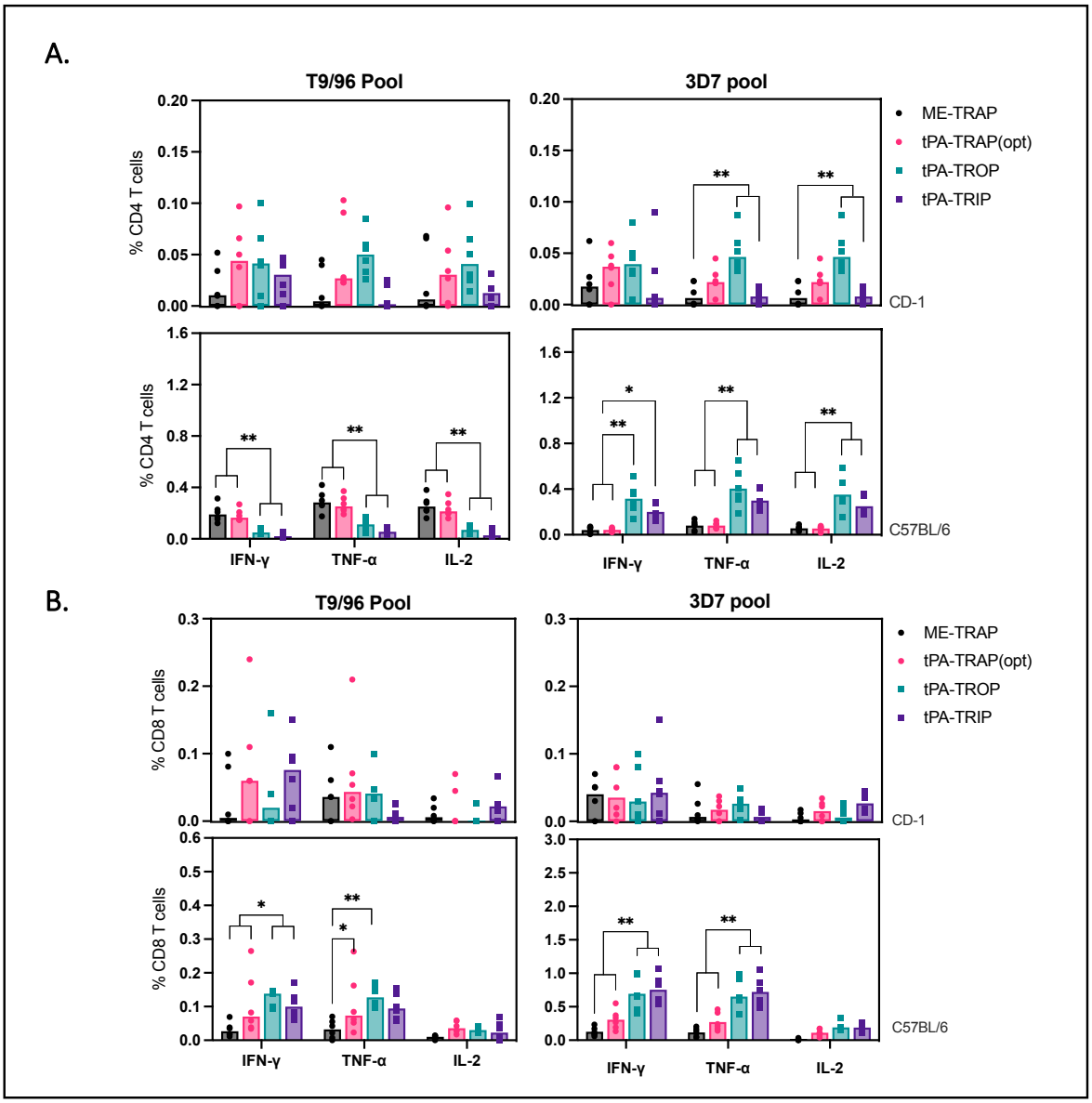


Figure 3.4 Functionality of CD4$^+$ and CD8$^+$ T-cell responses following vaccination with a single dose of ChAdOx1.

Splenocytes were stimulated for 6 hours with peptides prior to staining for intracellular cytokines. **A.** The graphs show the frequency of CD4$^+$ or **B.** CD8$^+$ T-cells producing IFN-γ, TNF-α or IL-2 in CD-1 (top panel) and C57BL/6 (top panel) mice following stimulation with TRAP T9/96 (left) or 3D7 (right) peptide pools. The bar represents each group's median (%) and single points indicate individual mice. Data in each graph was analysed with a two-way Anova followed by Tukey multiple comparison test to compare the difference in frequency of cytokines positive cells between vaccination groups. The data presented were representative of a single study. Asterisks indicate significant differences (*=p<0.05, **=p<0.01).

Antibody responses following a single dose ChAdOx1 vaccine were evaluated against TRAP 3D7. The responses were measured by standardised ELISA using positive serum from mice vaccinated with heterologous prime-boost ChAd63-MVA encoding ME-TRAP from the previous study. As predicted, inbred and outbred mice receiving tPA-TROP or tPA-TRIP 100% seroconverted after a single-dose ChAdOx1. Meanwhile, only 50% and around 17% of vaccinated CD-1 and C57BL/6 mice, respectively, produced antibodies that cross-reacted with TRAP 3D7. Surprisingly, no ME-TRAP vaccinated mice ME-TRAP showed detectable antibodies against TRAP 3D7 following a single dose of ChAdOx1 vaccine (Figure 3.5).

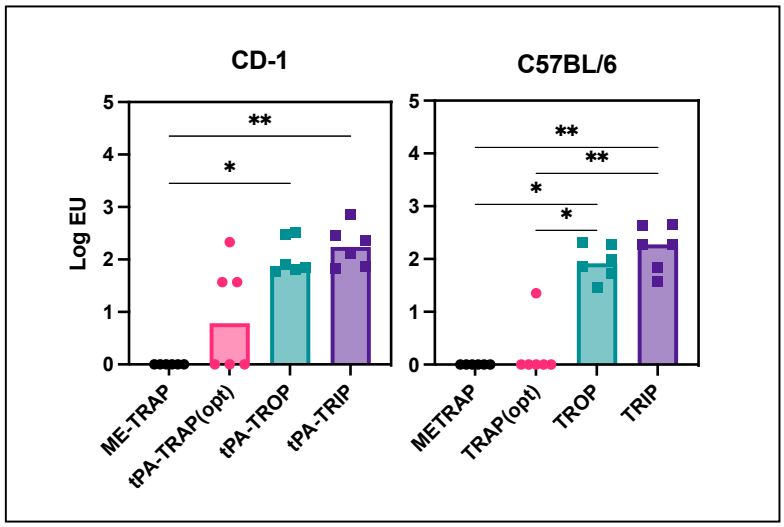


Figure 3.5 Antibody responses following a single dose of ChAdOx1 vaccine.

Antibodies against TRAP 3D7 in the serum of vaccinated CD-1 (left) and C57BL/6 mice were measured by standardised ELISA. Bars represents each group's median (Log Elisa Unit), and single point indicate each individual mouse. Data in each graph was analysed with a Kruskal-Wallis's test followed by Dunn's multiple comparison test to compare the difference between vaccination groups. The data presented were representative of a single study. Asterisks indicate significant differences (*=$p<0.05$, **=$p<0.01$).

3.3.2 Immunogenicity following single-dose MVA vaccinations.

Heterologous vaccination with MVA after priming with Adenovirus has been proven to elicit exceptional high antigen-specific $CD8^+$ T-cell responses [128, 129]. Therefore, MVA vaccines encoding the same transgene previously described in 3.3 were produced and immunogenicity evaluated at a single dose, prior to use in a heterologous ChAdOx1-MVA vaccination regimen. Similar to the single-dose ChAdOx1 experiment, the immunogenicity of these vectors was evaluated in inbred and outbred mice. However, in this experiment, we sacrificed mice seven days after vaccination which is around peak of the immune response after a single dose of MVA vaccination (Figure 3.6 A)[127].

Consistent with the previous work, peak immune responses induced following a single dose of MVA was lower than that observed after adenovirus vector administration [127]. Following immunisation, total T-cell responses in CD-1 mice were comparable across vaccination groups against all pool peptides tested; except T-cells responses in tPA-TRAP(opt) which were significantly ($p<0.05$) higher than tPA-TROP in response to T9/96 peptide pool.

When MVA vaccines were tested in C57BL/6 mice, total T-cell responses were dependant on the peptide strain used for stimulation. The tPA-TRAP(opt) induced significantly ($p<0.01$) higher immune responses compared to tPA-TROP and tPA-TRIP ($p<0.01$) after T9/96 pool stimulations; and interestingly, the response was also higher than ME-TRAP, albeit not statistically significant. Conversely, the tPA-TROP and tPA-TRIP induced significantly higher IFN-γ, in response to 3D7 peptide pool stimulation compared to ME-TRAP and tPA-(TRAP)opt. Meanwhile, immune responses against common pool peptides was comparable across the group (Figure 3.6 B). Antigen strain-specific immune responses

were also observed following vaccination with single dose MVA when the splenocytes were stimulated with individual T9 or TD9 peptides (CD4) but was comparable against T20 peptide (CD8) (Figure 3.6 C).

Similar with ChAdOx1 experiments, the functionality of $CD4^+$ and $CD8^+$ T-cells was measured by ICS. CD-1 mice contain diverse repertoire of MHC, resulted in high variability in $CD4^+$ and $CD8^+$ T-cell expressing IFN-γ, TNF-α or IL-2 response following a single dose of MVA. However, the results supported the ELISPOT data that a single dose of MVA was immunogenic. Consistent with previous finding, a single dose of MVA in inbred mice induced higher frequencies of $CD4^+$ compared to $CD8^+$ T-cells expressing IFN-γ, TNF-α or IL-2 cytokines [256]. Additionally, we also observed antigen strain-specific $CD4^+$ T-cell responses in C57BL/6 mice in response to TRAP T9/96 and 3D7 (Figure 3.7). Unlike vaccination with a single dose of ChAdOx1, single dose MVA failed to induced antibody response against TRAP 3D7 across the vaccination groups (Figure 3.8).

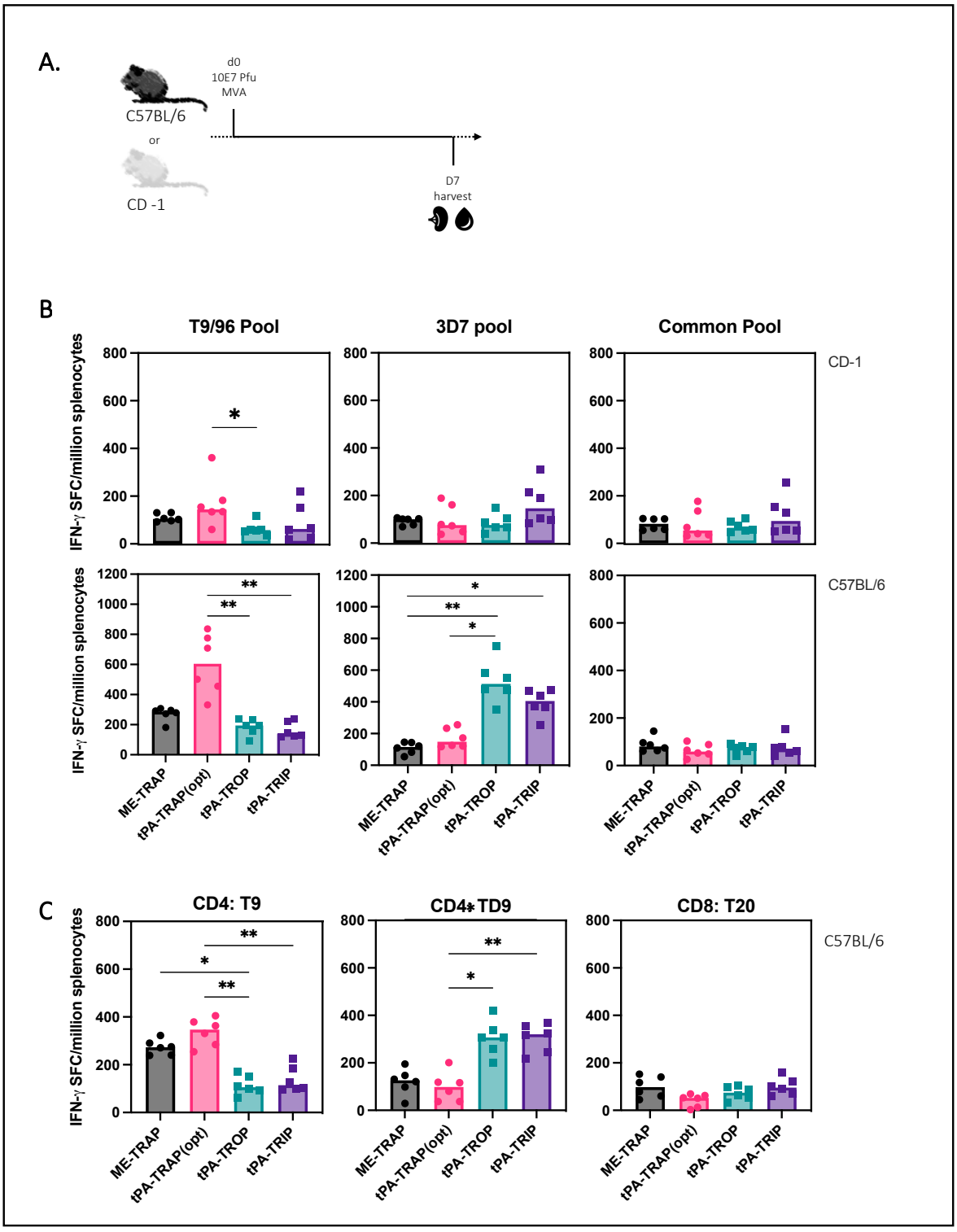


Figure 3.6 T-cell responses induced following a single dose of MVA vaccine.

A. Inbred and outbred mice were vaccinated with 10^7 Pfu of MVA encoding different versions of TRAP antigen. One week later, the mice were sacrificed, and spleen and blood harvested. T-cell responses were measured by *ex-vivo* IFN-γ ELISpot assay after stimulation with **B.** T9/96, 3D7 and a common peptide pool. **C**. Splenocytes from C57BL/6 mice were also stimulated with individual peptides, T9, TD9 and T20, that

contain $CD4^+$ or $CD8^+$ T cell restricted epitopes in $H\text{-}2^b$ mice. The bar represents each group's median (SFC/million splenocytes) and single point indicates individual mice. Data in each graph was analysed with Kruskal-Wallis's test followed by Dunn's multiple comparison test to compare the difference between vaccination groups. The data presented were representative of a single study. Asterisks indicate significant differences (*=p<0.05, **=p<0.01).

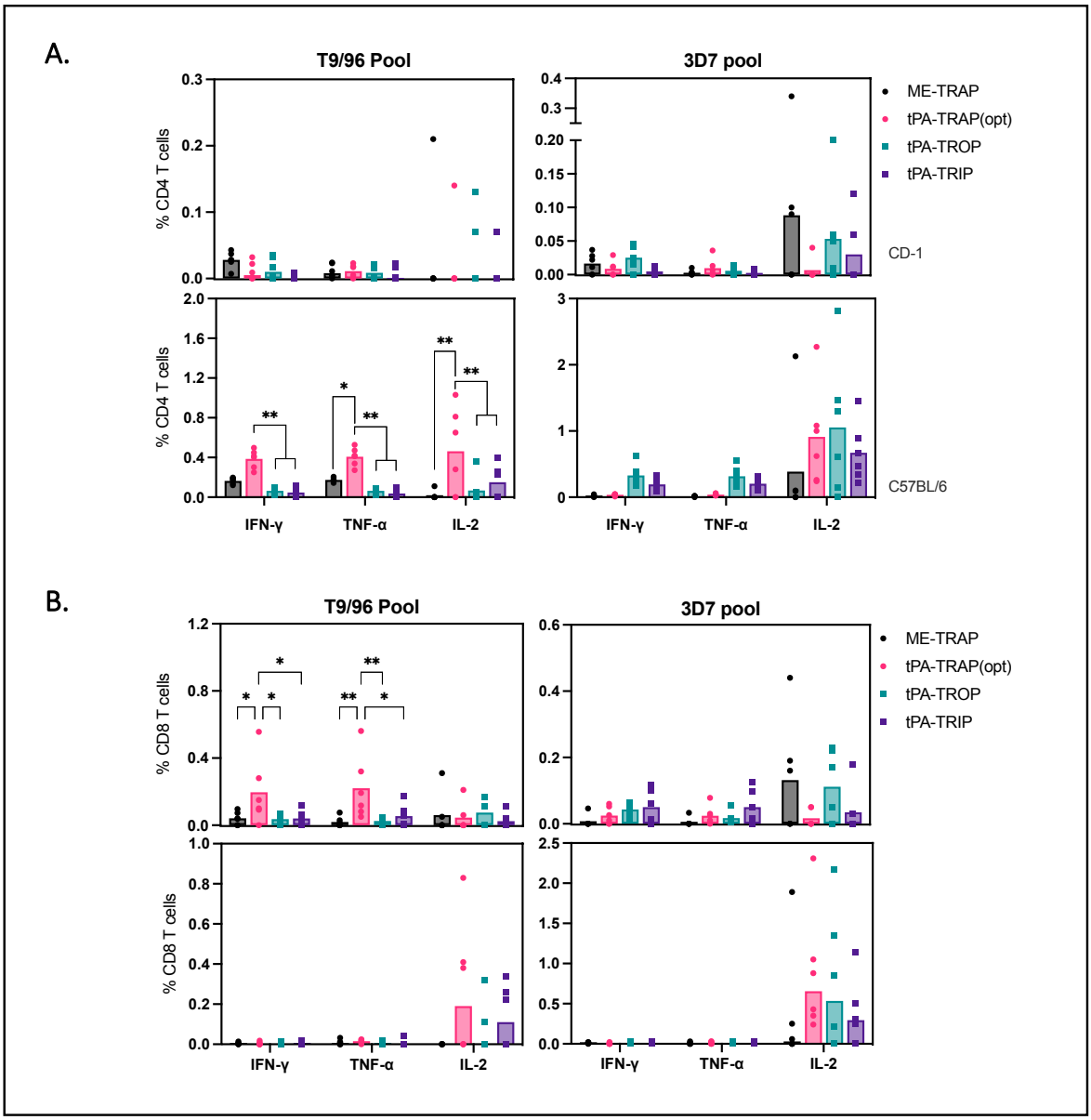


Figure 3.7 Functionality of $CD4^+$ and $CD8^+$ T-cell responses following vaccination with a single dose of MVA.

Splenocytes were stimulated for 6 hours with peptides prior to staining for intracellular cytokine. **A.** The graphs show the frequency of $CD4^+$ or **B.** $CD8^+$ T-cell producing IFN-γ, TNF-α or IL-2 in CD-1 (top panel) and C57BL/6 (top panel) mice after stimulation with TRAP T9/96 (left) or 3D7 (right) peptide pools. The bar represents each group's median (%) and single point indicates each individual mouse. Data in each graph was

analysed with two-way Anova followed by Tukey multiple comparison test to compare the difference of cytokines expression between vaccination groups. The data presented were representative of a single study. Asterisks indicate significant differences (*=p<0.05, **=p<0.01).

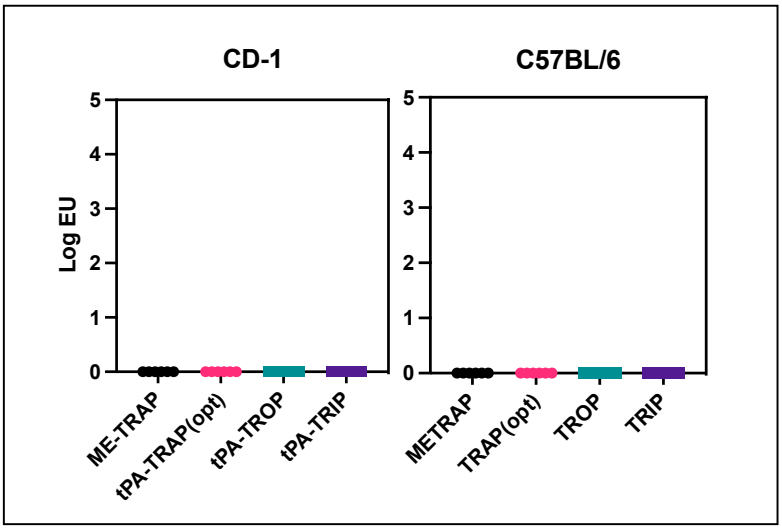


Figure 3.8 Antibody responses following a single dose of MVA vaccine.

Antibodies against TRAP 3D7 in serum from vaccinated CD-1 (left) and C57BL/6 mice were measured by standardised ELISA. The bar represents each group's median (Log Elisa Unit), and the single point indicates individual mice. The data presented were representative of a single study.

3.3.3 Immunogenicity following heterologous ChAdOx1-MVA vaccinations.

After establishing the immunogenicity of single-dose ChAdOx1 and MVA, immunogencity following a standard heterologous prime-boost regimen was compared. Five to six inbred and outbred mice per group were primed with 10^7 (C57BL/6) or 10^8 (CD1) IU of ChAdOx1 carrying different transgenes. Eight weeks later, the mice were boosted with 10^7 PFU of MVA encoding the respective antigen. Mice were sacrificed one week after MVA boost, with blood and spleens harvested for immunogenicity assays (Figure 3.9A).

Following prime-boost vaccination, T-cells responses in CD-1 mice specific to T9/96 or common pools were comparable across vaccination groups. A higher, but not statistically significant, response was observed in tPA-TROP and tPA-TRIP compared to ME-TRAP or

tPA-TRAP following stimulation with the 3D7 peptide pool. Meanwhile, responses in inbred mice showed a comparable response across all vaccination groups except ME-TRAP against T9/96 and 3D7 peptide pools. Responses induced following ME-TRAP vaccination were lower than all other groups, albeit not statistically significant. Interestingly, tPA-TROP ($p<0.05$) and tPA-TRIP ($p<0.01$) induced significantly higher T-cells responses after stimulation with common pool compared with ME-TRAP, and a trend towards higher responses compared to tPA-TRAP (opt) was also observed (Figure 3.9 B). Consistent with previous experiments, the response to T9 and TD9 peptide after the vaccination series was antigen strain-specific. Meanwhile, the production of IFN-γ was comparable across all transgenes except ME-TRAP, which showed a lower response, albeit not statistically significant (Figure 3.9 C).

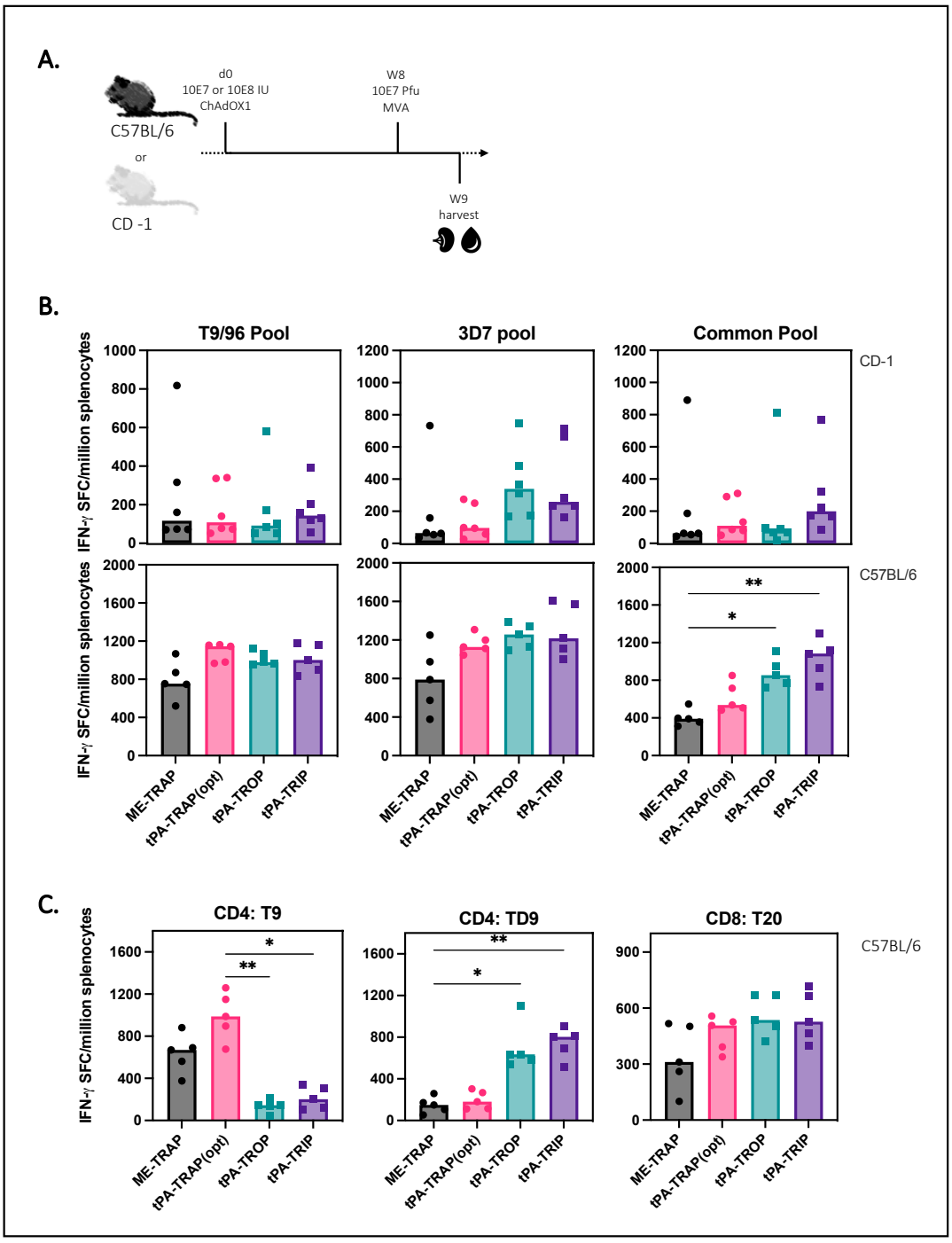


Figure 3.9 T-cell responses induced following heterologous ChAdOx1-MVA vaccination.

A Inbred and outbred mice were primed with 10^7 or 10^8 IU of ChAdOx1, respectively, encoding four different version of TRAP antigen. Mice were boosted with 10^7 Pfu of MVA encoding respective antigens 8 weeks later. One week following MVA vaccination T-cell responses were measured by *ex-vivo* IFN-γ ELISpot following stimulation with **B.** T9/96, 3D7 and a common peptide pool. **C**. Splenocytes from C57BL/6 mice were also stimulated with individual peptides, T9, TD9 and T20. The bar represents each group's median (SFC/million splenocytes) and single point indicates individual mice. The data in each graph was analysed with Kruskal-Wallis's test followed by Dunn's multiple comparison test to compare the difference between

vaccination groups. The data presented were representative of a single study. Asterisks indicate significant differences (*=p<0.05, **=p<0.01).

Functionality of TRAP specific $CD4^+$ and $CD8^+$ following stimulation with T9/96 and 3D7 pool peptides was evaluated by ICS. In CD1 mice, all vaccine groups, except ME-TRAP, showed comparable $CD4^+$ T-cell responses in terms of cells capable of producing IFN-γ, TNF-α or IL-2 cytokines after stimulation with T9/96 or 3D7 pool. Lower IFN-γ, TNF-α and IL-2 responses were observed in ME-TRAP vaccinated mice compared to tPA-TRIP when splenocytes were stimulated with 3D7 peptides. Meanwhile, consistent with ELISpot data against individual $CD4^+$ T-cell epitopes, in C57BL6 mice $CD4^+$ T-cells producing cytokines in responses to peptide pools were higher towards the peptides that matched the vaccine strain (Figure 3.10 A). When $CD4^+$ T-cells polyfunctionality was examined, in CD-1 mice the majority of $CD4^+$ T-cell induced produced IL-2-secreting monofunctional $CD4^+$ T-cell. Meanwhile in C57BL/6 mice, the highest frequency of $CD4^+$ T-cells was dominated by triple IFN-γ^+ TNF-α^+ IL-2^+ and double IFN-γ^+ TNF-α^+ IL-2^- positive $CD4^+$ T-cell in all vaccination groups regardless the peptide used for stimulation (Figure 3.10 B).

Regarding TRAP-specific $CD8^+$ T-cell responses, IFN-γ^+ or TNF-α^+ but not IL-2 strain-specific responses were observed following stimulation with T9/96 and 3D7 pool peptides in CD-1 mice. Interestingly, in C57BL/6 mice, the functionality of $CD8^+$ T-cell producing IFN-γ^+ or TNF-α^+, but not IL-2, were higher in tPA-TROP and tPA-TRIP after homologous stimulation with 3D7 pool; and were comparable in response to T9/96 pool compared to ME-TRAP and tPA-TRAP (opt). This pattern was also observed after single-dose vaccination with ChAdOx1. These results suggested that priming with ChAdOx1 determined $CD8^+$ T-cell cross-reactivity and boosting with MVA increased the magnitude of the responses (Figure 3.11 A). Additionally, matching the strain of peptides with the

vaccines increased the frequency of single IFN-γ^+ TNF-α^- IL-2^-, double IFN-γ^+ TNF-α^+ IL-2^-, and triple IFN-γ^+ TNF-α^+ IL-2^+ positive $CD8^+$ T-cells. Except, the polyfunctionality of $CD8^+$ T-cells responses from ME-TRAP and tPA-TROP were higher in response to 3D7 than T9/96 pool (Figure 3.11 B).

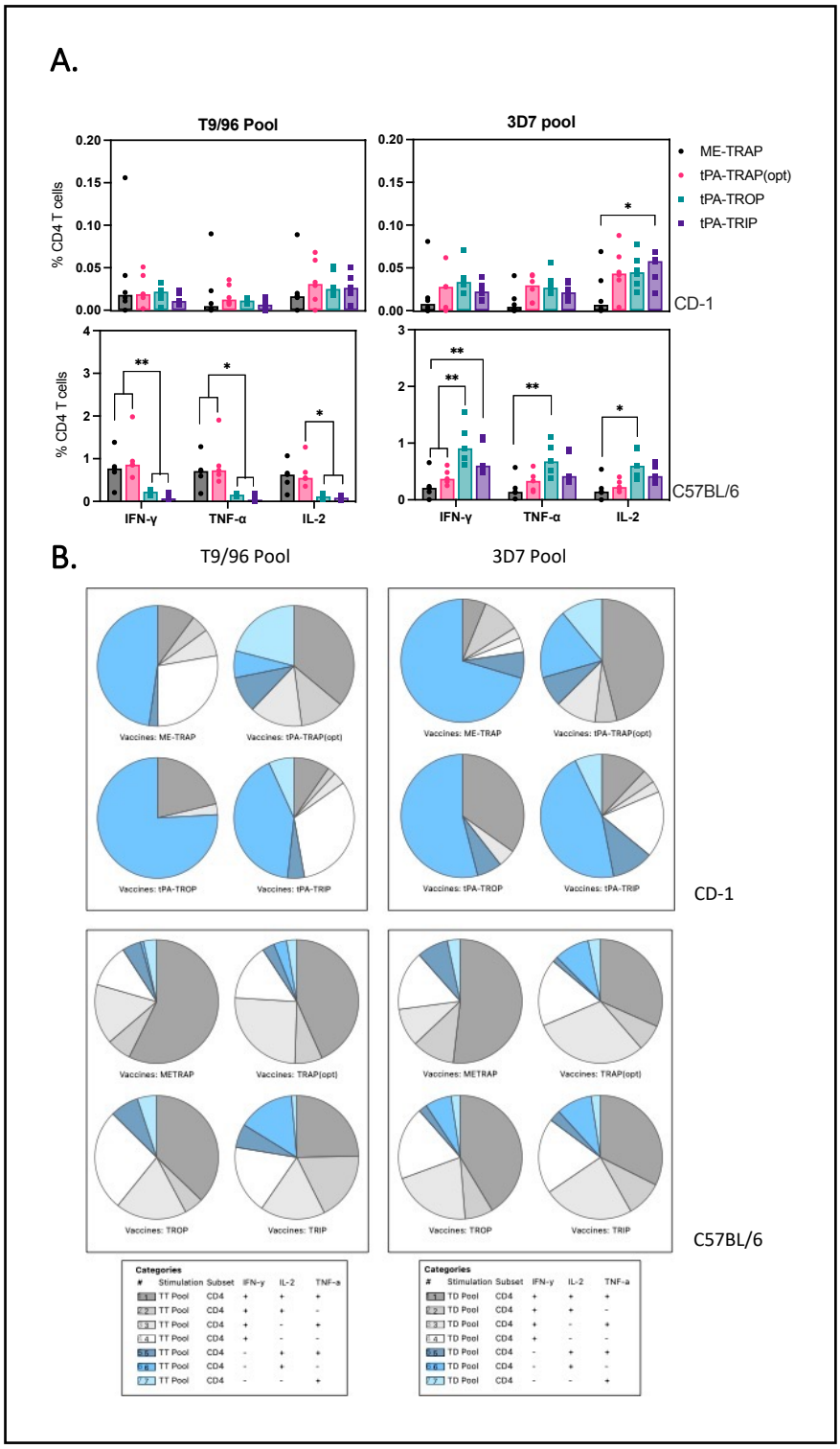


Figure 3.10 Functionality of TRAP-specific CD4$^+$T-cell responses following vaccination with ChAdOx1-MVA.

Splenocytes were stimulated with peptides prior to staining for intracellular cytokines. **A**. The graphs show the frequency of CD4$^+$ T-cells producing IFN-γ, TNF-α or IL-2 in CD-1 (top panel) and C57BL/6 (bottom panel) vaccinated mice following stimulation with TRAP T9/96 (left) or 3D7 (right) peptide pools. **B.** The pie charts summarise the proportion of TRAP-specific CD4$^+$ T-cells producing three, two or one cytokines in splenocytes from CD-1 (top panel) and C57BL/6 (bottom panel) mice after stimulation with TRAP T9/96 (left) or 3D7 (right) peptide pools. The bar represents each group's median (%) and single points indicating individual mice. Data in each graph was analysed with two-way Anova followed by Tukey multiple comparison test to compare the difference in cytokine production between vaccination groups. The data presented were representative of a single study. Asterisks indicate significant differences (*=$p<0.05$, **=$p<0.01$).

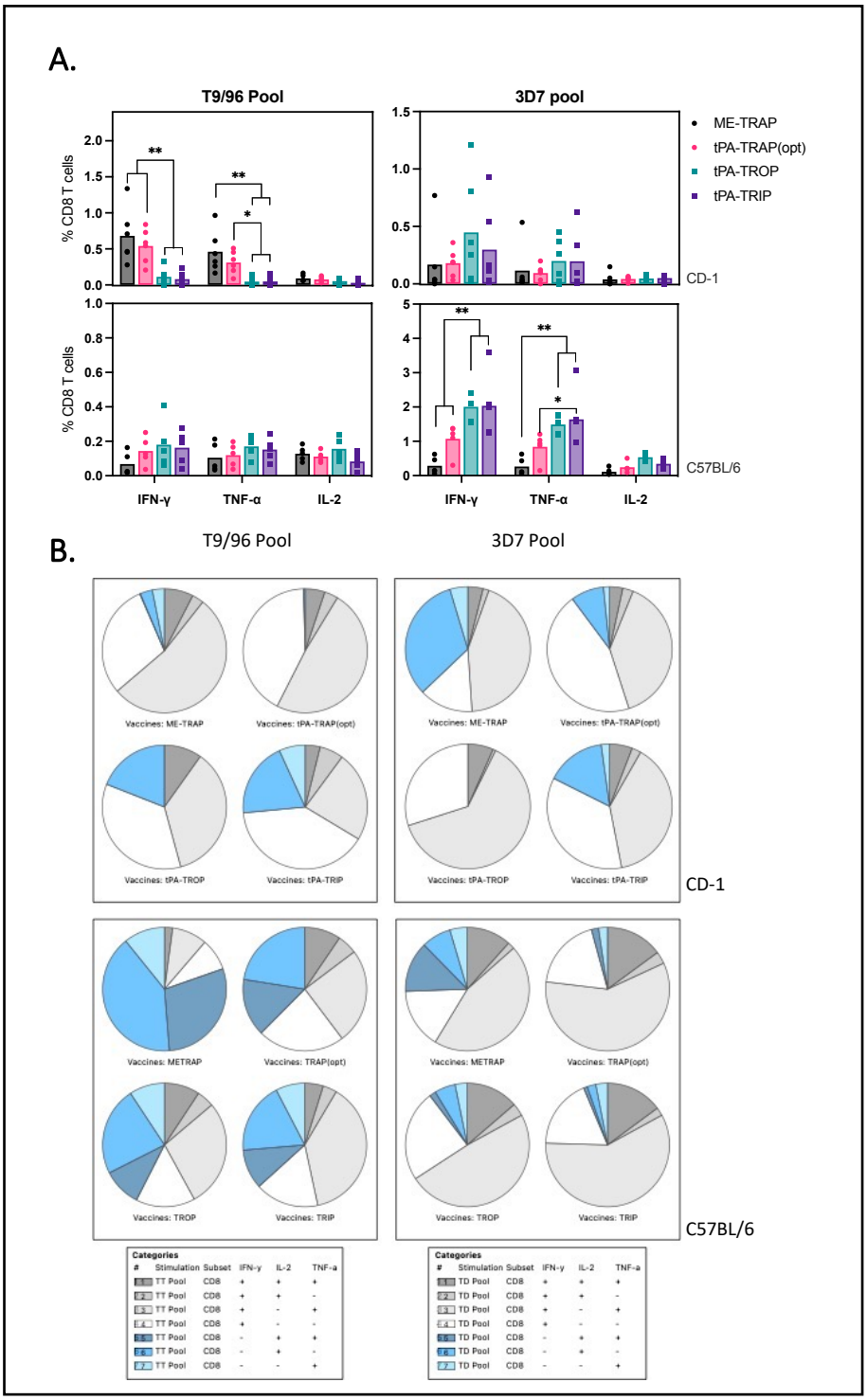


Figure 3.11 Functionality of TRAP-specific CD8+T-cell responses following vaccination with ChAdOx1-MVA.

Splenocytes were stimulated with peptides prior to staining for the production of intracellular cytokine. **A**. The graphs show the frequency of $CD8^+$ T-cell expressing IFN-γ, TNF-α or IL-2 in CD-1 (top panel) and C57BL/6 (bottom panel) vaccinated mice following stimulation with TRAP T9/96 (left) or 3D7 (right) peptide pools. **B.** The pie charts summarise the proportion of TRAP-specific $CD4^+$T-cell expressing three, two or one cytokines in CD-1 (top panel) and C57BL/6 (bottom panel) mice following stimulation with TRAP T9/96 (left) or 3D7

(right) peptide pools. The bar represents each group's median (%) and single point represent individual mice. Data in each graph was analysed with a two-way Anova followed by Tukey multiple comparison test to compare the difference of cytokines expression between vaccination groups. The data presented were representative of a single study. Asterisks indicate significant differences (*=$p<0.05$, **=$p<0.01$).

The total anti-TRAP IgG following heterologous ChAdOx1-MVA vaccination was measured against TRAP 3D7 protein. In inbred and outbred mice, the tPA-TROP and tPA-tPA-TRIP induced comparable anti-TRAP IgG levels, suggesting removing the CT-TM domain from the TRAP antigen did not affect the protein secretion and antigen presentation. The tPA-TRAP(opt) produced lower, but not significant, antibodies capable of binding to 3D7 TRAP. 100% of CD-1 and C57BL/6 mice immunised with ChAdOx1-MVA encoding tPA-TRAP(opt) were seropositive compared to only 50% and 16.7% in CD-1 and C57BL/6 mice that received only single dose ChAdOx1. These results indicate that although priming with single dose MVA poorly induced anti-TRAP IgG, boosting with MVA after ChAdOx1 prime induced robust antibody responses. Additionally, in C57BL/6 mice, ME-TRAP induced significantly lower anti-TRAP IgG compared to tPA-TROP ($p<0.01$) or tPA-TRIP ($p<0.05$); while only 1/6 of CD-1 mice receiving ME-TRAP seroconverted (Figure 3.12)

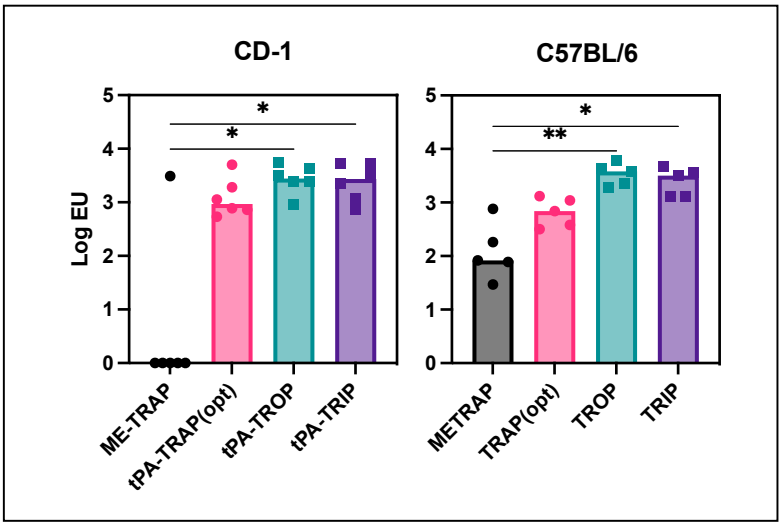


Figure 3.12 Antibody responses following ChAdOx1-MVA vaccinations.

Antibodies against TRAP 3D7 in serum from vaccinated CD-1 (left) and C57BL/6 mice were measured using a standardised ELISA. The bar represents each group's median (Log Elisa Unit) and single point indicate individual mice. Data in each graph was analysed with Kruskal-Wallis's test followed by Dunn's multiple comparison test to compare the difference between vaccination groups. The data presented were representative of a single study. Asterisks indicate significant differences (*=$p<0.05$, **=$p<0.01$).

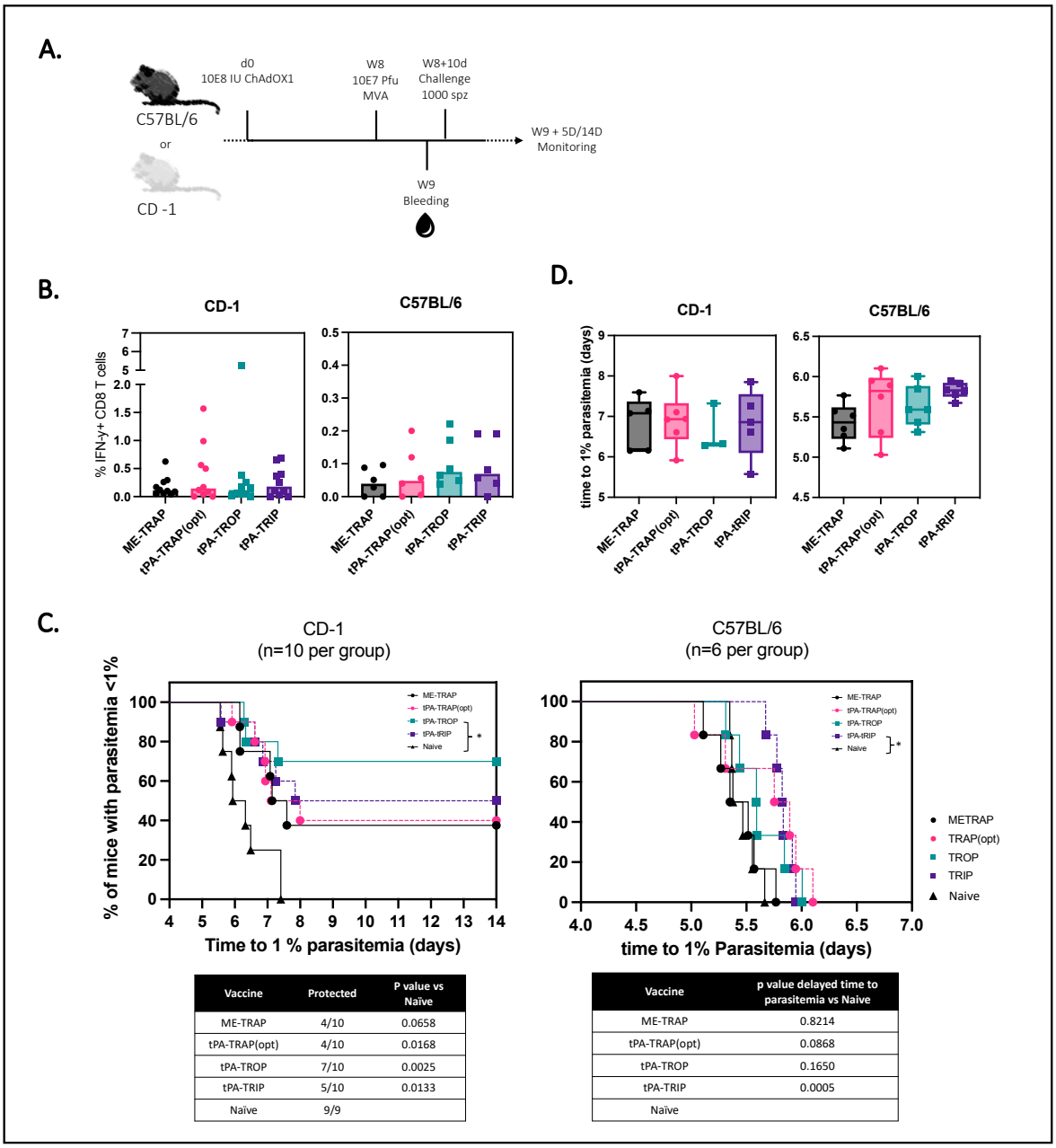
3.3.3 Viral vectors encoding TRAP 3D7 elicit higher levels of protection in mice.

To compare the efficacy of viral vectors encoding TRAP T9/96 and 3D7, C57BL/6 (n=6) or CD-1 mice (n=10) were primed with 10^8 IU of ChAdOx1 and boosted eight weeks later with 10^7 Pfu of MVA, in addition to a group of C57BL/6 and CD-1 naïve controls that remained unvaccinated. A blood sample was taken two days before challenge with malaria sporozoites. Due to limitations in the volume of the drawn blood, the PBMCs were only stimulated with the common pool peptide, and responses measured by ICS. Ten days after the last vaccination, mice were challenged by intravenous injection of 1000 transgenic *P. berghei* sporozoite expressing *Pf.* TRAP 3D7 and monitored for 14 days for the development of blood-stage malaria. Mice that did not develop blood-stage parasitaemia by day 14 were categorised as sterilely protected (Figure 3.13 A).

Following heterologous prime-boost vaccination, the frequency of IFN-γ^+ $CD8^+$ T-cells in vaccinated CD-1 and C57BL/6 mice were comparable across all vaccinated group. However, responses were lower than those measured against the intact antigens, indicating the importance of the strain-specific epitope in $CD8^+$ T-cells response (Figure 3.13 B). As predicted, no sterile protection was observed in C57BL/5 mice following challenge, as this strain of mice is highly susceptible to *P. berghei* infection. However, mice immunised with tPA-TRIP demonstrated a significant delay in time to 1% parasitaemia compared to naïve controls. In contrast, sterile protection after challenge with transgenic *P. berghei* sporozoites was observed in CD-1 mice. The highest level of protection (70%) was conferred in mice that received vaccines expressing tPA-TROP, which was statistically significant compared to naïve, followed by tPA-TRIP (50%). Meanwhile, only 40% and 37.5% of mice from tPA-TRAP(opt) and ME-TRAP, respectively, were protected against malaria (Figure 3.13 C). Time to parasitaemia was compared, but no differences were observed in median time to 1% parasitaemia from unprotected CD-1 mice across the groups. Meanwhile, a higher median time to 1% parasitaemia was observed in C57BL/6 mice immunised by tPA-TRIP compared to other vaccines, albeit not statistically significant (Figure 3.13 D).

Another study has demonstrated that double IFN-γ^+ TNF-α^+ IL-2^- and single IFN-γ^+ TNF-α^- IL-2^- positive $CD8^+$ T-cells significantly correlated with protection against malaria in vaccinated BALB/c mice [128]. To investigate whether similar findings were observed in our study, $CD8^+$ T-cells data from CD-1 mice was pooled and stratified based on protection status. No significant difference in the frequency of total IFN-γ^+ $CD8^+$ T-cells between protected and unprotected CD-1 mice was observed. In addition, when responses were classified based on co-expression with TNF-a or IL-2, neither frequency of monofunctional IFN-γ^+ TNF-α^- IL-2^- $CD8^+$ T-cells nor polyfunctional (IFN-γ^+ TNF-α^+ IL-2^+ or IFN-γ^+ TNF-

α^+ IL-2$^-$) CD8$^+$ T-cells differed between protected and unprotected mice when the PBMCs were stimulated using the common pool peptides. Suggesting the responses towards strain-specific epitopes were essential to determine protection (Figure 3.14).



Vaccine	Protected	P value vs Naïve
ME-TRAP	4/10	0.0658
tPA-TRAP(opt)	4/10	0.0168
tPA-TROP	7/10	0.0025
tPA-TRIP	5/10	0.0133
Naïve	9/9	

Vaccine	p value delayed time to parasitemia vs Naive
ME-TRAP	0.8214
tPA-TRAP(opt)	0.0868
tPA-TROP	0.1650
tPA-TRIP	0.0005
Naïve	

Figure 3.13 Efficacy of ChAdOx1-MVA vaccination in CD-1 and C57BL/6 mice.

A. Inbred and outbred mice were primed with 10^8 IU of ChAdOx1 encoding four different versions of TRAP antigen. Mice were boosted with 10^7 PFU of MVA encoding respective antigens eight weeks later. For the control group, ten CD-1 or six C57BL/6 mice were left unvaccinated. One week after the last dose, a blood samples was taken with PBMCs stimulated with a pool of common peptides, production of cytokine was measured by ICS. Two days later, all mice were challenged with 1000 transgenic *P. berghei* ANKA sporozoite expressing TRAP 3D7 protein and monitored for 14 days. **B.** TRAP-specific IFN-γ^+ CD8$^+$ T-cells from

vaccinated CD-1 (left) or C57BL/6 (right). C. Protective efficacy of four different vaccines in CD-1 (left) and C57BL/6 (right) mice presented in the Kaplan-Meier survival graphs. The survival curves were compared by Log-rank (Manter-Cox) with Bonferroni correction, a vaccine with p-value significantly lower than the Bonferroni-corrected threshold ($p<0.013$) were marked with *. **D**. Time to 1% parasitaemia from infected but vaccinated CD-1 (left) and C57BL/6 (right) mice. The ICS and time to 1% parasitaemia data were analysed with Kruskal-Wallis's followed by Dunn's multiple comparison tests to compare the difference between vaccination groups. The data presented were representative of a single study.

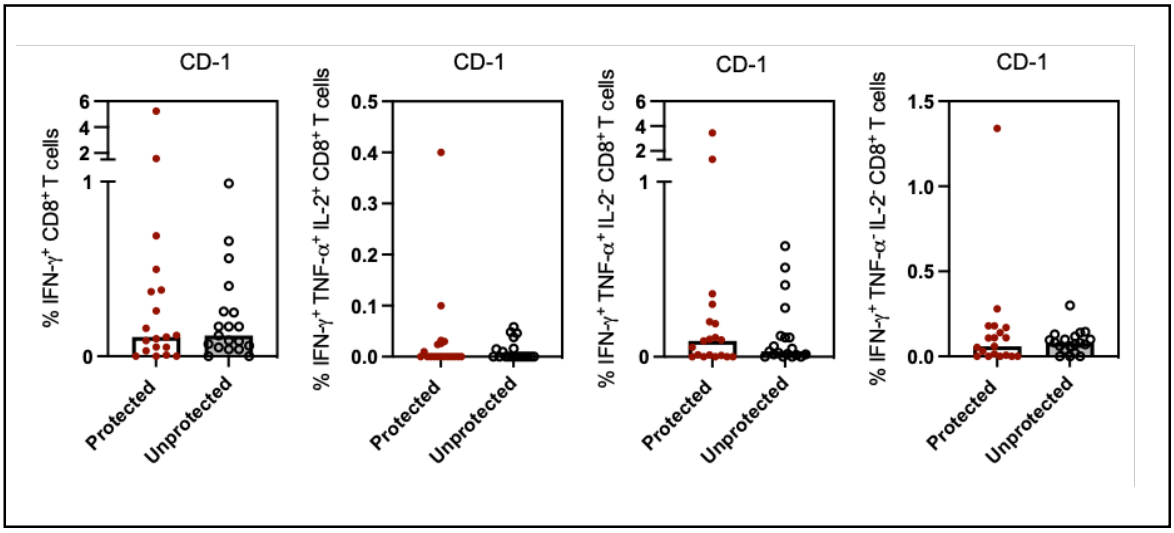


Figure 3.14 TRAP-specific CD8+ T-cell responses from protected vs unprotect CD-1 mice.
Pooled data on frequency of $CD8^+$ T-cell expressing IFN-γ with or without co-expression of TNF-α or IL-2 from protected and unprotected CD-1 mice two days before the challenge. Data in each graph was compared using the two-tailed Mann-Whitney test.

Next, the Spearman correlation coefficient was calculated to understand the relationship between the $CD8^+$ T-cells responses and time to 1% parasitaemia. In CD-1 mice, the polyfunctional (IFN-γ^+ TNF-α^+ IL-2^+ or IFN-γ^+ TNF-α^+ IL-2^-) $CD8^+$ T-cells, but not total IFN-γ^+ $CD8^+$ or monofunctional (IFN-γ^+ TNF-α^- IL-2^-) $CD8^+$ T-cells had a very weak positive correlation with time to 1% parasitaemia, however, these were not significant (Figure 3.15 A). In contrast, monofunctional IFN-γ^+ TNF-α^- IL-2^- $CD8^+$ T-cells in vaccinated C57BL/6 mice negatively correlated with time to 1% parasitaemia. Meanwhile, the IFN-γ^+ $CD8^+$ T-cells or polyfunctional $CD8^+$ T-cells positively correlated with time to 1% parasitaemia; but these relationships were not statistically significant (Figure 3.15 B).

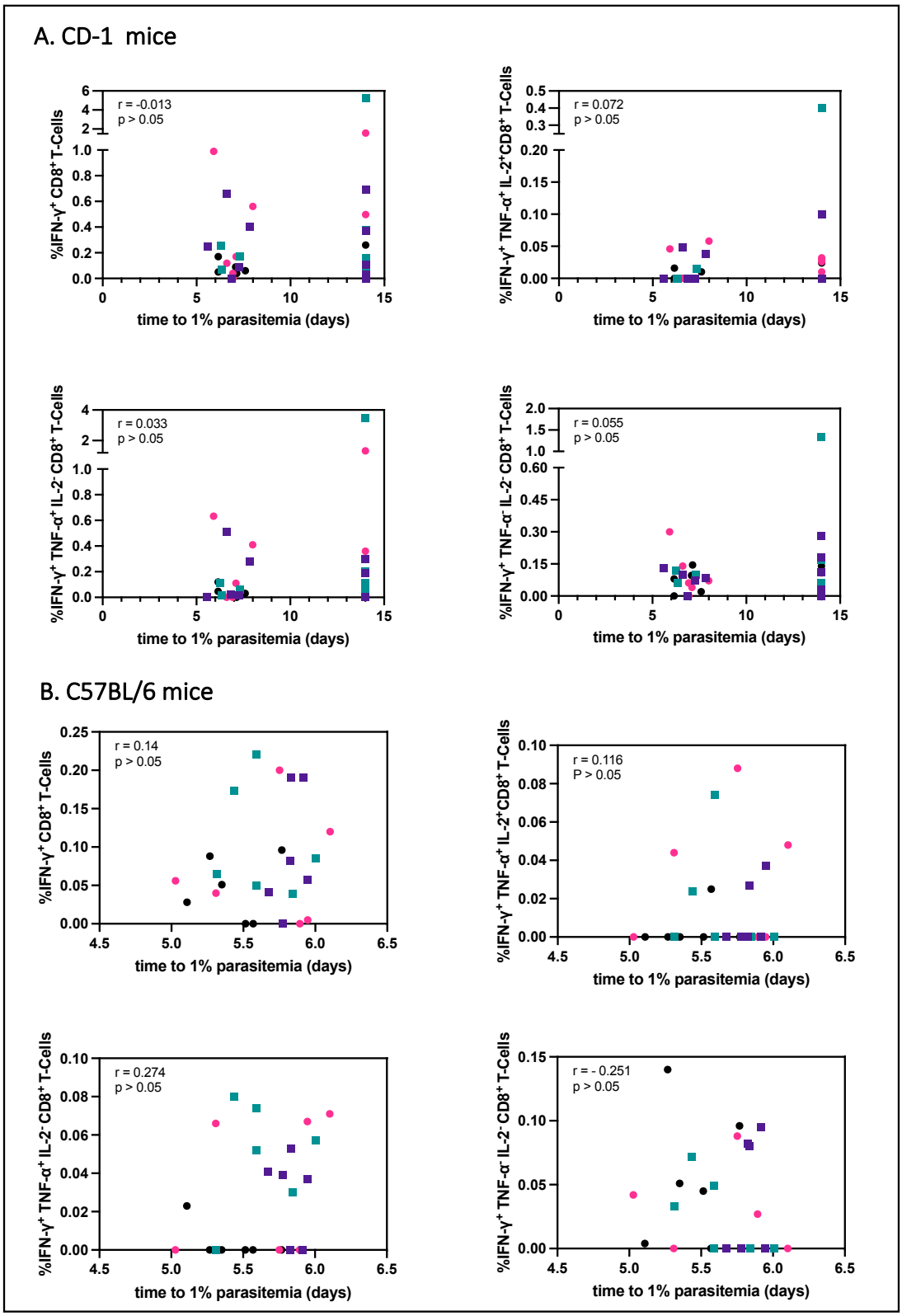


Figure 3.15 Correlation between CD8$^+$ T-cell responses with time to 1% parasitaemia.

Spearman correlation analysis between frequency of total IFN-γ^+, polyfunctional IFN-γ^+ TNF-α^+ IL-2^+ or IFN-γ^+ TNF-α^+ IL-2^-, and monofunctional IFN-γ^+ TNF-α^- IL-2 CD8$^+$ T-cells in response to common pool peptide vs. time to 1% parasitaemia in **A.** CD-1 and **B.** C57BL/6 mice.

Table 3.1 Summary of vaccines' immunogenicity in CD-1 mice.

Vaccine	Antigen Strain	Median T-cell response (IFN-γ+ SFC/million splenocytes)		
		T9/96 pool	3D7 pool	Common pool
Single dose **10^8 IU** ChAdOx1				
ME-TRAP	Pf. TRAP T9/96	130.5	99.5	58.0
tPA-TRAP(opt)	Pf. TRAP T9/96	334.5	242.0	213.0
tPA-TROP	Pf. TRAP 3D7	221.5	302.5	203.0
tPA-TRIP	Pf. TRAP 3D7	77.0	145.5	72.0
Single dose 10^7 Pfu MVA				
ME-TRAP	Pf. TRAP T9/96	104.0	100.5	82.5
tPA-TRAP(opt)	Pf. TRAP T9/96	144.5	75.5	44.0
tPA-TROP	Pf. TRAP 3D7	57.5	76.5	65.5
tPA-TRIP	Pf. TRAP 3D7	62.5	146.5	94.0
Prime-boost 10^8 IU ChAdOx1 – 10^7 Pfu MVA				
ME-TRAP	Pf. TRAP T9/96	117.0	64.0	54.0
tPA-TRAP(opt)	Pf. TRAP T9/96	109.0	96.0	86.0
tPA-TROP	Pf. TRAP 3D7	92.0	339.0	79.0
tPA-TRIP	Pf. TRAP 3D7	144.0	258.0	199.0

Table 3.2 Summary of vaccines' immunogenicity in C57BL/6 mice.

Vaccine	Antigen Strain	Median T-cell response (IFN-γ+ SFC/million splenocytes)		
		T9/96 pool	3D7 pool	Common poll
Single dose **10^7 IU** ChAdOx1				
ME-TRAP	Pf. TRAP T9/96	390.0	329.5	208.5
tPA-TRAP(opt)	Pf. TRAP T9/96	399.0	445.0	244.5
tPA-TROP	Pf. TRAP 3D7	343.5	741.5	350.0
tPA-TRIP	Pf. TRAP 3D7	201.0	619.5	268.0
Single dose 10^7 Pfu MVA				
ME-TRAP	Pf. TRAP T9/96	285.0	115.0	80.5
tPA-TRAP(opt)	Pf. TRAP T9/96	604.5	148.5	59.0
tPA-TROP	Pf. TRAP 3D7	194.5	513.5	75.5
tPA-TRIP	Pf. TRAP 3D7	137.0	405.0	68.5
Prime-boost 10^7 IU ChAdOx1 – 10^7 Pfu MVA				
ME-TRAP	Pf. TRAP T9/96	754.0	789.0	391.0
tPA-TRAP(opt)	Pf. TRAP T9/96	1145.0	1182.0	538.0
tPA-TROP	Pf. TRAP 3D7	979.0	1257.0	854.0
tPA-TRIP	Pf. TRAP 3D7	1002.0	1218.0	1084.0

3.4 Adjuvanting Adenoviral vector vaccines encoding Pf. TRAP 3D7.

Protection against liver-stage malaria requires an exceptionally high number of antigen-specific $CD8^+$ T-cells to scan, locate, and kill infected hepatocytes [257]. Such responses can be induced by employing viral vector vaccines, for instance, Adenovirus and MVA, in a heterologous prime-boost regimen. In addition, many studies have further evaluated the addition of adjuvants to enhance the immunogenicity of viral-vectored vaccines. However, co-formulating viral vector vaccines with chemical adjuvants have increased anti-vector immunity and failed to improve immunogenicity against the transgene [258, 259].

Another way to boost the immune responses against the transgene is by co-expressing a molecular adjuvant together with the antigen construct or by fusing the antigen to a potential adjuvant [256, 260, 261]. The canonical function of the Ii chain during the formation and transport of MHC class II has led scientists to utilise the Ii chain as an adjuvant to enhance $CD4^+$ and $CD8^+$ T-cells responses [262-265]. Our lab has previously demonstrated murine and human Ii chains can enhance $CD8^+$ T-cells responses against ME-TRAP encoded ChAd63 vector [256]. In a recent development, the Ii chains with low homology to human Ii chain were compared and systematically truncated to diminish the potential cross-reactivity [266]. The study found that the transmembrane domain (TMD) from the shark's invariant chain (denoted as SHIC) was sufficient to enhance T-cells responses with minimal reactivity towards Ii sequences itself observed. Therefore, in this study, fusing human-codon optimised TRAP 3D7, shown to induce higher Ag-specific $CD8^+$ T-cells response TRAP T9/96, to SHIC adjuvant was investigated to determine whether this could further enhance the TRAP specific responses.

Results:

3.4.1 Addition of SHIC enhanced T-cell responses in the suboptimal antigen but not in the optimised TRAP 3D7.

To evaluate whether adding SHIC adjuvant could enhance $CD8^+$ T cell responses induced by TRAP 3D7, a new entry vector was designed by removing the tPA leading sequence from tPA-TROP and replaced with SHIC at the N-terminal domain of the antigen. Similar to the previous study [256, 266], the endogenous signal peptide from the antigen was removed to avoid the protein cleavage between the antigen and SHIC adjuvant. Antigen constructs were subsequently transferred to the BAC vector carrying the ChAdOx1 genome and ChAdOx1 vector carrying the transgene produced by the vector core facility and denoted as SHIC-TROP and its immunogenicity was compared to tPA-TROP (Figure 3.16 A).

Following vaccination of C57BL/6 mice with 10^7 IU of ChAdOx1, spleens were harvested 2 weeks later to measure TRAP specific responses by IFN-γ ELIPOTs assay (Figure 3.16 B). Mice vaccinated with SHIC-TROP induced lower $CD4^+$ T-cells compared to tPA-TROP in response to the TD9 peptide. Interestingly, the SHIC-TROP sequence induced significant lower $CD8^+$ T-cell responses ($p<0.01$) compared with tPA-TROP (Figure. 3.16 C). To investigate whether similar responses were observed against the intact antigen, splenocytes were stimulated with a pool of 3D7 peptides and responses measured by ICS. Similar to previous findings, a lower frequency, but not significant, of IFN-γ^+ $CD4^+$ and significantly lower ($p<0.05$) IFN-γ^+ $CD8^+$ TRAP-specific responses were observed in SHIC-TROP compared with tPA-TROP (Figure 3.16 D). Meanwhile, the anti-TRAP 3D7 IgG was comparable between both vaccines (Figure 3.16 E). Similar responses were also observed when the SHIC adjuvant were added to the truncated version of TRAP 3D7 vaccine (TRIP) (Supplement Figure 8-2).

The addition of SHIC adjuvant did not enhance the immunogenicity of the TROP-encoded ChAdOx1 vector. The immunogenicity of tPA-TROP was likely optimised through the addition of the tPA leading sequence and human-codon optimisation. To investigate whether SHIC would enhance the immunogenicity of suboptimal antigens, a new ChAdOx1 vaccine was generated based on *Pf.* TRAP T9/96 wild-type and fused to the SHIC adjuvant at the end of the N-term (denoted as SHIC-TRAP(wt)) (Figure 3.17 A). $CD8^+$ T-cell responses induced by SHIC-TRAP(wt) in response to peptide T20 were comparable with TRAP(wt). Interestingly, a significant increase ($p<0.001$) in the frequency of $CD4^+$ T-cell responses against T9 peptide, around 8 times, was observed in SHIC-TRAP(wt) compared with TRAP(wt) (Figure 3.17 C). A similar observation was also found against the full-length of TRAP T9/96 protein when measured by ICS, with a significantly higher frequency of IFN-γ^+ $CD4^+$ but not IFN-γ^+ $CD8^+$ T-cells induced in SHIC-TRAP(wt) group compared to TRAP(wt) (Figure 3.17 D). Meanwhile, no improvement in anti-TRAP IgG levels were observed within adjuvanted antigens (Figure 3.17 E).

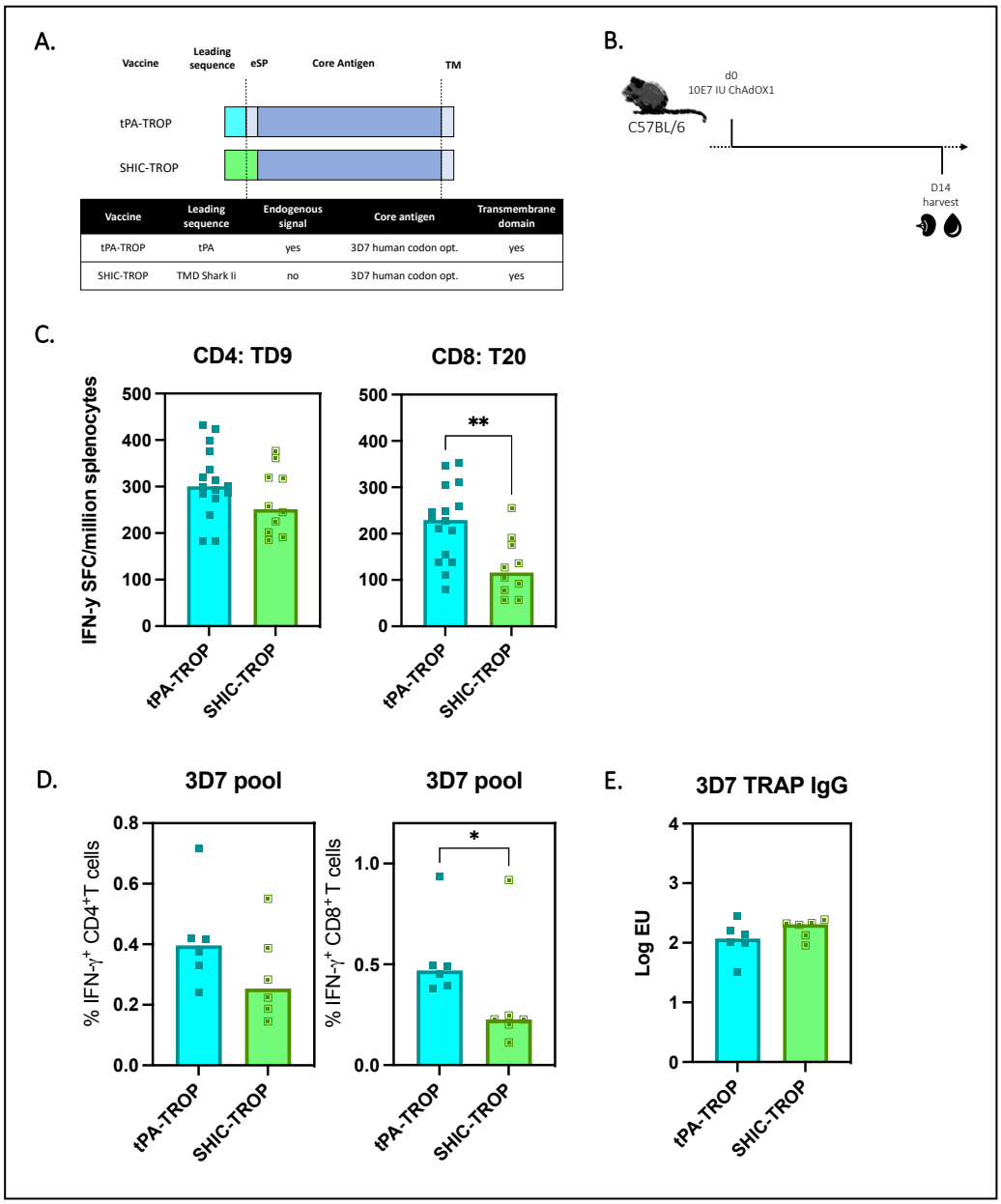
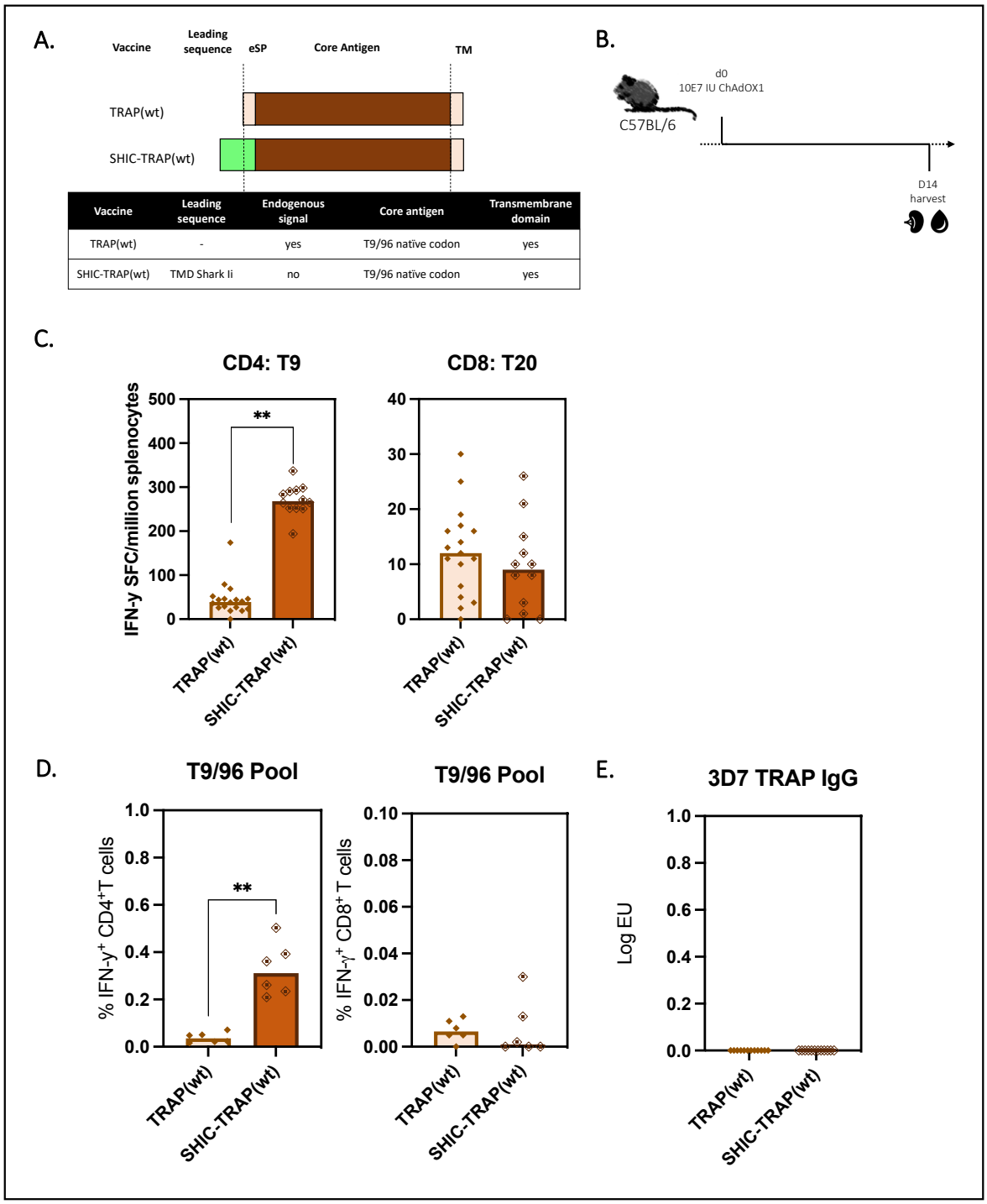


Figure 3.16 Impact of the addition of SHIC adjuvant to the immunogenicity TROP encoded ChAdOX-1 vector.

A. Full-length human-codon optimised *Pf.* TRAP 3D7 (TROP) was fused to the transmembrane domain of the shark invariant chain (SHIC) at the N-terminal of the antigen (denoted as SHIC-TROP), and the immunogenicity was compared to tPA-TROP. **B.** Inbred (C57BL/6) mice were immunised with 10^7 IU of ChAdOx1. Two weeks after vaccination, spleens and blood were harvested and processed for downstream assay. **C.** The $CD4^+$ and $CD8^+$ T-cell responses were measured by IFN-γ^+ ELISpot assays against TD9 ($CD4^+$) and T20 ($CD8^+$) peptides. **D.** TRAP-specific IFN-γ^+ $CD4^+$ and $CD8^+$ were measured by ICS after stimulation with 3D7 pool peptides. **E.** Anti-TRAP IgG levels in serum were measured by standardised ELISA against TRAP 3D7 protein. The data presented were representative of two independent studies. Groups were compared using the two-tail Mann-Whitney analysis. Asterisks indicate significant differences (*=$p<0.05$, **=$p<0.01$).



Vaccine	Leading sequence	Endogenous signal	Core antigen	Transmembrane domain
TRAP(wt)	-	yes	T9/96 native codon	yes
SHIC-TRAP(wt)	TMD Shark Ii	no	T9/96 native codon	yes

Figure 3.17 Impact of the addition of SHIC adjuvant to the immunogenicity TROP encoded ChAdOX-1 vector.

A. Full-length native *Pf.* TRAP T9/96 (TRAP(wt)) was fused to the transmembrane domain of the shark invariant chain (SHIC) at the N-terminal of the antigen (denoted as SHIC-TRAP(wt)), and the immunogenicity was compared to tPA-TRAP(wt). **B.** Inbred (C57BL/6) mice were immunised with 10^7 IU of ChAdOx1. Two weeks later, spleens and blood were harvested and processed for downstream assay. **C.** The $CD4^+$ and $CD8^+$

T-cell responses were measured by IFN-γ^+ ELISpot assays against T9 ($CD4^+$) and T20 ($CD8^+$) peptides. **D.** TRAP-specific IFN-γ^+ $CD4^+$ and $CD8^+$ measured by ICS after stimulation with T9/96 pool peptides. **E.** Anti-TRAP IgG levels in the serum was quantified by standardised ELISA against TRAP 3D7 protein. The data presented were representative of two independent studies. Groups were compared using the two-tail Mann-Whitney analysis. Asterisks indicate significant differences (*=p<0.05, **=p<0.01).

Table 3.3 Summary of vaccines' immunogenicity with or without SHIC in C57BL/6 mice.

Vaccine	Leading sequence	Median T-cell response (IFN-γ+ SFC/million splenocytes)	
		CD4(T9 or TD9)	CD8 (T20)
TRAP(wt)	-	39.0	12.0
SHIC-TRAP(wt)	Shark Invariant Chain (TMD)	268.0	9.0
tPA-TROP	tPA	300.5	229.5
SHIC-TROP	Shark Invariant Chain (TMD)	251.5	116.0

3.5 Inducing $CD8^+$ Tissue Resident (TRM) Memory in the liver using TRAP 3D7 encoded viral vectors.

$CD8^+$ T-cells play an essential role in providing immunity against liver-stage malaria [78, 96, 97]. Many studies have demonstrated that a high number of Ag-specific $CD8^+$ T-cells are required to scan, locate, and kill infected hepatocytes in the short period of sporozoite development before the infection progresses to erythrocytic malaria [257]. Although high-number Ag-specific $CD8^+$ T-cells in humans can be induced by heterologous prime-boost vaccination using viral vectors or high-dose vaccination with irradiated sporozoites [78, 129, 224], such effort possesses significant challenges. Moreover, the protection provided by circulating $CD8^+$ T-cells lasts for a short-time [267].

Following the identification of Tissue Resident Memory (TRM) cells and their role as sentinels, providing organ specific defence against pathogens, many studies have tried to induce TRMs enabling immunity in specific tissues following vaccinations. During hepatocyte infection, circulated $CD8^+$ T cells were not actively recruited into the liver [257]; therefore, high numbers of circulating Ag-specific $CD8^+$ T cells are needed to guarantee sporozoite infected cells will be detected whilst present in the liver. Therefore, a prime-target vaccination could be a potential alternative to protect against liver-stage malaria by bypassing the need for high-numbers of circulating Ag-specific $CD8^+$ T-cells. Our lab has recently demonstrated that the $CD8^+$ TRM (identified by $CD69^+CD44^+CXCR6^+$) could be induced through prime-target vaccination using nanoparticle or viral vectors [130]. The study demonstrated that the Ag-specific $CD8^+$ TRM population in the liver is sufficient to mediate protection against liver-stage malaria. While circulating $CD8^+$ T-cells protect against the acute phase of infection, the protection afforded by $CD8^+$ TRM was found to be more durable [267]. Therefore, this study investigated whether administering viral vectors

encoding *Pf* TRAP 3D7 in a prime-target regimen could induce higher protection than standard prime-boost vaccinations.

Results:

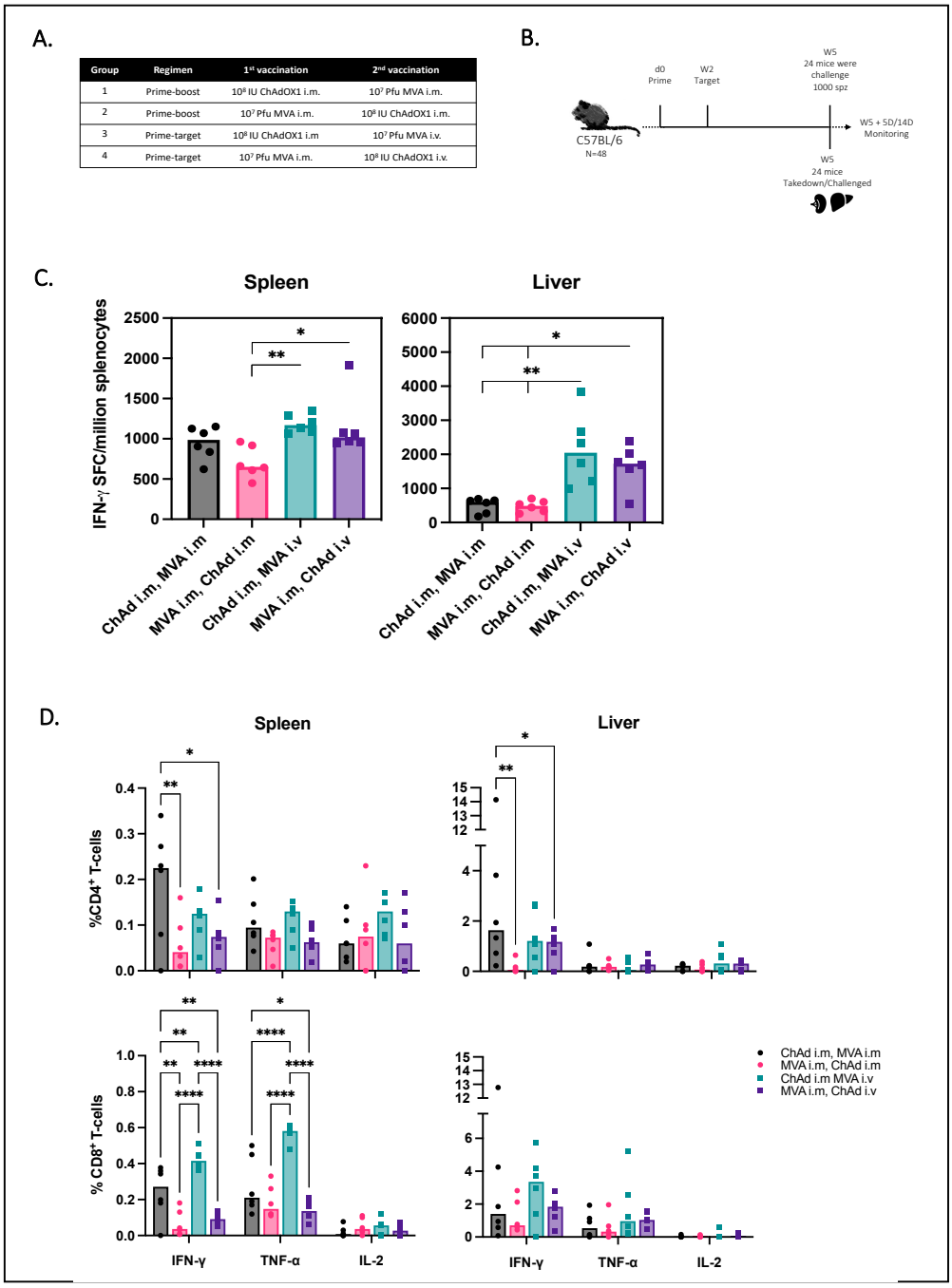
3.5.1 Prime-target vaccination using *Pf*. TRAP 3D7 encoded viral vectors induced $CD8^+$ liver-TRM in C57BL/6 mice.

To investigate the immunogenicity and efficacy of viral vectors encoding human codon-optimised TRAP 3D7 administered in a prime-target regimen; forty-eight C57BL/6 mice were divided into four groups and immunised with four different vaccination regimens. Although the previous study showed that prime-target vaccination could be achieved by using single viral vectors, we used combinations of two viral vectors, ChAdOx1 and MVA, to minimise the impact of anti-vector immunity (Spencer et al, manuscript in preparation). Mice were primed intramuscularly with ChAdOx1 or MVA, two weeks later they received the second dose alternating the vector administered either by standard booster (intramuscular) or targeted vaccinations (intravenous) (Figure 3.18 A). Six mice from each group were sacrificed three weeks after the last vaccination, with spleens & livers harvested further immunological analysis. The rest of the mice were challenged intravenously with 1000 transgenic *P. berghei* sporozoite expressing TRAP 3D7 (Figure 3.18 B).

Following vaccination, total T-cell responses measured in the spleen by IFN-γ ELISpot between prime-target, regardless of the vector order, and standard heterologous prime-boost vaccination $ChAd_{i.m}MVA_{i.m}$ were comparable. Mice immunised with $MVA_{i.m}ChAd_{i.m}$ induced significantly lower T-cell responses in the spleen compared to $ChAd_{i.m}MVA_{i.v}$ ($p<0.01$) or $MVA_{i.m}$ $ChAd_{i.v}$ ($p<0.05$). When antigen specific responses in the liver were

measured, $ChAd_{i.m}MVA_{i.v}$ ($p<0.01$) or $MVA_{i.m}ChAd_{i.v}$ ($p<0.05$) induced significantly higher T-cell responses compared to any standard prime-boost vaccinations (Figure 3.18 C).

Subsequent cytokine analysis by intracellular cytokine staining showed that priming with MVA, regardless of the second dose administration route, induced a significantly lower frequency of IFN-γ^+ $CD4^+$ T-cells in the spleen and liver compared to $ChAd_{i.m}MVA_{i.m}$ vaccination. While the expression of TNF-α and IL-2 by $CD4^+$ T-cell in the spleen were of similar magnitude with IFN-γ and comparable across the group, the majority of cytokine expressed by $CD4^+$ T-cells in the liver was IFN-γ. Interestingly, $ChAd_{i.m}MVA_{i.v}$ vaccination induced a significantly higher frequency of IFN-γ^+ and TNF-α^+ CD8 T-cells compared to other vaccination regimens in the spleen and in the liver (albeit not statistically significant).



Group	Regimen	1st vaccination	2nd vaccination
1	Prime-boost	10^8 IU ChAdOX1 i.m.	10^7 Pfu MVA i.m.
2	Prime-boost	10^7 Pfu MVA i.m.	10^8 IU ChAdOX1 i.m.
3	Prime-target	10^8 IU ChAdOX1 i.m	10^7 Pfu MVA i.v.
4	Prime-target	10^7 Pfu MVA i.m.	10^8 IU ChAdOX1 i.v.

Figure 3.18 T-cell responses induced by prime-boost or prime-target vaccination.

A. Six weeks old C57BL/6 mice were allocated into four different groups and vaccinated with the different regimens, prime-boost or prime-target, using combination of ChAdOx1 and MVA encoding tPA-TRIP antigen. **B**. Experimental design to evaluate the immune response and efficacy induced by prime-boost or prime-target vaccination. **C.** Total T-cell responses in the spleen (left) and liver (right) measured by IFN-γ ELISpot assay. **D.** Functionality of TRAP-specific $CD8^+$ and $CD4^+$ T-cell responses in the spleen (left) and liver (right) measured by ICS assay. The bar represents the median of each group, and single points indicate the response of individual mice. The ELISpot data was analysed with Kruskal-Wallis's followed by Dunn's multiple comparison tests. ICS data was analysed with two-way Anova followed by Tukey multiple

comparisons test. The data presented were representative of a single study. Asterisks indicate significant differences (*=p<0.05, **=p<0.01, ****=p<0.0001).

Next, the impact of different vaccination regimens on the induction of liver TRM was evaluated by quantifying the frequency of TRM within the $CD8^+$ T cell population that produced IFN-γ following peptide stimulation. By using $CD69^+CXCR6^+$ or $CD69^+CD11a^{hi}$ as markers of liver residency, a distinct population within the $CD8^+$ T cell population was observed in the liver but not in the spleen (Figure 3.19A, B). Mice vaccinated with $ChAd_{i.m}MVA_{i.v}$ induced significantly higher frequencies of liver $CD69^+CXCR6^+$ or $CD69^+CD11a^{hi}$ compared to all prime-boost vaccination groups. In addition, the frequency of $CD69^+CXCR6^+$ or $CD69^+CD11a^{hi}$ were not different between $ChAd_{i.m}MVA_{i.v}$ or $MVA_{i.m}ChAd_{i.v}$ groups. Interestingly, a statistically significant difference was observed between $MVA_{i.m}ChAd_{i.v}$ and $ChAd_{i.m}MVA_{i.m}$ or $MVA_{i.m}ChAd_{i.m}$ when $CD69^+CD11a^{hi}$ was used as the markers to identify Trm, but not when $CD69^+CXCR6^+$ was used, suggesting $CD69^+CD11a^{hi}$ are more robust markers to identify TRM in the liver as demonstrated previously [268] (Figure 3.19 B, C).

To further evaluate and compare the TRM population within $CD8^+$ T-cells, we performed t-distributed stochastic embedding t-SNE analysis by combining all markers associated with TRM phenotype on $CD8^+$ T-cells. The $CD8^+CD69^+$ and $CD8^+CD44^+$ T-cells were clustered together, showing TRMs as a distinct population within $CD8^+$ T-cells. $CD8^+$ T-cells were stratified between liver and spleen, then visualised for intensity of the TRM marker expression and cytokine production, a higher density of TRM cells with higher intensity of CD11a, CXCR6, CXCR3 marker were observed in the liver compared with spleen, indicating high proportion of $CD8^+$ TRM in the liver. After establishing that prime-target vaccination induced higher frequencies of liver $CD8^+$ TRM than standard prime-boost

vaccination, whether this would also impact the vaccine's efficacy was investigated. As predicted, sterile protection in C57BL/6 mice was not observed most likely due to high susceptibility of this strain to *P. berghei* infection. However, a delay in time to 1% parasitaemia in mice that received prime-target vaccination was observed, albeit this was not higher than the Bonferroni-corrected threshold (p=0.013). Additionally, the median times to 1% parasitaemia in $ChAd_{i.m}$ $MVA_{i.v}$ or $MVA_{i.m}ChAd_{i.v}$ were higher compared to $ChAd_{i.m}MVA_{i.m}$ or $MVA_{i.m}ChAd_{i.m}$; although this was not statistically significant.

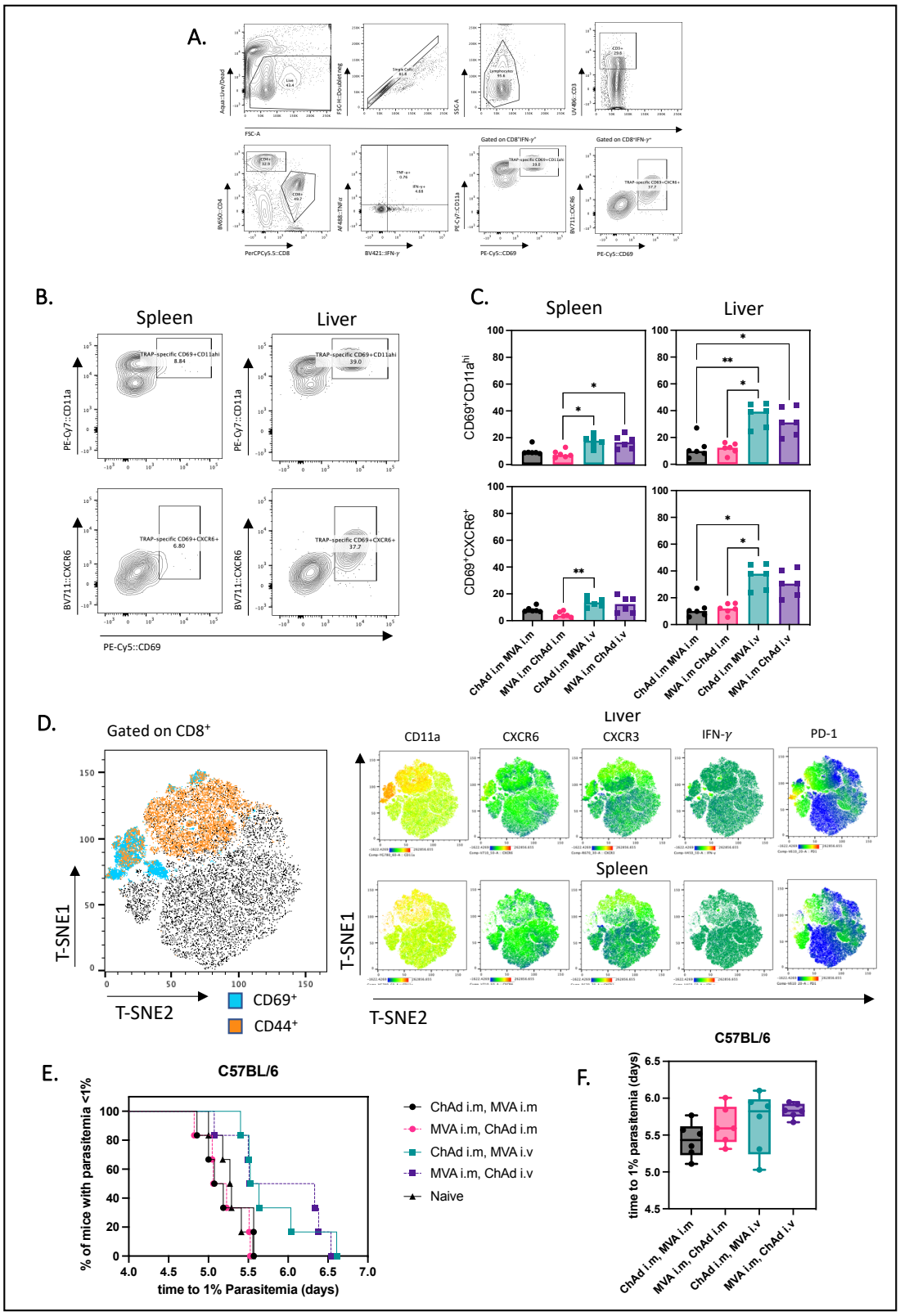


Figure 3.19. Prime-target vaccination with viral vectors.

A. Gating strategy to identify CD8$^+$ TRM using CD69$^+$CD11a^{hi} or CD69$^+$CXCR6$^+$ as marker of tissue residency. **B**. Representative of CD69$^+$CD11a^{hi} or CD69$^+$CXCR6$^+$ population in the liver and spleen. **C**. Median response of frequency of CD69$^+$CD11a^{hi} or CD69$^+$CXCR6$^+$ in the liver and spleen. **D**. t-SNE map

showing the distinct population of $CD8^+CD69^+$ and $CD8^+CD44^+$ and overlay of the t-SNE map, with heat map statistics from the expression of each marker. The t-SNE maps were representative of 48 samples from the spleen and liver. The samples were concatenated on $CD8^+$ T-cells with 3000 cells per sample. **E**. Protective efficacy of viral vectors encoding tPA-TRIP delivered in four vaccination regimens in C57BL/6 mice presented in the Kaplan-Meier survival graphs. The survival curves were compared by Log-rank (Mantel-Cox) with Bonferroni correction; regimens with p-value significantly lower than the Bonferroni-corrected threshold were marked with *****. **F.** Time to 1% parasitaemia from each vaccination group shown in the box and whisker plot. A single point indicates the response from individual mice. The data presented were representative of a single study. Data were analysed with Kruskal-Wallis's followed by Dunn's multiple comparison test to compare the difference between vaccination groups.

3.6 Discussion

Despite the recommendation given by WHO for the use of RTS,S, the first malaria vaccine with moderate protection against clinical malaria [13], the continuation to develop highly efficacious, durable and cost-effective next generation of malaria vaccines is pivotal to support malaria eradication programme. *Plasmodium falciparum*, the causative agent of severe malaria, has a complex life cycle in humans. The first phase of malaria parasite replication in humans requires infection of hepatocytes in the liver, where the parasites reside and replicate. This liver-stage development process takes around 7 to 14 days and is clinically silent; therefore, an attractive target for malaria vaccine development.

The RTS,S vaccine targets the sporozoite stage of the malaria parasite, which requires an extremely high amount of anti-CSP antibodies to rapidly neutralise the parasite in the short period between inoculation and transition to the liver [23, 269, 270]. Meanwhile, liver-stage malaria development takes 7 to 14 days in humans, allowing the immune system to have a longer window to eliminate the parasite. Immunisation with whole-sporozoite followed by chloroquine administration (CPS) or with irradiated sporozoites [78, 98], allowing parasite development in the liver without infection of RBCs, can elicit high levels of sterile protection (>75%) [161, 182, 208, 271]. This indicates that the induction of immune responses towards liver-stage malaria can be protective and therefore developing a liver-

stage malaria vaccine could be a viable alternative target for pre-erythrocytic malaria vaccine development.

The most clinically advanced subunit liver-stage malaria vaccine, ME-TRAP, was constructed based on *Pf.* TRAP T9/96 wild-type antigen fused to the multi-epitope string and delivered in heterologous Adenovirus (ChAd63)-MVA vaccination [101, 129, 204, 206, 223, 225, 226]. The vaccines induced exceptionally high Ag-specific $CD8^+$ T-cells, a response that was not observed in naturally exposed individuals, and provided partial protection against malaria challenge in malaria naïve individuals and reduced the risks of infection in malaria endemic countries [204, 228]. However, the vaccines induced lower T-cell responses and did not provide adequate levels of protection in children in endemic areas, the main target population for malaria vaccines [203].

P. falciparum has a lower GC% content in its genome (~20%) compared to humans (~59%), resulting in a difference in codon usage bias. Therefore, heterologous expression of *P. falciparum* proteins encoded in wild-type sequence in human cells is more likely to reduce protein expression leading to sub-optimal induction of immune responses. The core antigen of the ME-TRAP vaccine was constructed based on a wild-type sequence of *P. falciparum* T9/96. The sequence has not been optimised for expression in human/mammalian cells, a technique that was not widely available during the ME-TRAP construction two decades ago [200, 206]. In recent years, codon optimisation has become frequently used when designing genetic vaccines, e.g. DNA and viral vectors, against bacteria, viruses or parasites, including malaria [239, 242, 272-277]. Therefore, this study investigated whether such a technique could improve TRAP immunogenicity. Initial experiments using two-dose of DNA vaccine administered in a short-interval resulted in higher T-cell responses in codon-optimised TRAP, albeit not significant, compared with wild-type TRAP antigen. Interestingly, the ME-

TRAP, which also contains TRAP wild-type sequence but was fused to codon optimised ME string, induced higher T-cells than TRAP(wt) alone. The ME string consists of 20 T-Cell and B-cell epitopes from malaria antigens, BCG protein and tetanus toxin restricted to specific human HLA [206, 216, 227]; except the Pb9 epitope from murine malaria circumsporozoite protein, SYIPSAEKI, which is immunodominant in mouse H2-K^d [278]. In addition, the epitope string contains two epitopes from TRAP T9/96 protein: a heparin-binding motif, EWSPCSVTCGKG [200, 279], which is conserved across plasmodium species and a $CD8^+$ T-cell restricted epitope for C57BL/6 mice, DASKNKEKAL [127], which both are immunogenic in mice. Expression analysis using western-blot showed a higher intensity band of protein in the ME-TRAP construct compared to TRAP(wt) (Appendix 2), suggesting fused TRAP(wt) to ME sequences influenced antigen expression, which translated into higher immunogenicity in mice.

Increasing interval vaccination between doses, from 2 to 18 weeks, greatly reduced the magnitude of T-cell responses elicited by TRAP(wt) immunisation and a slight reduction in the TRAP(opt) but not in the ME-TRAP group. In contrast, long-interval vaccination with tPA-TRAP(opt) had a higher magnitude of total T-cell responses than delivered in the two-weeks interval. Delaying the second dose in DNA and viral vector vaccinations have been proven to enhance antibody responses [280-282] and the frequency and magnitude of $CD4^+$ and $CD8^+$ T-cell responses [283-285]. In addition, Brice et al. found that intervals between DNA vaccination significantly affect the magnitude of T-cells rather than the number of doses; Moreover, prolonged immunisation interval using a homologous DNA regimen induced T-cell response at a similar level with heterologous DNA-viral vector encoding *P. yoelii* CSP in standard regimen [283]. Meanwhile, administering the second dose of genetic vaccine after $CD8^+$ T-cell contraction and acquired memory phenotype (around nine weeks post-priming) resulted in a higher peak of $CD8^+$ T-cell response [284]. Although we did not

measure the immune response following a single dose of DNA vaccine encoding TRAP(wt). The protein expression from the TRAP(wt) construct showed a low intensity [Supplement Figure 8-1], it is possible that the first dose of TRAP(wt) failed to induced sufficient T-cell response, hence, prolonged the interval dose in this group failed to boost the immune response. One of the limitations of this experiment was that the comparison between native antigen versus human-codon optimised was conducted in DNA vaccine. Hence, this experiment's result must be interpreted carefully when the viral vectors are used to deliver the antigens.

Antigenic diversity within *P. falciparum* is a significant challenge in developing sub-unit vaccines against malaria, including TRAP antigen, which varies across geographic locations [207, 211, 286, 287]. A study from Gambian *P. falciparum* isolates showed that the amino acids in TRAP, but not CSP antigen, has undergone strong immune selection [288]. Additionally, a meta-population genetic analysis demonstrated that the variations of non-merozoites antigen, including TRAP, were restricted to the geographic area [289]. Both studies suggesting that the immunity induced by TRAP vaccine is likely to be influenced by *P. falciparum* strain and its geographic distribution. The original ME-TRAP vaccine construct was based on the TRAP sequence from T9/96, the Thailand-origin haplotype. Polymorphism analysis showed that the amino acids sequence from TRAP T9/96 differed by 6.1% compared with to TRAP from 3D7 strain (a laboratory strain originating from African haplotype NF59) and higher than the other haplotype found in Africa [207]. Although the origin of the original ME-TRAP vaccine strain differed from the origin of malaria in the main target population, i.e. children in sub-Saharan Africa, TRAP vaccine induced-T-cells were found to cross-react with TRAP 3D7, albeit in a lower levels [206, 223]. To improve vaccine efficacy, one may hypothesise that higher levels of 3D7 TRAP

specific T cells could be achieved by vaccinating with vaccine expressing 3D7 TRAP. Nevertheless, the actual immuno-potential of TRAP 3D7 has never been tested and compared. Therefore, in this study, a head-to-head comparison of viral vectors encoding TRAP T9/96 (ME-TRAP and tPA-TRAP(opt)) and 3D7 (tPA-TROP and tPA-TRIP) haplotype was performed.

TRAP T9/96 contains a $CD4^+$ (IHLYVNVFSNNAKEI) and $CD8^+$ (NVAFNRFLV) T-cell restricted epitope in H-$2K^b$ mice [127], which in this study is represented in peptide T9 and T20, peptides [127, 128, 256]. While the $CD8^+$ T-cell epitope is conserved between TRAP T9/96 and 3D7, the $CD4^+$ T-cell epitope sequence differs between strains by three amino acids, the 3D7 sequence is therefore referred to as TD9 (IHLYASVFSNNAREI). While both epitopes, T9 and TD9, were immunogenic in C57BL/6 mice, the $CD4^+$ T-cell response was significantly reduced when the splenocytes were stimulated with a peptide that was not matched to the vaccine. Interestingly, TRAP strain restriction was not limited to only a single epitope but also the intact antigen, as shown in ICS data, where low levels of CD4 cross-reactivity were observed when the splenocytes were stimulated with different strains of TRAP peptide pools. However, this effect was only observed in inbred mice and not in CD1 mice which possess a diverse array of MHC molecules and therefore more similar to humans. Interestingly, $CD4^+$ T-cell responses was higher in the tPA-TRAP(opt) or tPA-TROP vaccine, indicating codon-optimisation and full intact antigen were essential to induce higher $CD4^+$ T-cell responses following viral vector vaccinations.

C57BL/6 mice immunised with 3D7 vaccines elicited higher $CD8^+$ T-cell responses against homologous (3D7 pool) peptides and were comparable to TRAP T9/96 vaccines after heterologous (T9/96 pool) peptide stimulation. Suggesting that TRAP 3D7, but not TRAP T9/96 vaccines elicit one-way $CD8^+$ T-cell cross-reactivity in C57BL/6 mice. Similar

observations were also found in vaccine polymorphism model study using the Pb9 epitope, SYIPSAEKI and its isoform, from *P. berghei* CSP. The study found that immunisation with a mutant version of the Pb9 epitope, SYIPSAEDI, induced broader cross-reactivity of $CD8^+$ T-cells responses but not the wild Pb9 epitope, SYIPSAEKI [290]. Consistent with the immunogenicity study, strain selection positively impacts the protection afforded by vaccination with the 3D7 vaccine strain. Although no sterile protection was observed, the 3D7 vaccine strain induced a significant delay in time to 1% parasitaemia in C57BL/6 mice. Meanwhile, in CD-1 mice, viral-vectors encoding full-length TRAP 3D7 vaccine provided the highest protection (7/10) against challenges with transgenic *P. berghei* sporozoite expressing Pf. TRAP 3D7 protein. One limitation of this experiment was that the impact of different leading sequences between ME and tPA was not evaluated. However, efficacy data in CD-1 mice demonstrated that tPA-TROP (3D7). Induced higher efficacy than tPA-TRAP(opt) (T9/96) when challenged with transgenic P. berghei expressed Pf TRAP 3D7—suggesting that strain selection may contribute more to the immunity against malaria than the selection of the leading sequence in this case.

Experiments described in this section also investigated whether the immunogenicity of TROP could be further enhanced by fusing the core antigen to a molecular adjuvant. Invariant (Ii) chain, a type II integral membrane protein that functions during MHC class II biosynthesis, has been shown to enhance Ag-specific $CD8^+$ T-cell response in mice and non-human primates [256]. Adjuvating TROP with SHIC sequence reduced the $CD8^+$ T-cell response but induced comparable $CD4^+$ T-cell responses with tPA-TROP. Interestingly, when the TRAP(wt), found to be suboptimum, was fused to the SHIC adjuvant, the $CD4^+$ but not $CD8^+$ T-cell responses were enhanced by almost eight times. It is likely that the tPA-TROP construct has been optimised for inducing T-cells, as a similar experiment with SHIC-TRIP did not induce higher T-cell responses than tPA-TRIP (Appendix 1). In addition, the

reduction of $CD8^+$ T-cell responses, after fusing to SHIC adjuvant, has been observed in another optimised liver-stage antigen, *Pf* LSA1 [291]. The SHIC adjuvant is believed to enhance the T-cell responses by stabilising Ag expression and multimerization[266], therefore likely highly antigen-dependent.

It has been shown that Ag-specific $CD8^+$ T cells are not recruited into the liver during hepatocyte infection by sporozoites [257]. Therefore, protection relies on having a high number of circulating Ag-specific $CD8^+$ T-cells to reach the threshold required to rapidly eliminate infected cells. Heterologous vaccination using Adenovirus and MVA elicits exceptionally high $CD8^+$ T-cell responses. Using the same vaccination regimen, improvement in the construct through sequence and vaccine strain optimisation were shown to further enhance the response. However, the immune system may have a ceiling in terms of response against a particular antigen, as adding a SHIC adjuvant did not enhance T-cell responses from the optimised construct but did enhance the response against suboptimum antigen. To circumvent the need for high circulating Ag-specific T-cell responses, prime-target vaccination can be used to drive induction of $CD8^+$ TRM in the liver [130]. By using combinations of ChAdOx1 and MVA encoding *Pf.* TRAP 3D7 antigen, prime-target immunisation was shown to induce higher frequencies of $CD69^+CD11a^{hi}$ or $CD69^+CXCR6^+$ CD8 T-cells response in the liver compared to standard prime-boost vaccination. In the previous study, Adenoviral priming and MVA booster was found to induce a higher T-cell response and complete protection against murine malaria compared to MVA prime followed by Adenovirus boost in mice [128, 224]. Interestingly, priming with MVA and targeting with ChAdOx1 was shown to induce a similar frequency of $CD69^+CD11a^{hi}$ or $CD69^+CXCR6^+$ to $ChAd_{i.m}MVA_{i.v}$ vaccination. This result indicates the potential of the MVA vector as a priming agent in prime-target vaccinations.

In conclusion, optimising the transgene constructs on TRAP encoded viral vectors vaccine targeting liver-stage malaria elicits high immunogenicity and efficacy in mice. Additionally, selecting the relevant vaccine strain with the target geographic for the vaccine deployment may provide greater protection against malaria during transmission season in malaria-endemic countries. Therefore, it is interesting to progress the evaluation of the immunogenicity and efficacy of Pf. TRAP 3D7 encoded viral vector vaccine and compare its performance with ME-TRAP in a human clinical trial.

3.6.1 Chapter summary

Below is the summary of findings that have been demonstrated in this chapter:

1. The 3D7 strain vaccine (tPA-TROP and tPA-TRIP) induces comparable total T-cell responses to tPA-TRAP(opt) against TRAP T9/96 and 3D7 after prime-boost ChAdOx1-MVA vaccination in inbred mice.
2. The 3D7 strain vaccine induced higher T-cell response against any T9/96 vaccine after stimulation with TRAP 3D7 in outbred mice.
3. The tPA-TROP vaccine induces greater efficacy when challenged with transgenic P.berghei sporozoite expressing Pf. TRAP 3D7 in outbred mice.
4. Adding molecular adjuvant SHIC to the optimised TROP does not further enhance the T-cell responses after a single dose of ChAdOx1.

4

Design of a nanoparticle CSP antigen encoded in chimpanzee adenoviral vectors

4.1 Introduction

There is a broad agreement that, unlike most licensed vaccines which primarily induce antibody responses, an effective and durable malaria vaccine will require induction of both humoral and cell-mediated immunity to achieve sterile protection. Such immunity has been well demonstrated with whole sporozoite vaccination (WSV) using irradiated or genetically attenuated sporozoites or pathogenic sporozoites under chemoprophylaxis in murine models and humans clinical trials, resulting in a high level of protection against malaria challenge [78, 96, 170, 173, 182, 292, 293]. WSV induce antibody responses, mainly against the circumsporozoite protein (CSP) [292, 294-296]. Passive transfer of purified IgG from humans vaccinated with *Pf* sporozoite NF54 under chemoprophylaxis reduces the parasite burden in the liver of human liver-chimeric mice following challenge [294]. In addition, WSV prominently induces functional $CD8^+$ T-cell responses capable of killing infected hepatocytes and eliminating parasites, with CSP as the primary antigen target [78]. Although the role of $CD4^+$ T-cells in providing protection following WSV remain unclear, WSV induces detectable $CD4^+$ T-cell responses in human peripheral blood that elicits cytokine upon *ex-vivo* stimulation [78, 173, 297]. Notably, sporozoite-specific $CD4^+$ T-cell responses induced by RAS vaccination provided immunity against malaria [298]. Together, these data suggest that both humoral and cellular immune responses against CSP can provide protection against liver-stage malaria.

Despite practical challenges in scaling up, storage and translation into large-scale vaccination programs, WSV has become a gold standard in inducing a high level of sterile protection against pre-erythrocytic malaria. The induction of high titre and functional antibodies against CSP has sparked the development of subunit malaria vaccines targeting this protein. CSP is the major protein on the surface of sporozoite and has an essential role in hepatocyte invasion [299]. The protein consists of three domains: an N-terminus, a repeat domain and a C-terminus containing a GPI anchor. Later it was discovered that the antibody induced by WSV primarily reacted to the tetrapeptides, NANP, in the central repeat region of CSP [86, 300, 301]. The most advanced subunit vaccine targeting CSP, RTS, S/AS01, was developed based on 19 NANP repeats ("R") and the C-terminus of CSP without the GPI anchor ("T"). The antigen was fused to the hepatitis B-surface antigen, HBsAg ("S"), and is co-expressed with free HBsAg ("S") protein to create a virus-like particle (VLP) structure displaying the malaria antigen which is then formulated with adjuvant system 01 (AS01)[302, 303].

VLPs are virus derived structures made from structural protein capable of self-assembling into nanoparticle structure. Unlike viruses, VLPs do not contain any genetic material, therefore, are unable to replicate and be infectious. VLPs have been widely used as a vaccine platform, for example Hepatitis B and human papilloma virus (HPV) vaccines. The repeat structure of antigens in the VLP has become an attractive feature to effectively present antigen and promote cross-linking to B-cell receptors, resulting in higher and long-lasting antibody responses [304]. In the context of RTS,S/AS01, the vaccine elicits a high titre of anti-CSP antibodies and $CD4^+$ T-cell responses, with low to almost negligible $CD8^+$ T-cell responses [15, 303, 305, 306]. The vaccine provided short-lived protection for around 30 to 50% when assessed in children in a phase 3 study across seven sub-Saharan African

countries [307]. Although the short duration of protection highly was associated with the rapid waning of anti-CSP titre [14], poor induction of $CD8^+$ T-cell response following RTS, S vaccination may also contribute to low protection. Notably, many studies have demonstrated the importance of $CD8^+$ T-cell responses in providing protection against pre-erythrocytic malaria in murine and humans [78, 204, 278, 308-310]; this highlights the requirement for a malaria vaccine to induce potent $CD8^+$ T-cell alongside antibody responses.

Adenovirus-vectored vaccines have been proven to generate high cellular responses, particularly $CD8^+$ T-cells, as well as robust antibody responses. Recently, the capacity of adenovirus vector for use against infectious diseases have been validated through the licensing of three COVID-19 vaccines based on Adenovirus vector encoding spike protein, namely Adhu5 (Convidecia), Adhu26 (Jcovden) and chimpanzee adenovirus, ChAdOx1 (Vaxzevria)[311-313]. These vaccines induce robust neutralising antibodies with efficacy in preventing severe diseases caused by the SARS-CoV-2 virus varying between 50 to 80%. Additionally, the adenoviral vector has been extensively used to evaluate plasmodium antigens across different malaria stages, including sporozoite stage antigen, CSP [122, 129, 195, 233, 314, 315]. The vaccine, delivered in ChAd63-MVA encoding full-length CSP (minus GPI anchor), induced high T-cell responses although only moderate antibody responses. However, this vaccination regimen protected only 1 out of 15 volunteers from malaria challenge with efficacy primarily manifested in delayed time to treatment and reduced parasite burden in the liver [195]. It is highly likely that modest antibody responses against CSP, compared to the RTS,S/AS01, were primarily responsible for low levels of protection. However, several studies have tried to improve the immunogenicity of Adenovirus encoding CSP antigen by inserting the repeat NANP epitope in the hexon, fibre or protein IX of the Adenovirus capsid to mimic the repeat-antigen structure similar VLPs

[316-318]. Nevertheless, this approach is limited to the antigen's length and could affect adenovirus infectivity, transgene expression or yield production.

Therefore, while the VLP platform is capable of inducing high-titre antibodies, and the Adenovirus-vectored vaccine is potent at inducing T-cell mediated immunity, the work described in this chapter investigated whether combining VLP modalities within the adenovirus platform would enable delivery of CSP as a nanoparticle that could improve antibody and T-cell responses compared to adenovirus expressing CSP alone and the impact on vaccine efficacy.

Results:

4.2. Construction of chimpanzee adenoviral, ChAdOx1, vector encoding CSN nanoparticle.

Based on the antigen structure, VLPs are categorised into non-enveloped and enveloped VLPs. Non-enveloped VLPs can be formed using one or more viral structural proteins and act as the primary antigen, for example, in Hepatitis or HPV vaccine. Alternatively, these type of VLPs can also be engineered to display heterologous antigens by fusing the targeted antigen to the viral structural proteins, for example RTS,S, and R21 that both use HBsAg to display components of the CSP antigen. Non-enveloped VLPs are assembled *in-vitro*, hence, do not contain any materials from host cells. In contrast, the assembly process of enveloped VLP occurs *in-vivo*. Hence, when the VLPs are budded and released from the host cells, the VLPs contained plasma membrane from the host cells [319].

Similar to non-enveloped VLPs, the viral structural protein of enveloped VLP can become the target antigen or be engineered to display heterologous antigens. Unlike non-enveloped

VLPs, targeted antigens are expressed separately from structural proteins of enveloped VLPs. These antigens get trafficked to the plasma membrane and, together with viral structural protein, leads to formation of the VLP prior to budding and release. Therefore, this type of VLP can display larger antigen than non-enveloped VLP as the heterologous antigens' expression does not impair the assembly process (Figure 4.1). Because of this feature, in this study a ChAdOx1 vector was developed to encode an enveloped VLP displaying a modified but full-length version of CSP.

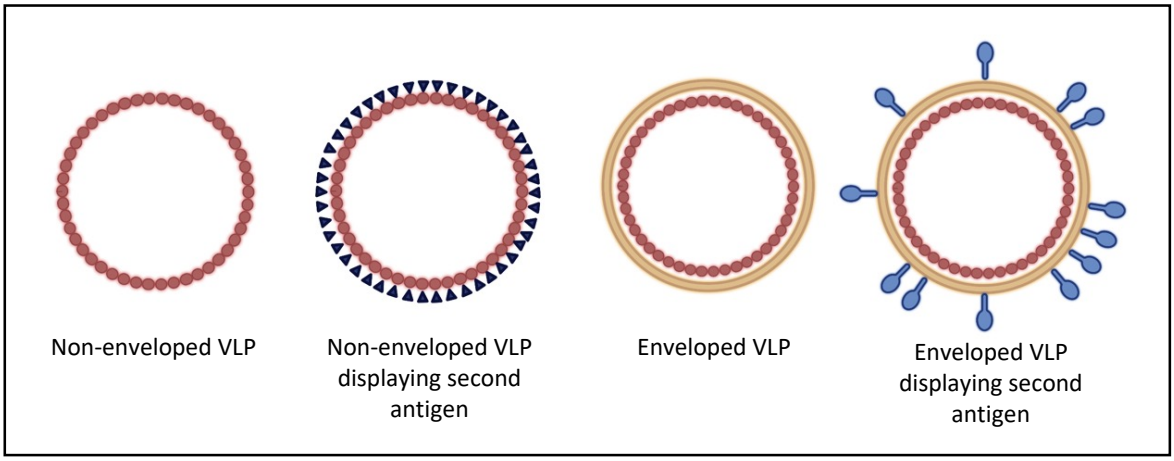


Figure 4.1 Illustration of different types of VLPs.

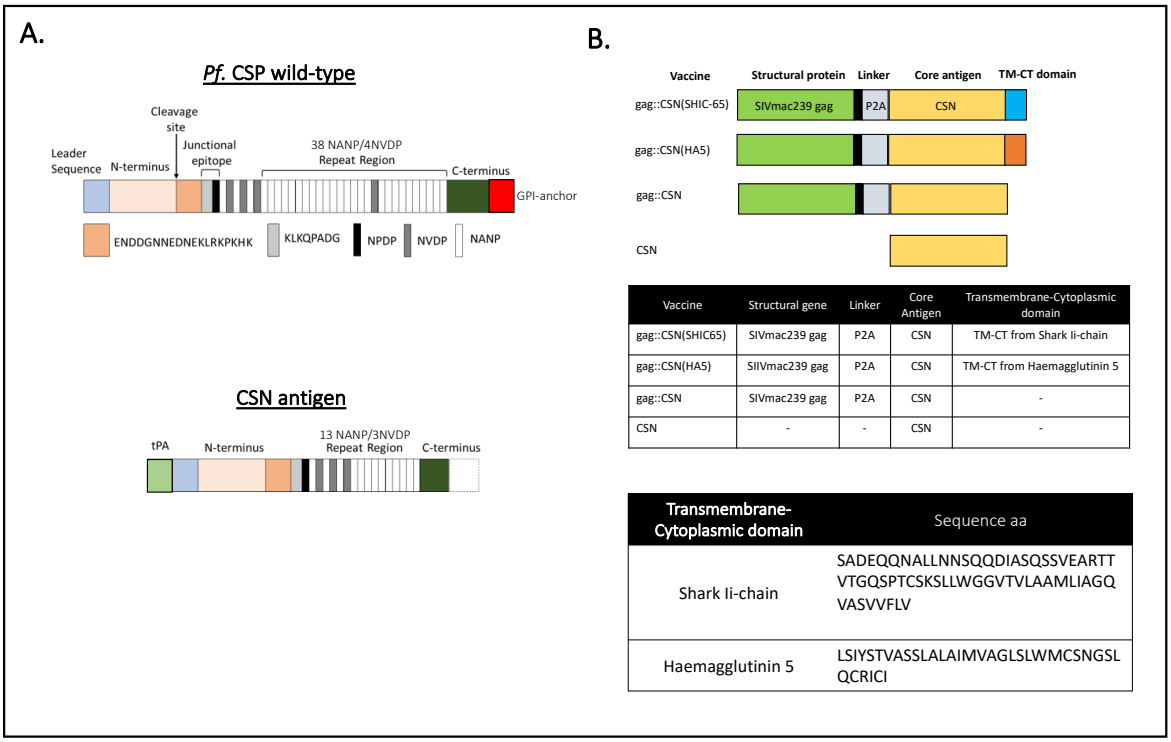
Non-enveloped VLPs are assembled *in-vitro* using one or more structural proteins. The structural protein in the non-enveloped VLP can act as the primary antigen or be used as a scaffold to display another antigens. Enveloped VLPs are assembled *in-vivo*; hence contain host membrane cells following budding and release. Incorporating heterologous antigens into host-membrane cells allow the enveloped VLPs to display target antigens.

.

The expression of full-length recombinant CSP has been problematic [320-323], and early studies using DNA or viral vectors encoding full-length CSP in our group showed poor transgene expression, that led to low immunogenicity of the vaccine [221, 324, 325]. However, a modified CSP antigen (denoted as CSN), generated by fusing the N-terminal protein to the tPA leading sequence and deleting the GPI-anchor at the C-terminus followed

by a reduction of the NANP repeats, showed improved immunogenicity [82, 195, 326-328]. In this study, the CSN construct was used as the primary target antigen (Figure 4.2 A). The pr55 gag polyprotein is a major structural protein from retroviruses. Unlike structural proteins from other enveloped viruses, the gag polyprotein can independently be recruited to the plasma membrane and form a VLP structure without any assistance of other proteins [329], as is required for Matrix protein 1 (M1) from Influenza virus [330]. Therefore, to simplify the construct, pr55 gag polyprotein from Simian Immunodeficiency Virus (SIV) mac293 (denoted as gag) was tested as a VLPs scaffold to display CSN.

The gag and CSN antigens were cloned into single cassette E1 under Early-Intermediate human CMV promotor. A self-cleaving sequence from porcine teschovirus-1 2A (P2A) was added in between these antigens to separate the expressed proteins during translation [331]. This strategy was chosen to maintain the stoichiometry between gag polyprotein and target antigen CSN. To allow incorporation of CSN antigen to the plasma membrane of the host cells, the transmembrane and cytoplasmic domain (TM-CT), from either Haemagglutinin A (HA) 5 or Shark's invariant chain (amino acids 1-65), was fused to the C terminal of CSN as an anchor. Vaccines were denoted as gag::CSN(HA5) and gag::CSN(SHIC65), respectively. For comparison, a CSN without TM-CT were constructed and denoted as gag::CSN. The ChAdOx1 encoding free CSN was used as a benchmark in this study (Figure 4.2B).



Vaccine	Structural gene	Linker	Core Antigen	Transmembrane-Cytoplasmic domain
gag::CSN(SHIC65)	SIVmac239 gag	P2A	CSN	TM-CT from Shark Ii-chain
gag::CSN(HA5)	SIIVmac239 gag	P2A	CSN	TM-CT from Haemagglutinin 5
gag::CSN	SIVmac239 gag	P2A	CSN	-
CSN	-	-	CSN	-

Transmembrane-Cytoplasmic domain	Sequence aa
Shark Ii-chain	SADEQQNALLNNSQQDIASQSSVEARTTVTGQSPTCSKSLLWGGVTVLAAMLIAGQVASVVFLV
Haemagglutinin 5	LSIYSTVASSLALAIMVAGLSLWMCSNGSLQCRICI

Figure 4.2 Construction of ChAdOx1 encoding nanoparticle CSP.

A. A schematic of Pf. CSP 3D7 and CSN antigen used in vaccine construct. The CSN antigen was constructed based on the full length of Pf. CSP 3D7. The antigen was modulated by fusing the N-term to the tPA leading sequence, reducing the NANP repeat number, and removing the last 15 amino acids at the C-term to inactivate the GPI-anchor. **B.** VLP-CSN were constructed by linking the CSN sequence to the pr55 gag polyprotein from SIVmac293 using a Self-cleaving 2A sequence from Porcine teschovirus-1 (P2A) and denoted as gag::CSN. Two other variants were derived from gag::CSN that were fused to the transmembrane and cytoplasmic domain from Haemagglutinin 5 (HA5) or Shark's invariant chain (SHIC65) and then denoted as gag::CSN(HA5) and gag::CSN(SHIC65), respectively. Subsequently, the free CSN construct was used as a benchmark.

4.3. Increased immunogenicity of ChAdOx1 encoding nanoparticle CSP in BALB/c mice.

To test the immunogenicity of newly constructed Adenovirus vaccines, 6 week old BALB/c mice were vaccinated intramuscularly with 10^7 IU of ChAdOx1 encoding four different constructs of CSN as described in 4.2. Two weeks later, spleens and blood were harvested and processed for subsequent assay (Figure 4.3 A). Following vaccination with a single-dose of ChAdOx1, total T-cell responses in mice vaccinated with gag::CSN(SHIC65) were significantly higher ($p<0.05$) compared to mice receiving CSN. Higher, but not significant, T-cell responses were also observed in gag::CSN vaccinated mice compared to CSN.

Surprisingly, a nonsignificant decrease in T-cell responses was observed in mice immunised with gag::CSN(HA) compared to CSN; gag::CSN(HA) elicited significantly ($p<0.001$) lower T-cell responses compared to gag::CSN or gag::CSN(SHIC65) (Figure 4.3 B). Antibody responses were measured against the NANP repeat by endpoint ELISA. Following vaccination with a low dose of ChAdOx1, anti-NANP IgG was comparable across all groups although antibodies were just above the level of detection (Figure 4.3 C).

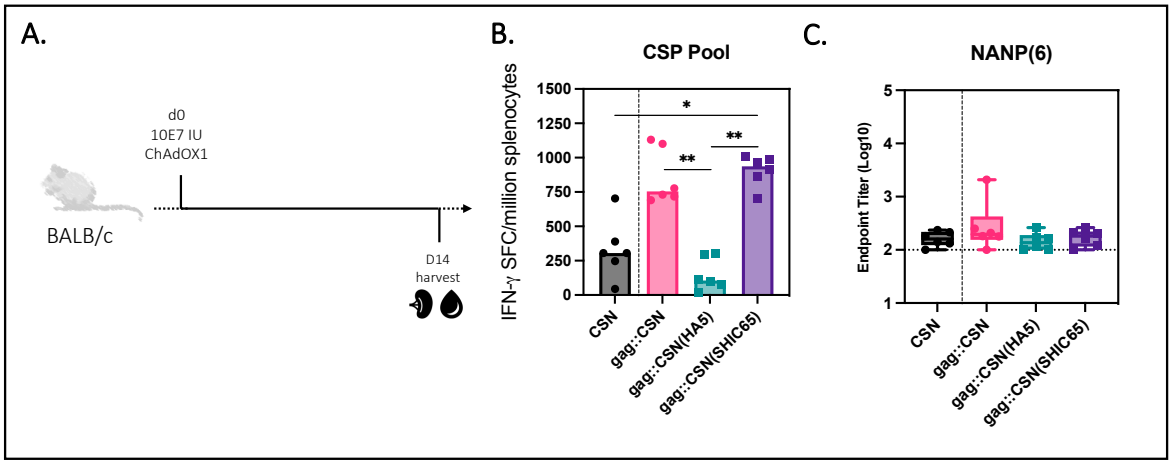


Figure 4.3. Immunogenicity following a single dose ChAdOx1 vaccines.

A. Groups of BALB/c mice (n=6) were immunised with 10^7 IU of ChAdOx1 encoding four different versions of CSN transgene. Mice were sacrificed two weeks later to harvest spleens and blood. **B.** Total T-cell responses were measured by *ex-vivo* IFN-γ ELISpot assay with splenocytes stimulated with a pool of CSP overlapping peptides spanning the full-length CSP antigen. The bar represents each group's median (SFC/million splenocytes) **C.** A box and whisker plot showing antibody response against the NANP repeat measured by Endpoint ELISA. Single points in all graphs indicate data from individual mice. Data in each graph was analysed with Kruskal-Wallis's test followed by Dunn's multiple comparison test to compare the difference between vaccination groups. The data presented were representative of a single study. Asterisks indicate significant differences (*=$p<0.05$).

To further evaluate immunogenicity, mice were immunised with two-doses of 10^8 IU ChAdOx1, ten times higher than the previous experiment, two weeks apart (Figure 4.4 A). Antibody responses were measured using a standardised ELISA against a full-length recombinant CSP and three peptides representing different regions of CSP: an N-interface peptide that contained junctional epitope KLKQPADGNPDPNANPNVDP, a central repeat (NANP6) and a PF16 peptide that represent the C-terminal region [199, 332]. In general, two doses of ChAdOx1 increased the production of antibodies against full-length CSP, NANP(6) and PF16 but not the N-interface peptide. Following two-dose vaccinations, the total anti-CSP IgG from mice immunised with gag::CSN ($p<0.01$) or gag::CSN(SHIC65) ($p<0.05$) were significantly higher compared to CSN. Additionally, a significantly higher level of anti-NANP(6) IgG was induced by gag::CSN(SHIC65) ($p<0.05$) than CSN. Antibody titres against NANP(6) were also higher in mice immunised with gag::CSN compared to CSN following the second dose of vaccine, although this was not significant. While the administration of a second dose did not increase antibody responses against the N-interface, anti-PF16 IgG was found to be boosted after a second dose with the titre significantly higher in gag::CSN ($p<0.05$) vaccinated mice compared to CSN and but non-significant higher titre in gag::CSN(SHIC65) compared with CSN (Figure 4.4 B, C).

To determine whether changes in the way antigen was constructed would affect the quality of antibody response, avidity of anti-NANP IgG was measured using sodium thiocyanate, NaSCN, as a chaotropic agent. Since antibodies induced by gag::CSN(HA5) were below the limit of detection, avidity of antibodies in this vaccine group was not measured. Following two-dose vaccination, the avidity of anti-NANP IgG induced by gag::CSN or gag::CSN(SHIC65) vaccination was higher than CSN, albeit this was not significant (Figure 4.4 D). Collectively, these data showed that ChAdOx1 encoding VLP-CSN enhanced the quantity and quality of antibody responses in BALB/c mice.

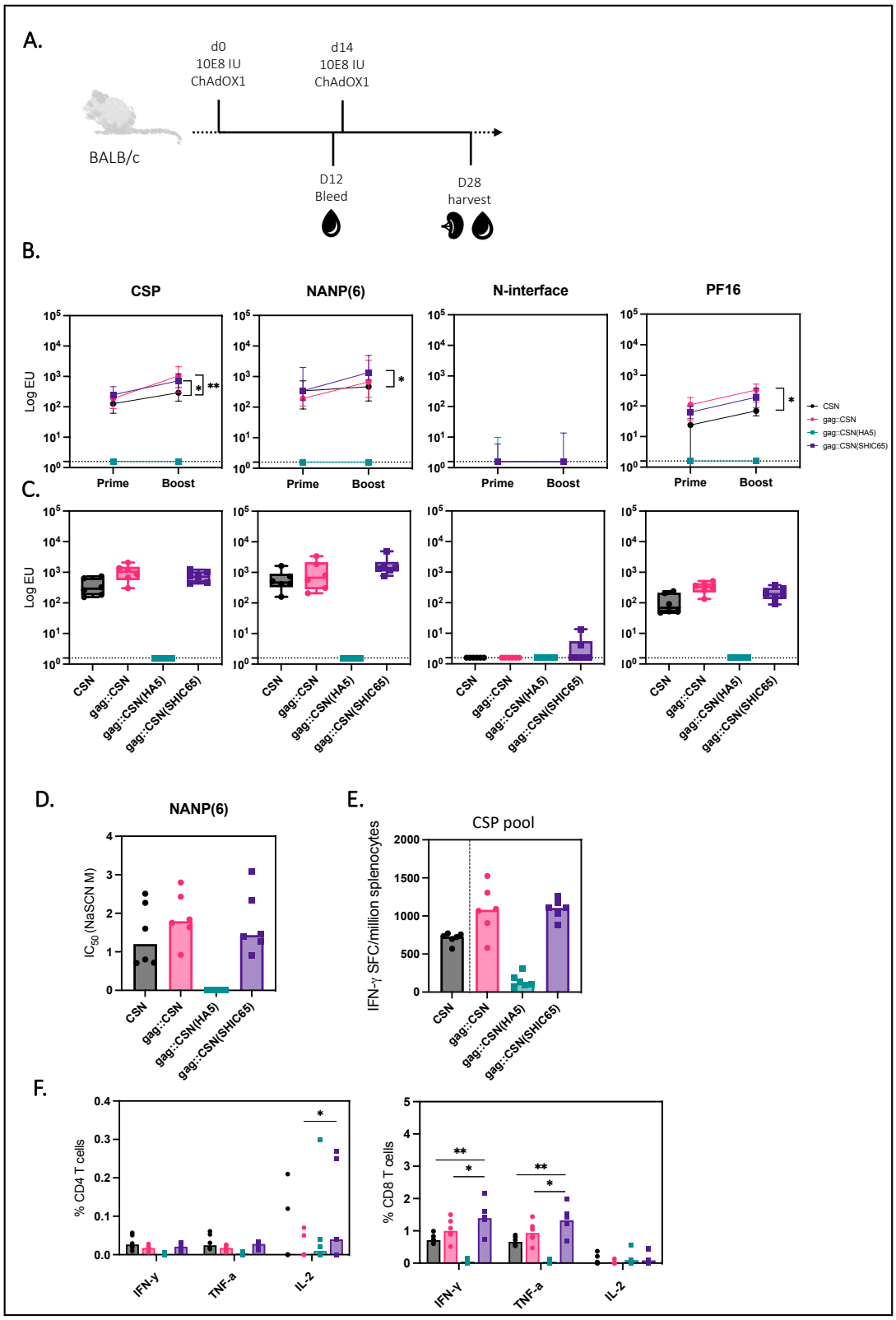


Figure 4.4. Humoral and cellular responses induced following prime-boost vaccination of ChAdOx1.

Groups of BALB/c mice were immunised with two doses of 10^8 IU ChAdOx1 encoding four different versions of CSN transgene, with two weeks between doses. Mice were sacrificed two weeks after the last dose, and spleens and blood harvested for subsequent assays. **B.** Median of antibody responses induced after prime and boost vaccinations against full-length recombinant CSP, Central terminal repeat (NANP6), junctional epitope

(N-interface), and C-terminal (PF16). **C.** Box and whisker plots show antibody response two weeks after a booster dose. **D.** Avidity of anti-NANP IgG measured by Avidity ELISA using NaSCN as chaotropic agent two weeks after a booster dose. **E.** Total T-cell responses measured by *ex-vivo* IFN-γ ELISpot assay following stimulation of splenocytes with a pool of CSP peptides two weeks after a booster dose. **F.** Functionality of CSP-specific $CD4^+$ and $CD8^+$ T-cells determined by production of IFN-γ, TNF-α or IL-2 cytokines. Bars represent each group's median, and single points indicate individual mice. ELISA and functionality of T-cell responses data were analysed with two-way Anova followed by Tukey multiple comparison test. The avidity of anti-NANP IgG data were analysed with Kruskal-Wallis's test, followed by Dunn's multiple comparison test. The data presented were representative of a single study. Asterisks indicate significant differences (*=$p<0.05$, **=$p<0.01$).

T-cell responses against CSP were measured by *ex-vivo* IFN-γ ELISpot assay. After two doses of vaccine, the magnitude of T-cell responses from mice receiving gag::CSN(HA5), was low and comparable to responses following a single low-dose of vaccine. Consistent with the single-dose ChAdOx1 immunisation data, total T-cell responses in mice immunised with two-doses of gag::CSN and gag::CSN(SHIC65) were higher compared to mice receiving CSN, albeit not statistically significant (Figure 4.4 E). In addition, using intracellular cytokine staining to measure T-cell function revealed a higher frequency of CSP-specific $CD8^+$ T-cell expressing IFN-γ in gag::CSN(SHIC65) vaccinated animals compared to CSN ($p<0.01$) or gag::CSN ($p<0.05$). Similar findings were also observed in the frequency of TNF-α^+ $CD8^+$ T-cells, with gag::CSN(SHIC65) vaccine inducing a higher proportion of TNF-α^+ $CD8^+$ T-cells than CSN ($p<0.01$) or gag::CSN ($p<0.05$). Meanwhile, the percentage of $CD4^+$ T-cells expressing IFN-γ, TNF-α^+, or IL-2 were comparable across vaccine groups (Figure 4.4 F). These data suggested that expressing CSN as nanoparticles with TM-CT from shark invariant chain as a protein anchor induced high antibodies and $CD8^+$ T-cells responses, much better than responses observed following vaccination with vector expressing CSN alone.

4.4. Confirmation of antigens expression encoded in ChAdOx1.

To confirm expression of CSN in the four different constructs, immuno-fluorescent assay (IFA) was performed. A549 cells were cultured in 6-well plates and transfected using lipofectamine and DNA plasmids-encoding each vaccine construct. 48 hours after transfection, cells were fixed and stained with 2A10 monoclonal antibody (mAb), which recognises the NANP repeat from the CSP antigen. 2A10 binding was detected by addition of an anti-mouse IgG antibody conjugated to Alexa fluorophore 488. IFA revealed the expression of CSN antigen from all DNA vaccine constructs with a distinct pattern between gag::CSN(SHIC65) compared to the other three constructs. Antigen expression in CSN, gag::CSN and gag::CSN(HA5) was brighter around the nucleus with a conglomeration structure observed across the cytoplasmic compartment. In contrast, the expression of CSN antigens in gag::CSN(SHIC-65) was distributed across cytoplasmic cells and most likely occurring on the cell surface (Figure 4.5 A).

To further evaluate the expression of CSP antigen on the cell plasma membrane, HeLa S3 cells were cultured in 6 wells plate and were transduced with ChAdOx1, at an MOI of 10, encoding each antigen construct. Following 48-72 hours of infection, cells were stained with three different antibodies: the mAb 2A10, sera from mice vaccinated with ChAd63-MVA encoding CSN or R21 followed by detection with anti-mouse IgG conjugated to Alexa fluorophore 488, the level of antibody binding was quantified by flow cytometry. As a control, cells were transduced with a ChAdOx1 encoding an irrelevant antigen, tPA-TROP, or left uninfected. Flow cytometry analysis revealed positive expression of CSP on the cell surface, around 38-48% (calculation data in appendix 4), from cells transduced with ChAdOx1 encoding gag::CSN(SHIC65). Surprisingly, the frequency of positive cells transduced with ChAdOx1-gag::CSN(HA5) was similar to cells transduced with CSN, tPA-

TROP or left uninfected. These result indicated that CSN from ChAdOx1-gag::CSN(HA5) was poorly expressed on the cell surface, although the IFA analysis detected CSN antigen from this construct. Meanwhile, the frequency of positive cells from ChAdOx1-gag::CSN was slightly higher than CSN or negative control. However, the histogram visualisation failed to separate this construct from the controls (Figure 4.5 B).

To determine whether CSP was being expressed as nanoparticles, HeLa cells were cultured in T75 flasks and infected with ChAdOx1 (MOI 10) encoding each vaccine construct. 72 hours after infection, the supernatant from each individual flask was harvested, clarified, and concentrated using 30% (w/v) sucrose cushion ultracentrifugation at 31000 rpm for 2 h at 4^{o}C with supernatants removed, and pellets resuspended in PBS for further analysis. In parallel, the cells from each culture were pelleted and lysed with a protease inhibitor cocktail containing M-PER buffer. Following incubation at 4^{o}C for 5 minutes, the cell lysates were separated from the debris by centrifugation at 13000 rpm for 5 minutes, and the supernatant transferred to clean microtubes prior to analysis of cellular and supernatant fractions by western-blot.

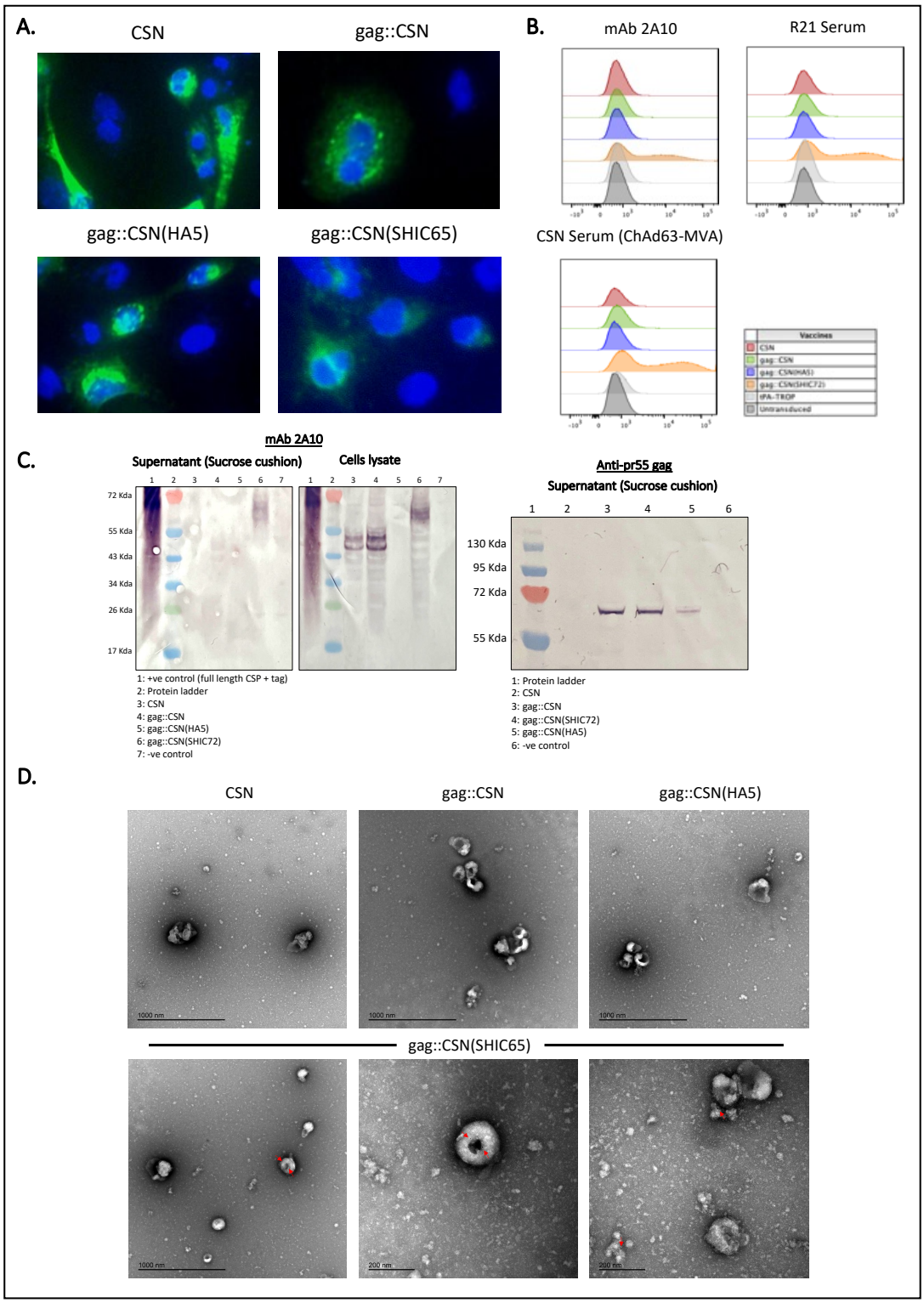


Figure 4.5 Expression of CSN antigens.

A. Immunofluorescent analysis (IFA) of A549 cells expressing CSN from four vaccine constructs. The expression of CSN antigens was detected by monoclonal antibody (mAb) 2A10 and anti-mouse IgG conjugate to AF488 (green). The nucleus was labelled with DAPI (blue). **B.** Histogram analysis of CSN antigen on the surface of HeLa S3 cells following transduction with ChAdOx1 (MoI=10) encoding different CSN constructs or irrelevant antigens, tPA-TROP. The expression of CSN on the cells' surface was detected with mAb 2A10,

serum from vaccinated mice with ChAd63-MVA, or R21 prior to being labelled with anti-mouse IgG conjugated to AF488 (green) and analysed by flow cytometry. **C.** Detection of CSN antigen from supernatant & cell lysate and **D.** Detection of pr55 gag in the supernatant using western blot and **E.** Immunogold labelling of pellet-containing extracellular vesicle from the supernatant after sucrose cushion centrifugation, from the HeLa S3 cells infected with ChAdOx1 (MoI=10) encoding different CSN constructs. The data from IFA, Flowcytometry and Western Blot analysis represent two to three replicate experiments.

The predicted molecular weight of SIV pr55 gag is around 57 kDa, with the residual amino acids from GSG-linker and self-cleaving peptides 2A; the total molecular weight of gag protein in the constructs was predicted to be around 60 kDa. The western blot analysis using polyclonal anti pr55gag from the pellet samples revealed the presence of proteins between 55 and 72 kDa from gag::CSN, gag::CSN(HA5) and gag::CSN(SHIC65) but not from the CSN construct or negative control, indicating gag proteins were successfully expressed and separated from CSN in VLP fusions. Additionally, western blot analysis showed the presence of CSN antigen in the cell lysate from cells infected with ChAdOx1 encoding CSN, gag::CSN and gag::CSN(SHIC65). Since the TM-CT from the Shark Invariant chain contains an additional 65 amino acids, fusing the CSN to this TM-CT increased the molecular weight of the antigen. Surprisingly, the assay did not detect the presence of CSN in the gag::CSN(HA) vaccine, suggesting poor expression of the CSN antigen in this construct. In contrast, western blot analysis using pellet samples detected the presence of CSN antigen only in cells transduced with ChAdOx1 encoding gag::CSN(SHIC65) (Figure 4.5 C), suggesting nanoparticle of CSP from gag::CSN(CHIC65) construct are present in the supernatant.

To further confirm whether CSN in the supernatant was expressed as nanoparticles, the pellet from sucrose cushion centrifugation were sent to Dunn School Bioimaging Facility for immunogold labelling and electron microscopy analysis following labelling with mAb

2A10. Immunogold analysis showed CSN was present in extracellular vesicles (EVs) from cells infected with gag::CSN(SHIC65) but not in any other construct. Notably, the density of EVs in the CSN construct was lower than vaccine construct containing gag antigen, indicating gag polyprotein's importance in producing enveloped VLPs. Collectively, these data suggested that CSN fused to TM-CT of Shark's invariant chain, successfully incorporated into enveloped VLPs using pr55 gag as the building block for the VLPs.

4.5. Two doses of ChAdOx1 did not protect mice from malaria following sporozoite challenge

To determine whether improvements in immunogenicity from ChAdOx1 expressing nanoparticle CSN also translated into improved efficacy, malaria challenge experiements were performed. Because the ChAdOx1-gag::CSN(HA5) construct was shown to express antigen poorly and led to low immunogenicity; the construct was excluded from efficacy studies. Six-week BABL/c mice were immunised twice with 10^8 IU of ChAdOx1 encoding CSN, gag::CSN or gag::CSN(SHIC65) in three weeks intervals. A group of mice were left unvaccinated to serve as infection controls. Mice were challenged three weeks after the last vaccination with 1000 transgenic *P. berghei* sporozoite expressing *Pf.* CSP 3D7 injected directly into the vein with mice monitored for 14 days or until they reached 1% parasitemia. All mice were bled two days before receiving the second dose or challenged (Figure 4.6 A).

Following challenge with sporozoites, all vaccinated and naïve mice developed parasitemia. However, mice immunised with gag::CSN(SHIC65) showed a higher median in the time taken to reach 1% parasitemia compared to mice receiving CSN, albeit this was not statistically significant (Figure 4.6 B, C). Consistent with previous data, gag::CSN(SHIC65) induced higher levels of antibodies against the full length of CSP and NANP(6) compared

to CSN or gag::CSN, although not significant in this experiment. In addition, a significantly higher anti-PF16 IgG was observed in gag::CSN ($p<0.05$) compared with CSN; higher levels of antibodies against PF16 were also observed in mice receiving gag::CSN(SHIC65) compared to CSN, albeit not significant. Antibody responses against the N-interface peptide from the majority of vaccinated mice were below the limit of detection (Figure 4.6 D).

To extend the analysis, Inhibition of Sporozoite Invasion (ISI) assays were performed to determine whether there was a difference in functional capacity of antibodies induced by different CSN constructs. A high frequency of Green Fluorescent Protein (GFP) positive cells were seen when cells were infected sporozoite plus serum from mice vaccinated with CSN. Meanwhile, cells incubated with sporozoite plus serum from gag::CSN or gag::CSN(SHIC65) vaccinated mice showed a higher reduction in the frequency of positive cells compared to CSN, suggesting more sporozoites were inhibited by serum containing antibodies from gag::CSN or gag::CSN(SHIC65) than CSN vaccine during invasion of the Huh7 cells *in-vitro*. When the % reduction was calculated based on the ratio between tested serum and control, cells incubated with sporozoite and media only, the percentage of inhibition was highest in serum samples from gag::CSN or gag::CSN(SHIC65) vaccinated mice compared to CSN vaccinated, again this was not statistically significant. Collectively, the improvement in the immunogenicity provided by ChAdOx1 expressing nanoparticle CSP translated into a moderate improvement in efficacy, primarily manifested in delaying time to parasitaemia and a higher percentage of sporozoite inhibition *in-vitro* [209].

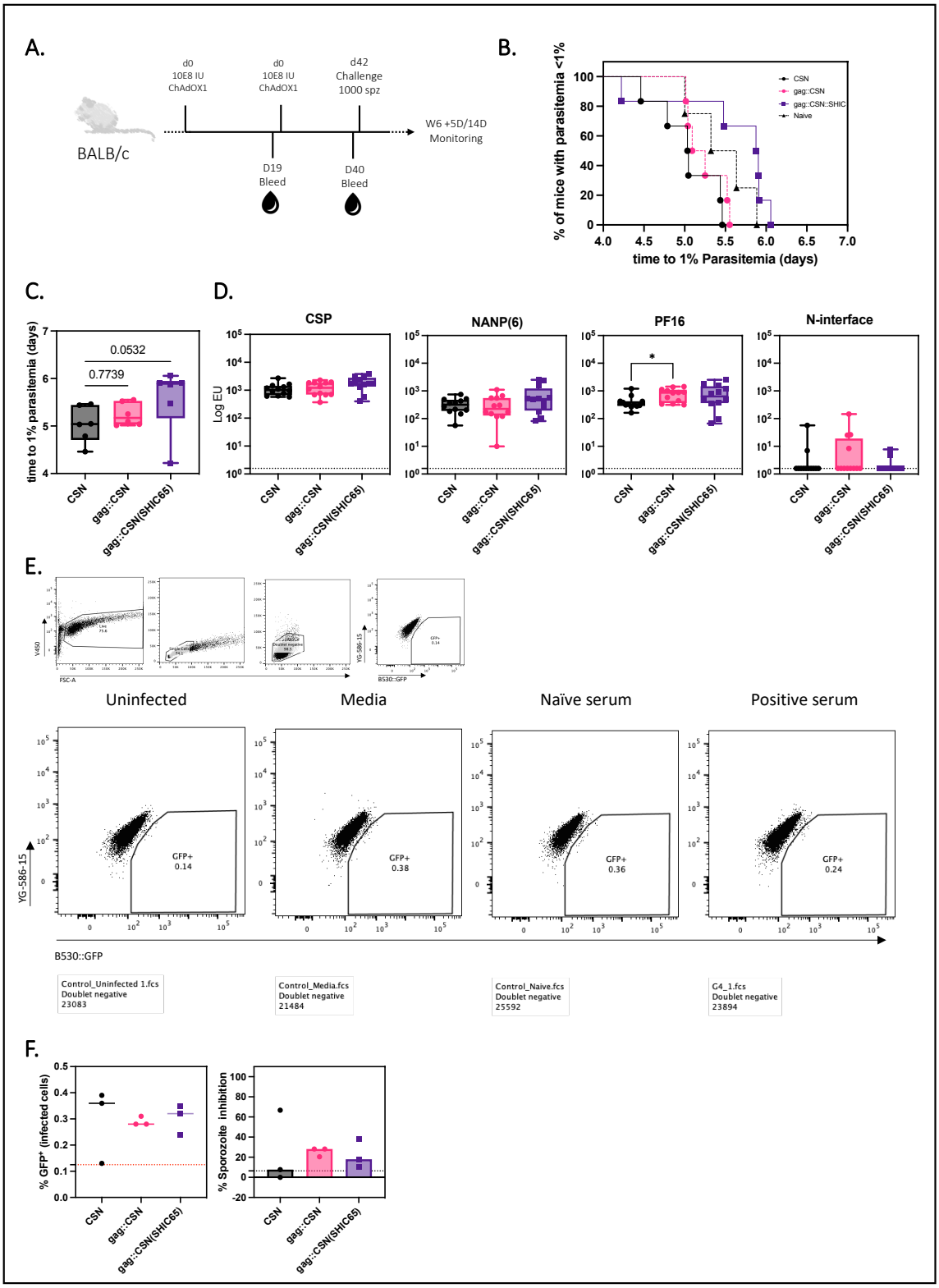


Figure 4.6 Efficacy 1 and functionality of antibody responses following prime-boost vaccination of ChAdOx1.

A. Groups of BALB/c mice were immunised with two doses of 10^8 IU of ChAdOx1 encoding four different versions of CSN transgene in three weeks interval. Three weeks after the last dose, all mice were challenged with 1000 transgenic *P. berghei* ANKA sporozoite expressing *Pf* CSP 3D7 protein and monitored for 14 days.

B. Protective efficacy of three different vaccines in BALB/c mice presented by the Kaplan-Meier survival curves. **C.** A box and whisker plot showing time to 1% parasitaemia induced by different CSN vaccines. **D.** A box and whisker plot showing antibody responses two days before challenge. **E.** Gating strategy for ISI assay and representative population from uninfected Huh7 cells or Huh7 cells that were incubated with sporozoite and media, naïve serum or positive serum. **F.** Percentage of Huh7 cells infected with sporozoites and percent inhibition induced by different CSN vaccine construct. The red dotted line shows the average frequency of uninfected cells, while the black dotted line represents the percent inhibition from naïve serum. The horizontal line or bar represents each group's median, single points indicate data from individual mice. Data were analysed with Kruskal-Wallis's test and Dunn's multiple comparison test. Experiment was repeated in duplicate. Data presented represent Asterisks indicate significant differences (*=$p<0.05$).

4.6. Towards multi-antigen pre-erythrocytic malaria vaccines.

Malaria parasites are known to use more than one ligand during host cell invasion. Therefore, an effective subunit malaria vaccine is likely required to target multiple antigens. While multiple antigens could be from the same phase of malaria development, a multi-stage antigen may increase the protection through different immune mechanisms. For example, CSP-based vaccines such as RTS,S/AS01 and R21 primarily induce protection through the production of antibodies against the central terminal repeat of CSP that neutralises sporozoites during their travel to the liver [149, 193, 333]. Meanwhile, antigen-specific $CD8^+$ T-cell induced by vaccination with viral vectors encoding TRAP antigen remove parasites by killing the infected hepatocytes in the liver [129, 204, 310].

Co-administration of vaccines targeting CSP and TRAP have been shown to improve protection in the preclinical model [193]. Initial clinical data from the combination of RTS,S/AS01, and ChAd63/MVA-ME-TRAP administered in a staggered regimen led to higher levels of protection than the administration of RTS,S/AS01 alone [334]. However, this study required five different clinical visits, which could be impractical for implementation. Interestingly, co-administration of RTS,S/AS01 and ChAd63/MVA-ME-TRAP induced lower anti-NANP antibodies than RTS,S/AS01 alone, leading to lower levels

of protection [335]. It was also found that co-administration of RTS,S/AS01, and ChAd63/MVA-ME-TRAP drives Th-1 biased responses that increase induction of $CXCR3^+$ circulated T follicular helper cells (Tfh) associated with lower antibody responses [336].

A combination of multiple antigens therefore requires further optimisation. Initial work in our group attempting to combine ME-TRAP and CSN in a single Adenovirus vector failed to induce immune responses against CSN to the same level of Adenovirus encoding CSN alone (data unpublished). However, when three filovirus antigens were inserted into a single cassette, E1, with the addition of a 2A self-cleaving sequence between the transgene, the trivalent vaccine induced similar levels of immunity to monovalent adenovirus encoding each of the three different filovirus antigens [337]. Moreover, in previous experiments, addition of P2A sequence between gag and CSN sequence has been shown to enable successful expression of the gag polyprotein separately to the CSN antigen.

Therefore, using the same strategy, DNA vaccines encoding optimised *Pf* TRAP 3D7 (TROP) and gag::CSN(SHIC65) (denoted as gCSN in this study) were constructed using pENTR4 plasmid backbone, enabling future transfer into BAC-ChAdOx1 genome for generation of ChAdOx1 vaccines. To evaluate whether antigen position in the construct affected immunogenicity, two different combinations were constructed, gCSN-TROP or TROP-gCSN. For comparison, DNA vaccines encoding monovalent TROP or gCSN vaccine were used (Figure 4.8A).

Groups of BALB/c mice were immunised twice with 50 μg of DNA vaccine with a two-week interval between doses. Two weeks after the final dose, mice were sacrificed with blood and spleens harvested and processed for further assays (Figure 4.8B). Following vaccination, CSP-specific T cell responses induced in the gCSN group were significantly

higher than TROP ($p<0.05$) but was non-significantly higher than gCSN-TROP or TROP-gCSN induced responses. Interestingly, comparable TRAP-specific T-cells responses were observed in mice receiving TROP, gCSN-TROP or TROP-gCSN. Surprisingly, mice vaccinated with the gCSN vaccine elicited TRAP-specific T-cell responses, albeit of lower magnitude than other vaccine that contain TRAP 3D7 in its construct ($p<0.05$). Meanwhile, all vaccine constructs induced lower T-cell responses against gag protein (Figure 4.8C).

The antibody responses against CSP were measured using NANP(6) ELISA, following vaccination we observed comparable anti-NANP IgG levels in mice immunised with gCSN, gCSN-TROP or TROP-gCSN. Although, the quartile range in TROP-gCSN was wider than gCSN-TROP, suggesting a more robust antibody response induced in the latter. Meanwhile, all vaccine constructs induced low anti-TRAP IgG responses. Together, these data showed the potential of this technique to combine two different antigens that target sporozoite and liver-stage malaria that requires further evaluation as a viral vector platform.

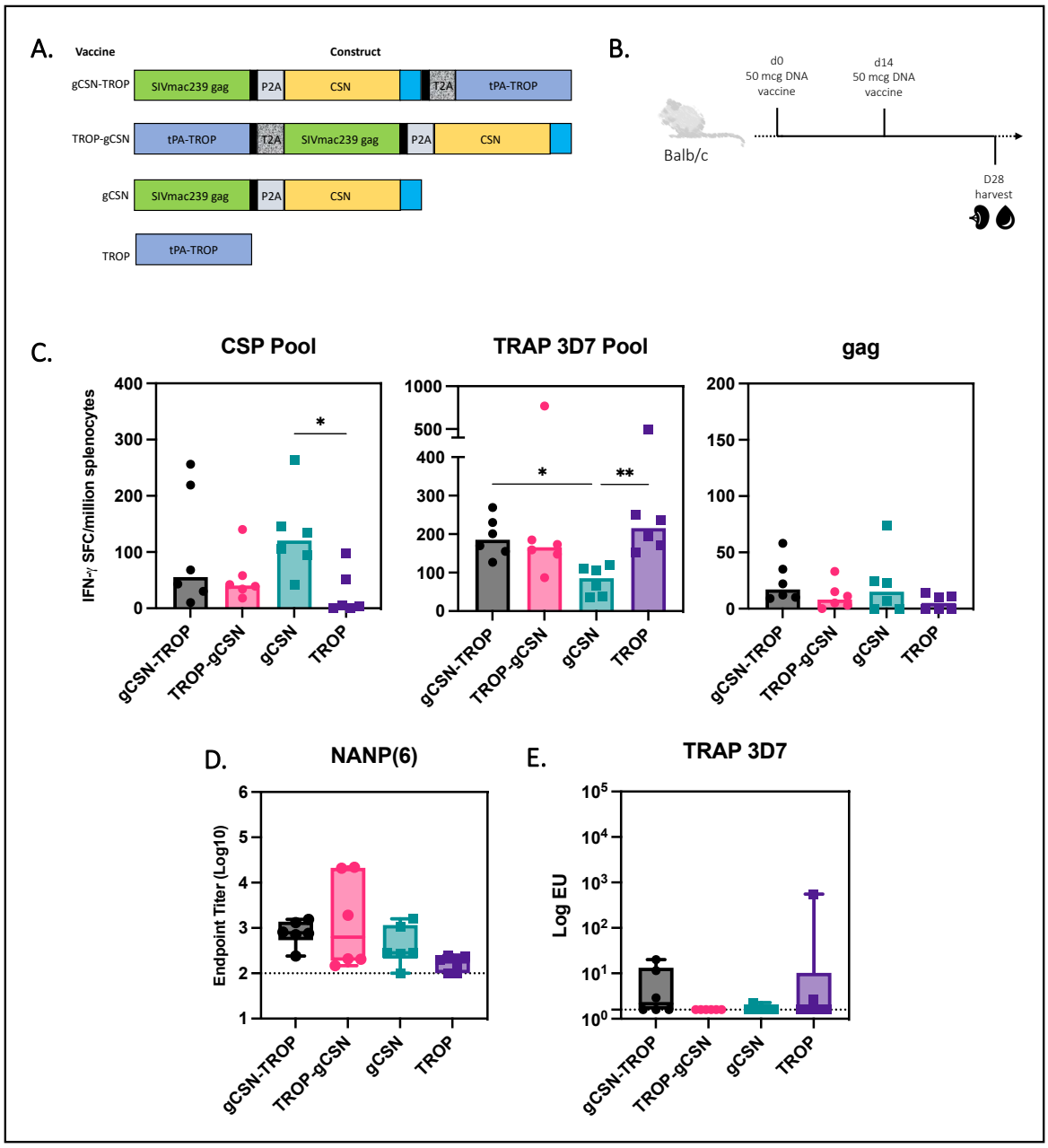


Figure 4.8 Immunogenicity of DNA vaccines encoding multi-pre-erythrocytic antigens.

A. Schematic of antigen construct encode in DNA vaccine using pENTR4 plasmid backbone. Similar to gCSN, which were linked by a P2A sequence, the gCSN and TROP antigens were linked using a self-cleaving 2A sequence from Thosea asigna virus (T2A). **B.** Groups of BALB/c mice were immunised with two doses of 50µg of DNA rwo weeks apart. Mice were sacrificed two weeks after the last dose, and spleens and blood harvested for subsequent assays. **C.** Total T-cell responses measured *ex-vivo* IFN-γ ELISpot response after splenocyte stimulation with CSP Pool, TRAP 3D7 Pool, or peptides representing gag protein. **D.** Anti-NANP IgG measured by endpoint ELISA **E.** Anti-TRAP IgG measured by standardised ELISA. The data in each graph was analysed with Kruskal-Wallis's test, followed by Dunn's multiple comparison test. The data presented were representative of a single study. Asterisks indicate significant differences (*=$p<0.05$, **=$p<0.01$).

4.7. Discussion.

An effective malaria vaccine is required to induce both arms of immune response to achieve high-levels of protection. While VLPs-based vaccines elicit high antibody response against the antigen target, Adenovirus vaccines are known to induce robust antigen-specific cellular responses. Here we investigated the possibility of combining two vaccine modalities, VLPs and Adenovirus, into a single platform to induce humoral and cellular immunity.

Gag polyprotein is the major structural protein in retroviral viruses. During the retroviral virion assembly, the enveloped glycoproteins is synthesised and translocated to the cell membrane. Simultaneously, the gag polyproteins are translated and recruited to the cell membrane and bind with the membrane lipid bilayer and multimerises, then together with the enveloped glycoproteins, results in budding and release of viral particles. While structural protein in other enveloped viruses, such as in influenza, require interactions with their enveloped glycoproteins to enable trafficking to the plasma membrane, the recruitment of gag polyproteins can occur independently of their enveloped glycoprotein. Therefore, the gag polyprotein is an attractive structural protein to use in developing enveloped VLPs vaccines [338-340]. Additionally, the assembly process of enveloped VLPs can occurred *in-vivo*, allowing them to be combined with other modalities, such as Adenoviral vectors. This combination strategy has been tested in preclinical studies targeting HIV [340, 341], placenta malaria [342], and colorectal cancer [343] and have been shown to induce potent cellular and humoral responses. In this chapter, Chimpanzee adenovirus vaccine, ChAdOx1, was constructed which encoded an enveloped VLPs displaying a modified full-length CSP antigen, using pr55 Gag polyprotein from Simian Immunodeficiency Virus, SIVmac293.

The gag polyprotein was constructed using the same cassette (E1) as the CSN antigen, this strategy has been shown previously to be more genetically stable than inserting the transgene in different locus, such as in E1 and E3 cassette [344]. Using the self-cleaving 2A sequence from porcine teschovirus-1 (P2A) to separate the proteins, antigens were inserted under a single human CMV immediate early promotor and BGH-derived polyadenylation signals to maintain the stoichiometry between the antigens. The P2A sequence is known to have high cleavage efficiency in human cell lines, zebrafish embryo and adult mice [331]; and in this study the gag polyprotein and CSN antigen were successfully expressed as separate intact proteins (Figure 4.3C).

Incorporating antigen targets into the plasma membrane requires a transmembrane and cytoplasmic domain (TM-CT) to act as an anchor and signal for protein trafficking. Addition of TM-CT from MMTV or influenza virus to the placenta malaria antigen, ID1-DBL2X-ID2a domains of VAR2CS that lack of TM-CT domain, successfully incorporated the antigen to the enveloped VLP when the antigen was administered in recombinant human adenovirus 5 [342]. In addition, the TM-CT sequence determined the abundancy of antigen incorporated into the cell membrane. For instance, replacing the endogenous TM-CT of HIV-1 enveloped protein with heterologous TM-CT sequence from the mouse mammary tumour virus (MMTV) or hemagglutinin of influenza virus (HA) has been shown to increase the incorporation of env to the membrane protein by around 15 and 6 fold, respectively, compared to endogenous TM-CT of env HIV-1 [345].

Since CSP lacks TM-CT and the GPI anchor in the CSN construct has been deleted to improve antigen expression, we fused the CSN antigen to the TM-CT domain of haemagglutinin 5 from the influenza virus. Previous studies have shown that TM-CT from the shark invariant chain can enhance $CD8^+$ T-cell responses, albeit this enhancement is

antigen-specific [266]. Invariant chain (Ii), or CD74, is a type-II membrane glycoprotein with multifaceted roles in antigen presentation and trafficking of MHC class II. During the MHC class II transfer, Ii creates a complex with the α and β chain, (αβIi)3. This complex is subsequently transferred to the membrane surface. On the surface of membrane, the complex is rapidly internalised with the foreign antigen and targeted to early endosomes where the Ii starts to be degraded [346]. However, in the case of excess production of Ii, the proteins are translocated to the cell membrane in the absence of MHC II [347].For this reason, CSN was fused to the TM-CT of the shark invariant chain intending to achieve high incorporation of CSN to the plasma membrane.

Flow cytometry analysis showed that the CSN antigen successfully translocated to the cell surface plasma membrane when the antigen was fused to the TM-CT from the shark Ii. Surprisingly, the flow cytometry analysis failed to detect CSN antigen with TM-CT from HA5 (Figure 4.5). Immunogenicity experiments showed that ChAdOx1 encoding gag::CSN(HA5) was less immunogenic than other CSN-VLP constructs or CSN alone. The low immunogenicity of the ChAdOx1-gag::CSN(HA5) was likely due to poor CSN antigen expression as western-blot analysis from HeLa S3 transduced by this ChAdOx1 vaccine failed to detect CSN antigen but not gag polyprotein. Sequencing analysis of the gag::CSN(HA5) transgene in BAC ChAdOx1 revealed a deletion of single nucleotide guanine at position 4 in the CSN sequence that changed the open reading from the CSN antigen. Hence, the CSN antigen but not the gag protein, was poorly translated in this construct. It was likely that the deletion occurred during recombination homolog between the entry vector and BAC of ChAdOx1, as the IFA analysis from the transfected A549 with plasmid encoding this contract was able to detect CSN expression. Consequently, this limits

myself from evaluating the impact of different TM-CT sequences on incorporating the antigen of interest in the VLP.

Although the ChAdOx1-gag::CSN(SHIC65) elicited significantly higher antibodies and $CD8^+$ T-cell responses compared to CSN alone, the vaccine did not sterilely protect BALB/c mice from malaria infection following challenge with transgenic *P. berghei* sporozoites expressing *Pf.* CSP 3D7. However, the vaccine did delay the time to parasitaemia and induced higher levels of inhibition against the invasion of sporozoite *in vitro*, albeit these were not statistically significant. It is therefore likely that the antibody responses induced by ChAdOx1-gag::CSN(SHIC65) was insufficient to protect the mice against a stringent challenge.

In the murine model, vaccination with the whole sporozoite induces antibody and T-cell responses against CSP associated with protection. Meanwhile, the protection induced by subunit CSP-based vaccine in humans correlates with antibodies that act against the extracellular phase of sporozoite. In contrast, T-cell mediated immunity against liver-stage malaria is observed in vaccination with a subunit TRAP-based vaccine, which killed the intracellular phase of the malaria parasite inside infected hepatocytes. Hence, multi-stage antigen vaccines containing CSP and TRAP may induce higher protection than individual CSP or TRAP subunit vaccines. Early experiments combined Pb TRAP and CSP using bidirectional promotors or inserted in the different locus of Adenovirus vector induced lower T-cell response than individual Adenovirus encoding TRAP or CSP antigen [348]. Here, using the P2A sequence, the multi-antigen malaria vaccine was evaluated. Early investigation using DNA vaccine showed that the vaccine was immunogenic and induced antibody responses against CSP and T-cell response against TRAP to a similar level to that

observed following vaccination with individual CSP and TRAP vaccines. Based on this early data, it is interesting to investigate further the immunogenicity of this multi-antigen CSP-TRAP vaccine in viral vectors, which was not performed in this thesis due to insufficient time.

In summary, the work described in this chapter has demonstrated the possibility of the Adenovirus vaccine encoding pre-erythrocytic malaria antigen expressed as a nanoparticle VLPs. Fusing the CSN antigen to the TM-CT of the shark invariant chain allowed the antigen to be incorporated into the VLPs and led to improved humoral and cellular responses.

4.7.1 Chapter summary

Below is the summary of findings that have been demonstrated in this chapter:

1. The gag::CSN(SHIC65) vaccine construct successfully expressed CSN antigen on the surface of enveloped VLP.
2. The gag::CSN(SHIC65) moderately induces higher antibody and T-cell responses in comparison to the CSN vaccine construct.
3. Vaccination with two doses of ChAdOx1 encoding gag::CSN(SHIC65) confers a higher median of delayed time to 1% parasitaemia compared with two doses of ChAdOx1-CSN.
3. Constructing multi-antigen gag::CSN(SHIC65) and tPA-TROP into a single cassette using ribosomal skipping sequence induced comparable antibody and T-cell responses compared to individual antigens.

5

Broadening antibody responses towards different CSP domains by heterologous vaccination

5.1 Introduction

Many subunit malaria vaccines in development target the circumsporozoite protein which is expressed on the sporozoite surface and plays a critical role in sporozoite invasion of hepatocytes. The rationale for selecting CSP as the target antigen was derived from observation that whole sporozoite vaccination induces antibodies mainly to CSP protein [86, 87, 96, 97, 349]. In addition, serum transfer from humans vaccinated with whole sporozoite vaccination (WSV) protects mice from malaria infection after challenge with transgenic *P. berghei* sporozoite expressing *P. falciparum* CSP [294]. Hypothetically, antibodies that recognise CSP can avert malaria by neutralising sporozoites before hepatocyte infection. The structure of CSP protein consists of three domains: N-terminus (ntCSP), central repeat region (central CSP), and C-terminus (ctCSP). Although the number of tetrapeptide NANP (major repeat) varies between parasite strains, CSP from *P. falciparum* 3D7 contains 38 major repeat of NANP and 1 NVDP (minor repeat) in central domain of CSP [350, 351]. Upstream of the central region, a tetrapeptide NPDP together with major and minor repeats form the junctional region NP-DPNA-NPNV-DPNA followed by interspersed minor NPNV-DPNA (Figure 5.1).

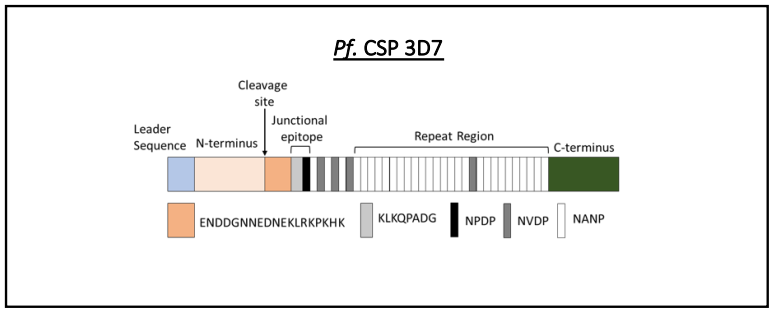


Figure 5.1 Schematic diagram of Pf. CSP 3D7.

The CSP protein consists of an N-terminal domain, a central repeat region and a C-terminal domain containing a GPI anchor. The central repeat region of Pf. CSP 3D7 is comprised of 38 major repeat NANP tetrapeptides interspersed by minor repeat NVDP and NPDP.

Early characterisation of antibodies against CSP focused on the repeat region of CSP [86, 87]. Murine monoclonal antibodies that recognised major repeat NANP from RAS-vaccinated mice were found to inhibit sporozoite invasion *in-vitro* and *in-vivo* [87, 89]. Correspondingly, a human monoclonal antibody that recognises the same epitope, NANP, was shown to provide sterilising immunity [352]. In recent years, the exploration of humoral immunity against CSP has been expanded to other CSP regions. The fact that ntCSP and ctCSP have essential roles in parasite infectivity corroborated this endeavour [22, 353]. A monoclonal antibody, 5D5, derived from RAS-vaccinated mice, recognises the highly conserved Region I (RI) in the ntCSP, which contains the proteolytic site of CSP, and was found to block CSP processing and inhibit infection *in-vivo* [354]. Recently, human monoclonal antibodies that bind to the junctional Region (CSI43 and MGG4) and interspersed minor (L9) were found to effectively neutralise sporozoites and block sporozoite infection [198, 199, 355]. Remarkably, passive immunisation with mAb CIS43 provided protection against malaria challenges in human clinical trials [356]. Meanwhile, the characterisation of the humoral response against ctCSP has led to the discovery of a few mAbs capable of reducing liver parasite burden [357]. Although these mAbs did not provide sterilising immunity, antibody responses against ctCSP from humans vaccinated with CSP-

based vaccines were associated with protection [358]. Together, these data demonstrate why diversification of antibody responses against the different domains of CSP is a plausible strategy to increase protection against malaria.

Despite having relatively low efficacy and short-live protection, RTS,S/AS01, has received WHO recommendation to be used among children in sub-Saharan and other regions with moderate to high malaria transmission [13]. RTS,S/AS01 were constructed based on the truncated version of CSP – i.e. 18 NANP repeat and C-terminal region [359]. The vaccine is given as three doses with a 1-month interval, plus an additional dose one year later. Data from phase III trials showed that the vaccine induces high titres of anti-NANP antibodies but these titres wane rapidly in the first six months following the last-dose of vaccine [14, 191]. The next generation of RTS,S-like vaccine, R21, is currently in clinical development with promising results in the two years of follow-up [149]. The vaccine was constructed based on a similar antigen construct to RTS,S but has higher malaria antigen density on the VLP [193].

High anti-NANP IgG titres are associated with protection [360]. However, a recent finding suggests that a high titre of anti-NANP IgG promotes antibody feedback limiting NANP-specific B-cell expansion, resulting in plateauing antibody response after administering the first booster [361]. Importantly, the limit for anti-NANP titre to promote antibody feedback is below the threshold of anti-NANP titre to induce protection [361]. Consequently, repeat malaria vaccine administration will not optimally boost antibody responses, and complete sterile protection will be challenging to achieve. Furthermore, it has been thought that the dominance of NANP repeat masks other vulnerable site among CSP, such as junctional epitope and interspersed minor repeat [362, 363]. The passive transfer of mAb CIS43 and

L9 has elegantly demonstrated these protective epitopes [198, 355]. However, early vaccine development based solely on junctional epitopes induced antibody responses that reduced parasite burden in the liver, but did not achieve sterilising immunity [364, 365], suggesting immune responses to NANP repeat are also necessary for sterile protection. Therefore, inducing a balanced immune response towards different protective regions within CSP may promote long-lasting protection against malaria infection.

To induce immune response towards different regions of CSP, the antigen construct needs to contain ntCSP, central CSP and ctCSP. But production of recombinant full-length CSP has been challenging [190, 320-323, 366]. The previous chapter described the construction a ChAdOx1 vaccine encoding modified full-length CSP antigen expressed as nanoparticles (gag::CSN(SHIC65). Although two doses of ChAdOx1 gag::CSN(SHIC65) did not provide sterile protection, this construct induced higher antibody and T-cell responses compared to Adenovirus-expressed soluble CSP. In addition, antibodies induced by this vaccine recognised full-length CSP, the junctional region, NANP repeat and ctCSP, albeit antibody titres towards the junctional region were minimal. In recent studies, heterologous vaccination using Adenovirus and protein in adjuvant was reported to induce broader T-cell and antibody responses compared to homologous Adenovirus or homologous protein in adjuvant vaccination regimens [342, 367]. Using a similar approach, the work described in this chapter investigated whether heterologous vaccination using ChAdOx1 gag::CSN(SHIC65) and booster with protein VLP displaying junctional epitope of CSP could induce a more diverse immune response towards the different regions of CSP and whether this could improve vaccine efficacy.

Results:

5.2. Comparison of immune response induced by viral vector and protein VLP vaccines in outbred mice.

Antibody titres against NANP repeat region correlate highly with protection from sporozoite challenge [333]. It seems likely that antibody titres induced by Adenovirus vaccines are insufficient to provide sterile protection. Work presented in the previous chapter showed that two doses of Adenovirus encoding different CSN constructs did not protect BALB/c mice from sporozoite challenge. To get a better understanding of why sterile protection is not induced by Adenoviral vaccines, a head-to-head comparison between viral vectors vaccines encoding CSN antigen with R21 was performed. R21 is a virus-like particle vaccine similar to RTS, S, that has previously been shown to provide complete protection even when administered at ultra-low doses (0.05 μg/dose) [194]. Because of limited access to Matrix-M used in human clinical trial [148] (due to IP reasons), R21 in these studies was formulated in Addavax, a preclinical grade oil-in-water adjuvant that previously has been shown to enhanced immune response against CSP, albeit to a lesser extent than Matrix-M or MF59 adjuvants in pre-clinical study [193].

Viral vector vaccines were administered in heterologous prime-boost Adenovirus-MVA regimen, a clinically relevant regimen that has been shown to induce robust CSP-specific antibody and T-cell responses [195]. Two types of Adenoviral vector, ChAd63 (an Adenovirus chimpanzee that was used in a previous human clinical trial) and ChAdOx1, both encoding CSN, were used to prime mice and MVA-CSN was used as the booster. In addition, mice were primed with the recent ChAdOx1 construct that expresses CSN as a nanoparticle, ChAdOx1-gag::CSN(SHIC65). Using outbred mice that harbour high genetic diversity, CD-1 mice received either three doses of 0.5 μg R21/Addavax in three weeks

intervals or heterologous Adenovirus prime and MVA boost with 8 weeks between vaccines. Mice were bled at week 3, week 6 and week 9 (where all groups had completed vaccinations). At the end of the experiment, week 15, mice were sacrificed, spleens and blood were harvested and processed for further analysis (Figure 5.2 A, B).

Kinetic analysis showed that anti-NANP IgG levels significantly increased ($p<0.01$) following each dose of R21/Addavax given in the R,R,R vaccination group. The antibody titre peaked at week 9, three weeks after the last R21 vaccination but had significantly decreased ($p<0.01$) by week 15. Similar observations were also found in mice vaccinated with viral vectors. The titre of anti-NANP IgG was significantly increased and peaked one week after the administration of MVA compared to 6 weeks after Adenovirus priming ($p<0.01$). Although a slight increase in anti-NANP IgG levels were observed at week-6 following Adenovirus priming, compared to week-3, a statistically significant difference ($p<0.05$) in antibody responses at week 6 compared with week-3 was only observed in mice primed with Cx1(gag::CSN(SHIC65)). Meanwhile, the titre of anti-NANP IgG was significantly decreased at week-15 compared to week-9 in all mice receiving viral vector vaccines (Figure 5.1 C). When the titre of antibody responses across vaccination groups was compared at each peak time point, a significantly lower (1 log) antibody titre was observed in mice vaccinated with viral vectors compared to mice immunised using R21 (Figure 5.2 D).

To extend the analysis, the cellular responses induced following different vaccination regimens was compared. Using flow cytometry, NANP-specific B-cells in the spleen were identified by antigen-fluorochrome tetramer staining. NANP-specific B-cell populations were separated from total B-cell population by combining two NANP-tetramer stains (Figure 5.1 F), all vaccination regimens induce comparable numbers of NANP-specific B-

cells. A higher number of plasmablast cells were observed in R,R,R and C63(CSN)-MVA groups compared to Cx1(CSN)-MVA or Cx1(-gag::CSN(SHIC65))-MVA, albeit this was not statistically significant. Meanwhile, a higher number of germinal centre (GC) B-cells were observed in mice immunised using C63(CSN)-MVA or Cx1(gag::CSN(SHIC65))-MVA compared to R,R,R or Cx1(CSN)-MVA regimens, although this was also not significant. In addition, comparable isotype class switch B-cells were observed in all vaccination regimens (Figure 5.1 G). To complete the analysis, total T-cell responses were measured by *ex-vivo* IFN-γ ELISpot assays. Consistent with previous finding, higher CSP-specific T-cell responses were induced in mice immunised using any Adenovirus-MVA compared with protein-VLP (R21) albeit this was not significant (Figure 5.2 E). Together, these data suggest that although vaccination with viral vector encoding CSN antigen induced robust antibody and T-cell responses, the magnitude of anti-NANP IgG was lower than vaccination using protein VLP R21.

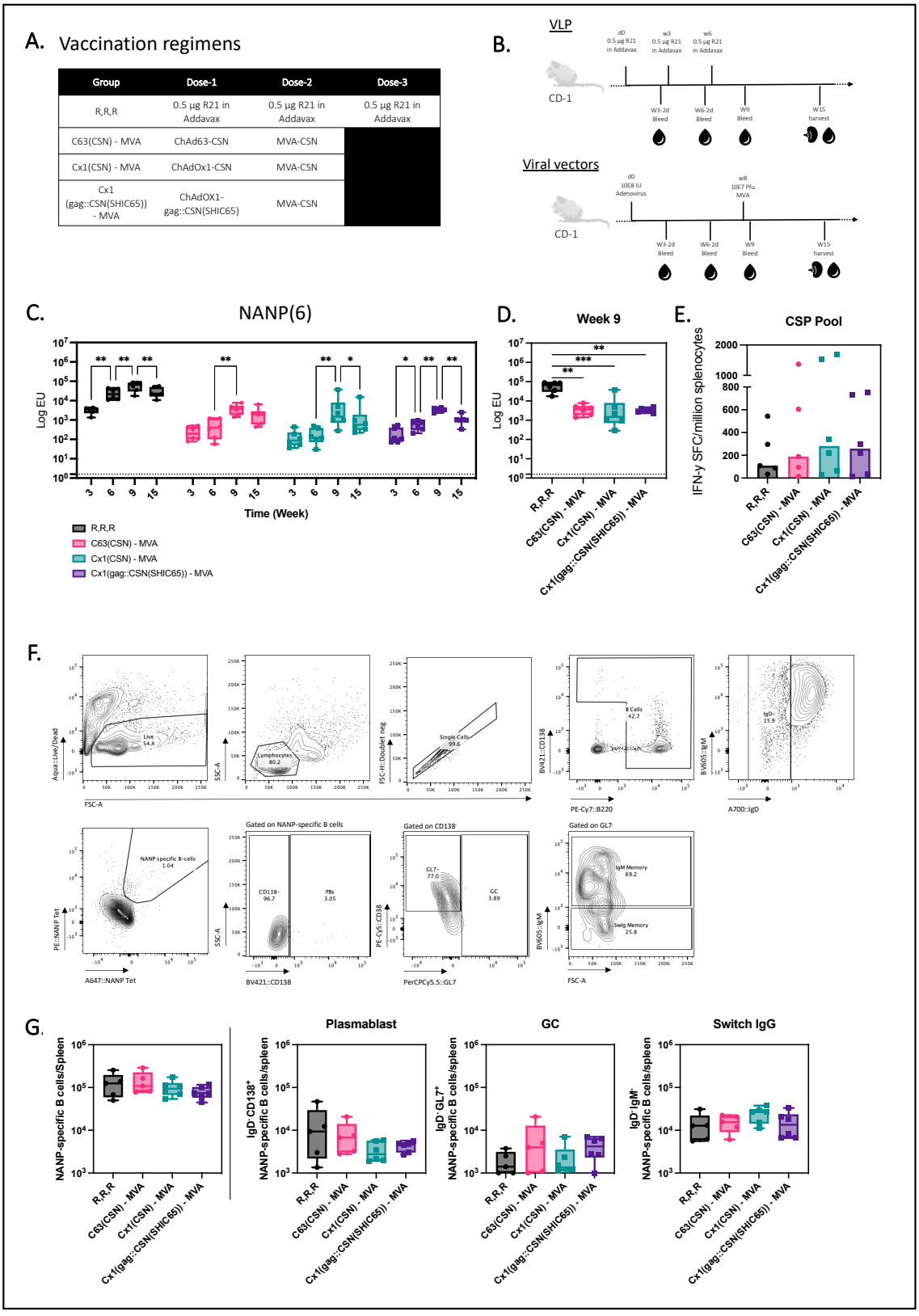


Figure 5.2 Humoral and cellular responses induced by VLP or viral vector vaccination.

A. Vaccinations group to compare the immunogenicity of VLP and viral vectored vaccines. **B.** CD-1 mice were vaccinated with three doses of 0.5 µg R21 formulated in Addavax in three weeks intervals or heterologous

Adenovirus – MVA prime-boost in an 8 week interval. At week-15, the mice were sacrificed, spleens and blood harvested for subsequent assays. **C.** A box and whisker plot showing the time course of anti-NANP IgG induced by four different vaccination regimens. **D.** A box and whisker plot showing anti-NANP IgG titres across vaccination groups at the peak time point. **E.** Total CSP-specific T-cell responses measured by *ex-vivo* IFN-γ ELISpot assay from splenocytes stimulated with a pool of CSN peptides. **F.** Gating strategy to identify NANP-specific B-cells in the spleen **G.** A box and whisker plot showing the total number of NANP-specific B-cells, plasmablast, GC and isotype class switched B-cells in the spleen. Data was analysed using a two-way Anova followed by Tukey multiple comparison test. The data presented were representative of a single study. Asterisks indicate significant differences (*=$p<0.05$, **=$p<0.01$).

5.3. Heterologous vaccinations induced broad antibody responses to different regions of CSP in inbred mice.

In the seminal study, in addition to NANP major repeat, the CSP antigen contained other protective epitopes at the junctional region and interspersed minor repeat that are not contained in RTS,S or R21 vaccine construct [198, 199, 355, 368]. Early studies of vaccines targeting the junctional region demonstrated a reduced parasite burden in the liver but did not prevent infection in vaccinated mice following malaria challenge [364, 365]. Indicating immune response to protective epitope from NANP major repeat is also required to achieve sterile protection. Therefore, this study investigated whether balancing immune responses towards different protective epitopes could be induced by heterologous vaccination. ChAdOx1 gag::CSN(SHIC65) was used to prime the immune response against different domains across CSP antigen, this response was then boosted with a VLP targeting the junctional region of CSP. This VLP was constructed by fusing the highly conserved region I and junctional epitope to the Hepatitis B surface antigen (HBsAg) and expressed in *P. pastoris* system similar to R21, hence denoted as R21-G1 (Figure 5.3A). The R21-G1 used in this study were constructed, produced, and provided by Ekta Mukhopadhyay and Ahmed Salman (manuscript in preparation).

BABL/c mice were allocated into four group. Group numbers 1 and 2 received homologous immunisation using three doses of 0.5 μg of either R21 or R21-G1 formulated in Addavax. Meanwhile, the 3rd and 4th groups were immunised in a heterologous regimen using one dose of 10^8 IU of ChAdOx1 encoding gag::CSN(SHIC65) followed by two doses of either 0.5μg R21/Addavax or R21-G1/Addavax in three weeks interval. Mice were bled three weeks after receiving each vaccination and sacrificed at week 15 (Figure 5.2 B, C). Antibody responses were measured towards full-length recombinant CSP, major repeat NANP (NANP6), junctional region (N-interface peptide) and C-term (PF16 peptide) (Figure 5.3 B, C).

Following vaccination, kinetic analysis showed that anti-CSP IgG levels increased following each dose administered across the vaccination groups and peaked at week-9, three weeks after the last dose of vaccine. Interestingly, the administration of the second dose of R21-G1 in the G1,G1,G1 group boosted the anti-CSP antibodies by at least 3 log Elisa Units, followed by plateauing phase after the administration of the third dose. Similar patterns were also observed in anti-NANP IgG, the administration of the second dose boosted the production of anti-NANP IgG, but the response plateaued after the third dose in all vaccination groups except in C,R,R group, which, surprisingly, decreased following the second dose in this group. While the first vaccine dose in each group induced limited antibodies against junctional epitope (N-interface), the administration of the second dose boosted antibodies responses to this region in all groups. Responses peaked after the third immunisation with the highest titre observed in G1,G1,G1 group. As expected, mice vaccinated with three doses of R21-G1 did not elicit antibodies against the C-terminal region at any time point, as this vaccine lacks a C-terminal domain. Additionally, boosting with R21-G1 after priming with ChAdOx1 did not increase anti-PF16 IgG in C,G1,G group. In

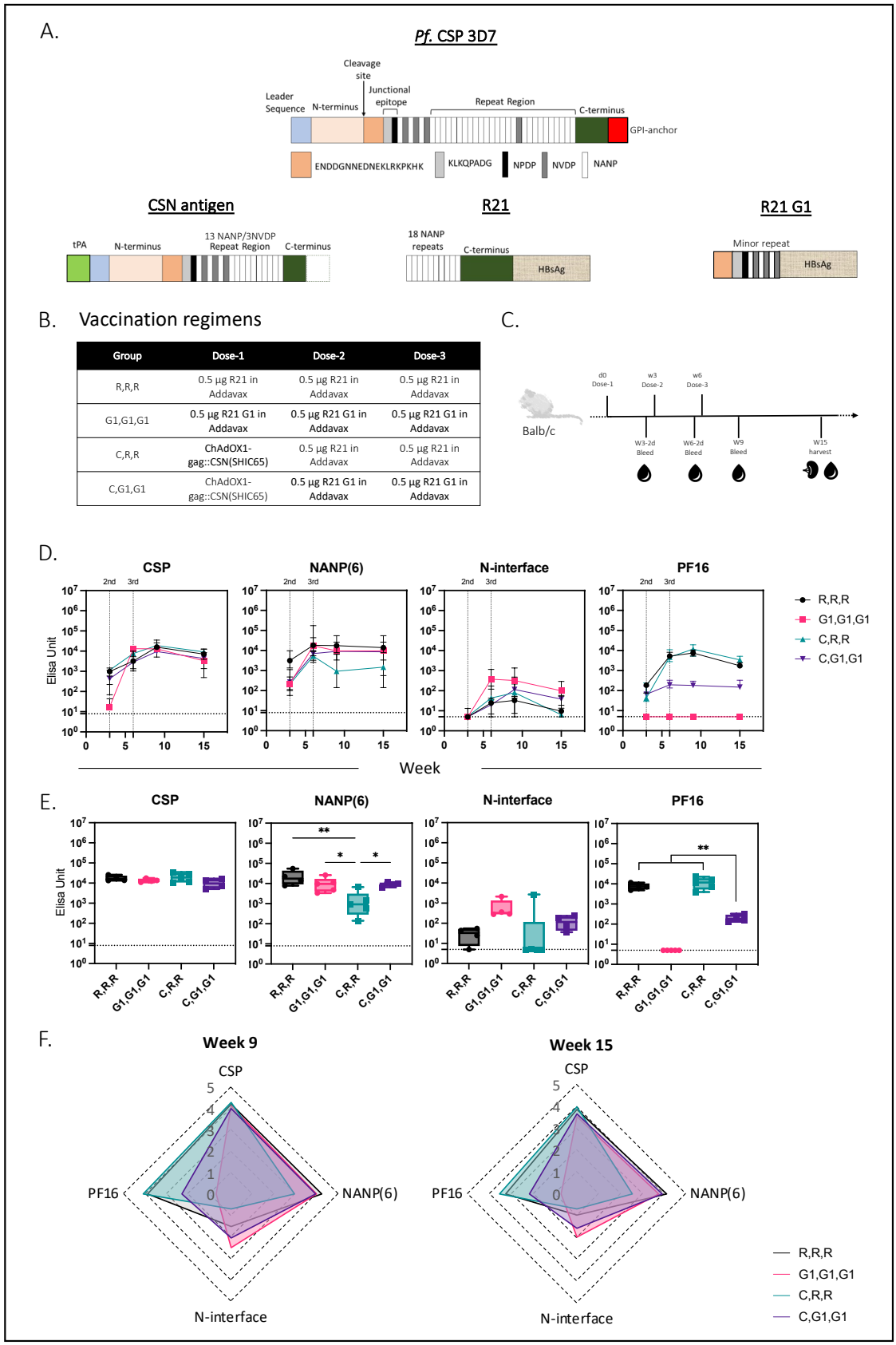
contrast, the anti-C-term antibodies were increased following each dose given in R,R,R or C,R,R group (Figure 5.3 D).

At the peak time point (week 9 since the first dose), all vaccine groups elicited comparable levels of anti-CSP IgG. Meanwhile a significant lower anti-NANP IgG titre was observed in the heterologous C,R,R group compared to homologous R,R,R ($p<0.01$), G1,G1,G1 ($p<0.05$) or heterologous C,G1,G1 ($p<0.05$). In addition, a higher antibody response against the junctional epitope was observed in mice vaccinated with homologous G1,G1,G1 or heterologous C,G1,G1 compared to vaccination with homologous R,R,R or heterologous C,R,R, albeit this was not statistically significant. In contrast vaccination with homologous R,R,R or heterologous C,R,R induced significantly ($p<0.01$) higher anti-C term IgG compared to heterologous C,G1,G. Homologous G1,G1,G1 did not elicit antibodies that recognised C-terminal domain of CSP (Figure 5.3 E), as expected.

Spider charts were used to visualise the median antibody responses induced against different regions of CSP across all vaccination groups. At the peak time-point (week-9), antibody responses in mice vaccinated with homologous R,R,R group was biased towards full-length CSP, NANP and C-terminal domain with minimum response toward the junctional epitope. In contrast, mice that received homologous G1,G1,G1 vaccines produced more antibodies recognising the junctional epitope, with high titre antibodies towards CSP and NANP(6); however, these mice lacked anti-C term IgG compared to homologous R,R,R vaccination. Heterologous C,R,R vaccination reduced the responses towards NANP compared to homologous R,R,R, and the majority of antibody responses were skewed towards full-length CSP and C-terminal domain with minimal antibodies that bound to the junctional region. In contrast, heterologous C,G1,G1 vaccination elicited anti-CSP and anti-NANP IgG to a comparable level with homologous R,R,R with a robust and balanced response towards N-

interface and C-terminal domain compared to homologous G1,G1,G1. Week-15 antibody response patterns were similar to week-9 patterns, with a reduction in magnitude observed at this point (Figure 5.3 F). Collectively, these data suggest that priming with full-length CSP and boosting with the vaccine-targeted junctional region induced balanced antibody responses towards different regions of CSP.

To complete the analysis, T-cell responses were compared. At the end of the experiment, splenocytes from vaccinated mice were stimulated with CSP peptide pools, and total T-cell responses measured using *ex-vivo* IFN-γ ELISpot assays. As expected, minimal T-cell responses were induced after three doses of homologous R,R,R or G1,G1,G1. In contrast, mice vaccinated with heterologous C,R,R ($p<0.01$) or C,G1,G1 ($p<0.05$) elicited higher T-cell responses compared to mice receiving three doses of homologous VLPs. Meanwhile, no statistical differences were observed in T-cell responses between C,R,R and C,G1,G1 groups, suggesting priming with a single dose of ChAdOx1 vaccine effectively rescued the T-cell response. Subsequently, functional analysis using ICS assay showed that the majority of CSP specific-$CD8^+$ T-cells induced in mice vaccinated with heterologous C,R,R or C,G1,G1 produced significantly higher levels of IFN-γ and TNF-α than any homologous VLPs group. Meanwhile, the frequency of CSP-specific $CD4^+$ T-cell producing IFN-γ, TNF-α or IL-2 were comparable across the group (Figure 5.4 A, B).



Group	Dose-1	Dose-2	Dose-3
R,R,R	0.5 µg R21 in Addavax	0.5 µg R21 in Addavax	0.5 µg R21 in Addavax
G1,G1,G1	0.5 µg R21 G1 in Addavax	0.5 µg R21 G1 in Addavax	0.5 µg R21 G1 in Addavax
C,R,R	ChAdOX1-gag::CSN(SHIC65)	0.5 µg R21 in Addavax	0.5 µg R21 in Addavax
C,G1,G1	ChAdOX1-gag::CSN(SHIC65)	0.5 µg R21 G1 in Addavax	0.5 µg R21 G1 in Addavax

Figure 5.3 Antibody responses following homologous and heterologous vaccinations in BALB/c mice. **A.** Illustration of antigen construct, CSN, R21 and R21-G1 compared to wild-type CSP antigen from *Plasmodium falciparum* 3D7. **B.** BALB/c mice were allocated into four different groups to receive either three

doses of VLPs, 0.5µg of R21/Addavax or R21-G1/Addavax, or a single dose of 10^8 IU ChAdOx1 encoding gag::CSN(SHIC65) followed by two doses of either R21/Addavax or R21-G1/Addavax. **C.** BALB/c mice were immunised in three-week intervals and bled three weeks after each vaccination. At the week-15 timepoint, mice were sacrificed with spleens and blood harvested for subsequent assays. **D.** Kinetics of antibody responses with interquartile range, induced by different vaccination groups against full-length CSP, NANP(6), N-interface (junctional region) and PF16 peptide (represent C-terminal domain). The vertical dotted lines indicates the timing for administration of the 2nd and 3rd doses. Meanwhile, the horizontal dotted lines indicates the lower limit of detection in each assay **E.** A box and whisker plot showing the total IgG response induced against CSP, NANP(6), N-interface and PF16 three weeks following the last vaccination. **F.** Spider plot showing the antibody responses against CSP and different domains of CSP antigen from different vaccination groups at week-9 (left) and week 15 (right). The data presented were representative of a single study.

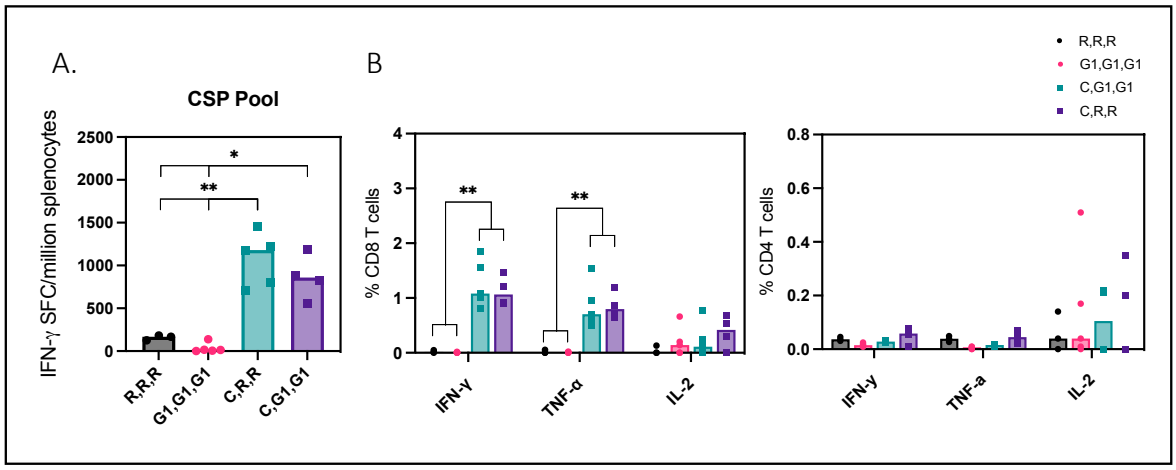
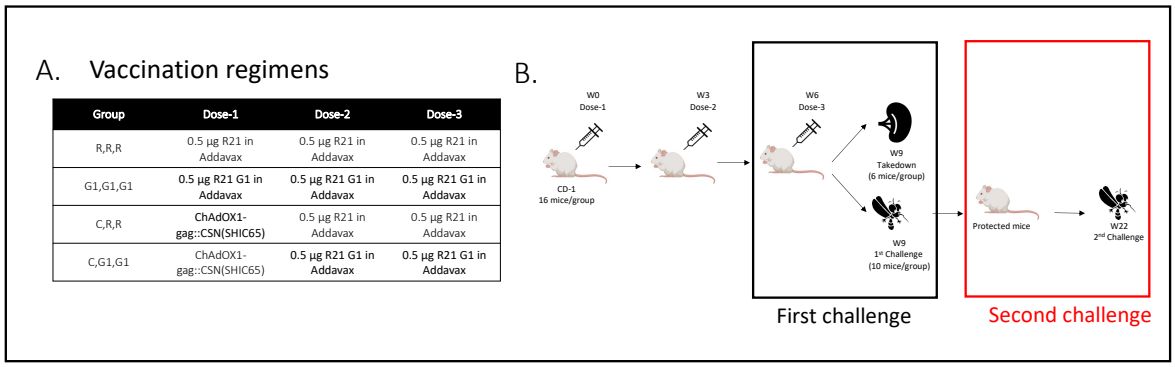


Figure 5.4 T-cells responses following homologous and heterologous vaccinations in BALB/c mice.

.A. Total T-cell responses were measured by *ex-vivo* IFN-γ ELISpot assay following splenocytes stimulation with a pool of CSP peptides at the final timepoint (week-15). **B.** Functionality of CSP-specific $CD4^+$ and $CD8^+$ T-cells producing IFN-γ, TNF-α or IL-2 cytokines. The bar represents each group's median, and single points indicate individual mice. Data was analysed with two-way Anova followed by Tukey multiple comparison test. Asterisks indicate significant differences (*=$p<0.05$, **=$p<0.01$).

5.4 Heterologous vaccinations induced broad antibody responses to different regions of CSP in outbred mice.

A similar experiment was repeated in outbred mice. Sixty-four CD-1 mice (n= 16/group) were allocated into four groups, similar to Figure 5.3B. After receiving the third dose of vaccine, 6 mice per group were sacrificed for cellular immune response analysis. Meanwhile, the remaining mice (10 mice/group) were challenged with 1000 transgenic *P. berghei* ANKA sporozoite expressing *P. falciparum* CSP (Pb(PfCSP)). Previously, three doses of R21 have been shown to induce high-level of protection against malaria challenge in mice; therefore, to test the durability of the immune response induced by each vaccination regiment, a second challenge was administered to the mice from each group, which shown sterile protection after the first challenged. (Figure 5.4 A,B).



Group	Dose-1	Dose-2	Dose-3
R,R,R	0.5 µg R21 in Addavax	0.5 µg R21 in Addavax	0.5 µg R21 in Addavax
G1,G1,G1	0.5 µg R21 G1 in Addavax	0.5 µg R21 G1 in Addavax	0.5 µg R21 G1 in Addavax
C,R,R	ChAdOX1-gag::CSN(SHIC65)	0.5 µg R21 in Addavax	0.5 µg R21 in Addavax
C,G1,G1	ChAdOX1-gag::CSN(SHIC65)	0.5 µg R21 G1 in Addavax	0.5 µg R21 G1 in Addavax

Figure. 5.5 Design experiment to evaluate immunogenicity and efficacy of four different vaccination regiment.

A. CD-1 mice were allocated into four different groups to receive either three doses of VLPs, 0.5µg of R21/Addavax or R21-G1/Addavax, or a single dose of 10^8 IU ChAdOx1 encoding gag::CSN(SHIC65) followed by two doses of either R21/Addavax or R21-G1/Addacax. **B.** The CD-1 mice were immunised in three-week intervals and bled three weeks after each vaccination. Six mice per group were sacrificed at week-15 with spleens and blood collected and processed for downstream analysis. The remaining mice (10 mice per group), including the additional naïve group, were challenged with 1000 transgenic *P. berghei* ANKA sporozoite expressing Pf CSP 3D7 protein and monitored for 11 days. The protected mice were re-challenged three months later.

Consistent with the initial immunogenicity study in BALB/c mice (Figure 5.3), the magnitude of anti-CSP IgG levels increased following each vaccine dose and peaked at week-9, when the mice were challenged with transgenic Pb(PfCSP) sporozoites, followed by a decreased in anti-CSP IgG titres three months later (at the time point of the second challenge). Similar patterns were also observed in the kinetic of anti-NANP IgG levels across all vaccination groups. In agreement with WSV or vaccination using RTS,S/AS01 [361, 369], the titre of anti-NANP IgG was only marginally boosted by administering the third dose in all vaccination groups. In contrast, antibodies that bound to the junctional region were found to increase following each dose and peaked at week-9 in mice immunised with homologous G1,G1,G1 or heterologous C,G1,G1 vaccine. Meanwhile, the titre of antibodies binding to junctional epitope plateaued after administration of the second dose in the R,R,R of C,R,R group. Interestingly, mice immunised with heterologous C,R,R or C,G1,G1 had an increase in antibody titre to the junctional region at week 22. In contrast, the titre of anti-N-interface IgG was decreased in homologous R,R,R or G1,G1,G1 group. As expected, homologous R,R,R or heterologous C,R,R vaccination induced a high titre of anti-C-term IgG and peaked at the three weeks following the last vaccination. As expected, R21-G1/Addavax did not induce anti-C-term IgG at any time point. Meanwhile, consistent with immunogenicity data in BALB/c mice, G1/Addavax did not boost the antibody titre to the C-term region in the heterologous C,G1,G1 group. (Figure 5.6 A).

To investigate further, antibody responses at the time point before the first challenge (week-9) were compared across all vaccination groups. Anti-CSP IgG in the homologous R,R,R group was significantly higher than in homologous G1,G1,G1 ($p<0.01$), or heterologous C,R,R ($p<0.05$) and C,G1,G1 ($p<0.01$) groups. However, antibodies against central repeat region NANP were comparable across all vaccination groups. In contrast, significantly

higher antibody titres against the junctional epitope were observed in mice immunised with homologous G1,G1,G1 vaccine compared to homologous R,R,R ($P<0.01$) or heterologous C,R,R group ($p<0.01$). Mice in the heterologous C,G1,G1 group also elicited higher titre of anti-N-interface IgG compared to mice in the homologous R,R,R or heterologous C,R,R, albeit this difference was not statistically significant. Meanwhile, no statistical difference in the titre of anti-N-interface IgG was observed between homologous G1,G1,G1 and heterologous C,G1,G1 vaccination. In addition, mice immunised with homologous R,R,R or heterologous C,R,R had a significantly higher antibody to Cterm region compared to mice vaccinated with heterologous C,R,R at the time of first challenge. Meanwhile, no anti-C term IgG was detected at the first challenge time point in the homologous G1,G1,G1 group (Figure 5.6 B).

To extend the analysis, antibodies' avidity against different CSP regions was measured using NaSCN as a chaotropic agent. Three weeks after the last vaccination, a significantly higher anti-NANP IgG avidity was observed in mice receiving homologous R,R,R compared to mice in homologous G1,G1,G1 ($p<0.01$) or heterologous C,G1,G1 ($p<0.05$) group. A higher, but not significant, anti-NANP IgG avidity was also observed in mice immunised with heterologous C,R,R compared to homologous G1,G1,G1 or heterologous C,G1,G1 group. Additionally, antibodies that bound to the junctional region were found to have low avidity in all vaccine groups. Meanwhile, anti-C-term IgG in mice receiving the homologous R,R,R vaccine had a higher avidity index compared to the heterologous C,G1,G1 group ($p<0.05$); but were comparable with heterologous C,R,R group. Since R21-G1 did not contain any C-terminal domain in its vaccine construct, the avidity of anti-C-term IgG in homologous G1,G1,G1 group was not assessed (Figure 5.6 C).

Consistent with immunogenicity data in BALB/c mice (Figure 5.3), spider chart plotting revealed that antibody responses in mice receiving homologous R,R,R or heterologous C,R,R skewed towards full-length CSP, NANP, and C-terminal domain with minimum antibodies from this vaccination group recognising the junctional epitope. In contrast, the majority of antibodies induced by homologous G1,G1,G1 bound to the full-length CSP, NANP and junctional epitope, with no antibody responses detected towards the C-terminal domain. Meanwhile, immunisation with heterologous C,G1,G1 elicited high antibody responses that bound to full-length CSP and NANP but with balanced responses towards junctional epitope and C-terminal domain (Figure 5.6 D).

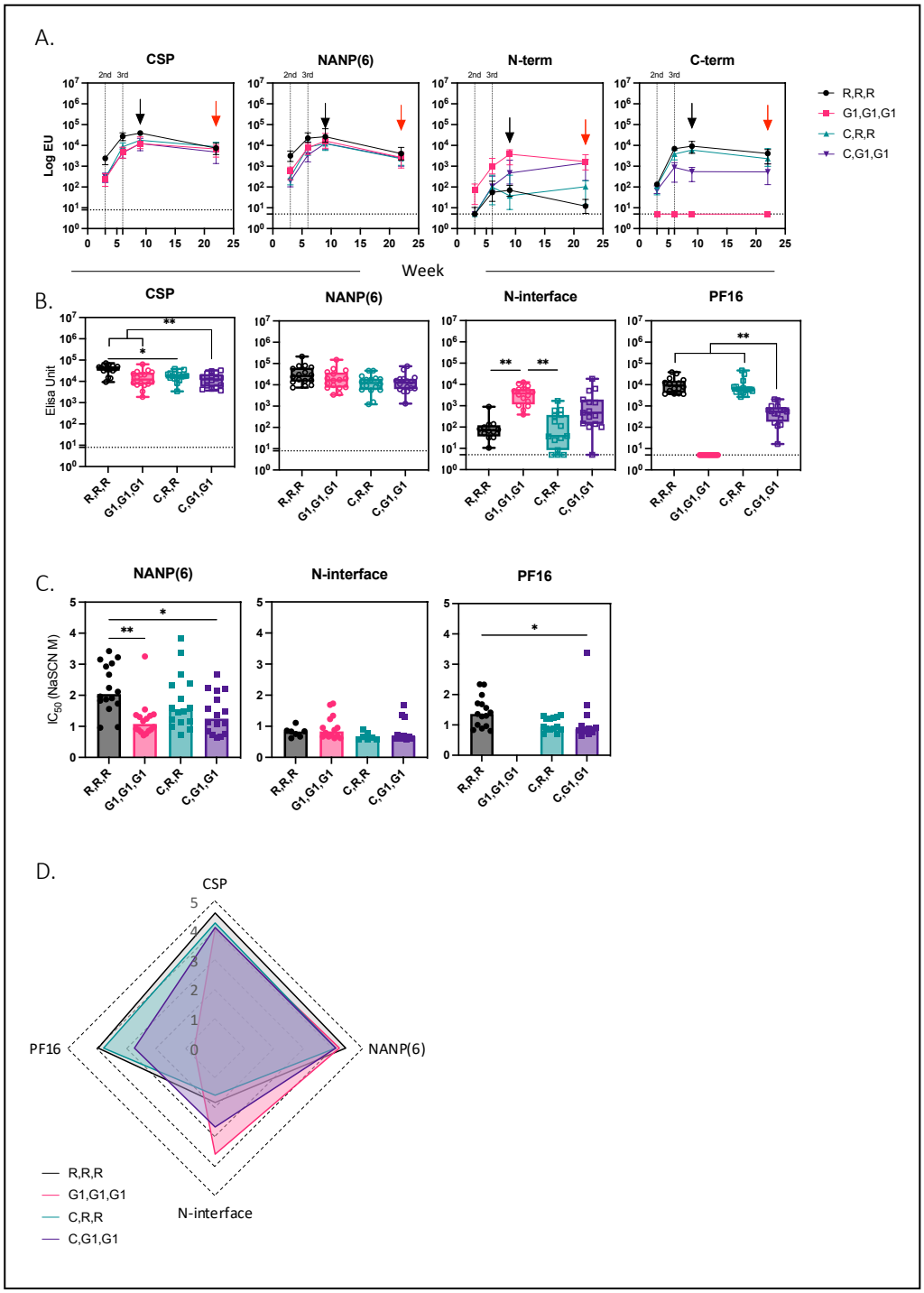


Figure 5.6 Antibody responses following homologous and heterologous vaccination in CD-1 mice.

A. Kinetics of median antibody responses with interquartile ranges, induced by different vaccination groups against full-length CSP, NANP(6), N-interface (junctional region) and PF16 peptide (represent C-terminal domain). The black and red arrows indicate the time point of the first and second sporozoite challenge, respectively. The vertical dotted lines indicate the timing for administration of the 2nd and 3rd doses. Meanwhile, the horizontal dotted lines indicate the lower limit of detection in each assay. **B.** Box and whisker plot showing the total IgG responses induced against full-length CSP, NANP(6), N-interface (junctional region) and PF16 peptide (represent C-terminal domain) at the time of the first challenge (three weeks

following the last vaccinations). **C.** Avidity of antibodies against different regions of CSP measured by Avidity ELISA using NaSCN as a chaotropic agent prior to the first challenge (three weeks following the last vaccinations). The bar represents each group's median, and single point indicates individual mice. **D.** Spider plot shows antibody responses to CSP and its different domains prior to the first challenge (three weeks following the last vaccinations). Data in B and C were analysed with Kruskal-Wallis's test, followed by Dunn's multiple comparison test. Asterisks indicate significant differences (*=p<0.05, **=p<0.01).

5.5. Cellular immunity following homologous and heterologous vaccination in CD-1 mice.

Cellular responses induced by homologous or heterologous vaccination were also measured. At time of the first challenge, 6 mice from each group were sacrificed, with spleens harvested and processed using the technique and gating strategy as in previous experiments (Figure 5.2). Splenocytes were aliquoted and stimulated with a pool of CSP peptides and functionality measured using *ex-vivo* IFN-γ ELISpot and ICS assays. Although T-cell responses in CD-1 mice showed more variability than in BALB/c mice, due to diverse MHC repertoires, the results were consistent. Mice primed with a single dose ChAdOx1 followed by two doses of VLPs induced higher T-cell responses compared to mice immunised with homologous VLPs, confirming the Adenoviral vector's potency in inducing T-cell responses (Figure 5.7 A, B).

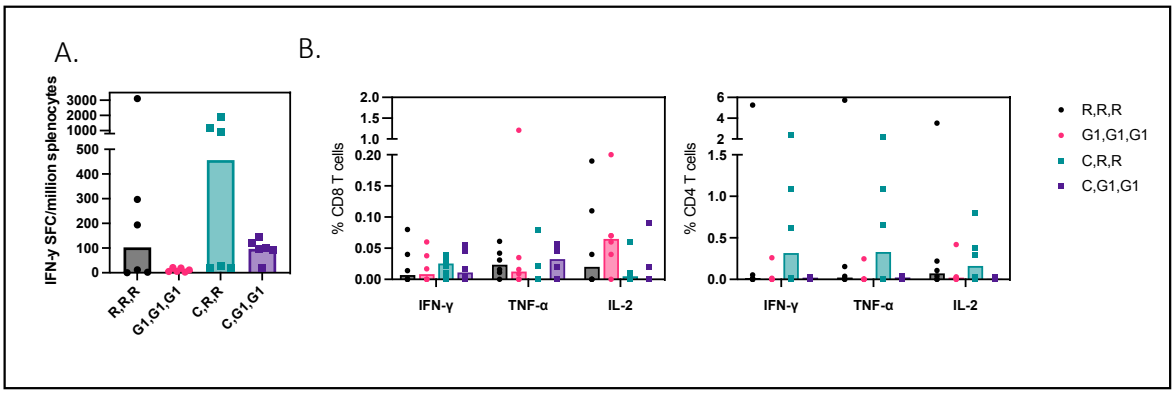


Figure 5.7 T-cells responses following homologous and heterologous vaccinations in CD-1 mice.

A. Total T-cell responses was measured by *ex-vivo* IFN-γ ELISpot assay of splenocytes stimulated with a pool of CSP peptides three weeks after the last vaccinations. **B.** Functionality of CSP-specific $CD4^+$ and $CD8^+$ T-

cell in terms of production of IFN-γ, TNF-α or IL-2 cytokines. The bar represents each group's median, and single point indicates individual mice. Data were analysed with Kruskal-Wallis's test and Dunn's multiple comparison test.

Some aliquots of splenocytes were also stained for B-cell analysis. Following surface B-cell specific staining, NANP-specific B-cells were detected in all vaccine groups, with the highest number observed in the homologous R,R,R group. A significantly higher number of NANP-specific plasmablasts ($p<0.05$) and isotype class switch B-cells were also observed in homologous R,R,R compared to other vaccination groups, albeit the NANP-specific switched IgG in homologous R,R,R was only significant when compared with heterologous C,G1,G1 group. Meanwhile, NANP-specific germinal centre B-cell numbers were comparable across all vaccine groups (Figure 5.9).

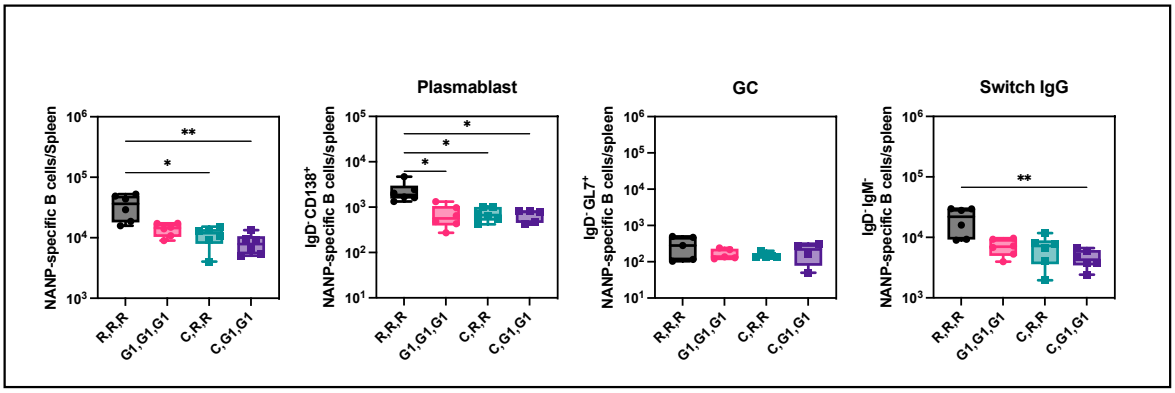


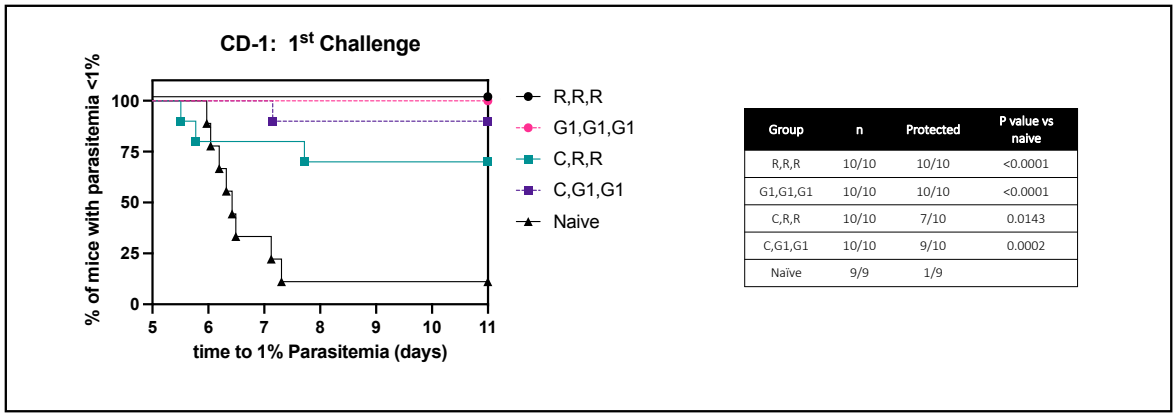
Figure 5.8 B-cell responses following homologous and heterologous vaccination in CD-1 mice.
Box and whisker plots showing the total number of NANP-specific: B-cells, plasma blast, GC and isotype class switched B-cells in the spleen. Data were analysed with Kruskal-Wallis's test and Dunn's multiple comparison test. Asterisks indicate significant differences (*=$p<0.05$, **=$p<0.01$).

5.6. All vaccination regimens induced high-level protection against the first malaria challenge.

To determine whether differences in immune responses induced by homologous and heterologous vaccinations could influence the protection against malaria infection, challenge experiments were performed. Three weeks after the last vaccination, 10 mice from

each group were were challenged with 1000 transgenic *P. berghei* ANKA sporozoite expressing *P. falciparum* CSP (Pb(PfCSP)). For the control, 10 naïve CD-1 mice were also challenged; one of the mice from the naïve group was taken down within 24 hours as this mouse showed hunched posture, piloerection, and reduced movement one day after being challenged and, therefore, was excluded from analysis (Figure 5.9).

As expected, complete protection was achieved in mice vaccinated with homologous R,R,R. Interestingly, mice that received three doses of homologous G1,G1,G1 were also completely protected. Although not all mice were protected, heterologous C,R,R vaccination provided high-level protection, with 7 out of 10 sterilely protected. Meanwhile, 9 out of 10 mice were sterilely protected after receiving heterologous C,G1,G1 vaccination.



Group	n	Protected	P value vs naive
R,R,R	10/10	10/10	<0.0001
G1,G1,G1	10/10	10/10	<0.0001
C,R,R	10/10	7/10	0.0143
C,G1,G1	10/10	9/10	0.0002
Naïve	9/9	1/9	

Figure 5.9. Efficacy following homologous and heterologous vaccinations – The first challenge.

Protective efficacy of four different vaccine groups in CD-1 mice after the first sporozoite challenged, presented in the Kaplan-Meier survival graphs. The survival curves were compared by Log-rank (Manter-Cox) with Bonferroni correction (p=0.013). The p-value of each vaccination group was presented in the table. The data presented were representative of a single study.

5.7. Broad antibody responses to different regions of CSP were maintained in heterologous C,G1,G1 vaccination regimen prior the second challenge.

Before the second challenge, antibody levels from the sterile mice from the first challenge were characterised. Three months after the first challenge, anti-CSP and anti-NANP IgG titres were comparable in all vaccination groups. Meanwhile, the titre of antibodies against junctional region in mice immunised with homologous R,R,R or heterologous C,R,R were significantly low compared to homologous G1,G1,G1 or C,G1,G1 group. In addition, only a few mice in homologous R,R,R or heterologous C,R,R had detectable antibodies to the junction region at the time of the second challenge (week-22). Meanwhile, no statistical difference in anti-N interface IgG titres were observed between homologous G1,G1,G1 and heterologous C,G1,G1 group. While the antibodies targeting the C-terminal domain were absent in homologous G1,G1,G1 group, the titre of anti-PF16 IgG remained high in mice vaccinated with homologous R,R,R or heterologous C,R,R. In addition, a lower antibody anti-C term was observed in heterologous C,G1,G1 compared to homologous R,R,R or heterologous C,R,R group; however, this was not statistically significant (Figure 5.10 A).

Visualisation of antibody responses at the second challenge using spider chart showed that antibody responses in the homologous R,R,R or heterologous C,R,R group remained skewed towards CSP, NANP(6) and C term. Importantly, antibody responses against the junctional epitope were minimal in heterologous C,R,R, to almost negligible in the homologous R,R,R group. The responses to the C term remained absent in the homologous G1,G1,G1 group, while antibody responses against NANP(6) and CSP remained high. Notably, high titre of anti-CSP and anti-NANP IgG with proportional antibodies binding junctional epitope and C-terminal domain were maintained in heterologous C,G1,G1 group (Figure 5.10 B).

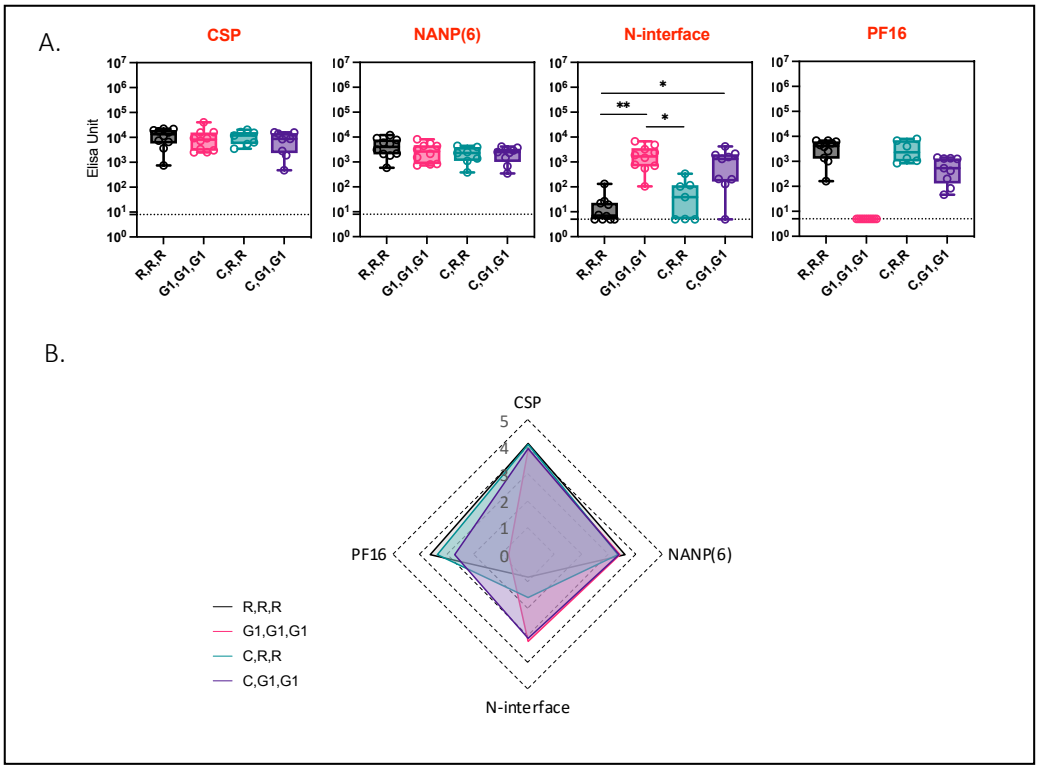


Figure 5.10 Antibody responses following homologous and heterologous vaccination in CD-1 mice at the second challenge time point.

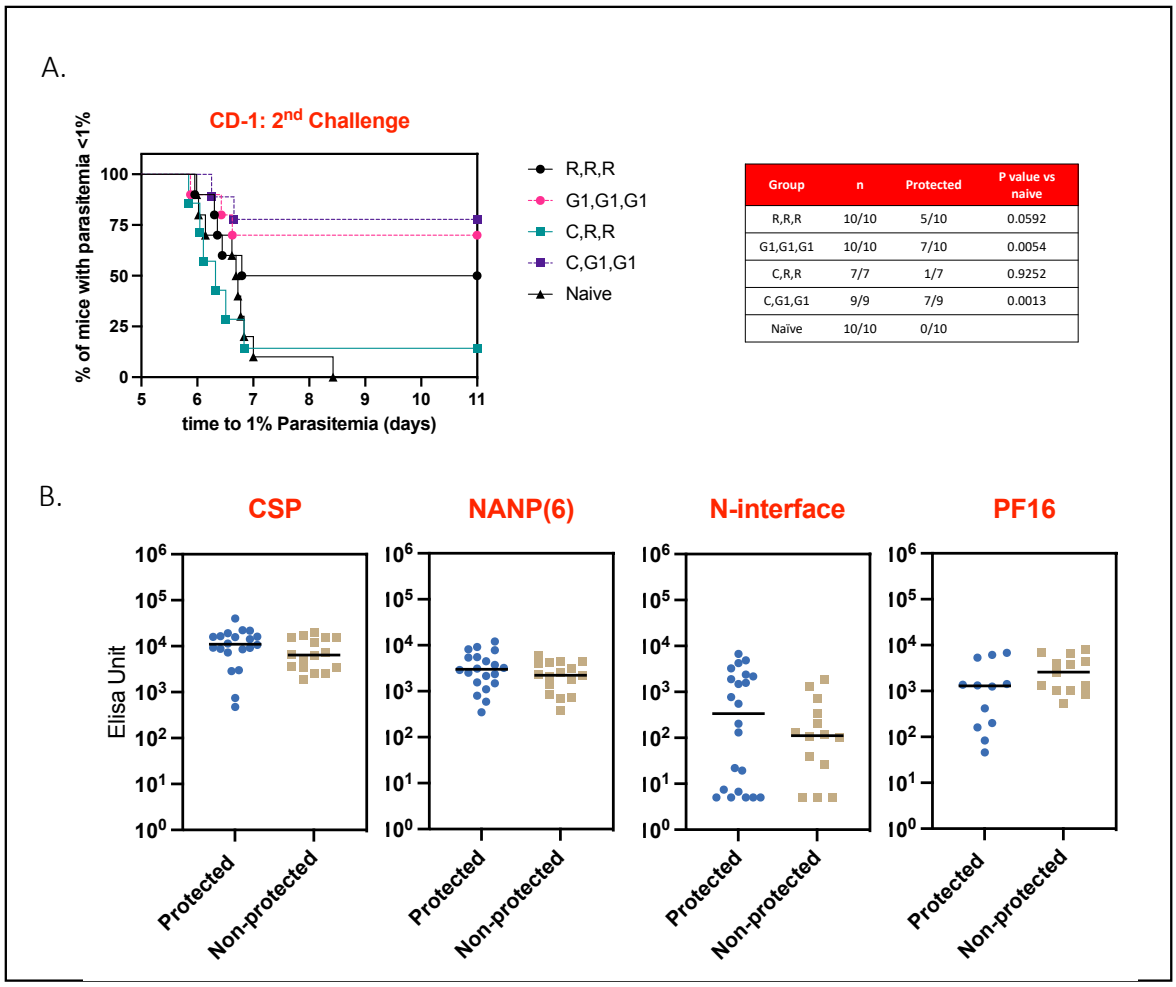
A. A box and whisker plot showing the total IgG responses induced against CSP, NANP(6), N-interface and PF16. **B.** Spider plot showing the antibody responses against the different domains of CSP. Data in A were analysed with Kruskal-Wallis's test, followed by Dunn's multiple comparison test. Asterisks indicate significant differences (*=p<0.05, **=p<0.01)

5.8. Homologous G1,G1,G1 and Heterologous C,G1,G1 vaccination regimens conferred high-level protection against the second malaria challenge.

To determine the durability of protection in each vaccination regimen, protected mice were re-challenged with 1000 Pb(PfCSP) sporozoite three months after the first challenge. Following the second sporozoite challenge, fifty per cent of mice from the homologous R,R,R group developed blood-stage malaria. Meanwhile, only 1 out of 7 mice immunised with C,R,R remained sterilely protected after the second challenge. Interestingly, high-level

protection remained in mice receiving homologous G1,G1,G1 or C,G1,G1 vaccination, with around 70% and 77% of mice protected, respectively (Figure 5.11A).

As more mice developed blood-stage malaria after the second challenge, it allow the comparison of antibody responses between protected and unprotected mice. Data across vaccination groups were pooled and stratified based on protection status. To compare antibody anti C-term between protected and unprotected mice, we excluded the data from homologous G1,G1,G1 group in the analysis as the anti-C-term IgG were absent in this group. Levels of anti-CSP and anti-NANP IgG were comparable between protected and non-protected mice. Interestingly, antibodies binding to the junctional region were higher in protected mice compared with unprotected, albeit this was not significant. Surprisingly, the protected mice had a non-significant lower anti-PF16 IgG compared to unprotected mice at the time of the second challenge (Figure 5.11 B).



Group	n	Protected	P value vs naive
R,R,R	10/10	5/10	0.0592
G1,G1,G1	10/10	7/10	0.0054
C,R,R	7/7	1/7	0.9252
C,G1,G1	9/9	7/9	0.0013
Naïve	10/10	0/10	

Figure 5.11. Efficacy following homologous and heterologous vaccinations – The second challenge.

A. Protective efficacy of four different vaccine groups in CD-1 mice after the first sporozoite challenged, presented in the Kaplan-Meier survival graphs. The survival curves were compared by Log-rank (Manter-Cox) with Bonferroni correction (p=0.013). The p-value of each vaccination group was presented in the table. **B.** Pooling of antibody response data stratified by protection status. The horizontal line represents the median of each group. The data presented were representative of a single study.

5.9. Correlation analysis between antibody responses and protection.

To gain a better understanding on the role of antibody responses towards different region of CSP in providing protection against malaria infection, we further analysed the correlation between antibody responses and protection status following the challenge with transgenic Pb(PfCSP) sporozoites. In the first challenge, spearman correlation analysis revealed that anti-NANP ($p<0.01$) and anti-N-interface ($p<0.05$) IgG significantly positively correlated

with time to 1% parasitaemia. A weak positive correlation was observed between NANP IgG avidity with time to 1% parasitaemia, albeit this was not significant. Surprisingly, anti-PF16 IgG did not correlate with protection in CD-1 mice. Nevertheless, the anti-PF16 IgG was negatively correlated with anti-N-interface IgG ($p<0.05$), suggesting no cross-reaction between antibodies that bind to N-term and C-term. In contrast, the antibodies bound to C-term significantly correlated ($p<0.0001$) with antibody that bound to the full-length CSP. (Figure 5.11 A).

At the second challenge, spearman correlation analysis showed that antibodies that recognised junctional epitope had a higher positive correlation with time to 1% parasitaemia at the second challenge compared to anti-NANP IgG titres. However, this was not statistically significant. Meanwhile, anti-PF16 titres were negatively correlated with protection in the second challenge, but again this was not significant (Figure 5.11 B)Together, these data suggest that high antibody titre towards major repeat NANP and junctional epitope may contribute to protection in CD-1 mice after challenge with transgenic Pb(PfCSP) sporozoites in mice.

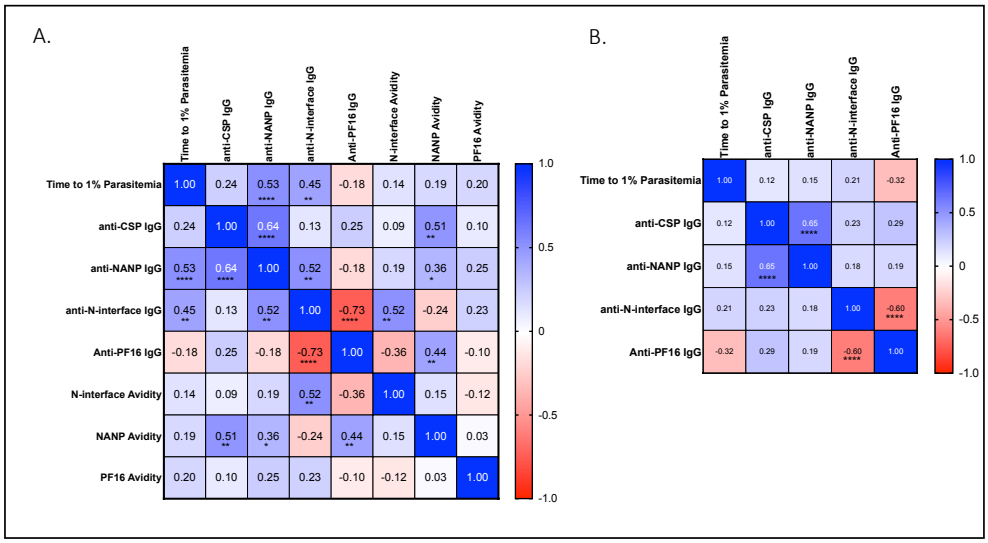


Figure 5.11. Spearman correlation analysis.

Matrix analysis from Spearman correlation test showing the relationship between different antibody responses and time-to-1 % parasitaemia in **A.** the first challenge and **B.** the second challenge.

5.10. Serum from homologous and heterologous vaccination inhibit sporozoite invasion *in-vitro*.

The level of antibodies that bound to NANP repeat major and junctional epitope positively correlated with sterile protection against malaria in the first challenge. To complement the analysis, Inhibition of Sporozoite Invasion assay was performed using the serum from the mice that were taken down at three weeks following the last vaccination (at the time point of the first challenge). All serum from vaccinated mice showed a reduction in the frequency of GFP-positive cells compared to naïve serum. Serum from mice vaccinated with homologous G1,G1,G1 showed the highest reduction of the frequency of GFP-positive cells among the different vaccination groups. Additionally, all serum from vaccinated mice showed higher levels of inhibition compared to naïve serum, suggesting all vaccination groups serum contained antibodies that have the functionality to block sporozoite invasion *in-vitro*. Serum from mice immunised with homologous G1,G1,G1 vaccines induced higher level of inhibition, albeit this was not statistically significant. In addition, a comparable level of inhibition was observed when sporozoites were incubated with serum from mice in the homologous R,R,R or heterologous C,G1,G1 group. Meanwhile, serum from mice immunised with heterologous C,R,R had the lowest level of inhibition compared to all other vaccine groups, although this was not significant (Figure 5.9 A, B).

The correlation between percent inhibition with IgG titre against different epitopes was analysed using Spearman correlation analysis. Titre of anti-CSP (r=0.42), anti-NANP (r=0.59) and anti-junctional epitope (r=0.38) IgG all positively correlated with percentage of sporozoite inhibition. Only anti-NANP IgG was statistically significant ($p<0.50$). Meanwhile, consistent with *in-vivo* data, anti-C-term IgG (r=-0.01) had a weak negative

correlation with percentage inhibition, but once again this trend was not statistically significant (Figure 5.9 C).

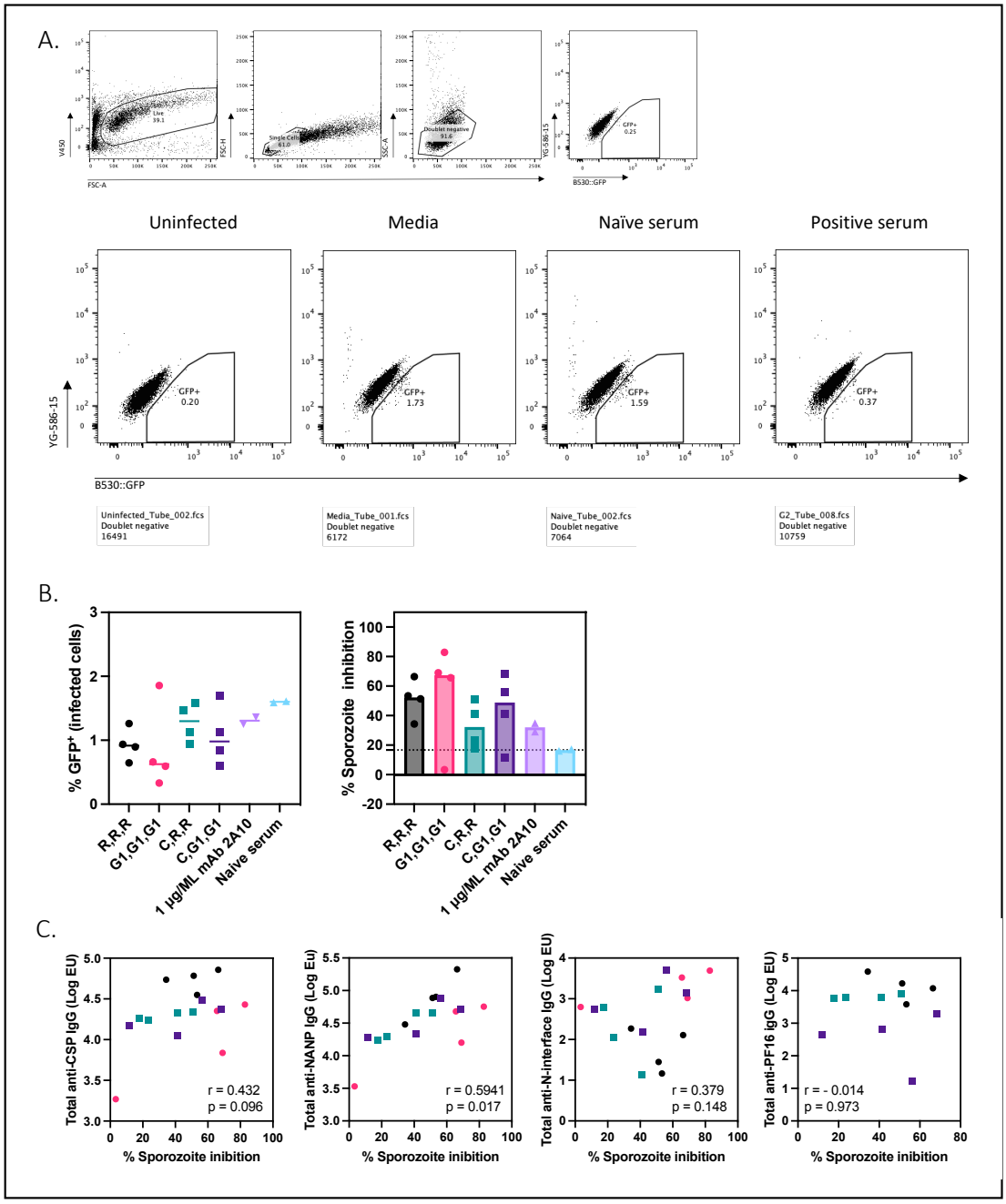


Figure 5.12 Serum from mice vaccinated with homologous and heterologous vaccination inhibit sporozoite invasion in-vitro.

A. Gating strategy for ISI assay and representative of GFP^{+}Huh7 cells population from uninfected Huh7 cells or Huh7 cells that were incubated with sporozoite and media, naïve serum or positive serum. **B.** Frequency of GFP^{+}Huh7 cells and percent inhibition induced by different vaccination regimens, mAb 2A10 control and

naïve serum. **C.** Spearman correlation analysis between titre of anti-CSP, anti-NANP, anti-N-interface and anti-PF16 versus per cent sporozoite inhibition. The data presented represent two independent experiments.

Table 3.1 Summary of antibody responses induced by four different vaccination regiment in CD-1 mice.

Vaccination regiment	Median of total IgG (EU)			
	CSP	NANP(6)	N-interface	PF16
Time point week-9 (First challenge)				
R,R,R	39219.31	26302.68	69.98	9141.13
G1,G1,G1	12147.87	16443.87	3793.15	LLOD
C,R,R	17803.28	12161.86	37.84	6018.66
C,G1,G1	12288.53	12457.08	475.34	550.81
Time point week-22 (Second challenge)				
R,R,R	13365.96	4073.80	7.09	4120.98
G1,G1,G1	8147.04	2630.27	1671.09	LLOD
C,R,R	11912.42	2290.87	38.73	2293.51
C,G1,G1	8709.64	2511.89	1333.52	530.88

5.11. Discussion

Alongside cellular responses, antibodies have a major role in providing immunity against malaria. Early studies in the murine models demonstrated passive transfer of serum from mice vaccinated with a single dose of RAS significantly could reduce parasite burden in the liver of naïve mice following sporozoite challenge with murine malaria [96, 97]. In the seminal study, mice immunised with genetically attenuated *P. yoelii* sporozoites, induced antibodies that partially protected mice from sporozoite challenge, administered by mosquito bites, in the absence of T-cells [370]. In humans, repeating vaccination using RAS provide complete sterile protection against malaria challenge using a homologous parasite strain (*P. falciparum* 3D7). Although the main mechanism of RAS-induced immunity in humans is via induction of Ag-specific $CD8^+$ T-cells that function to kill infected hepatocytes [78], protective and sterilising antibodies have been isolated from human RAS-vaccinee [198, 199, 352, 355]. Notably, the majority of antibodies induced by WSV bound to the CSP antigen [86, 87], highlighting the potential of CSP protein as the antigen target for subunit malaria vaccines.

RTS,S/AS01 targets CSP's NANP repeat region and C-terminal domain. In the phase III trials, the vaccine induced a high titre of anti-circumsporozoite antibodies (measured towards NANP repeat) with Geometric Mean Titre (GMT) 539.6 EU/mL one month after the third dose among Kenyan and Tanzanian children aged 5-17 months [191]. However, titres waned in a biphasic exponential decay with only 71.9 EU/mL in the first 6.5 months in the 5-17 months age group and even lower in infants aged 6-12 weeks [14, 191]. A high titre of anti-NANP antibodies is required for protection, with an estimated titre of 121

EU/mL providing 50% efficacy against malaria infection [14]. Suppose the protection relies solely on the antibody binding to the repeat regions (NANP); in that case, a vaccine platform that induced high titre antibodies could be more favourable, such as virus-like particles (VLPs). CSN encoding viral-vector vaccines induced at least one log lower anti-NANP IgG compared to R21, the second generation of RTS/S-like vaccine using VLP technology (Figure 5.1). Likely, there is no protection after two-dose of ChAdOx1 encoding different CSP construct in the efficacy study in the previous experiment (Figure 4.6) due to the low titre of anti-NANP antibodies unable to mediate protection. While at the same time, the vaccination regimen used (Adenovirus-Adenovirus) in the study was not designed to maximise T-cell responses as would be achiueved with a Adenovirus-MVA regimen (Figure 4.6). Vaccine platforms can significantly impact the outcome of the immune response, for instance, in blood-stage malaria, where antibodies predominantly mediate the immune effector function. Administration of Rh5 vaccine using protein in adjuvant (AS01) is found to promote higher T-follicular helper cells than viral vector vaccination, and these cells drive high-titre of antibody response associated with reduction in parasite growth [155, 371].

Despite the licensing of RTS,S/AS01, concerns over its antigen construct and other vaccines targeting NANP repeat major are rising. It has been argued that despite being immunodominant, the NANP repeat region masks other vulnerable site on CSP [362, 363]. Recently, the junctional epitope and interspersed minor, two sites not included in RTS,S or R21, have been identified as the sites of protective monoclonal antibody binding (CIS43, MGG4, L9) [198, 199, 355]. Interestingly, passive transfer of mAbs L9 that bind to interspersed minor NANV (combination between major and minor repeat, NANP/NVDP) protect more mice from malaria infection at lower doses than mAbs (317) targeting major

NANP repeat [355]. Remarkably, passive immunisation with mAb CIS43, a human monoclonal antibody that recognises a junctional epitope, protect humans from malaria infection in a CHMI study [356]. However, translating this information into vaccine design requires signification optimisation. Early studies using NPDP(19) peptide showed robust antibody responses but lacked inhibitory function [199]. Subsequently, junctional epitope peptides chemically conjugated to Qβ or expressed in the N-terminus and B domain GS loop of CHIK VLP were found to reduce parasite burden in the liver but did not prevent malaria infection [364, 365]. Recently, junctional epitopes expressed and displayed on the surface of TMV partially protected mice from malaria infection [372]. These findings highlight the importance of different regions of CSP as a target for protective antibodies and suggest that balancing immune response across CSP regions may promote sterile and long-lasting protection.

The work described in this chapter investigated the possibility of diversification of the immune responses against different regions of CSP via a heterologous vaccination approach. ChAdOx1 encoding nanoparticle CSP was used to prime immune responses to the full length of CSP followed by a booster dose with VLP targeting the junctional region. In the first immunogenicity study, this heterologous vaccination approach resulted in comparable anti-NANP IgG with homologous vaccination using R21/Addavax (R,R,R), a VLP mainly targeting NANP repeat major and C terminal region. Importantly, this approach also promoted a high titre of antibodies that bound to the junctional region, with proportional antibodies that recognised the C-terminal region.

When the efficacy of different vaccination regimens was tested in outbred mice, it was not surprising that vaccination with homologous (R,R,R) R21 induced complete protection in

the first challenge. Three doses of R21 induced high titre antibody against NANP major repeat, which was correlated with protection (Figure 5.6). Surprisingly, immunisation with homologous (G1,G1,G1) and heterologous (C,G1,G1) R21-G1 also induced complete protection in the first challenge (Figure 5.5). This high-level of protection was maintained in mice immunised by homologous or heterologous R21-G1 when challenged again a further three months later. Meanwhile, mice immunised with homologous R21 were partially protected at the second challenge, while the protection of heterologous R21 decreased drastically after the second challenge (Figure 5.4). Vaccination with homologous or heterologous R21-G1 induced higher titres of antibodies that bound to the junctional region than homologous and heterologous R21; this significantly correlated with protection in the first challenge (Figure 5.5). However, the titre of anti-NANP IgG induced by homologous and heterologous R21-G1 was comparable to homologous vaccination using R21. The construct of R21-G1 contains three NANP epitopes interspersed with NPDP and NVDP tetrapeptide. Therefore, in mice receiving R21-G1, it is highly likely that most antibodies bound to the NANP were cross-reactive to anti-junctional epitope and have different specificity with anti-NANP IgG induced by R21. mAbs CIS34 and L9 bind to recombinant *P. falciparum* CSP (rCSP) in two-step high-affinity binding; while mAb CIS34 recognise NPDP and NANP site, mAb L9 binds to NVDP and NANP[198, 355]. Structural binding analysis revealed that antibodies binding to junctional epitopes rely upon the NANP sequence at the junctional region [373]. While antibodies that solely bind to NPDP or NVDP have not been identified, it is interesting to characterise further the antibodies induced by R21-G1 vaccination.

Following the second challenge, protected mice had a higher trend of antibodies binding to the junctional region compared to unprotected mice. However, the exact mechanism of protection induced by these antibodies remains unclear. Early findings showed that the mAb

CIS34 contributed to the inhibition of proteolytic cleavage of *Pf* CSP, an obligatory step before the CSP binds to hepatocytes during cell invasion. Albeit to a lesser extent than mAb 5D5 that binds to highly-conserved Region I (RI), which is situated adjacent to the upstream junctional region[198]. Meanwhile, using intravital liver imaging, Wang et al. showed that mAb L9 inhibit sporozoite egress from liver sinusoid during the invasion process [355]; however, the exact molecular mechanism remain unknown. Homologous G1,G1,G1 and heterologous C,G1,G1 induced comparable antibodies against NANP and junctional regions; however, heterologous R21-G1 induced more durable anti-junctional antibodies compared to homologous R21 vaccination. Notably, a single dose of ChAdOx1-gag::CSN(SHIC65) in a heterologous vaccination regimen was able to rescue the immune response towards C-terminal region that lacked following homologous G1 immunisation. However, in this study, avidity of anti-PF16 antibodies were not measured at the time of the second malaria challenge. Among RTS,S/AS01 vaccinees, the avidity of anti-C terminal antibodies is associated with protection against first clinical malaria [333]. Delaying and fractional dose at the third vaccine administration increased the avidity of antibodies against the C terminal region [374]. However, the immunity against the C terminal is hindered by the high polymorphism of amino acids between *P. falciparum* strains. Recently, a human mAbs (mAb 1512) that recognises the B sheet domain, a conserved epitope in the TSR homology region, has been identified among RTS,S vaccinee. Although this mAb does not provide sterilising immunity, passive transfer of this mAb reduced parasite burden in the liver of mice [357].

It is possible that antibodies bind to different regions of CSP, have different biological functions or degrees of functionality [375]. Indeed, the synergy between these antibodies in mediating protection against malaria infection requires further investigation. Initial analysis using a logistic regression model and receiver operating characteristic (ROC) analysis

reveals that a combination of region-specific antibody leads to higher confidence in predicting protection than individual region-specific antibody responses (Appendix 1). Notably, synergy between monoclonal antibodies against different epitopes of blood-stage malaria antigen, CyRPA, led to a stronger growth inhibitory effect than individual mAb alone [376]. If such synergy is proven to exist in CSP-mediated immunity, CSP-based vaccines need to be able to induce immune responses towards different regions of CSP antigen. In conclusion, data presented in this chapter has shown that immune responses against different regions of CSP could be induced by heterologous vaccination. Priming immune response towards the full length of CSP and boosting with a junctional epitope targeted vaccine results in diverse antibody responses against different epitopes of CSP that can lead to higher and more durable protection against malaria infection.

5.11.1 Chapter summary:

Below is the summary of findings that have been demonstrated in this chapter:

1. Heterologous C,R,R or C,G1,G1 vaccination regimens induce broader antibody response against different regions of CSP than homologous R,R,R or G1,G1,G1 in inbred and outbred mice.
2. Homologous G1,G1,G1 or heterologous C,G1,G1 vaccination regimens induced higher antibodies against the junctional region of CSP with comparable anti-NANP IgG compared to homologous R,R,R or heterologous C,R,R.
3. All vaccination regimens confer high protection in the first challenge against transgenic P. berghei expressing Pf. CSP 3D7 in outbred mice. However, in the second challenge, heterologous C,G1,G1 vaccination protects more mice than other regimens.
4. The Anti-NANP IgG are not boosted after the first challenge across all vaccination regimens. However, the first sporozoite challenge boosts the antibody recognising the junctional epitope in mice vaccinated with heterologous C,R,R or C,G1,G1.

5. The Anti-NANP IgG significantly correlated with the inhibition of sporozoite invasion in-vitro

6

Concluding remarks

6.1 Summary findings

The field of malaria vaccine research has reached its significant milestone with the licensing of RTS,S/AS01, adding a new valuable tool for global health efforts to control and reduce malaria burden worldwide. The vaccine provides short-lived protection and protects around 25-50% of children and infants in malaria-endemic areas. Surely, improving malaria vaccines is still needed to achieve 75% efficacy as targeted in the malaria vaccine technology roadmap.

Whole sporozoite vaccination has become the gold standard for vaccine-induced immunity against malaria infection. Nevertheless, the implementation of such a vaccine worldwide is hindered by technical and logistical challenges. Indeed, studies on WSV have demonstrated that sterile immunity against malaria infection can be achieved by vaccination. Both humoral and cellular responses have been shown to have essential roles in achieving immunity against malaria infection. WSV induces immune responses against broad-range antigens; however, targeting individual antigens in subunit vaccines has not been able to achieve the same level of protection as WSV. CSP and TRAP proteins are two antigens that have been extensively used and currently, are the most advanced antigen in pre-erythrocytic subunit vaccine development. While, in parallel, efforts to investigate other potential antigens are still ongoing, this thesis aimed to improve subunit CSP and TRAP-based vaccines.

The effectiveness of liver-stage malaria vaccines, such as ME-TRAP, relies on the antigen presentation by HLA-1 from the infected hepatocytes. Therefore, selecting the antigen with the most relevant strain for the target population is essential. The tPA-TROP encoded in ChAdOx1 and MVA vector was constructed based on full-length *Pf.* TRAP 3D7 strain, which originated in Africa. The antigen sequence was human codon-optimised and fused to the tPA-leading sequence and appears to be optimum as an addition molecular adjuvant did not further enhance the T-cell response. In contrast, adding a molecular adjuvant to the suboptimum antigen increased T-cell responses 8 times higher than without an adjuvant.

Head-to-head comparison between viral vector vaccines encoding TRAP T9/96 and 3D7 showed that heterologous ChAdOx1-MVA vaccination showed that tPA-TROP induced higher-levels of protection compared to either tPA-TRAP (opt) or ME-TRAP (which both are T9/96 vaccine strain). Remarkably, T-cell responses induced in mice immunised with tPA-TROP appeared to cross-react with TRAP T9/96 protein with a magnitude similar to those immunised with tPA-TRAP (opt) or ME-TRAP. Indeed, it is interesting to evaluate the immunogenicity and efficacy of tPA-TROP further and compare it with ME-TRAP in a clinical trial.

Early studies of WSV in murine models suggested that both humoral and cellular immune responses, mainly against CSP, can induce sterile protection against malaria infection. Meanwhile, clinical data of subunit CSP-based vaccine, RTS,S, showed that antibody responses primarily mediate protection. RTS,S was constructed using virus-like particle (VLP) technology known to induce a high-titre antibody response. While vaccination with RTS,S elicited high anti-CSP antibodies, the vaccine was found to poorly induce cellular immunity, particularly CD8 T-cells, whereas vaccination with Adenovirus encoding CSP

antigen-induced high T-cell responses. Here a state-of-the-art strategy was tested to construct Adenovirus vaccines expressing self-forming nanoparticle CSP (CSN). Using gag pr55 from SIVmac293 as a structural protein for enveloped VLPs, CSN was successfully displayed on VLPs when the antigen was fused to the transmembrane and cytoplasmic tail domain of shark invariant chain (gag::CSN(SHIC65)). Improvement in T-cell and antibody responses compared to ChAdOx1 expressing CSN alone were observed. Although not sterilising, two doses of ChAdOx1-gag::CSN(SHIC65) induced a delay in the time mice succumbed to malaria after challenge and showed increased ability to inhibit sporozoite invasion *in-vitro*. Indeed, further optimisation is required to maximise the incorporation of antigens on VLPs or combine with two or more antigens. Optimised tPA-TROP was added and combined with the gag::CSN(SHIC65) construct to test this concept further and evaluate it as a multi-antigen DNA vaccine. Initial investigation suggested that no immune interference was observed when these two antigens were combined and separated by T2A sequence in a single DNA plasmid. TRAP-specific T-cell responses induced by multiantigen gCSN-TROP or TROP-gCSN vaccine was comparable to DNA vaccine encoding tPA-TROP alone. Similarly, no antagonistic effect was observed in anti-NANP antibody production between multiantigen gCSN-TROP or TROP-gCSN vaccine with the gCSN vaccine alone. Therefore, it would be interesting to further evaluate this multiantigen vaccine in a viral vector vaccination regimen and evaluate its efficacy in preclinical studies.

6.2 Future directions

6.2.1 Head-to-Head comparison of viral vectors vaccine encoding ME-TRAP and tPA-TROP in clinical trial

WSV data showed that vaccination against liver-stage malaria development could achieve sterile protection. While subunit CSP-based vaccine mainly induced antibodies that act against the extracellular phase of sporozoite, liver-stage antigen-based vaccines, such as TRAP, target parasite development in the liver, adding more layers of protection against malaria. Therefore, it is pivotal to keep the development of the liver-stage malaria vaccine. Indeed, the current subunit pre-erythrocytic vaccine landscape is dominated by vaccines targeting CSP. Hence, it is essential for other potential or improved candidates, such as tPA-TROP, to progress to clinical trial and compare with the current most advanced candidate that has been tested, i.e. ME-TRAP.

6.2.2 Optimisation of nanoparticle CSP encoded in chimpanzee adenoviral vectors.

It has been reported that different transmembrane and cytoplasmic tail domains can affect the number of proteins incorporated into plasma membrane cells. For instance, only 1.5% of env HIV-1 are incorporated into enveloped VLP when endogenous TM-CT is used; Meanwhile, around 58 and 29% of env are incorporated when the endogenous TM-CT were replaced with TM-CT from Mouse mammary tumour virus (MMTV) env or Haemagglutinin (HA) are used, respectively. Therefore, an attractive approach would be to investigate further different sources of TM-CT that allow the incorporation of CSP antigen into enveloped VLPs.

6.2.3 Multi-antigen and multi-stage malaria vaccine.

Antibodies against CSP neutralise extracellular sporozoite and inhibit invasion of hepatocytes, reducing the number of infected hepatocytes. Meanwhile, antigen-specific T-cells can recognise infected hepatocytes and kill them to disrupt parasite development in the liver. Hence combining vaccines targeting the extracellular- and intracellular-phase of sporozoite may add layers of protection, increasing vaccine efficacy. Initial investigation of DNA vaccines containing multi pre-erythrocytic antigen gag::CSN(SHIC) and tPA-TROP showed that the vaccine elicited immune responses similar to DNA vaccines encoding individual gag::CSN(SHIC) or tPA-TROP. Therefore, it is interesting to evaluate further this vaccine's immunogenicity and efficacy in viral vector immunisation.

6.2.4 Investigating mRNA vaccine technology to deliver large and complex malaria antigen.

Many liver-stage malaria proteins, such as LSA1, LSA2, LISP1 and SLARP, are large antigens with no clear immunodominant regions. There is limited information on the development of liver-stage malaria vaccine using these antigens, possibly due to the large size and complex structure possessed by these antigens that limit the evaluation of these antigens using available vaccine technology. Nevertheless, many of these proteins are functionally pivotal for parasite development in the liver [377-379]. Suggesting these proteins is a potential target for a liver-stage malaria vaccine. During the COVID-19 pandemic, two mRNA vaccines received Emergency Use Listing (EUL) from WHO. This has validated mRNA technology's potential to be used for prophylactic/therapeutic purposes. In addition, the vaccine-induced robust humoral and cellular immune response and conferred high protection against severe COVID-19 Diseases. Therefore, it is interesting to

investigate whether the mRNA technology can also be used to deliver malaria antigens, especially large-size and complex antigens.

6.3 Final remarks

This work described in this thesis aimed to improve current viral vector vaccines targeting pre-erythrocytic malaria. Viral vector vaccines encoding TRAP antigen from *P. falciparum* 3D7 were developed to achieve this. Their performance was compared to vaccines derived from the T9/96 strain, including ME-TRAP, that has been evaluated in Phase II trials. The tPA-TROP (3D7) induced higher levels of protection against transgenic *P. berghei* sporozoite expressing Pf. TRAP 3D7 (homologous protection) compared with ME-TRAP (T9/96). Suggesting this vaccine construct might induce higher protection in the field than vaccines expressing ME-TRAP. Although tPA-TROP was demonstrated to confer higher protection against challenges in CD-1 mice, it is also worth evaluating other liver-stage antigens that are less polymorphic and compared with tPA-TROP before progressing to clinical trial. Additionally, this thesis has demonstrated that it is possible to express malaria antigens as self-forming nanoparticles when the construct is delivered in an Adenovirus vector. This concept could be further developed to include two or more malaria antigens, increasing the diversity of malaria responses.

7

References

1. WHO, *World malaria report 2022.* World Health Organisation, 2022.
2. WHO, *Global technical strategy for malaria 2016-2030, 2021 update.* World Health Organisation, 2021.
3. Kleinschmidt, I., et al., *Implications of insecticide resistance for malaria vector control with long-lasting insecticidal nets: a WHO-coordinated, prospective, international, observational cohort study.* Lancet Infect Dis, 2018. **18**(6): p. 640-649.
4. Riveron, J.M., et al., *Rise of multiple insecticide resistance in Anopheles funestus in Malawi: a major concern for malaria vector control.* Malar J, 2015. **14**: p. 344.
5. Sokhna, C., M.O. Ndiath, and C. Rogier, *The changes in mosquito vector behaviour and the emerging resistance to insecticides will challenge the decline of malaria.* Clin Microbiol Infect, 2013. **19**(10): p. 902-7.
6. Uwimana, A., et al., *Emergence and clonal expansion of in vitro artemisinin-resistant Plasmodium falciparum kelch13 R561H mutant parasites in Rwanda.* Nat Med, 2020. **26**(10): p. 1602-1608.
7. Balikagala, B., et al., *Evidence of Artemisinin-Resistant Malaria in Africa.* N Engl J Med, 2021. **385**(13): p. 1163-1171.
8. Imwong, M., et al., *Molecular epidemiology of resistance to antimalarial drugs in the Greater Mekong subregion: an observational study.* Lancet Infect Dis, 2020. **20**(12): p. 1470-1480.
9. Grignard, L., et al., *A novel multiplex qPCR assay for detection of Plasmodium falciparum with histidine-rich protein 2 and 3 (pfhrp2 and pfhrp3) deletions in polyclonal infections.* EBioMedicine, 2020. **55**: p. 102757.
10. Berhane, A., et al., *Major Threat to Malaria Control Programs by Plasmodium falciparum Lacking Histidine-Rich Protein 2, Eritrea.* Emerg Infect Dis, 2018. **24**(3): p. 462-470.
11. Weiss, D.J., et al., *Indirect effects of the COVID-19 pandemic on malaria intervention coverage, morbidity, and mortality in Africa: a geospatial modelling analysis.* Lancet Infect Dis, 2021. **21**(1): p. 59-69.
12. WHO, *WHO recommends groundbreaking malaria vaccine for children at risk.* WHO News, 2021.
13. WHO, *Malaria vaccine: WHO Position paper.* 2022.
14. White, M.T., et al., *Immunogenicity of the RTS,S/AS01 malaria vaccine and implications for duration of vaccine efficacy: secondary analysis of data from a phase 3 randomised controlled trial.* Lancet Infect Dis, 2015. **15**(12): p. 1450-8.
15. RTS, S.C.T.P.A.S., Lell B, Fernandes JF, Abossolo BP, Methogo BG, Kabwende AL, Adegnika AA, Mordmüller B, Issifou S, Kremsner PG, Sacarlal J, Aide P, Lanaspa M, Aponte JJ, Machevo S, Acacio S, Bulo H, Sigauque B, Macete E, Alonso P, Abdulla S, Salim N, Minja R, Mpina M, Ahmed S, Ali AM, Mtoro AT, Hamad AS, Mutani P, Tanner M, Tinto H, D'Alessandro U, Sorgho H, Valea I, Bihoun B, Guiraud I, Kaboré

B, Sombié O, Guiguemdé RT, Ouédraogo JB, Hamel MJ, Kariuki S, Oneko M, Odero C, Otieno K, Awino N, McMorrow M, Muturi-Kioi V, Laserson KF, Slutsker L, Otieno W, Otieno L, Otsyula N, Gondi S, Otieno A, Owira V, Oguk E, Odongo G, Woods JB, Ogutu B, Njuguna P, Chilengi R, Akoo P, Kerubo C, Maingi C, Lang T, Olotu A, Bejon P, Marsh K, Mwambingu G, Owusu-Agyei S, Asante KP, Osei-Kwakye K, Boahen O, Dosoo D, Asante I, Adjei G, Kwara E, Chandramohan D, Greenwood B, Lusingu J, Gesase S, Malabeja A, Abdul O, Mahende C, Liheluka E, Malle L, Lemnge M, Theander TG, Drakeley C, Ansong D, Agbenyega T, Adjei S, Boateng HO, Rettig T, Bawa J, Sylverken J, Sambian D, Sarfo A, Agyekum A, Martinson F, Hoffman I, Mvalo T, Kamthunzi P, Nkomo R, Tembo T, Tegha G, Tsidya M, Kilembe J, Chawinga C, Ballou WR, Cohen J, Guerra Y, Jongert E, Lapierre D, Leach A, Lievens M, Ofori-Anyinam O, Olivier A, Vekemans J, Carter T, Kaslow D, Leboulleux D, Loucq C, Radford A, Savarese B, Schellenberg D, Sillman M, Vansadia P., *A phase 3 trial of RTS,S/AS01 malaria vaccine in African infants.* N Engl J Med, 2012. **367**(24): p. 2284-95.

16. WHO, *Malaria vaccine: Preferred Product Characteristic and Clinical Development Considerations*. 2022.
17. Cowman, A.F., et al., *Malaria: Biology and Disease.* Cell, 2016. **167**(3): p. 610-624.
18. Vanderberg, J.P., *Plasmodium berghei: Quantisation of sporozoites injected by mosquitoes feeding on a rodent host.* Experimental Parasitology, 1977. **42**(1): p. 12.
19. Kebaier, C., T. Voza, and J. Vanderberg, *Kinetics of mosquito-injected Plasmodium sporozoites in mice: fewer sporozoites are injected into sporozoite-immunized mice.* PLoS Pathog, 2009. **5**(4): p. e1000399.
20. Sidjanski, S., and Vanderberg, J.P., *Delayed Migration of Plasmodium Sporozoites from the Mosquito Bite Site to the Blood.* The American Journal of Tropical Medicine and Hygiene, 1997. **57**(4).
21. Yamauchi, L.M., et al., *Plasmodium sporozoites trickle out of the injection site.* Cell Microbiol, 2007. **9**(5): p. 1215-22.
22. Herrera, R., et al., *Reversible Conformational Change in the Plasmodium falciparum Circumsporozoite Protein Masks Its Adhesion Domains.* Infect Immun, 2015. **83**(10): p. 3771-80.
23. Prudencio, M., A. Rodriguez, and M.M. Mota, *The silent path to thousands of merozoites: the Plasmodium liver stage.* Nat Rev Microbiol, 2006. **4**(11): p. 849-56.
24. Sturm, A., Amino, R., van de Sand, C., Regen, T., Retzlaff, S., Rennenberg, A., Krueger, A., Pollok, J.M., Menard, R., and Heussler, V.T. Science 313, 1287–1290., *Manipulation of host hepatocytes by the malaria parasite for delivery into liver sinusoids.* Science, 2006. **313**: p. 4.
25. Lin, C.S., et al., *Multiple Plasmodium falciparum Merozoite Surface Protein 1 Complexes Mediate Merozoite Binding to Human Erythrocytes.* J Biol Chem, 2016. **291**(14): p. 7703-15.
26. Weiss, G.E., et al., *Revealing the sequence and resulting cellular morphology of receptor-ligand interactions during Plasmodium falciparum invasion of erythrocytes.* PLoS Pathog, 2015. **11**(2): p. e1004670.
27. Tham, W.H., et al., *Plasmodium falciparum Adhesins Play an Essential Role in Signalling and Activation of Invasion into Human Erythrocytes.* PLoS Pathog, 2015. **11**(12): p. e1005343.

28. Singh, S., et al., *Distinct external signals trigger sequential release of apical organelles during erythrocyte invasion by malaria parasites.* PLoS Pathog, 2010. **6**(2): p. e1000746.
29. Chen, L., et al., *An EGF-like protein forms a complex with PfRh5 and is required for invasion of human erythrocytes by Plasmodium falciparum.* PLoS Pathog, 2011. **7**(9): p. e1002199.
30. Reddy, K.S., et al., *Multiprotein complex between the GPI-anchored CyRPA with PfRH5 and PfRipr is crucial for Plasmodium falciparum erythrocyte invasion.* Proc Natl Acad Sci U S A, 2015. **112**(4): p. 1179-84.
31. Crosnier, C., et al., *Basigin is a receptor essential for erythrocyte invasion by Plasmodium falciparum.* Nature, 2011. **480**(7378): p. 534-7.
32. Smith TG, L.P., Carter R, Walliker D, Ranford-Cartwright LC, *Commitment to sexual differentiation in the human malaria parasite, Plasmodium falciparum.* Parasitology., 2000. **121**(2): p. 7.
33. Silvestrini F, A.P., Williams JL Parasitology. 2000 Nov;121 Pt 5:465-71. doi: 10.1017/s0031182099006691. PMID: 11128797., *Commitment to the production of male and female gametocytes in the human malaria parasite Plasmodium falciparum.* Parasitology, 2000. **121**(5): p. 7.
34. Joice, R., et al., *Plasmodium falciparum transmission stages accumulate in the human bone marrow.* Sci Transl Med, 2014. **6**(244): p. 244re5.
35. Mackintosh CL, B.J., Marsh K. , *Clinical features and pathogenesis of severe malaria.* Trends Parasitol., 2004. **20**(12): p. 7.
36. Leech JH, B.J., Miller LH, Howard RJ. J, *Identification of a strain-specific malarial antigen exposed on the surface of Plasmodium falciparum-infected erythrocytes.* Exp Med., 1984. **159**(6): p. 9.
37. Newbold CI, C.A., Kyes S, Berendt AR, Snow RW, Peshu N, Marsh K. Ann *PfEMP1, polymorphism and pathogenesis.* Trop Med Parasitol., 1997. **91**(5): p. 7.
38. Fried M, D.P., *Adherence of Plasmodium falciparum to chondroitin sulfate A in the human placenta.* Science., 1996. **272**(5267): p. 3.
39. Beeson JG, R.S., Cooke BM, Reeder JC, Chai W, Lawson AM, Molyneux ME, Brown GV. , *Adhesion of Plasmodium falciparum-infected erythrocytes to hyaluronic acid in placental malaria.* Nat Med., 2000. **6**(1): p. 5.
40. Chakravorty SJ, C.A., *The role of ICAM-1 in Plasmodium falciparum cytoadherence.* Eur J Cell Biol., 2005. **84**(1): p. 15.
41. Mota MM, J.W., Hirst E, Patnaik PK, Holder AA. , *Plasmodium chabaudi-infected erythrocytes adhere to CD36 and bind to microvascular endothelial cells in an organ-specific way.* Infect Immun., 2000. **68**(7): p. 4135.
42. Rogerson SJ, H.L., Duffy PE, Leke RF, Taylor DW. , *Malaria in pregnancy: pathogenesis and immunity.* Lancet Infect Dis., 2007 Feb. **7**(2): p. 13.
43. Rowe JA, M.J., Newbold CI, Miller LH. , *P. falciparum rosetting mediated by a parasite-variant erythrocyte membrane protein and complement-receptor 1.* Nature., 1997. **388**(6639): p. 292.
44. Xia, S., et al., *Effect of an Inactivated Vaccine Against SARS-CoV-2 on Safety and Immunogenicity Outcomes: Interim Analysis of 2 Randomized Clinical Trials.* JAMA, 2020.
45. Roberts DJ, P.A., Kai O, Kortok M, Marsh K. , *Autoagglutination of malaria-infected red blood cells and malaria severity.* Lancet., 2000 Apr 22. **355**(9213): p. 3.

46. Looareesuwan S, H.M., Wattanagoon Y, White NJ, Warrell DA, Bunnag D, Harinasuta T, Wyler DJ. , *Dynamic alteration in splenic function during acute falciparum malaria.* N Engl J Med., 1987. **10**(317): p. 5.
47. Awandare GA, G.B., Boeuf P, Tetteh JK, Kurtzhals JA, Behr C, Akanmori BD. , *Increased levels of inflammatory mediators in children with severe Plasmodium falciparum malaria with respiratory distress.* J Infect Dis., 2006. **194**(10): p. 3.
48. Ayimba E, H.J., Ségbéna AY, Gantin RG, Lechner CJ, Agosssou A, Banla M, Soboslay PT. , *Proinflammatory and regulatory cytokines and chemokines in infants with uncomplicated and severe Plasmodium falciparum malaria.* Clin Exp Immunol., 2011 Nov. **166**(2): p. 3.
49. MJ., W., *Complement. First of two parts.* N Engl J Med., 2001 Apr 5;. **344**(13): p. 13.
50. MJ., W., *Complement. Second of two parts.* N Engl J Med., 2001 Apr 12. **344**(15): p. 5.
51. Medzhitov, R., *Recognition of microorganisms and activation of the immune response.* Nature., 2007 Oct 18. **449**(7164): p. 8.
52. Joffre, O.P., et al., *Cross-presentation by dendritic cells.* Nat Rev Immunol, 2012. **12**(8): p. 557-69.
53. Kawai T, A.S., *The roles of TLRs, RLRs and NLRs in pathogen recognition.* Int Immunol., 2009 Apr. **21**(3): p. 317.
54. Murphy, K., Walport, M. , *Janeway's Immunobiology. 9th Edition.* 2016, New York: Garland Science.
55. Farber, D.L., N.A. Yudanin, and N.P. Restifo, *Human memory T cells: generation, compartmentalization and homeostasis.* Nat Rev Immunol, 2014. **14**(1): p. 24-35.
56. Neefjes, J., et al., *Towards a systems understanding of MHC class I and MHC class II antigen presentation.* Nat Rev Immunol, 2011. **11**(12): p. 823-36.
57. Wong, P. and E.G. Pamer, *CD8 T cell responses to infectious pathogens.* Annu Rev Immunol, 2003. **21**: p. 29-70.
58. Mahnke, Y.D., et al., *The who's who of T-cell differentiation: human memory T-cell subsets.* Eur J Immunol, 2013. **43**(11): p. 2797-809.
59. Harty JT, T.A., White DW. 2000;18:275-308. , *CD8+ T cell effector mechanisms in resistance to infection.* Annu Rev Immunol., 2000. **18**: p. 29.
60. Zhu, J. and W.E. Paul, *Peripheral CD4+ T-cell differentiation regulated by networks of cytokines and transcription factors.* Immunol Rev, 2010. **238**(1): p. 247-62.
61. McHeyzer-Williams, L.J., et al., *Follicular helper T cells as cognate regulators of B cell immunity.* Curr Opin Immunol, 2009. **21**(3): p. 266-73.
62. Baird JK, M.S., Basri H, Tirtokusumo S, Subianto B, Hoffman SL. , *Age-dependent susceptibility to severe disease with primary exposure to Plasmodium falciparum.* J Infect Dis., 1998 Aug. **178**(2): p. 4.
63. Owusu-Agyei S, K.K., Baird JK, Utz GC, Binka FN, Nkrumah FK, Fryauff DJ, Hoffman SL. , *Incidence of symptomatic and asymptomatic Plasmodium falciparum infection following curative therapy in adult residents of northern Ghana.* Am J Trop Med Hyg, 2001. **65**(3): p. 7.
64. Smith, T., Felger, I., Tanner, M., Beck, H.P., *The epidemiology of multiple Plasmodium falciparum infections 11. Premunition in Plasmodium falciparum infection: Insights from the epidemiology of multiple infections.* Transactions of the Royal Society of Tropical Medicine and Hygiene,, 1999. **93**(1): p. 6.

65. Schuffner, W.A.P., *Two subjects relating to the epidemiology of malaria.* Mededeelingen van der Burgerlijken Geneeskundingen Dienst in Nederlandsche-Indie, 1919. **9**: p. 35.
66. Gupta S, S.R., Donnelly CA, Marsh K, Newbold C. , *Immunity to non-cerebral severe malaria is acquired after one or two infections.* Nat Med., 1999. **5**(3): p. 4.
67. Marsh K, S.R., *Host-parasite interaction and morbidity in malaria endemic areas.* Philos Trans R Soc Lond B Biol Sci., 1997 Sep 29;. **352**(1359): p. 10.
68. Okell, L.C., et al., *Submicroscopic infection in Plasmodium falciparum-endemic populations: a systematic review and meta-analysis.* J Infect Dis, 2009. **200**(10): p. 1509-17.
69. Medzhitov, R., D.S. Schneider, and M.P. Soares, *Disease tolerance as a defense strategy.* Science, 2012. **335**(6071): p. 936-41.
70. Menendez, C., et al., *Development of vaccines to prevent malaria in pregnant women: WHO MALVAC meeting report.* Expert Rev Vaccines, 2011. **10**(9): p. 1271-80.
71. Amino, R., et al., *Quantitative imaging of Plasmodium transmission from mosquito to mammal.* Nat Med, 2006. **12**(2): p. 220-4.
72. Chakravarty, S., et al., *CD8+ T lymphocytes protective against malaria liver stages are primed in skin-draining lymph nodes.* Nat Med, 2007. **13**(9): p. 1035-41.
73. Khan ZM, V.J., *Role of host cellular response in differential susceptibility of nonimmunized BALB/c mice to Plasmodium berghei and Plasmodium yoelii sporozoites.* Infect Immun., 1991.
74. Khan ZM, N.C., Vanderberg JP., *Early hepatic stages of Plasmodium berghei: release of circumsporozoite protein and host cellular inflammatory response.* Infect Immun., 1992.
75. Epiphanio, S., et al., *Heme oxygenase-1 is an anti-inflammatory host factor that promotes murine plasmodium liver infection.* Cell Host Microbe, 2008. **3**(5): p. 331-8.
76. Khan ZM, N.C., Vanderberg JP. , *Early hepatic stages of Plasmodium berghei: release of circumsporozoite protein and host cellular inflammatory response.* Infect Immun, 1992 Jan. **60**.
77. Leiriao P, M.M., Rodriguez A. AJ ;191(10):, *poptotic Plasmodium-infected hepatocytes provide antigens to liver dendritic cells.* Infect Dis., 2005 May 15. **191**(10): p. 14.
78. R. A. Seder, L.C., M. E. Enama, K. L. Zephir, U. N. Sarwar, I. J. Gordon, L. A. Holman, E. R. James, P. F. Billingsley, A. Gunasekera, A. Richman, S. Chakravarty, A. Manoj, S. Velmurugan, M. Li, A. J. Ruben, T. Li, A. G. Eappen, R. E. Stafford, S. H. Plummer, C. S. Hendel, L. Novik, P. J. M. Costner, F. H. Mendoza, J. G. Saunders, M. C. Nason, J. H. Richardson, J. Murphy, S. A. Davidson, T. L. Richie, M. Sedegah, A. Sutamihardja, G. A. Fahle, K. E. Lyke, M. B. Laurens, M. Roederer, K. Tewari, J. E. Epstein, B. K. L. Sim, J. E. Ledgerwood, B. S. Graham, S. L. Hoffman, *Protection Against Malaria by Intravenous Immunization with a Nonreplicating Sporozoite Vaccine.* Science, 2013. **341**(6152): p. 1359-1365.
79. Frevert, U., et al., *Intravital observation of Plasmodium berghei sporozoite infection of the liver.* PLoS Biol, 2005. **3**(6): p. e192.
80. Liehl, P. and M.M. Mota, *Innate recognition of malarial parasites by mammalian hosts.* Int J Parasitol, 2012. **42**(6): p. 557-66.

81. Usynin, I., C. Klotz, and U. Frevert, *Malaria circumsporozoite protein inhibits the respiratory burst in Kupffer cells.* Cell Microbiol, 2007. **9**(11): p. 2610-28.
82. Singh AP, B.C., Wang Q, Levay A, Nussenzweig DR, Walker JR, Winzeler EA, Fujii H, Fontoura BM, Nussenzweig V. , *Plasmodium circumsporozoite protein promotes the development of the liver stages of the parasite.* Cell, 2007 Nov 2. **131**(3): p. 13.
83. Leiriao, P., et al., *HGF/MET signalling protects Plasmodium-infected host cells from apoptosis.* Cell Microbiol, 2005. **7**(4): p. 603-9.
84. van de Sand, C., et al., *The liver stage of Plasmodium berghei inhibits host cell apoptosis.* Mol Microbiol, 2005. **58**(3): p. 731-42.
85. Esposito F, L.S., Modiano D, Zavala F, Reeme J, Lamizana L, Coluzzi M, Nussenzweig RS. , *Prevalence and levels of antibodies to the circumsporozoite protein of Plasmodium falciparum in an endemic area and their relationship to resistance against malaria infection.* Trans R Soc Trop Med Hyg., 1988. **82**(6): p. 6.
86. Zavala, F., Cochrane, A.H., Nardin, E.H., Nussenzweig, R.S., Nussenzweig, V, *Circumsporozoite proteins of malaria parasites contain a single immunodominant region with two or more identical epitopes.* J Exp Med, 1983. **157**(6): p. 1947–1957.
87. Zavala, F., Tam, J.P., Hollingdale, M.R., Cochrane, A.H., Quakyi, I., Nussenzweig, R.S., Nussenzweig V, *Rationale for development of a synthetic vaccine against Plasmodium falciparum malaria.* Science, 1985. **228,**(4706): p. 1436-1440.
88. Vanderberg, J.P. and U. Frevert, *Intravital microscopy demonstrating antibody-mediated immobilisation of Plasmodium berghei sporozoites injected into skin by mosquitoes.* Int J Parasitol, 2004. **34**(9): p. 991-6.
89. Nardin, E.H., Nussenzweig, V., Nussenzweig, R.S., Collins, W.E., Harinasuta, K.T., Tapchaisri, P., Chomcharn Y., *Circumsporozoite proteins of human malaria parasites Plasmodium falciparum and Plasmodium vivax.* J Exp Med, 1982. **156**.
90. Stewart MJ, N.R., Schulman S, Vanderberg JP. , *Plasmodium berghei sporozoite invasion is blocked in vitro by sporozoite-immobilizing antibodies.* Infect Immun., 1986 Mar. **51**(3): p. 6.
91. John, C.C., et al., *Antibodies to the Plasmodium falciparum antigens circumsporozoite protein, thrombospondin-related adhesive protein, and liver-stage antigen 1 vary by ages of subjects and by season in a highland area of Kenya.* Infect Immun, 2003. **71**(8): p. 4320-5.
92. John, C.C., et al., *Antibodies to pre-erythrocytic Plasmodium falciparum antigens and risk of clinical malaria in Kenyan children.* J Infect Dis, 2008. **197**(4): p. 519-26.
93. Reece, W.H., et al., *A CD4(+) T-cell immune response to a conserved epitope in the circumsporozoite protein correlates with protection from natural Plasmodium falciparum infection and disease.* Nat Med, 2004. **10**(4): p. 406-10.
94. Migot-Nabias F, D.P., Ringwald P, Dubois B, Mayombo J, Minh TN, Fievet N, Millet P, Luty A., *Immune response to Plasmodium falciparum liver stage antigen-1: geographical variations within Central Africa and their relationship with protection from clinical malaria.* Trans R Soc Trop Med Hyg., 2000 Sep-Oct;. **94**(5): p. 6.
95. John CC, S.P., Ouma JH, Nahlen BL, King CL, Kazura JW. , *Cytokine responses to Plasmodium falciparum liver-stage antigen 1 vary in rainy and dry seasons in highland Kenya.* Infect Immun., 2000 Sep. **68**(9): p. 7.
96. Nussenzweig RS, V.J., Most H, Orton C., *Protective Immunity produced by the Injection of X-irradiated Sporozoites of Plasmodium berghei.* Nature, 1967. **216**.

97. Rodrigues, M., Nussenzweig, R S and Zavala, , *The relative contribution of antibodies, CD4+ and CD8+ T cells to sporozoite-induced protection against malaria.* Immunology., 1993. **80**(1): p. 6.
98. Clyde, D.F., *mmunization of man against falciparum and vivax malaria by use of attenuated sporozoites.* I Am J Trop Med Hyg., 1975. **24**(3): p. 4.
99. Hoffman SL, G.L., Luke TC, Schneider I, Le TP, Doolan DL, Sacci J, de la Vega P, Dowler M, Paul C, Gordon DM, Stoute JA, Church LW, Sedegah M, Heppner DG, Ballou WR, Richie TL. , *Protection of humans against malaria by immunization with radiation-attenuated Plasmodium falciparum sporozoites.* J Infect Dis, 2002 Apr. **185**(8): p. 10.
100. Schmidt, N.W., et al., *Memory CD8 T cell responses exceeding a large but definable threshold provide long-term immunity to malaria.* Proc Natl Acad Sci U S A, 2008. **105**(37): p. 14017-22.
101. Ogwang, C., et al., *Safety and immunogenicity of heterologous prime-boost immunisation with Plasmodium falciparum malaria candidate vaccines, ChAd63 ME-TRAP and MVA ME-TRAP, in healthy Gambian and Kenyan adults.* PLoS One, 2013. **8**(3): p. e57726.
102. Overstreet, M.G., et al., *CD4+ T cells modulate expansion and survival but not functional properties of effector and memory CD8+ T cells induced by malaria sporozoites.* PLoS One, 2011. **6**(1): p. e15948.
103. Rénia L, G.D., Marussig M, Corradin G, Miltgen F, Lambert PH, Mazier D, Del Giudice G. , *Effector functions of circumsporozoite peptide-primed CD4+ T cell clones against Plasmodium yoelii liver stages.* J Immunol., 1993. **150**(14): p. 8.
104. McGregor, I.A., *Studies in the acquisition of immunity of plasmodium falciparum infections in africa.* Trans R Soc Trop Med Hyg., 1964. **58**: p. 80.
105. Snow RW, N.B., Palmer A, Donnelly CA, Gupta S, Marsh K. 177(3):819-22. , *Risk of severe malaria among African infants: direct evidence of clinical protection during early infancy.* J Infect Dis., 1998 Mar;. **177**(3): p. 4.
106. Golgi, C., *Sulle febbri malariche estivo-autunnali di Roma.* Gazzetta Medica di Pavia, 1893. **2**(2): p. 13.
107. Bautista, J.M., et al., *Malaria proteomics: insights into the parasite-host interactions in the pathogenic space.* J Proteomics, 2014. **97**: p. 107-25.
108. Schofield L, H.F., *Signal transduction in host cells by a glycosylphosphatidylinositol toxin of malaria parasites.* J Exp Med., 1993 Jan 1. **177**(1): p. 9.
109. Krishnegowda, G., et al., *Induction of proinflammatory responses in macrophages by the glycosylphosphatidylinositols of Plasmodium falciparum: cell signaling receptors, glycosylphosphatidylinositol (GPI) structural requirement, and regulation of GPI activity.* J Biol Chem, 2005. **280**(9): p. 8606-16.
110. Carvalho LH, F.C., Krettli AU. ;60(4):674-9., *Cellular responses to Plasmodium falciparum major surface antigens and their relationship to human activities associated with malaria transmission.* Am J Trop Med Hyg., 1999 Apr. **60**(4): p. 6.
111. Elloso MM, v.d.H.H., vande Waa JA, Manning DD, Weidanz WP. , *Inhibition of Plasmodium falciparum in vitro by human gamma delta T cells.* J Immunol., 1994 Aug 1. **153**: p. 8.
112. Riley, E.M., et al., *Naturally acquired cellular and humoral immune responses to the major merozoite surface antigen (PfMSP1) of Plasmodium falciparum are*

associated with reduced malaria morbidity. Parasite Immunol, 1992. **14**(3): p. 321-37.
113. Podoba JE, S.M., *CD4+ and CD8+ T lymphocytes both contribute to acquired immunity to blood-stage Plasmodium chabaudi AS.* Infect Immun., 1991 Jan. **59**(1): p. 8.
114. Langhorne J, M.S., Eichmann K, Gillard SS. , *The response of CD4+ T cells to Plasmodium chabaudi chabaudi.* Immunol Rev. 1, 1989 Dec;. **12**: p. 29.
115. McCall, M.B. and R.W. Sauerwein, *Interferon-gamma--central mediator of protective immune responses against the pre-erythrocytic and blood stage of malaria.* J Leukoc Biol, 2010. **88**(6): p. 1131-43.
116. Stevenson MM, T.M.-. *Differential induction of helper T cell subsets during blood-stage Plasmodium chabaudi AS infection in resistant and susceptible mice.* Clin Exp Immunol., 1993 Apr. **92**(1): p. 7.
117. Cohen S. McGregor, I.A., Carrington, S. , *Gamma-globulin and acquired immunity to human malaria.* Nature., 1961 Nov 25;. **1192**: p. 5.
118. Chan, J.A., F.J. Fowkes, and J.G. Beeson, *Surface antigens of Plasmodium falciparum-infected erythrocytes as immune targets and malaria vaccine candidates.* Cell Mol Life Sci, 2014. **71**(19): p. 3633-57.
119. Fowkes, F.J., et al., *The relationship between anti-merozoite antibodies and incidence of Plasmodium falciparum malaria: A systematic review and meta-analysis.* PLoS Med, 2010. **7**(1): p. e1000218.
120. Tran, T.M., et al., *Naturally acquired antibodies specific for Plasmodium falciparum reticulocyte-binding protein homologue 5 inhibit parasite growth and predict protection from malaria.* J Infect Dis, 2014. **209**(5): p. 789-98.
121. Chiu, C.Y., et al., *Association of antibodies to Plasmodium falciparum reticulocyte binding protein homolog 5 with protection from clinical malaria.* Front Microbiol, 2014. **5**: p. 314.
122. Douglas, A.D., et al., *The blood-stage malaria antigen PfRH5 is susceptible to vaccine-inducible cross-strain neutralizing antibody.* Nat Commun, 2011. **2**: p. 601.
123. Duffy, P.E., et al., *Pre-erythrocytic malaria vaccines: identifying the targets.* Expert Rev Vaccines, 2012. **11**(10): p. 1261-80.
124. Goodman, A.L. and S.J. Draper, *Blood-stage malaria vaccines - recent progress and future challenges.* Ann Trop Med Parasitol, 2010. **104**(3): p. 189-211.
125. Nunes, J.K., et al., *Development of a transmission-blocking malaria vaccine: progress, challenges, and the path forward.* Vaccine, 2014. **32**(43): p. 5531-9.
126. Offeddu, V., et al., *Naturally acquired immune responses against Plasmodium falciparum sporozoites and liver infection.* Int J Parasitol, 2012. **42**(6): p. 535-48.
127. Reyes-Sandoval, A., et al., *Single-dose immunogenicity and protective efficacy of simian adenoviral vectors against Plasmodium berghei.* Eur J Immunol, 2008. **38**(3): p. 732-41.
128. Reyes-Sandoval, A., et al., *Prime-boost immunization with adenoviral and modified vaccinia virus Ankara vectors enhances the durability and polyfunctionality of protective malaria CD8+ T-cell responses.* Infect Immun, 2010. **78**(1): p. 145-53.
129. O'Hara, G.A., et al., *Clinical assessment of a recombinant simian adenovirus ChAd63: a potent new vaccine vector.* J Infect Dis, 2012. **205**(5): p. 772-81.
130. Gola A, S.D., Walters AA, Sridhar S, Uderhardt S, Salman AM, Halbroth BR, Bellamy D, Bowyer G, Powlson J, Baker M, Venkatraman N, Poulton I, Berrie E, Roberts R,

Lawrie AM, Angus B, Khan SM, Janse CJ, Ewer KJ, Germain RN, Spencer AJ, Hill AVS. , *Prime and target immunization protects against liver-stage malaria in mice.* Sci Transl Med., 2018. **10**(460).
131. Draper, S.J., et al., *Malaria Vaccines: Recent Advances and New Horizons.* Cell Host Microbe, 2018. **24**(1): p. 43-56.
132. Spring, M., M. Polhemus, and C. Ockenhouse, *Controlled human malaria infection.* J Infect Dis, 2014. **209 Suppl 2**: p. S40-5.
133. Laurens, M.B., et al., *A consultation on the optimization of controlled human malaria infection by mosquito bite for evaluation of candidate malaria vaccines.* Vaccine, 2012. **30**(36): p. 5302-4.
134. Langhorne J, B.P., Galinski M, Good M, Harty J, Leroy D, Mota MM, Pasini E, Renia L, Riley E, Stins M, Duffy P. 10:23, *The relevance of non-human primate and rodent malaria models for humans.* Malar J., 2011 Feb 2;. **10**(23).
135. Wykes, M.N. and M.F. Good, *What have we learnt from mouse models for the study of malaria?* Eur J Immunol, 2009. **39**(8): p. 2004-7.
136. Espinosa, D.A., et al., *Development of a chimeric Plasmodium berghei strain expressing the repeat region of the P. vivax circumsporozoite protein for in vivo evaluation of vaccine efficacy.* Infect Immun, 2013. **81**(8): p. 2882-7.
137. Mlambo, G. and N. Kumar, *Transgenic rodent Plasmodium berghei parasites as tools for assessment of functional immunogenicity and optimization of human malaria vaccines.* Eukaryot Cell, 2008. **7**(11): p. 1875-9.
138. de Koning-Ward TF, J.C., Waters AP. , *The development of genetic tools for dissecting the biology of malaria parasites.* Annu Rev Microbiol., 2000. **54**: p. 11.
139. Janse, C.J., et al., *High efficiency transfection of Plasmodium berghei facilitates novel selection procedures.* Mol Biochem Parasitol, 2006. **145**(1): p. 60-70.
140. Foquet L, H.C., van Gemert GJ, Libbrecht L, Sauerwein R, Meuleman P, Leroux-Roels G. ;12:430. , *Molecular detection and quantification of Plasmodium falciparum-infected human hepatocytes in chimeric immune-deficient mice.* Malar J., 2013 Nov 24. **12**(430).
141. Genito, C.J., et al., *Liposomes containing monophosphoryl lipid A and QS-21 serve as an effective adjuvant for soluble circumsporozoite protein malaria vaccine FMP013.* Vaccine, 2017. **35**(31): p. 3865-3874.
142. Seth, L., et al., *Development of a self-assembling protein nanoparticle vaccine targeting Plasmodium falciparum Circumsporozoite Protein delivered in three Army Liposome Formulation adjuvants.* Vaccine, 2017. **35**(41): p. 5448-5454.
143. Itsara, L.S., et al., *The Development of Whole Sporozoite Vaccines for Plasmodium falciparum Malaria.* Front Immunol, 2018. **9**: p. 2748.
144. Oneko, M., et al., *Safety, immunogenicity and efficacy of PfSPZ Vaccine against malaria in infants in western Kenya: a double-blind, randomized, placebo-controlled phase 2 trial.* Nat Med, 2021. **27**(9): p. 1636-1645.
145. Coulibaly, D., et al., *PfSPZ-CVac malaria vaccine demonstrates safety among malaria-experienced adults: A randomized, controlled phase 1 trial.* EClinicalMedicine, 2022. **52**: p. 101579.
146. Roestenberg M, W.J., van der Boor SC, Langenberg MCC, Hoogerwerf MA, Janse JJ, Manurung M, Yap XZ, García AF, Koopman JPR, Meij P, Wessels E, Teelen K, van Waardenburg YM, van de Vegte-Bolmer M, van Gemert GJ, Visser LG, van der Ven AJAM, de Mast Q, Natasha KC, Abebe Y, Murshedkar T, Billingsley PF, Richie TL, Sim

BKL, Janse CJ, Hoffman SL, Khan SM, Sauerwein RW. , *A double-blind, placebo-controlled phase 1/2a trial of the genetically attenuated malaria vaccine PfSPZ-GA1.* Sci Transl Med., 2020 May 20;. **12**.
147. Franke-Fayard, B., et al., *Creation and preclinical evaluation of genetically attenuated malaria parasites arresting growth late in the liver.* NPJ Vaccines, 2022. **7**(1): p. 139.
148. Datoo, M.S., et al., *Efficacy of a low-dose candidate malaria vaccine, R21 in adjuvant Matrix-M, with seasonal administration to children in Burkina Faso: a randomised controlled trial.* The Lancet, 2021. **397**(10287): p. 1809-1818.
149. Datoo, M.S., et al., *Efficacy and immunogenicity of R21/Matrix-M vaccine against clinical malaria after 2 years' follow-up in children in Burkina Faso: a phase 1/2b randomised controlled trial.* The Lancet Infectious Diseases, 2022.
150. Friedman-Klabanoff, D.J., et al., *Low dose recombinant full-length circumsporozoite protein-based Plasmodium falciparum vaccine is well-tolerated and highly immunogenic in phase 1 first-in-human clinical testing.* Vaccine, 2021. **39**(8): p. 1195-1200.
151. Urakami A, S.A., Ishikawa M, Yap ML, Flores-Garcia Y, Haseda Y, Aoshi T, Zavala FP, Rossmann MG, Kuno S, Ueno R, Akahata W., *Development of a Novel Virus-Like Particle Vaccine Platform That Mimics the Immature Form of Alphavirus.* Clin Vaccine Immunol., 2017 Jul 5. **24**(7).
152. Ezoe, S., et al., *First-in-human randomised trial and follow-up study of Plasmodium falciparum blood-stage malaria vaccine BK-SE36 with CpG-ODN(K3).* Vaccine, 2020. **38**(46): p. 7246-7257.
153. Payne, R.O., et al., *Human vaccination against RH5 induces neutralizing antimalarial antibodies that inhibit RH5 invasion complex interactions.* JCI Insight, 2017. **2**(21).
154. Stanisic, D.I., et al., *Vaccination with chemically attenuated Plasmodium falciparum asexual blood-stage parasites induces parasite-specific cellular immune responses in malaria-naive volunteers: a pilot study.* BMC Med, 2018. **16**(1): p. 184.
155. Minassian, A.M., et al., *Reduced blood-stage malaria growth and immune correlates in humans following RH5 vaccination.* Med (N Y), 2021. **2**(6): p. 701-719 e19.
156. Druilhe, P., *Biofusion proteins as anti-malaria vaccines*, in *WIPO*, V.a.P. Ltd, Editor. 2018: Canada.
157. Ragotte, R.J., M.K. Higgins, and S.J. Draper, *The RH5-CyRPA-Ripr Complex as a Malaria Vaccine Target.* Trends Parasitol, 2020. **36**(6): p. 545-559.
158. Mulamba, C., et al., *Evaluation of the Pfs25-IMX313/Matrix-M malaria transmission-blocking candidate vaccine in endemic settings.* Malar J, 2022. **21**(1): p. 159.
159. Sirima, S.B., et al., *PRIMVAC vaccine adjuvanted with Alhydrogel or GLA-SE to prevent placental malaria: a first-in-human, randomised, double-blind, placebo-controlled study.* Lancet Infect Dis, 2020. **20**(5): p. 585-597.
160. Ko, K.T., et al., *Structure of the malaria vaccine candidate Pfs48/45 and its recognition by transmission blocking antibodies.* Nat Commun, 2022. **13**(1): p. 5603.
161. Roestenberg M, M.M., Hopman J, et al. Protection against a malaria challenge by sporozoite inoculation. , *Protection against a Malaria Challenge by Sporozoite Inoculation.* N Engl J Med., 2009(361): p. 468-477.

162. Rieckmann KH, B.R., Cassells JS, Sell KW. , *Use of attenuated sporozoites in the immunization of human volunteers against falciparum malaria.* Bull World Health Organ., 1979. **57**: p. 5.
163. Hoffman, S.L., et al., *Development of a metabolically active, non-replicating sporozoite vaccine to prevent Plasmodium falciparum malaria.* Hum Vaccin, 2010. **6**(1): p. 97-106.
164. Luke, T.C. and S.L. Hoffman, *Rationale and plans for developing a non-replicating, metabolically active, radiation-attenuated Plasmodium falciparum sporozoite vaccine.* J Exp Biol, 2003. **206**(Pt 21): p. 3803-8.
165. Oakley, M.S., et al., *Molecular Markers of Radiation Induced Attenuation in Intrahepatic Plasmodium falciparum Parasites.* PLoS One, 2016. **11**(12): p. e0166814.
166. James, E.R., et al., *A First for Human Vaccinology: GMP Compliant Radiation Attenuation of Plasmodium falciparum Sporozoites for Production of a Vaccine Against Malaria.* Front Immunol, 2022. **13**: p. 851028.
167. Mueller, A.K., et al., *Plasmodium liver stage developmental arrest by depletion of a protein at the parasite-host interface.* Proc Natl Acad Sci U S A, 2005. **102**(8): p. 3022-7.
168. van Dijk, M.R., et al., *Genetically attenuated, P36p-deficient malarial sporozoites induce protective immunity and apoptosis of infected liver cells.* Proc Natl Acad Sci U S A, 2005. **102**(34): p. 12194-9.
169. Hoffman, S.L., et al., *The March Toward Malaria Vaccines.* Am J Prev Med, 2015. **49**(6 Suppl 4): p. S319-33.
170. VanBuskirk, K.M., et al., *Preerythrocytic, live-attenuated Plasmodium falciparum vaccine candidates by design.* Proc Natl Acad Sci U S A, 2009. **106**(31): p. 13004-9.
171. Annoura, T., et al., *Assessing the adequacy of attenuation of genetically modified malaria parasite vaccine candidates.* Vaccine, 2012. **30**(16): p. 2662-70.
172. van Schaijk, B.C., et al., *Gene disruption of Plasmodium falciparum p52 results in attenuation of malaria liver stage development in cultured primary human hepatocytes.* PLoS One, 2008. **3**(10): p. e3549.
173. Spring, M., et al., *First-in-human evaluation of genetically attenuated Plasmodium falciparum sporozoites administered by bite of Anopheles mosquitoes to adult volunteers.* Vaccine, 2013. **31**(43): p. 4975-83.
174. Kublin, J.G., et al., *Complete attenuation of genetically engineered Plasmodium falciparum sporozoites in human subjects.* Sci Transl Med, 2017. **9**(371).
175. van Schaijk, B.C., et al., *A genetically attenuated malaria vaccine candidate based on P. falciparum b9/slarp gene-deficient sporozoites.* Elife, 2014. **3**.
176. Beaudoin RL, S.C., Mitchell F, Tubergen TA., *Plasmodium berghei: immunization of mice against the ANKA strain using the unaltered sporozoite as an antigen.* Exp Parasitol., 1977 Jun;. **42**(1): p. 1.
177. Orjih AU, C.A., Nussenzweig RS. , *Comparative studies on the immunogenicity of infective and attenuated sporozoites of Plasmodium berghei.* Trans R Soc Trop Med Hyg., 1982. **76**(1): p. 4.
178. Belnoue, E., et al., *Protective T cell immunity against malaria liver stage after vaccination with live sporozoites under chloroquine treatment.* J Immunol, 2004. **172**(4): p. 2487-95.

179. Golenser J, H.J., Verhave JP, Kaay HJ, Meuwissen JH. , *Crossreactivity with sporozoites, exoerythrocytic forms and blood schizonts of Plasmodium berghei in indirect fluorescent antibody tests with sera of rats immunized with sporozoites or infected blood.* Clin Exp Immunol., 1977 Jul. **29**(1): p. 9.
180. Slater, A.F., *Chloroquine: mechanism of drug action and resistance in Plasmodium falciparum.* Pharmacol Ther., 1993 Feb-Mar;57. **2**(3): p. 33.
181. Lewis, M.D., et al., *CD8(+) T cells mediate robust stage-specific immunity to P. berghei under chemoprophylaxis and this protective environment is not downregulated by the presence of blood-stage infection.* PLoS One, 2014. **9**(2): p. e88117.
182. Bijker, E.M., et al., *Protection against malaria after immunization by chloroquine prophylaxis and sporozoites is mediated by preerythrocytic immunity.* Proc Natl Acad Sci U S A, 2013. **110**(19): p. 7862-7.
183. Pfeil, J., et al., *Protection against malaria by immunization with non-attenuated sporozoites under single-dose piperaquine-tetraphosphate chemoprophylaxis.* Vaccine, 2014. **32**(45): p. 6005-11.
184. Friesen, J. and K. Matuschewski, *Comparative efficacy of pre-erythrocytic whole organism vaccine strategies against the malaria parasite.* Vaccine, 2011. **29**(40): p. 7002-8.
185. Friesen, J., S. Borrmann, and K. Matuschewski, *Induction of antimalaria immunity by pyrimethamine prophylaxis during exposure to sporozoites is curtailed by parasite resistance.* Antimicrob Agents Chemother, 2011. **55**(6): p. 2760-7.
186. Peng, X., et al., *Artesunate versus chloroquine infection-treatment-vaccination defines stage-specific immune responses associated with prolonged sterile protection against both pre-erythrocytic and erythrocytic Plasmodium yoelii infection.* J Immunol, 2014. **193**(3): p. 1268-77.
187. Joe, C.C.D., et al., *Manufacturing a chimpanzee adenovirus-vectored SARS-CoV-2 vaccine to meet global needs.* Biotechnol Bioeng, 2022. **119**(1): p. 48-58.
188. Potocnjak, P., Yoshida, N., Nussenzweig, R.S., Nussenzweig, V., *Monovalent fragments (Fab) of monoclonal antibodies to a sporozoite surface antigen (Pb44) protect mice against malarial infection.* J Exp Med, 1980. **152**(6): p. 10.
189. Yoshida, N., Nussenzweig, R.S., Potocnjak, P., Nussenzweig, V., Aikawa, M., *Hybridoma Produces Protective Antibodies Directed against the Sporozoite Stage of Malaria Parasite.* Science, 1980. **207**(446).
190. Gordon DM, M.T., Krzych U, Cohen JC, Schneider I, LaChance R, Heppner DG, Yuan G, Hollingdale M, Slaoui M, et al., *Safety, immunogenicity, and efficacy of a recombinantly produced Plasmodium falciparum circumsporozoite protein-hepatitis B surface antigen subunit vaccine.* J Infect Dis., 1995. **171**(6): p. 10.
191. Olotu, A., et al., *Efficacy of RTS,S/AS01E malaria vaccine and exploratory analysis on anti-circumsporozoite antibody titres and protection in children aged 5-17 months in Kenya and Tanzania: a randomised controlled trial.* Lancet Infect Dis, 2011. **11**(2): p. 102-9.
192. White, M.T., et al., *The relationship between RTS,S vaccine-induced antibodies, CD4(+) T cell responses and protection against Plasmodium falciparum infection.* PLoS One, 2013. **8**(4): p. e61395.
193. Collins, K.A., et al., *Enhancing protective immunity to malaria with a highly immunogenic virus-like particle vaccine.* Sci Rep, 2017. **7**: p. 46621.

194. Collins, K.A., et al., *Ultra-low dose immunization and multi-component vaccination strategies enhance protection against malaria in mice.* Sci Rep, 2021. **11**(1): p. 10792.
195. Hodgson, S.H., et al., *Evaluation of the efficacy of ChAd63-MVA vectored vaccines expressing circumsporozoite protein and ME-TRAP against controlled human malaria infection in malaria-naive individuals.* J Infect Dis, 2015. **211**(7): p. 1076-86.
196. Mallory, K.L., et al., *Messenger RNA expressing PfCSP induces functional, protective immune responses against malaria in mice.* NPJ Vaccines, 2021. **6**(1): p. 84.
197. Langowski, M.D., et al., *Optimization of a Plasmodium falciparum circumsporozoite protein repeat vaccine using the tobacco mosaic virus platform.* Proc Natl Acad Sci U S A, 2020. **117**(6): p. 3114-3122.
198. Kisalu, N.K., et al., *A human monoclonal antibody prevents malaria infection by targeting a new site of vulnerability on the parasite.* Nat Med, 2018. **24**(4): p. 408-416.
199. Tan, J., et al., *A public antibody lineage that potently inhibits malaria infection through dual binding to the circumsporozoite protein.* Nat Med, 2018. **24**(4): p. 401-407.
200. Robson, K.J., et al., *A highly conserved amino-acid sequence in thrombospondin, properdin and in proteins from sporozoites and blood stages of a human malaria parasite.* Nature, 1988. **335**(6185): p. 79-82.
201. Akhouri, R.R., et al., *Structural and functional dissection of the adhesive domains of Plasmodium falciparum thrombospondin-related anonymous protein (TRAP).* Biochem J, 2004. **379**(Pt 3): p. 815-22.
202. Akhouri, R.R., et al., *Role of Plasmodium falciparum thrombospondin-related anonymous protein in host-cell interactions.* Malar J, 2008. **7**: p. 63.
203. Tiono, A.B., et al., *First field efficacy trial of the ChAd63 MVA ME-TRAP vectored malaria vaccine candidate in 5-17 months old infants and children.* PLoS One, 2018. **13**(12): p. e0208328.
204. Ewer, K.J., et al., *Protective CD8+ T-cell immunity to human malaria induced by chimpanzee adenovirus-MVA immunisation.* Nat Commun, 2013. **4**: p. 2836.
205. Gantt, S., et al., *Antibodies against thrombospondin-related anonymous protein do not inhibit Plasmodium sporozoite infectivity in vivo.* Infection and Immunity, 2000. **68**(6): p. 3667--3673.
206. McConkey, S.J., et al., *Enhanced T-cell immunogenicity of plasmid DNA vaccines boosted by recombinant modified vaccinia virus Ankara in humans.* Nat Med, 2003. **9**(6): p. 729-35.
207. Robson, K.J., et al., *Natural polymorphism in the thrombospondin-related adhesive protein of Plasmodium falciparum.* Am J Trop Med Hyg, 1998. **58**(1): p. 81-9.
208. Schats, R., et al., *Heterologous Protection against Malaria after Immunization with Plasmodium falciparum Sporozoites.* PLoS One, 2015. **10**(5): p. e0124243.
209. Rodriguez-Galan, A., et al., *An in vitro assay to measure antibody-mediated inhibition of P. berghei sporozoite invasion against P. falciparum antigens.* Sci Rep, 2017. **7**(1): p. 17011.
210. ROSARIO, V., *Cloning of Naturally Occurring Mixed Infections of Malaria Parasites.* Science, 1981. **212**(4498): p. 2.
211. Robson, K.J., et al., *Polymorphism of the TRAP gene of Plasmodium falciparum.* Proc Biol Sci, 1990. **242**(1305): p. 205-16.

212. Robson, K.J.H., *Thrombospondin-related adhesive protein (TRAP) of Plasmodium falciparum: Expression during sporozoite ontogeny and binding to human hepatocytes.* Parasitology Today, 1995. **11**(11): p. 410.
213. Cowan, G., et al., *Expression of thrombospondin-related anonymous protein in Plasmodium falciparum sporozoites.* The Lancet, 1992. **339**(8806): p. 1412--1413.
214. Sultan, A.A., et al., *TRAP is necessary for gliding motility and infectivity of Plasmodium sporozoites.* Cell, 1997. **90**(3): p. 511--522.
215. Aidoo, M., et al., *Recombinant vaccinia viruses for the characterization of Plasmodium falciparum-specific cytotoxic T lymphocytes: recognition of processed antigen despite limited re-stimulation efficacy.* Int Immunol, 1997. **9**(5): p. 731-7.
216. Gilbert, S.C., et al., *A protein particle vaccine containing multiple malaria epitopes.* Nature biotechnology, 1997. **15**(November): p. 498--502.
217. Schneider, J., et al., *A prime-boost immunisation regimen using DNA followed by recombinant modified vaccinia virus Ankara induces strong cellular immune responses against the Plasmodium falciparum TRAP antigen in chimpanzees.* Vaccine, 2001. **19**(32): p. 4595-602.
218. Moorthy, V.S., et al., *Safety and immunogenicity of DNA/modified vaccinia virus ankara malaria vaccination in African adults.* J Infect Dis, 2003. **188**(8): p. 1239-44.
219. Moorthy, V.S., et al., *Safety of DNA and modified vaccinia virus Ankara vaccines against liver-stage P. falciparum malaria in non-immune volunteers.* Vaccine, 2003. **21**(17-18): p. 1995-2002.
220. Bejon, P., et al., *A phase 2b randomised trial of the candidate malaria vaccines FP9 ME-TRAP and MVA ME-TRAP among children in Kenya.* PLoS Clin Trials, 2006. **1**(6): p. e29.
221. Dunachie, S.J., et al., *A DNA prime-modified vaccinia virus ankara boost vaccine encoding thrombospondin-related adhesion protein but not circumsporozoite protein partially protects healthy malaria-naive adults against Plasmodium falciparum sporozoite challenge.* Infect Immun, 2006. **74**(10): p. 5933-42.
222. Webster, D.P., et al., *Safety of recombinant fowlpox strain FP9 and modified vaccinia virus Ankara vaccines against liver-stage P. falciparum malaria in non-immune volunteers.* Vaccine, 2006. **24**(15): p. 3026-34.
223. Kimani, D., et al., *Translating the immunogenicity of prime-boost immunization with ChAd63 and MVA ME-TRAP from malaria naive to malaria-endemic populations.* Mol Ther, 2014. **22**(11): p. 1992-2003.
224. Gilbert, S.C., et al., *Enhanced CD8 T cell immunogenicity and protective efficacy in a mouse malaria model using a recombinant adenoviral vaccine in heterologous prime-boost immunisation regimes.* Vaccine, 2002. **20**(7-8): p. 1039--1045.
225. Mensah, V.A., et al., *Safety, Immunogenicity and Efficacy of Prime-Boost Vaccination with ChAd63 and MVA Encoding ME-TRAP against Plasmodium falciparum Infection in Adults in Senegal.* PLoS One, 2016. **11**(12): p. e0167951.
226. Bliss, C.M., et al., *Viral Vector Malaria Vaccines Induce High-Level T Cell and Antibody Responses in West African Children and Infants.* Mol Ther, 2017. **25**(2): p. 547-559.
227. Aidoo M, L.A., Allsopp CE, Plebanski M, Meisner SJ, Krausa P, Browning M, Morris-Jones S, Gotch F, Fidock DA, et al., *Identification of conserved antigenic components for a cytotoxic T lymphocyte-inducing vaccine against malaria.* Lancet., 1995 Apr 22. **345**(8956): p. 5.

228. Ogwang, C., et al., *Prime-boost vaccination with chimpanzee adenovirus and modified vaccinia Ankara encoding TRAP provides partial protection against Plasmodium falciparum infection in Kenyan adults.* Sci Transl Med, 2015. **7**(286): p. 286re5.
229. Bejon, P., et al., *The induction and persistence of T cell IFN-gamma responses after vaccination or natural exposure is suppressed by Plasmodium falciparum.* J Immunol, 2007. **179**(6): p. 4193-201.
230. Ramalingam, T.R., Reiman, R. M. & Wynn, T. A., *Exploiting worm and allergy models to understand Th2 cytokine biology.* Current Opinion in Allergy and Clinical Immunology, 2005. **5**(5): p. 7.
231. Liebeschuetz, S., et al., *Diagnosis of tuberculosis in South African children with a T cell-based assay: a prospective cohort study.* The Lancet, 2004. **364**(9452): p. 2196-2203.
232. Schneider, J., et al., *Enhanced immunogenicity for CD8+ T cell induction and complete protective efficacy of malaria DNA vaccination by boosting with modified vaccinia virus Ankara.* Nature Medicine, 1998. **4**(4): p. 397--402.
233. Longley, R.J., et al., *Comparative assessment of vaccine vectors encoding ten malaria antigens identifies two protective liver-stage candidates.* Sci Rep, 2015. **5**: p. 11820.
234. Longley, R.J., A.V. Hill, and A.J. Spencer, *Malaria vaccines: identifying Plasmodium falciparum liver-stage targets.* Front Microbiol, 2015. **6**: p. 965.
235. Bettencourt, P., *Current Challenges in the Identification of Pre-Erythrocytic Malaria Vaccine Candidate Antigens.* Front Immunol, 2020. **11**: p. 190.
236. Mauro, V.P. and S.A. Chappell, *A critical analysis of codon optimization in human therapeutics.* Trends Mol Med, 2014. **20**(11): p. 604-13.
237. Mauro, V.P., *Codon Optimization in the Production of Recombinant Biotherapeutics: Potential Risks and Considerations.* BioDrugs, 2018. **32**(1): p. 69-81.
238. Narum, D.L., et al., *Codon optimization of gene fragments encoding Plasmodium falciparum merzoite proteins enhances DNA vaccine protein expression and immunogenicity in mice.* Infect Immun, 2001. **69**(12): p. 7250-3.
239. Ko, H.J., et al., *Optimization of codon usage enhances the immunogenicity of a DNA vaccine encoding mycobacterial antigen Ag85B.* Infect Immun, 2005. **73**(9): p. 5666-74.
240. Datta, D., et al., *Evaluation of the Impact of Codon Optimization and N-Linked Glycosylation on Functional Immunogenicity of Pfs25 DNA Vaccines Delivered by In Vivo Electroporation in Preclinical Studies in Mice.* Clin Vaccine Immunol, 2015. **22**(9): p. 1013-9.
241. Lorenz, F.K., et al., *Codon optimization of the human papillomavirus E7 oncogene induces a CD8+ T cell response to a cryptic epitope not harbored by wild-type E7.* PLoS One, 2015. **10**(3): p. e0121633.
242. Stachyra, A., et al., *Codon optimization of antigen coding sequences improves the immune potential of DNA vaccines against avian influenza virus H5N1 in mice and chickens.* Virol J, 2016. **13**(1): p. 143.
243. Liang, B., et al., *Improved Prefusion Stability, Optimized Codon Usage, and Augmented Virion Packaging Enhance the Immunogenicity of Respiratory Syncytial Virus Fusion Protein in a Vectored-Vaccine Candidate.* J Virol, 2017. **91**(15).

244. Lopes, A., et al., *Codon-Optimized P1A-Encoding DNA Vaccine: Toward a Therapeutic Vaccination against P815 Mastocytoma.* Mol Ther Nucleic Acids, 2017. **8**: p. 404-415.
245. Latanova, A.A., et al., *Codon optimization and improved delivery/immunization regimen enhance the immune response against wild-type and drug-resistant HIV-1 reverse transcriptase, preserving its Th2-polarity.* Sci Rep, 2018. **8**(1): p. 8078.
246. Punde, N., et al., *Codon harmonization reduces amino acid misincorporation in bacterially expressed P. falciparum proteins and improves their immunogenicity.* AMB Express, 2019. **9**(1): p. 167.
247. Luo, M., et al., *Immunization with plasmid DNA encoding influenza A virus nucleoprotein fused to a tissue plasminogen activator signal sequence elicits strong immune responses and protection against H5N1 challenge in mice.* J Virol Methods, 2008. **154**(1-2): p. 121-7.
248. Kou, Y., et al., *Tissue plasminogen activator (tPA) signal sequence enhances immunogenicity of MVA-based vaccine against tuberculosis.* Immunol Lett, 2017. **190**: p. 51-57.
249. Alharbi, N.K., et al., *ChAdOx1 and MVA based vaccine candidates against MERS-CoV elicit neutralising antibodies and cellular immune responses in mice.* Vaccine, 2017. **35**(30): p. 3780-3788.
250. Walliker, D.Q., Isabella A. ; Wellems, Thomas E. ; McCutchan, Thomas F. ; Szarfman, Ana ; London, William T. ; Corcoran, Lynn M. ; Burkot, Thomas R. ; Carter, Richard, *Genetic Analysis of the Human Malaria Parasite Plasmodium falciparum.* American Association for the Advancement of Science, 1987. **236**(4809): p. 7.
251. Preston, M.D., et al., *A barcode of organellar genome polymorphisms identifies the geographic origin of Plasmodium falciparum strains.* Nat Commun, 2014. **5**: p. 4052.
252. Sallberg, M., et al., *A malaria vaccine candidate based on a hepatitis B virus core platform.* Intervirology, 2002. **45**(4-6): p. 350-61.
253. Walk, J., et al., *Modest heterologous protection after Plasmodium falciparum sporozoite immunization: a double-blind randomized controlled clinical trial.* BMC Med, 2017. **15**(1): p. 168.
254. Epstein, J.E., et al., *Protection against Plasmodium falciparum malaria by PfSPZ Vaccine.* JCI Insight, 2017. **2**(1): p. e89154.
255. Dicks, M.D.J., et al., *A novel chimpanzee adenovirus vector with low human seroprevalence: Improved systems for vector derivation and comparative immunogenicity.* PLoS ONE, 2012. **7**(7).
256. Spencer, A.J., et al., *Enhanced vaccine-induced CD8+ T cell responses to malaria antigen ME-TRAP by fusion to MHC class ii invariant chain.* PLoS One, 2014. **9**(6): p. e100538.
257. Spencer, A.J., et al., *The Threshold of Protection from Liver-Stage Malaria Relies on a Fine Balance between the Number of Infected Hepatocytes and Effector CD8(+) T Cells Present in the Liver.* J Immunol, 2017. **198**(5): p. 2006-2016.
258. Padron-Regalado, E., et al., *STING-pathway modulation to enhance the immunogenicity of adenoviral-vectored vaccines.* Sci Rep, 2022. **12**(1): p. 14464.
259. Milicic, A., et al., *Adjuvanting a viral vectored vaccine against pre-erythrocytic malaria.* Sci Rep, 2017. **7**(1): p. 7284.
260. Ogun, S.A., et al., *The oligomerization domain of C4-binding protein (C4bp) acts as an adjuvant, and the fusion protein comprised of the 19-kilodalton merozoite*

surface protein 1 fused with the murine C4bp domain protects mice against malaria. Infect Immun, 2008. **76**(8): p. 3817-23.
261. Capone, S., et al., *Fusion of HCV nonstructural antigen to MHC class II-associated invariant chain enhances T-cell responses induced by vectored vaccines in nonhuman primates.* Mol Ther, 2014. **22**(5): p. 1039-47.
262. Mikkelsen, M., et al., *Enhanced and sustained CD8+ T cell responses with an adenoviral vector-based hepatitis C virus vaccine encoding NS3 linked to the MHC class II chaperone protein invariant chain.* J Immunol, 2011. **186**(4): p. 2355-64.
263. Rowe, H.M., et al., *Immunization with a lentiviral vector stimulates both CD4 and CD8 T cell responses to an ovalbumin transgene.* Mol Ther, 2006. **13**(2): p. 310-9.
264. Diebold, S.S., Cotten, M., Koch, N., Zenke, M., *MHC class II presentation of endogenously expressed antigens by transfected dendritic cells.* Gene Ther., 2001 Mar. **8**(6): p. 7.
265. Malcherek, G., et al., *MHC class II-associated invariant chain peptide replacement by T cell epitopes: engineered invariant chain as a vehicle for directed and enhanced MHC class II antigen processing and presentation.* European Journal of Immunology, 1998. **28**(5): p. 1524-1533.
266. Halbroth, B.R., et al., *Development of a Molecular Adjuvant to Enhance Antigen-Specific CD8(+) T Cell Responses.* Sci Rep, 2018. **8**(1): p. 15020.
267. Olsen, T.M., et al., *Prime-and-Trap Malaria Vaccination To Generate Protective CD8(+) Liver-Resident Memory T Cells.* J Immunol, 2018. **201**(7): p. 1984-1993.
268. McNamara, H.A.C., Y.; Wagle M.V.; Sontani, Y.; Roots, C. M.; Miosge, L.A. O'Connor, J.H.O.; Sutton, H.J.; Ganusov, V.V.; Heath, W.R.; Bertolino, P.; Goodnow, C.G.; Parish, I.A.; Enders, A.; Cockburn, I.A., *Up-regulation of LFA-1 allows liver-resident memory T cells to patrol and remain in the hepatic sinusoids.* Science immunology, 2017. **2**(9).
269. Alonso, P.L., et al., *Efficacy of the RTS,S/AS02A vaccine against Plasmodium falciparum infection and disease in young African children: randomised controlled trial.* The Lancet, 2004. **364**(9443): p. 1411-1420.
270. Rts, S.C.T.P., *Efficacy and safety of the RTS,S/AS01 malaria vaccine during 18 months after vaccination: a phase 3 randomized, controlled trial in children and young infants at 11 African sites.* PLoS Med, 2014. **11**(7): p. e1001685.
271. Roestenberg, M., et al., *Long-term protection against malaria after experimental sporozoite inoculation: an open-label follow-up study.* The Lancet, 2011. **377**(9779): p. 1770-1776.
272. Crosby, C.M., et al., *A Novel Codon-optimized SIV Gag-pol Immunogen for Gene-based Vaccination.* Virol Rep, 2015. **5**: p. 47-55.
273. Jiang, S., et al., *Comparison of Wild Type DNA Sequence of Spike Protein from SARS-CoV-2 with Optimized Sequence on The Induction of Protective Responses Against SARS-Cov-2 Challenge in Mouse Model.* Hum Vaccin Immunother, 2022. **18**(1): p. 2016201.
274. Pei, J., et al., *Codon optimization of G protein enhances rabies virus-induced humoral immunity.* J Gen Virol, 2019. **100**(8): p. 1222-1233.
275. Lee, D.H., et al., *Protection induced by malaria virus-like particles containing codon-optimized AMA-1 of Plasmodium berghei.* Malar J, 2019. **18**(1): p. 394.

276. Ternette, N., et al., *Immunogenicity and efficacy of codon optimized DNA vaccines encoding the F-protein of respiratory syncytial virus.* Vaccine, 2007. **25**(41): p. 7271-9.
277. Lin, C.T., et al., *A DNA vaccine encoding a codon-optimized human papillomavirus type 16 E6 gene enhances CTL response and anti-tumor activity.* J Biomed Sci, 2006. **13**(4): p. 481-8.
278. Romero, P., Maryanskl, J.L., Corradin, G., Nussenzweig, R.S., Nussenzweig, V., and Zavala,, *Cloned cytotoxic T cells recognize an epitope in the circumsporozoite protein and protect against malaria.* Nature, 1997(341): p. 323-326.
279. Bharadwaj, A., et al., *Induction of protective immune responses by immunization with linear multiepitope peptides based on conserved sequences from Plasmodium falciparum antigens.* Infect Immun, 1998. **66**(7): p. 3232-41.
280. Ledgerwood, J.E., et al., *Prime-boost interval matters: a randomized phase 1 study to identify the minimum interval necessary to observe the H5 DNA influenza vaccine priming effect.* J Infect Dis, 2013. **208**(3): p. 418-22.
281. Flaxman, A., et al., *Reactogenicity and immunogenicity after a late second dose or a third dose of ChAdOx1 nCoV-19 in the UK: a substudy of two randomised controlled trials (COV001 and COV002).* The Lancet, 2021. **398**(10304): p. 981-990.
282. Das, J., et al., *Delayed fractional dosing with RTS,S/AS01 improves humoral immunity to malaria via a balance of polyfunctional NANP6- and Pf16-specific antibodies.* Med (N Y), 2021. **2**(11): p. 1269-1286 e9.
283. Brice, G.T., et al., *Extended immunization intervals enhance the immunogenicity and protective efficacy of plasmid DNA vaccines.* Microbes Infect, 2007. **9**(12-13): p. 1439-46.
284. Knudsen, M.L., et al., *Kinetic and phenotypic analysis of CD8+ T cell responses after priming with alphavirus replicons and homologous or heterologous booster immunizations.* J Virol, 2014. **88**(21): p. 12438-51.
285. Nayrac, M., et al., *Temporal associations of B and T cell immunity with robust vaccine responsiveness in a 16-week interval BNT162b2 regimen.* Cell Rep, 2022. **39**(13): p. 111013.
286. Jongwutiwes, S., et al., *Variation in the thrombospondin-related adhesive protein (TRAP) gene of Plasmodium falciparum from Thai field isolates.* Mol Biochem Parasitol, 1998. **92**(2): p. 349-53.
287. Mehrizi, A.A., et al., *Population genetic structure analysis of thrombospondin-related adhesive protein (TRAP) as a vaccine candidate antigen in worldwide Plasmodium falciparum isolates.* Infect Genet Evol, 2020. **80**: p. 104197.
288. Weedall, G.D., et al., *Differential evidence of natural selection on two leading sporozoite stage malaria vaccine candidate antigens.* Int J Parasitol, 2007. **37**(1): p. 77-85.
289. Barry, A.E., et al., *Contrasting population structures of the genes encoding ten leading vaccine-candidate antigens of the human malaria parasite, Plasmodium falciparum.* PLoS One, 2009. **4**(12): p. e8497.
290. Wilson, K.L., S.D. Xiang, and M. Plebanski, *A Model to Study the Impact of Polymorphism Driven Liver-Stage Immune Evasion by Malaria Parasites, to Help Design Effective Cross-Reactive Vaccines.* Front Microbiol, 2016. **7**: p. 303.

291. Halbroth, B.R., et al., *Preclinical Development and Assessment of Viral Vectors Expressing a Fusion Antigen of Plasmodium falciparum LSA1 and LSAP2 for Efficacy against Liver-Stage Malaria.* Infect Immun, 2020. **88**(2).
292. Finney, O.C., et al., *Immunization with genetically attenuated P. falciparum parasites induces long-lived antibodies that efficiently block hepatocyte invasion by sporozoites.* Vaccine, 2014. **32**(19): p. 2135-8.
293. van der Velden, M., et al., *Protective Efficacy Induced by Genetically Attenuated Mid-to-Late Liver-Stage Arresting Plasmodium berghei Deltamrp2 Parasites.* Am J Trop Med Hyg, 2016. **95**(2): p. 378-82.
294. Behet, M.C., et al., *Sporozoite immunization of human volunteers under chemoprophylaxis induces functional antibodies against pre-erythrocytic stages of Plasmodium falciparum.* Malar J, 2014. **13**: p. 136.
295. Nahrendorf, W., et al., *Memory B-cell and antibody responses induced by Plasmodium falciparum sporozoite immunization.* J Infect Dis, 2014. **210**(12): p. 1981-90.
296. Zenklusen, I., et al., *Immunization of Malaria-Preexposed Volunteers With PfSPZ Vaccine Elicits Long-Lived IgM Invasion-Inhibitory and Complement-Fixing Antibodies.* J Infect Dis, 2018. **217**(10): p. 1569-1578.
297. Lyke, K.E., et al., *Attenuated PfSPZ Vaccine induces strain-transcending T cells and durable protection against heterologous controlled human malaria infection.* Proc Natl Acad Sci U S A, 2017. **114**(10): p. 2711-2716.
298. Doolan, D.L. and S.L. Hoffman, *The complexity of protective immunity against liver-stage malaria.* J Immunol, 2000. **165**(3): p. 1453-62.
299. Coppi, A., et al., *The malaria circumsporozoite protein has two functional domains, each with distinct roles as sporozoites journey from mosquito to mammalian host.* J Exp Med, 2011. **208**(2): p. 341-56.
300. Cochrane, A., Aikawa, M., Jeng, M., Nussenzweig, RS., *Antibody-Induced Ultrastructural Changes of Malarial Sporozoites.* J Immunol 1, 1976. **116**: p. 859-867.
301. Young, J.F., Ballou., WR., Hockmeyer W.T, *Developing a human malaria sporozoite vaccine.* Microb Pathog, 1987. **2**: p. 237-240.
302. Cohen, J., et al., *From the circumsporozoite protein to the RTS, S/AS candidate vaccine.* Hum Vaccin, 2010. **6**(1): p. 90-6.
303. RTS, S.C.T.P., *Efficacy and safety of RTS,S/AS01 malaria vaccine with or without a booster dose in infants and children in Africa: final results of a phase 3, individually randomised, controlled trial.* The Lancet, 2015. **386**(9988): p. 31-45.
304. Zepeda-Cervantes, J., J.O. Ramirez-Jarquin, and L. Vaca, *Interaction Between Virus-Like Particles (VLPs) and Pattern Recognition Receptors (PRRs) From Dendritic Cells (DCs): Toward Better Engineering of VLPs.* Front Immunol, 2020. **11**: p. 1100.
305. Kester, K.E., et al., *Randomized, double-blind, phase 2a trial of falciparum malaria vaccines RTS,S/AS01B and RTS,S/AS02A in malaria-naive adults: safety, efficacy, and immunologic associates of protection.* J Infect Dis, 2009. **200**(3): p. 337-46.
306. The RTS, S.C.T.P., *First Results of Phase 3 Trial of RTS,S/AS01 Malaria Vaccine in African Children.* 2011. **365**(20).
307. Tinto, H., et al., *Long-term incidence of severe malaria following RTS,S/AS01 vaccination in children and infants in Africa: an open-label 3-year extension study*

of a phase 3 randomised controlled trial. The Lancet Infectious Diseases, 2019. **19**(8): p. 821-832.

308. J. E. Epstein, K.T., K. E. Lyke, B. K. L. Sim, P. F. Billingsley, M. B. Laurens, A. Gunasekera, S. Chakravarty, E. R. James, M. Sedegah, A. Richman, S. Velmurugan, S. Reyes, M. Li, K. Tucker, A. Ahumada, A. J. Ruben, T. Li, R. Stafford, A. G. Eappen, C. Tamminga, J. W. Bennett, C. F. Ockenhouse, J. R. Murphy, J. Komisar, N. Thomas, M. Loyevsky, A. Birkett, C. V. Plowe, C. Loucq, R. Edelman, T. L. Richie, R. A. Seder, S. L. Hoffman, *Live Attenuated Malaria Vaccine Designed to Protect Through Hepatic CD8+ T Cell Immunity.* Science, 2011. **334**(6055): p. 475-480.
309. W R Weiss, M.S., R L Beaudoin, L H Miller, and M F Good, *CD8+ T cells (cytotoxic/suppressors) are required for protection in mice im- munized with malaria sporozoites.* PNAS, 1988. **85**(2): p. 573-576.
310. Reyes-Sandoval, A., et al., *CD8+ T effector memory cells protect against liver-stage malaria.* J Immunol, 2011. **187**(3): p. 1347-57.
311. Halperin, S.A., et al., *Final efficacy analysis, interim safety analysis, and immunogenicity of a single dose of recombinant novel coronavirus vaccine (adenovirus type 5 vector) in adults 18 years and older: an international, multicentre, randomised, double-blinded, placebo-controlled phase 3 trial.* The Lancet, 2022. **399**(10321): p. 237-248.
312. Voysey, M., et al., *Safety and efficacy of the ChAdOx1 nCoV-19 vaccine (AZD1222) against SARS-CoV-2: an interim analysis of four randomised controlled trials in Brazil, South Africa, and the UK.* The Lancet, 2021. **397**(10269): p. 99-111.
313. Sadoff, J., et al., *Safety and Efficacy of Single-Dose Ad26.COV2.S Vaccine against Covid-19.* N Engl J Med, 2021. **384**(23): p. 2187-2201.
314. Sheehy, S.H., et al., *Phase Ia clinical evaluation of the safety and immunogenicity of the Plasmodium falciparum blood-stage antigen AMA1 in ChAd63 and MVA vaccine vectors.* PLoS One, 2012. **7**(2): p. e31208.
315. de Graaf, H., et al., *Safety and Immunogenicity of ChAd63/MVA Pfs25-IMX313 in a Phase I First-in-Human Trial.* Front Immunol, 2021. **12**: p. 694759.
316. Salisch, N.C., et al., *Antigen capsid-display on human adenovirus 35 via pIX fusion is a potent vaccine platform.* PLoS One, 2017. **12**(3): p. e0174728.
317. Palma, C., et al., *Adenovirus particles that display the Plasmodium falciparum circumsporozoite protein NANP repeat induce sporozoite-neutralizing antibodies in mice.* Vaccine, 2011. **29**(8): p. 1683-9.
318. Shiratsuchi, T., et al., *A potent malaria vaccine based on adenovirus with dual modifications at Hexon and pVII.* Vaccine, 2017. **35**(50): p. 6990-7000.
319. Yan, D., et al., *The application of virus-like particles as vaccines and biological vehicles.* Appl Microbiol Biotechnol, 2015. **99**(24): p. 10415-32.
320. Noe, A.R., et al., *A full-length Plasmodium falciparum recombinant circumsporozoite protein expressed by Pseudomonas fluorescens platform as a malaria vaccine candidate.* PLoS One, 2014. **9**(9): p. e107764.
321. Schwenk, R., et al., *IgG2 antibodies against a clinical grade Plasmodium falciparum CSP vaccine antigen associate with protection against transgenic sporozoite challenge in mice.* PLoS One, 2014. **9**(10): p. e111020.
322. Plassmeyer, M.L., et al., *Structure of the Plasmodium falciparum circumsporozoite protein, a leading malaria vaccine candidate.* J Biol Chem, 2009. **284**(39): p. 26951-63.

323. Kedees, M.H., et al., *Plasmodium falciparum: glycosylation status of Plasmodium falciparum circumsporozoite protein expressed in the baculovirus system.* Exp Parasitol, 2002. **101**(1): p. 64-8.
324. Walther, M., et al., *Safety, immunogenicity, and efficacy of prime-boost immunization with recombinant poxvirus FP9 and modified vaccinia virus Ankara encoding the full-length Plasmodium falciparum circumsporozoite protein.* Infect Immun, 2006. **74**(5): p. 2706-16.
325. Imoukhuede, E.B., et al., *Safety and immunogenicity of the malaria candidate vaccines FP9 CS and MVA CS in adult Gambian men.* Vaccine, 2006. **24**(42-43): p. 6526-33.
326. Bruna-Romero, O., et al., *Enhanced protective immunity against malaria by vaccination with a recombinant adenovirus encoding the circumsporozoite protein of Plasmodium lacking the GPI-anchoring motif.* Vaccine, 2004. **22**(27-28): p. 3575-84.
327. Coppi, A., et al., *The Plasmodium circumsporozoite protein is proteolytically processed during cell invasion.* J Exp Med, 2005. **201**(1): p. 27-33.
328. de Barra, E., et al., *A phase Ia study to assess the safety and immunogenicity of new malaria vaccine candidates ChAd63 CS administered alone and with MVA CS.* PLoS One, 2014. **9**(12): p. e115161.
329. Bell, N.M. and A.M. Lever, *HIV Gag polyprotein: processing and early viral particle assembly.* Trends Microbiol, 2013. **21**(3): p. 136-44.
330. Wang, D., et al., *The lack of an inherent membrane targeting signal is responsible for the failure of the matrix (M1) protein of influenza A virus to bud into virus-like particles.* J Virol, 2010. **84**(9): p. 4673-81.
331. Kim, J.H., et al., *High cleavage efficiency of a 2A peptide derived from porcine teschovirus-1 in human cell lines, zebrafish and mice.* PLoS ONE, 2011. **6**(4): p. 1--8.
332. Regules, J.A., et al., *Fractional Third and Fourth Dose of RTS,S/AS01 Malaria Candidate Vaccine: A Phase 2a Controlled Human Malaria Parasite Infection and Immunogenicity Study.* J Infect Dis, 2016. **214**(5): p. 762-71.
333. Dobano, C., et al., *Concentration and avidity of antibodies to different circumsporozoite epitopes correlate with RTS,S/AS01E malaria vaccine efficacy.* Nat Commun, 2019. **10**(1): p. 2174.
334. Rampling, T., et al., *Safety and High Level Efficacy of the Combination Malaria Vaccine Regimen of RTS,S/AS01B With Chimpanzee Adenovirus 63 and Modified Vaccinia Ankara Vectored Vaccines Expressing ME-TRAP.* J Infect Dis, 2016. **214**(5): p. 772-81.
335. Rampling, T., et al., *Safety and efficacy of novel malaria vaccine regimens of RTS,S/AS01B alone, or with concomitant ChAd63-MVA-vectored vaccines expressing ME-TRAP.* NPJ Vaccines, 2018. **3**: p. 49.
336. Bowyer, G., et al., *CXCR3(+) T Follicular Helper Cells Induced by Co-Administration of RTS,S/AS01B and Viral-Vectored Vaccines Are Associated With Reduced Immunogenicity and Efficacy Against Malaria.* Front Immunol, 2018. **9**: p. 1660.
337. Sebastian, S., et al., *A Multi-Filovirus Vaccine Candidate: Co-Expression of Ebola, Sudan, and Marburg Antigens in a Single Vector.* Vaccines (Basel), 2020. **8**(2).
338. Fontana, D., et al., *Chimeric VLPs Based on HIV-1 Gag and a Fusion Rabies Glycoprotein Induce Specific Antibodies against Rabies and Foot-and-Mouth Disease Virus.* Vaccines (Basel), 2021. **9**(3).

339. Boix-Besora, A., et al., *Optimization, Production, Purification and Characterization of HIV-1 GAG-Based Virus-like Particles Functionalized with SARS-CoV-2.* Vaccines (Basel), 2022. **10**(2).
340. Andersson, A.M.C., et al., *Effect of HIV-1 envelope cytoplasmic tail on adenovirus primed virus encoded virus-like particle immunizations.* Vaccine, 2016. **34**(44): p. 5344--5351.
341. Andersson, A.-M., M. Schwerdtfeger, and P. Holst, *Virus-Like-Vaccines against HIV.* Vaccines, 2018. **6**(1): p. 10.
342. Andersson, A.M.C., et al., *Novel adenovirus encoded virus-like particles displaying the placental malaria associated VAR2CSA antigen.* Vaccine, 2017. **35**(8): p. 1140--1147.
343. Neukirch, L., et al., *Adenovirus based virus-like-vaccines targeting endogenous retroviruses can eliminate growing colorectal cancers in mice.* Oncotarget, 2019. **10**(14): p. 1458--1472.
344. Vujadinovic, M., et al., *Adenoviral Type 35 and 26 Vectors with a Bidirectional Expression Cassette in the E1 Region Show an Improved Genetic Stability Profile and Potent Transgene-Specific Immune Response.* Hum Gene Ther, 2018. **29**(3): p. 337-351.
345. Wang, B.Z., et al., *Incorporation of High Levels of Chimeric Human Immunodeficiency Virus Envelope Glycoproteins into Virus-Like Particles.* Journal of Virology, 2007. **81**(20): p. 10869--10878.
346. Romagnoli P, L.C., Yewdell J, Bakke O, Germain RN., *Relationship between invariant chain expression and major histocompatibility complex class II transport into early and late endocytic compartments.* J Exp Med., 1991. **177**(3): p. 583-596.
347. Lindner, R., *Invariant Chain Complexes and Clusters as Platforms for MIF Signaling.* Cells, 2017. **6**(1).
348. Halbroth, B.R., *Development of Adjuvanted Multi-Antigen Liver-Stage Malaria Vaccines*
, in *Nuffield Department of Clinical Medicine*. 2016, University of Oxford.
349. Ishizuka, A.S., et al., *Protection against malaria at 1 year and immune correlates following PfSPZ vaccination.* Nat Med, 2016. **22**(6): p. 614-23.
350. Gardner MJ, H.N., Fung E, White O, Berriman M, Hyman RW, Carlton JM, Pain A, Nelson KE, Bowman S, Paulsen IT, James K, Eisen JA, Rutherford K, Salzberg SL, Craig A, Kyes S, Chan MS, Nene V, Shallom SJ, Suh B, Peterson J, Angiuoli S, Pertea M, Allen J, Selengut J, Haft D, Mather MW, Vaidya AB, Martin DM, Fairlamb AH, Fraunholz MJ, Roos DS, Ralph SA, McFadden GI, Cummings LM, Subramanian GM, Mungall C, Venter JC, Carucci DJ, Hoffman SL, Newbold C, Davis RW, Fraser CM and Barrell B, *Genome sequence of the human malaria parasite Plasmodium falciparum.* Nature, 2002. **419**.
351. Lockyer, M.J., Schwarz., R.T, *Strain variation in the circumsporozoite protein gene of Plasmodium falciparum.* Mol Biochem Parasitol, 1987. **22**(1).
352. Oyen, D., et al., *Structural basis for antibody recognition of the NANP repeats in Plasmodium falciparum circumsporozoite protein.* Proc Natl Acad Sci U S A, 2017. **114**(48): p. E10438-e10445.
353. Bongfen, S.E., et al., *The N-terminal domain of Plasmodium falciparum circumsporozoite protein represents a target of protective immunity.* Vaccine, 2009. **27**(2): p. 328-35.

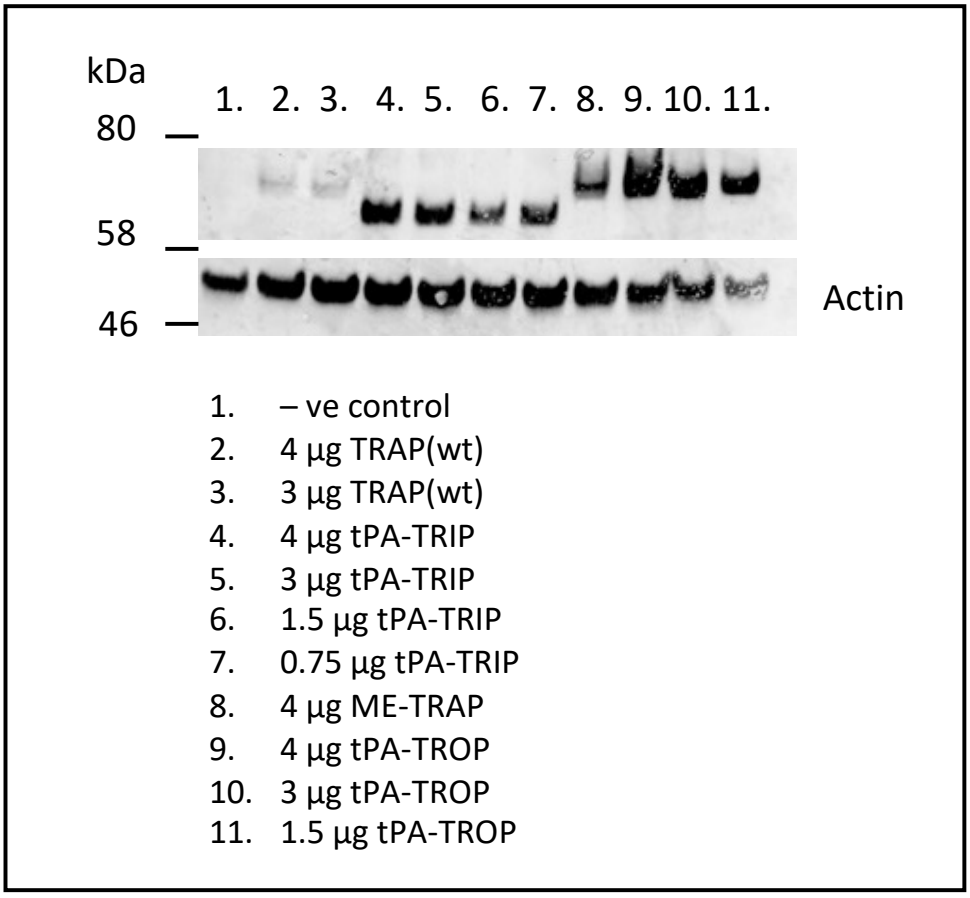
354. Espinosa, D.A., et al., *Proteolytic Cleavage of the Plasmodium falciparum Circumsporozoite Protein Is a Target of Protective Antibodies.* J Infect Dis, 2015. **212**(7): p. 1111-9.
355. Wang, L.T., et al., *A Potent Anti-Malarial Human Monoclonal Antibody Targets Circumsporozoite Protein Minor Repeats and Neutralizes Sporozoites in the Liver.* Immunity, 2020. **53**(4): p. 733-744 e8.
356. Gaudinski, M.R., et al., *A Monoclonal Antibody for Malaria Prevention.* N Engl J Med, 2021. **385**(9): p. 803-814.
357. Beutler, N., et al., *A novel CSP C-terminal epitope targeted by an antibody with protective activity against Plasmodium falciparum.* PLoS Pathog, 2022. **18**(3): p. e1010409.
358. Chaudhury, S., et al., *Breadth of humoral immune responses to the C-terminus of the circumsporozoite protein is associated with protective efficacy induced by the RTS,S malaria vaccine.* Vaccine, 2021. **39**(6): p. 968-975.
359. Garcon, N., D.G. Heppner, and J. Cohen, *Development of RTS,S/AS02: a purified subunit-based malaria vaccine candidate formulated with a novel adjuvant.* Expert Rev Vaccines, 2003. **2**(2): p. 231-8.
360. Bejon, P., et al., *Efficacy of RTS,S malaria vaccines: individual-participant pooled analysis of phase 2 data.* Lancet Infect Dis, 2013. **13**(4): p. 319-27.
361. McNamara, H.A., et al., *Antibody Feedback Limits the Expansion of B Cell Responses to Malaria Vaccination but Drives Diversification of the Humoral Response.* Cell Host Microbe, 2020.
362. Kurtovic, L., M.J. Boyle, and J.G. Beeson, *Epitope masking may limit antibody boosting to malaria vaccines.* Immunol Cell Biol, 2021. **99**(2): p. 126-129.
363. Chatterjee, D., et al., *Avid binding by B cells to the Plasmodium circumsporozoite protein repeat suppresses responses to protective subdominant epitopes.* Cell Rep, 2021. **35**(2): p. 108996.
364. Jelinkova, L., et al., *An epitope-based malaria vaccine targeting the junctional region of circumsporozoite protein.* NPJ Vaccines, 2021. **6**(1): p. 13.
365. Francica, J.R., et al., *Design of Alphavirus Virus-Like Particles Presenting Circumsporozoite Junctional Epitopes That Elicit Protection against Malaria.* Vaccines (Basel), 2021. **9**(3).
366. Young JF, H.W., Gross M, Ballou WR, Wirtz RA, Trosper JH, Beaudoin RL, Hollingdale MR, Miller LH, Diggs CL, et al., *Expression of Plasmodium falciparum circumsporozoite proteins in Escherichia coli for potential use in a human malaria vaccine.* Science., 1985. **228**(4702): p. 5.
367. Andersson, A.M.C. and P.J. Holst, *Increased t cell breadth and antibody response elicited in prime-boost regimen by viral vector encoded homologous siv gag/env in outbred cd1 mice.* Journal of Translational Medicine, 2016. **14**(1): p. 1--10.
368. Flores-Garcia, Y., et al., *The P. falciparum CSP repeat region contains three distinct epitopes required for protection by antibodies in vivo.* PLoS Pathog, 2021. **17**(11): p. e1010042.
369. Kester, K.E., et al., *Phase 2a trial of 0, 1, and 3 month and 0, 7, and 28 day immunization schedules of malaria vaccine RTS,S/AS02 in malaria-naive adults at the Walter Reed Army Institute of Research.* Vaccine, 2008. **26**(18): p. 2191-202.
370. Keitany, G.J., M. Vignali, and R. Wang, *Live attenuated pre-erythrocytic malaria vaccines.* Hum Vaccin Immunother, 2014. **10**(10): p. 2903-9.

371. Nielsen, C.M., et al., *Protein/AS01(B) vaccination elicits stronger, more Th2-skewed antigen-specific human T follicular helper cell responses than heterologous viral vectors.* Cell Rep Med, 2021. **2**(3): p. 100207.
372. Langowski, M.D., et al., *Restricted valency (NPNA)n repeats and junctional epitope-based circumsporozoite protein vaccines against Plasmodium falciparum.* NPJ Vaccines, 2022. **7**(1): p. 13.
373. Oyen, D., et al., *Structure and mechanism of monoclonal antibody binding to the junctional epitope of Plasmodium falciparum circumsporozoite protein.* PLoS Pathog, 2020. **16**(3): p. e1008373.
374. Dennison, S.M., et al., *Magnitude, Specificity, and Avidity of Sporozoite-Specific Antibodies Associate With Protection Status and Distinguish Among RTS,S/AS01 Dose Regimens.* Open Forum Infectious Diseases, 2021. **8**(2).
375. Feng, G., et al., *Mechanisms and targets of Fcgamma-receptor mediated immunity to malaria sporozoites.* Nat Commun, 2021. **12**(1): p. 1742.
376. Ragotte, R.J., et al., *Heterotypic interactions drive antibody synergy against a malaria vaccine candidate.* Nat Commun, 2022. **13**(1): p. 933.

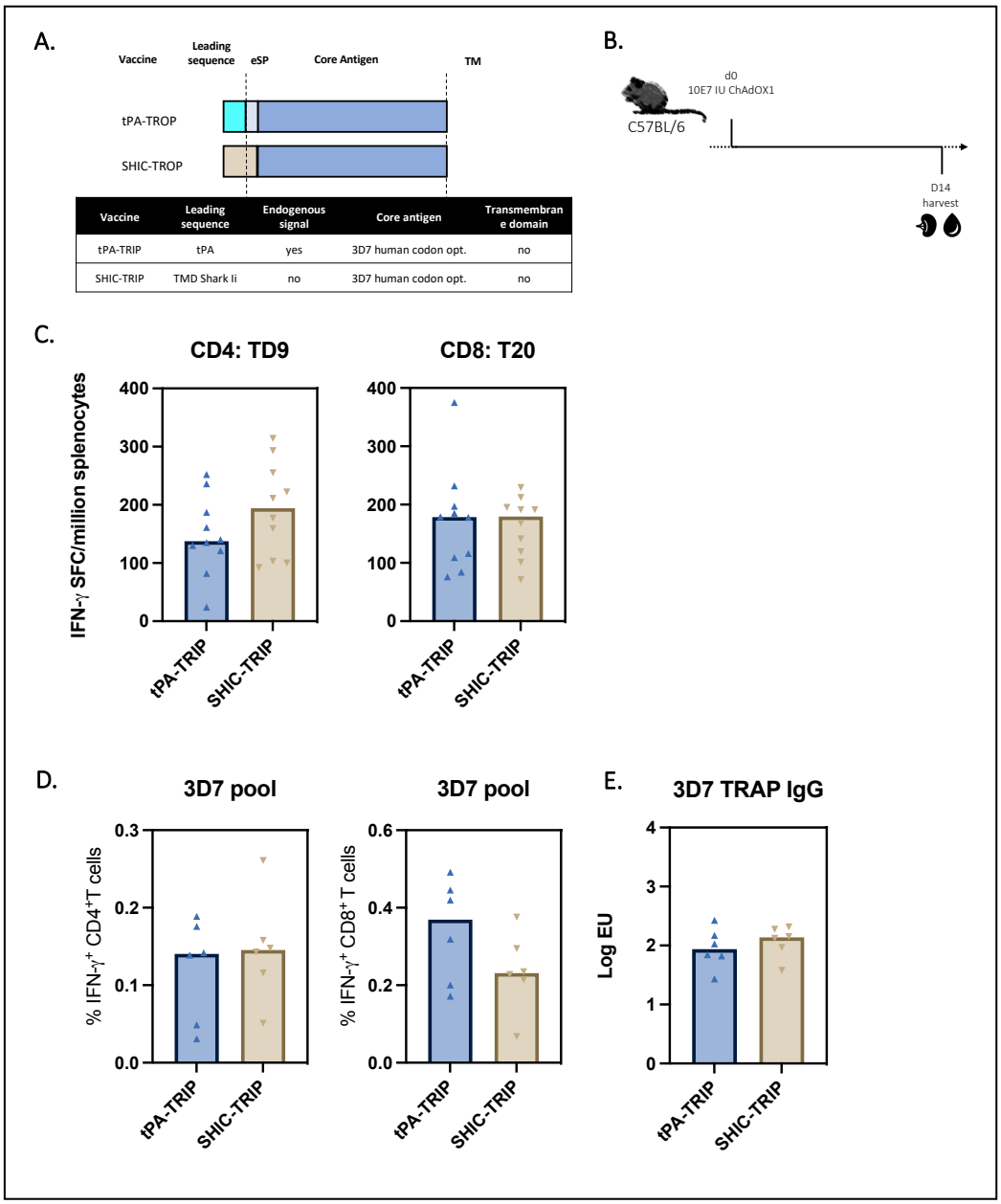
8

Appendix

8.1 Supplemental Figures



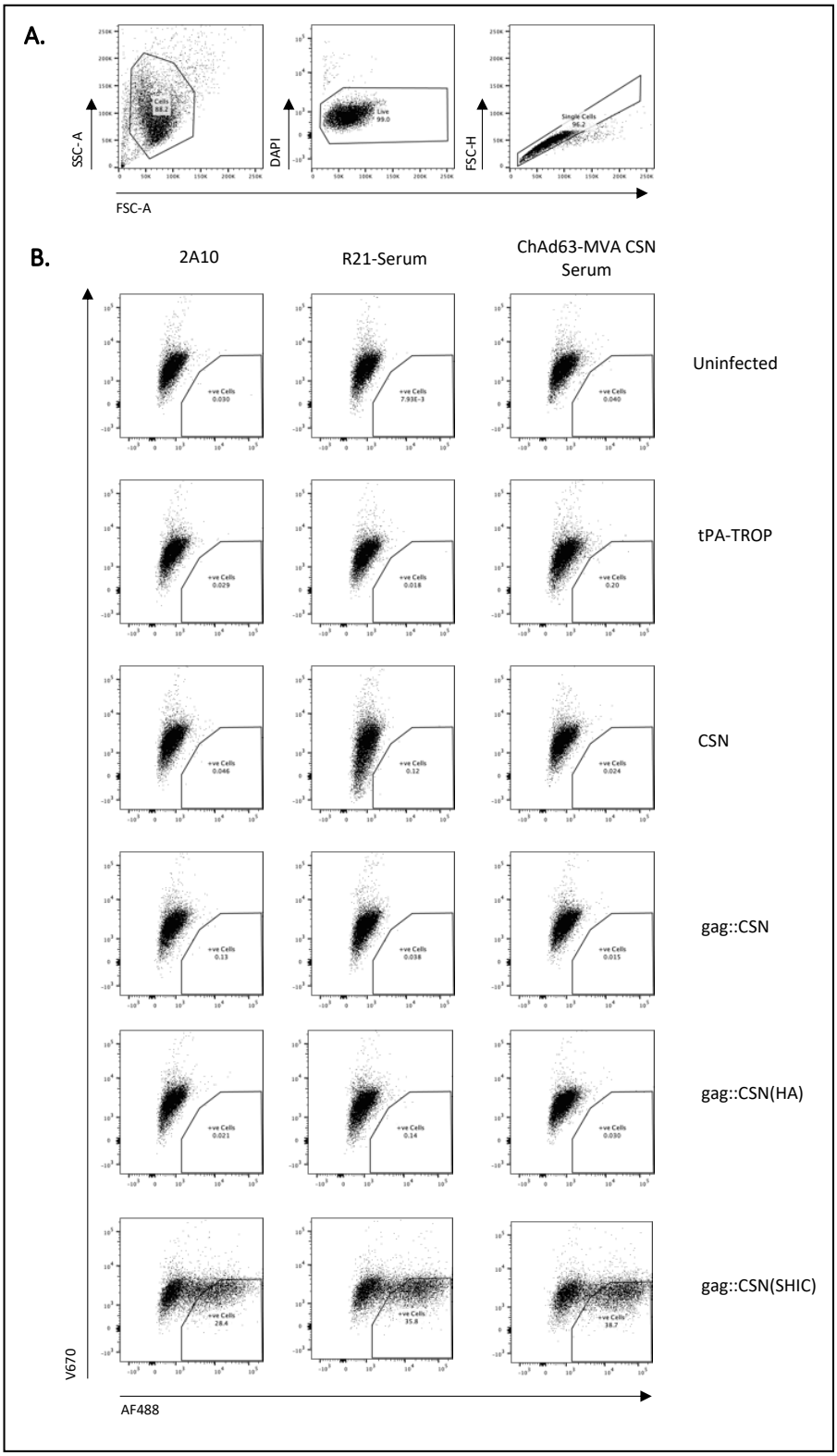
Supplement Figure 8-1. Expression analysis of various TRAP construct using Western Blot.
HEK293 cells were transfected using entry vector encoding various TRAP construct at different concentration. After 48 hours, the cells were lysed, and the lysate was running on the 12% Bis-Tris Protein Gel under reducing condition. β-actin represents the housekeeping gene that was selected as a loading control.



Vaccine	Leading sequence	Endogenous signal	Core antigen	Transmembrane domain
tPA-TRIP	tPA	yes	3D7 human codon opt.	no
SHIC-TRIP	TMD Shark Ii	no	3D7 human codon opt.	no

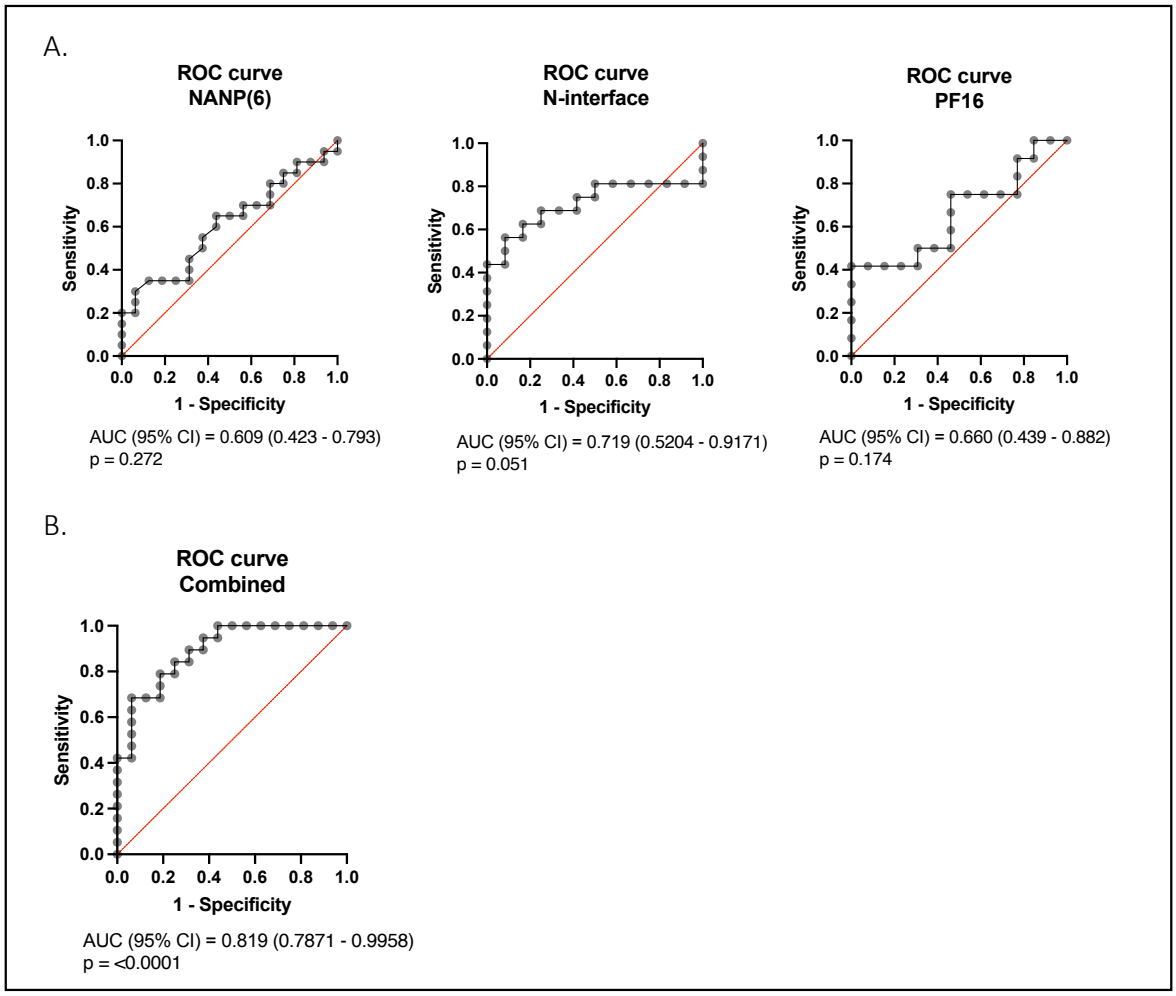
Supplement Figure 8-2 Impact of the addition of SHIC adjuvant to the immunogenicity TRIP encoded ChAdOX-1 vector.

A. Truncated human-codon optimised *Pf.* TRAP 3D7 (TRIP) was fused to the transmembrane domain of the shark invariant chain (SHIC) at the N-terminal of the antigen (denoted as SHIC-TRIP), and the immunogenicity was compared to tPA-TRIP. **B.** Inbred (C57BL/6) mice were immunised with 10^7 IU of ChAdOx1. Two weeks after vaccination, spleens and blood were harvested and processed for downstream assay. **C.** The $CD4^+$ and $CD8^+$ T-cell responses were measured by IFN-γ^+ ELIPOTs assays against a single peptide TD9 (CD4) and T20 (CD8). **D.** TRAP-specific IFN-γ^+ $CD4^+$ and $CD8^+$ were measured by ICS after stimulation with 3D7 pool peptides. **E.** Anti-TRAP IgG levels in serum were measured by standardised ELISA against TRAP 3D7 protein. The data presented were representative of two independent studies. Groups were compared using the two-tail Mann-Whitney analysis. Asterisks indicate significant differences (*=$p<0.05$, **=$p<0.01$).



Supplement Figure 8-3. Analysis of antigen expression on the cells surface

A. Gating strategy for analysis of antigen expression on the surface of HeLa S3 Cells. **B.** Representative population of positive cells expressing antigen CSN on the cells surface detected using either mAb 2A10, R21 serum or ChAd63-MVA CSN vaccinated mice.



Supplement Figure 8-4 ROC curve analysis of predicting the performance of antibody responses in mediating protection.

Antibody data and protection status from mice in the second challenge study were used to model the relationship between antibody responses vs immune outcome (protected/unprotected) using simple logistic regression and ROC analysis. **A.** ROC curve based on univariate logistic regression from each region-specific antibody responses. **B.** ROC curve based on multivariate logistic regression combining each region-specific antibody response.

8.2 Supplemental Tables

Supplement table 8.1 Peptide sequence of *P. falciparum* TRAP

TRAP T9/96 Pools		TRAP 3D7 Pools	
T1	**MNHLGNVKYLVIVFLIFFDL**	TD1	**MNHLGNVKYLVIVFLIFFDL**
T2	**VIVFLIFFDLFLVNGRDVQN**	TD2	**VIVFLIFFDLFLVNGRDVQN**
T3	FLVNGRDVQNNIVDEIKYSE	TD3	FLVNGRDVQNNIVDEIKYRE
T4	NIVDEIKYSEEVCNDQVDLY	TD4	NIVDEIKYREEVCNDEVDLY
T5	EVCNDQVDLYLLMDCSGSIR	TD5	EVCNDEVDLYLLMDCSGSIR
T6	**LLMDCSGSIRRHNWVNHAVP**	TD6	**LLMDCSGSIRRHNWVNHAVP**
T7	**RHNWVNHAVPLAMKLIQQLN**	TD7	**RHNWVNHAVPLAMKLIQQLN**
T8	LAMKLIQQLNLNDNAIHLYV	TD8	LAMKLIQQLNLNDNAIHLYA
T9	LNDNAIHLYVNVFSNNAKEI	TD9	LNDNAIHLYASVFSNNAREI
T10	NVFSNNAKEIIRLHSDASKN	TD10	SVFSNNAREIIRLHSDASKN
T11	IRLHSDASKNKEKALIIIRS	TD11	IRLHSDASKNKEKALIIIKS
T12	KEKALIIIRSLLSTNLPYGR	TD12	KEKALIIIKSLLSTNLPYGK
T13	LLSTNLPYGRTNLTDALLQV	TD13	LLSTNLPYGKTNLTDALLQV
T14	**TNLTDALLQVRKHLNDRINR**	TD14	**TNLTDALLQVRKHLNDRINR**
T15	**RKHLNDRINRENANQLVVIL**	TD15	**RKHLNDRINRENANQLVVIL**
T16	**ENANQLVVILTDGIPDSIQD**	TD16	**ENANQLVVILTDGIPDSIQD**
T17	**TDGIPDSIQDSLKESRKLSD**	TD17	**TDGIPDSIQDSLKESRKLSD**
T18	**SLKESRKLSDRGVKIAVFGI**	TD18	**SLKESRKLSDRGVKIAVFGI**
T19	**RGVKIAVFGIGQGINVAFNR**	TD19	**RGVKIAVFGIGQGINVAFNR**
T20	**GQGINVAFNRFLVGCHPSDG**	TD20	**GQGINVAFNRFLVGCHPSDG**
T21	**FLVGCHPSDGKCNLYADSAW**	TD21	**FLVGCHPSDGKCNLYADSAW**
T22	**KCNLYADSAWENVKNVIGPF**	TD22	**KCNLYADSAWENVKNVIGPF**
T23	**ENVKNVIGPFMKAVCVEVEK**	TD23	**ENVKNVIGPFMKAVCVEVEK**
T24	**MKAVCVEVEKTASCGVWDEW**	TD24	**MKAVCVEVEKTASCGVWDEW**
T25	**TASCGVWDEWSPCSVTCGKG**	TD25	**TASCGVWDEWSPCSVTCGKG**
T26	**SPCSVTCGKGTRSRKREILH**	TD26	**SPCSVTCGKGTRSRKREILH**
T27*	TRSRKREILHEGCTSEIQEQ	TD27	TRSRKREILHEGCTSELQEQ
T28	EGCTSEIQEQCEEERCPPKW	TD28	EGCTSELQEQCEEERCLPKR
T29	CEEERCPPKWEPLDVPDEPE	TD29	CEEERCLPKREPLDVPDEPE
T30	**EPLDVPDEPEDDQPRPRGDN**	TD30	**EPLDVPDEPEDDQPRPRGDN**
T31	DDQPRPRGDNSSVQKPEENI	TD31	DDQPRPRGDNFAVEKPNENI

TRAP T9/96 Pools		TRAP 3D7 Pools	
T32	SSVQKPEENIIDNNPQEPSP	TD32	FAVEKPNENIIDNNPQEPSP
T33	IDNNPQEPSPNPEEGKDENP	TD33	IDNNPQEPSPNPEEGKGENP
T34	NPEEGKDENPNGFDLDENPE	TD34	NPEEGKGENPNGFDLDENPE
T35*	NGFDLDENPENPPNPDIPEQ	TD35	NGFDLDENPENPPNPPNPPN
T36	NPPNPDIPEQKPNIPEDSEK	TD36	NPPNPPNPPNPPNPPNPPNP
T37		TD37	*PPNPPNPPNPDIPEQKPNIP*
T38	DIPEQKPNIPEDSEKEVPSD	TD38	*DIPEQKPNIPEDSEKEVPSD*
T39	**EDSEKEVPSDVPKNPEDDRE**	TD39	**EDSEKEVPSDVPKNPEDDRE**
T40	**VPKNPEDDREENFDIPKKPE**	TD40	**VPKNPEDDREENFDIPKKPE**
T41	**ENFDIPKKPENKHDNQNNLP**	TD41	**ENFDIPKKPENKHDNQNNLP**
T42	NKHDNQNNLPNDKSDRNIPY	TD42	NKHDNQNNLPNDKSDRYIPY
T43	NDKSDRNIPYSPLPPKVLDN	TD43	NDKSDRYIPYSPLAPKVLDN
T44*	SPLPPKVLDNERKQSDPQSQ	TD44	SPLAPKVLDNERKQSDPQSQ
T45	**ERKQSDPQSQDNNGNRHVPN**	TD45	**ERKQSDPQSQDNNGNRHVPN**
T46	**DNNGNRHVPNSEDRETRPHG**	TD46	**DNNGNRHVPNSEDRETRPHG**
T47	**SEDRETRPHGRNNENRSYNR**	TD47	**SEDRETRPHGRNNENRSYNR**
T48	RNNENRSYNRKYNDTPKHPE	TD48	RNNENRSYNRKHNNTPKHPE
T49	KYNDTPKHPEREEHEKPDNN	TD49	KHNNTPKHPEREEHEKPDNN
T50	REEHEKPDNNKKKGESDNKY	TD50	REEHEKPDNNKKKAGSDNKY
T51	**KKKGESDNKYKIAGGIAGGL**	TD51	KKKAGSDNKYKIAGGIAGGL
T52	**KIAGGIAGGLALLACAGLAY**	TD52	**KIAGGIAGGLALLACAGLAY**
T53*	**ALLACAGLAYKFVVPGAATP**	TD53	**ALLACAGLAYKFVVPGAATP**
T54	**KFVVPGAATPYAGEPAPFDE**	TD54	**KFVVPGAATPYAGEPAPFDE**
T55	**YAGEPAPFDETLGEEDKDLD**	TD55	**YAGEPAPFDETLGEEDKDLD**
T56	**TLGEEDKDLDEPEQFRLPEE**	TD56	**TLGEEDKDLDEPEQFRLPEE**
T57	**EPEQFRLPEENEWN**	TD57	**EPEQFRLPEENEWN**

Supplement table 8.2 Peptide sequence of *P. falciparum* CSP 3D7

***P. falciparum* CSP 3D7 Pools**	
CSP-1	MRKLAILSVSSFLFV
CSP-2	ILSVSSFLFVEALFQ
CSP-3	SFLFVEALFQEYQCY
CSP-4	EALFQEYQCYGSSSN
CSP-5	EYQCYGSSSNTRVLN
CSP-6	GSSSNTRVLNELNYD
CSP-7	TRVLNELNYDNAGTN
CSP-8	ELNYDNAGTNLYNEL
CSP-9	NAGTNLYNELEMNYY
CSP-10	LYNELEMNYYGKQEN
CSP-11	EMNYYGKQENWYSLK
CSP-12	GKQENWYSLKKNSRS
CSP-13	WYSLKKNSRSLGEND
CSP-14	KNSRSLGENDDGNNE
CSP-15	LGENDDGNNEDNEKL
CSP-16	DGNNEDNEKLRKPKH
CSP-17	DNEKLRKPKHKKLKQ
CSP-18	RKPKHKKLKQPADGN
CSP-19	KKLKQPADGNPDPNA
CSP-20	PADGNPDPNANPNVD
CSP-21	PDPNANPNVDPNANP
CSP-22	NPNVDPNANPNVDPN
CSP-23	PNANPNVDPNANPNV
CSP-24	NVDPNANPNVDPNAN
CSP-25	ANPNVDPNANPNANP
CSP-26	DPNANPNANPNANPN
CSP-27	PNANPNANPNANPNA
CSP-28	NANPNANPNANPNAN
CSP-29	ANPNANPNANPNANP
CSP-30	NPNANPNANPNANPN
CSP-31	PNANPNANPNANPNA
CSP-32	NANPNANPNANPNKN
CSP-33	ANPNANPNKNNQGNG
CSP-34	NPNKNNQGNGQGHNM
CSP-35	NQGNGQGHNMPNDPN
CSP-36	QGHNMPNDPNRNVDE
CSP-37	PNDPNRNVDENANAN

P. falciparum CSP 3D7 Pools	
CSP-38	RNVDENANANSAVKN
CSP-39	NANANSAVKNNNNEE
CSP-40	SAVKNNNNEEPSDKH
CSP-41	NNNEEPSDKHIKEYL
CSP-42	PSDKHIKEYLNKIQN
CSP-43	IKEYLNKIQNSLSTE
CSP-44	NKIQNSLSTEWSPCS
CSP-45	SLSTEWSPCSVTCGN
CSP-46	WSPCSVTCGNGIQVR
CSP-47	VTCGNGIQVRIKPGS
CSP-48	GIQVRIKPGSANKPK
CSP-49	IKPGSANKPKDELDY
CSP-50	ANKPKDELDYANDIE
CSP-51	DELDYANDIEKKICK
CSP-52	ANDIEKKICKMEKCS
CSP-53	KKICKMEKCSSVFNV
CSP-54	MEKCSSVFNVVNSSI
CSP-55	SVFNVVNSSI